

Peripheral Inflammation Remotely Triggers Global Gene Expression Changes in the Brain

Carolyn Ann Thomson
BSc

Submitted in fulfilment of the requirements for the degree
of Doctor of Philosophy

College of Medical, Veterinary and Life Sciences
Institute of Infection, Immunity and Inflammation
University of Glasgow

March 2014

Abstract

Although the central nervous system (CNS) was once considered an immunologically privileged site, in recent years it has become increasingly evident that cross talk between the immune system and the CNS does occur. As a result, patients with chronic inflammatory diseases such as rheumatoid arthritis, inflammatory bowel disease or psoriasis are often further burdened with neuropsychiatric symptoms such as depression, anxiety and fatigue. Despite the recent advances in our understanding of neuroimmune communication pathways, the precise effect peripheral immune activation has on neural circuitry remains unclear. Therefore, the primary aim of this thesis was to develop a better understanding of the bidirectional relationship, and communication pathways, that exist between the immune system and the nervous system.

By utilising transcriptomics in a well-characterised murine model of systemic inflammation, I have investigated the molecular mechanisms by which inflammation originating in the periphery can induce transcriptional modulation in the brain. Systemic inflammation was induced in male C57BL/6 mice via intraperitoneal injection of lipopolysaccharide (LPS). After 48 hours, whole brain transcriptional profiles were assessed, and compared to that of a vehicle-treated control group, using Affymetrix GeneChip microarrays. Target gene induction, identified by microarray analysis was validated independently using QPCR. Expression of the same panel of target genes was then investigated, in the brains of mice, following the induction of different sterile, and TLR-dependent, models of peripheral inflammation.

Microarray analysis of whole brains collected 48hr after LPS challenge revealed increased transcription of a range of interferon-stimulated genes (ISGs) in the brain, including a significant upregulation of the classic interferon-induced chemokine CXCL10. This transcriptional profile could not be reproduced by the systemic administration of TNF α , or following lipoteichoic acid-induced systemic inflammation. However, target genes remained induced in the brain following daily LPS injections, in the absence of a detectable inflammatory cytokine response in the periphery.

The central induction of CXCL10 suggests that acute exposure to LPS in the periphery may prime the brain for T cell infiltration. This prompted an investigation into whether leukocytes infiltrated the brain following daily systemic LPS injections. First, the inflammatory chemokine repertoire in the brains of LPS treated mice was systematically characterised. In addition to *Cxcl10*, repeated injection of LPS in the periphery triggered a transient increase in the transcription of a number of other inflammatory chemokines in the brain. Chemokine induction was associated with an influx of leukocytes from the periphery, and an increase in mRNA encoding the relevant chemokine receptors. Therefore, chemokine induction in the brain following daily systemic LPS injections may mediate the recruitment of leukocytes from the periphery.

The transcriptional response in the brain following systemic LPS challenge is indicative of a peripherally triggered inflammatory response in the brain. The data described in this thesis highlight a potential mechanism of gene modulation in the brain which may be dependent on a TLR-induced type I interferon response. Considerable evidence links type I interferons to psychiatric disorders, and consequently, interferon production in the brain could represent an important mechanism linking peripheral TLR-induced inflammation with behavioural changes. In addition, the data described in this thesis demonstrate that chronic exposure to LPS in the periphery may remotely modulate the recruitment of leukocytes to the brain. This highlights a potential protective mechanism that could prevent a chronic bacterial infection from spreading from the periphery to the brain.

Table of Contents

Abstract.....	1
Table of Contents.....	3
List of Tables	7
List of Figures	8
Author's declaration	11
Acknowledgments	12
List of abbreviations	14
1 Introduction	18
1.1 The Immune Response	19
1.1.1 Innate Immunity	20
1.1.2 Adaptive Immunity	24
1.1.3 Cytokines: an intercellular communication system	26
1.1.4 Inflammatory cytokines	26
1.1.5 Interferons.....	27
1.1.6 Chemokines	30
1.2 Immune Components of the CNS	38
1.2.1 Innate components.....	39
1.2.2 Adaptive components in the CNS	43
1.3 Chemokines in the CNS	48
1.3.1 Chemokines in CNS disorders	49
1.3.2 Chemokines in CNS homeostasis	57
1.4 Peripheral inflammation and behaviour	60
1.4.1 Evidence of inflammation-induced behavioural changes	61
1.4.2 Routes of immune-to-brain communication.....	65
1.4.3 Mechanisms of cytokine-induced behavioural changes	74
1.5 Thesis aims	84
2 Materials & Methods	86
2.1 General Reagents & Buffers	87
2.1.1 Materials & Reagents	87
2.1.2 Buffers	87
2.2 <i>In Vivo</i> Procedures.....	87
2.2.1 Animal welfare.....	87
2.2.2 Mice	88
2.2.3 Induction of systemic inflammation using LPS.....	88
2.2.4 Induction of systemic inflammation using TNF α	88
2.2.5 Induction of systemic inflammation using LTA	89
2.3 <i>Ex Vivo</i> Procedures	89
2.3.1 Perfusion.....	89
2.3.2 Brain dissection.....	89
2.3.3 Preparation of brain samples for histological analysis	89
2.3.4 Preparation of brain samples for gene expression analysis.....	90
2.3.5 Isolation of plasma from peripheral blood	90
2.3.6 Isolation of leukocytes from peripheral blood	91
2.3.7 Isolation of bone marrow	91
2.3.8 Generation of single-cell suspension from brain digests	92
2.4 Human Primary Cell Procedures.....	92

2.4.1	Patients & clinical samples	92
2.4.2	Isolation of mononuclear cells from peripheral blood.....	92
2.5	Gene Expression Analysis.....	93
2.5.1	RNA purification	93
2.5.2	Assessment of RNA integrity	95
2.5.3	Microarrays	96
2.5.4	Microarray analysis.....	97
2.5.5	cDNA Synthesis.....	98
2.5.6	Polymerase chain reactions.....	101
2.5.7	Quantitative real-time PCR	102
2.5.8	TaqMan low density array.....	108
2.5.9	RNA amplification	110
2.6	Protein Analysis.....	112
2.6.1	ELISA	112
2.6.2	Flow Cytometry.....	112
2.6.3	Histology.....	113
3	Transcriptional profiling of CNS following systemic inflammation	115
3.1	Introduction and aims.....	116
3.2	Acute model of systemic LPS-induced inflammation	117
3.2.1	Model validation	117
3.2.2	Processing of RNA samples.....	119
3.3	Determining how systemic LPS injection affects the transcriptional profile of the brain	121
3.3.1	Pre-processing of Affymetrix chip data using Partek	122
3.3.2	Gene expression analysis of Affymetrix chips using Partek.....	127
3.3.3	Gene ontology clustering.....	133
3.3.4	Ingenuity Pathway Analysis	134
3.3.5	Re-analysing the Affymetrix data using GeneSpring	139
3.3.6	Analysis of Affymetrix data using GeneSpring	140
3.3.7	Defining the genes commonly identified by both Partek and GeneSpring	145
3.4	QPCR analysis of target genes in the brain, blood and BM of LPS challenged mice.....	149
3.4.1	Validation of differential gene expression using QPCR.....	149
3.4.2	Comparison of central response to peripheral response	150
3.4.3	Determining kinetics of ISGs expression in the brain	156
3.5	Discussion and conclusions.....	157
4	Defining mechanisms of target gene induction in the CNS following systemic LPS challenge	163
4.1	Introduction and aims.....	164
4.2	Target gene expression following systemic cytokine-induced inflammation	167
4.2.1	Model validation	167
4.2.2	Target gene modulation in the brain, PBL and BM following systemic TNF α injection	169
4.3	Temporal target gene expression in PBL and brain following repeated LPS challenge	174
4.3.1	Model validation	174
4.3.2	Comparing cytokine induction in the brain and PBL during endotoxin tolerance	177
4.3.3	Comparing target gene induction in the brain.....	178
4.3.4	Type I IFN induction in the brain	181

4.4	Target gene expression following TLR2-induced MyD88 activation.....	182
4.4.1	Determining how systemic LTA challenge affects target gene expression in the brain, PBL and BM	182
4.4.2	Detecting peripheral inflammation following LTA injection.....	188
4.5	Discussion and conclusions.....	190
5	Characterising the chemokine repertoire and leukocyte infiltrate present in the brains of LPS-challenged mice	196
5.1	Introduction and aims.....	197
5.2	Regulation of chemokine and chemokine receptor transcripts following repeated systemic LPS injections.....	198
5.2.1	Chemokine transcripts are induced in the brain following multiple systemic LPS challenges	198
5.2.2	Chemokines are differentially regulated in the brain and PBL.....	202
5.2.3	Chemokine receptor transcripts are differentially induced in the brain and PBL	203
5.3	Leukocytes infiltrate the brain in response to chronic systemic LPS exposure	204
5.3.1	CD45 ^{hi} cells are increased in the brain following multiple systemic LPS challenges	205
5.3.2	Proportions of microglial cells varied following two doses of LPS..	208
5.3.3	CD11b ⁺ leukocytes infiltrate the brain following multiple systemic LPS challenges	210
5.3.4	CD3 ⁺ cell populations infiltrate the brain following multiple systemic LPS challenges	214
5.4	Identification of infiltrating leukocyte populations in the brain using histology.....	218
5.4.1	Neutrophil accumulation in the brain.....	218
5.4.2	CD3 ⁺ leukocyte accumulation in the brain	222
5.4.3	Monocyte accumulation in the brain	224
5.5	Discussion and conclusions.....	227
6	Defining the chemokine receptor profile of CNS-derived pathogenic leukocytes.....	234
6.1	Introduction and aims.....	235
6.2	Optimising RNA extraction and cDNA synthesis protocols.....	237
6.2.1	RNA extraction optimisation.....	237
6.2.2	cDNA synthesis optimization.....	241
6.3	Developing a protocol to amplify RNA from low cell numbers	243
6.3.1	Testing the efficiency of the RNA amplification kit using control HeLa cell RNA.....	243
6.3.2	Testing the limitations of the IVT kit using different starting quantities of template RNA.....	244
6.3.3	Testing the limitations of the IVT kit using PBMCs.....	245
6.3.4	Determining the transcriptional fidelity of aRNA	246
6.3.5	Determining the integrity of aRNA generated from different starting quantities of template RNA.....	248
6.3.6	Determining the integrity of aRNA generated from PBMCs	251
6.4	Discussion and conclusions.....	253
7	General Discussion	257
7.1	Introduction	258
7.2	Characterisation of the transcriptional profile in the brains of systemic LPS-challenged mice.....	259

7.3	Characterising the chemokine profile and leukocyte infiltrate in the brains of LPS-treated mice	264
7.3.1	Potential brain-specific effects of chemokine induction in the inflamed brain	267
7.4	Overview and hypotheses	270
7.5	Conclusions	274
7.6	Future directions	275
	References	277

List of Tables

Table 1.1 Chemokine receptors and their specific ligands.	32
Table 2.1 QPCR primer sequences	104
Table 2.2 Standard primer sequences	105
Table 2.3 Fluorescently-conjugated antibodies used for flow cytometry	113
Table 2.4 Primary antibodies used for immunohistochemistry.	114
Table 3.1 Integrity of RNA samples	121
Table 3.2 Differentially expressed entities identified using Partek	132
Table 3.3 Differentially expressed entities identified using GeneSpring	145
Table 3.4 Functional properties of differentially expressed genes, common to both Table 3.2 and Table 3.3.	147
Table 3.5 List of target genes upregulated specifically in the brain	151
Table 6.1 Yield of control amplifications from HeLa RNA.....	244

List of Figures

Figure 1.1 IFN receptor signalling pathways.....	30
Figure 1.2 Conserved Structures of the Four Chemokine Families.	31
Figure 1.3 Leukocyte recruitment to tissues.	35
Figure 1.4 The kynurenine pathway.	81
Figure 3.1 Plasma concentration of inflammatory cytokines following systemic LPS injection.....	118
Figure 3.2 Quality of RNA samples and efficiency of DNA fragmentation.....	120
Figure 3.3 Signal histogram of normalised intensity values	125
Figure 3.4 Principle component analysis of microarray samples	127
Figure 3.5 Top 10 enriched biological annotations.	134
Figure 3.6 Top 10 significantly altered biological pathways.	135
Figure 3.7 The Leukocyte extravasation signalling pathway	137
Figure 3.8 The Activation of IRF by cytosolic pattern recognition receptors signalling pathway	138
Figure 3.9 The Interferon signalling pathway	139
Figure 3.10 Normalised intensity values of individual entities.	142
Figure 3.11 Heatmap of the signal intensity of individual entities relative to baseline	143
Figure 3.12 Differentially expressed entities identified using Partek and GeneSpring.....	146
Figure 3.13 Interferon subtype analysis of ISGs induced in the brain	148
Figure 3.14 Differential ISG expression in the brain, PBL and BM of LPS-treated mice compared to vehicle control group.....	153
Figure 3.15 Differential expression of acute phase response genes in the brain, PBL and BM of LPS-treated mice compared to vehicle control group.	154
Figure 3.16 Differential expression of remaining target genes in the brain, PBL and BM of LPS-treated mice compared to vehicle control group.....	155
Figure 3.17 Temporal expression of ISGs in the brains of LPS-injected mice ...	156
Figure 4.1 TLR-induced signalling pathways.....	166
Figure 4.2 Plasma concentration of inflammatory cytokines following systemic TNF α injection	168
Figure 4.3 Differential expression of ISGs in the brain, PBL and BM of TNF-treated mice compared to vehicle control group.....	171
Figure 4.4 Differential expression of acute phase response genes in the brain, PBL and BM of TNF α -injected mice compared to vehicle control group.	172
Figure 4.5 Differential expression of remaining target genes in the brain, PBL and BM of TNF α -injected mice compared to vehicle control group.	173

Figure 4.6 Plasma concentration of inflammatory cytokines following acute LPS challenge and during endotoxin tolerance.....	176
Figure 4.7 Cytokine expression in the brain and in the PBL during endotoxin tolerance.....	178
Figure 4.8 Temporal gene expression in the brain and PBL of mice following repeated LPS injections.....	180
Figure 4.9 Temporal expression of type I IFNs in the brains of mice following repeated LPS injections.....	181
Figure 4.10 Differential expression of ISGs in the brain, PBL and BM of LTA-challenged mice compared to vehicle control group.....	185
Figure 4.11 Differential expression of acute phase response genes in the brain, PBL and BM of LTA-challenged mice compared to vehicle control group.....	186
Figure 4.12 Differential expression of remaining target genes in the brain, PBL and BM of LTA-challenged mice compared to vehicle control group.....	187
Figure 4.13 Plasma concentration of inflammatory cytokines following systemic LTA injection	189
Figure 5.1 Temporal expression of inflammatory chemokines in the brains of mice following repeated LPS injections.....	199
Figure 5.2 Temporal expression of CC chemokine and chemokine receptor in the brain and PBL of mice following repeated LPS injections.....	201
Figure 5.3 Temporal expression of CXC chemokine and chemokine receptor in the brain and PBL of mice following repeated LPS injections.....	202
Figure 5.4 Gating on live, single cells in the brain and PBL.....	205
Figure 5.5 Proportions of CD45 ^{hi} cells in the brains of LPS and vehicle-challenged mice.....	207
Figure 5.6 Variations in microglial cell numbers.....	209
Figure 5.7 Characterisation and quantification of CD11b ⁺ leukocyte populations in the brains of LPS-challenged mice	211
Figure 5.8 Characterisation and quantification of CD11b ⁺ leukocyte populations in the peripheral blood of LPS-challenged mice	213
Figure 5.9 Characterisation and quantification of CD3 ⁺ leukocyte populations in the brains of LPS-challenged mice	215
Figure 5.10 Characterisation and quantification of CD3 ⁺ leukocyte populations in the peripheral blood of LPS-challenged mice	217
Figure 5.11 Accumulation of neutrophils in the brain over time.....	220
Figure 5.12 Relative neutrophil numbers in the brains of LPS-treated mice compared to naïve control mice	221
Figure 5.13 Accumulation of T cells in the brain over time.....	223
Figure 5.14 Relative T cell numbers in the brains of LPS-treated mice compared to naïve control mice	224
Figure 5.15 Detection of monocytes/macrophages in the brain over time.....	226
Figure 6.1 Comparison of different methods of RNA extraction.....	239

Figure 6.2 Integrity of RNA samples extracted from 1×10^3 , 1×10^4 and 1×10^5 PBMCs	241
Figure 6.3 Comparison of High Capacity and SuperScript™ III reverse transcription kits.....	242
Figure 6.4 Yield of aRNA from different starting quantities	245
Figure 6.5 Comparison of the transcriptional profile of template RNA and aRNA	247
Figure 6.6 Integrity of RNA before and after amplification from different RNA starting quantities	250
Figure 6.7 Integrity of RNA before and after amplification from different numbers of cells	252
Figure 7.1 <i>Ifnar1</i> expression in the mouse brain.....	262
Figure 7.2 Response in the brain to a single systemic LPS injection: Observations and hypotheses.....	271
Figure 7.3 Response in the brain to daily systemic LPS injections: Observations and hypotheses.....	273

Author's declaration

I declare that the work described in this thesis is original and was generated entirely as a result of my own efforts. None of the data, submitted as part of this thesis, has been submitted for any other degree, either at the University of Glasgow, or at any other institution.

Signature:

Printed name: Carolyn Thomson

Acknowledgments

First of all I would like to say an enormous thank you to my supervisors, Dr Jonathan Cavanagh and Prof Gerry Graham, for all the support, help and guidance they have given me throughout my PhD. Gerry, I would have struggled to get through my PhD had you not let me defect to your lab group. Jonathan, thank you for all the encouragement you have given me over the years. You have had to put up with me through all sorts of emotional states and I'm sure this would have caused you to fire me a long time ago if you hadn't been such an excellent psychiatrist. I'm glad you didn't!

Although there are far too many of you to mention, I'd like to thank everyone in the GBRC who has given me support, or helped me in the lab, since I started my PhD. I have thoroughly enjoyed working in the Chemokine Research Group and every member of this group, past and present, has helped me in some form throughout my PhD. Special mentions go to Derek Gilchrist for all his help in the beginning of my project, Daniela Michlmayr for her help with IHC, and Clive McKimmie, Mairi Clarke and Alasdair Fraser for giving me various pieces of advice throughout my PhD. Also, special thanks to Chris Hansell and Vuk Cerovic, for each reading a chapter of my thesis. And to Michelle Le Brocq and Fabian Shütte, for always knowing when it's time for beer. In particular, I'd like to say a massive thank you to Darren Asquith and Alison McColl. I don't know how I would have made it through the last few years if it hadn't been for the two of you and, although I hide it well behind a lot of friendly abuse, I am incredibly grateful to you both. Darren, not only did you read over my paper, and a decent chunk of my thesis, but you have been stuck answering my relentless science questions for the last four years (sorry). Alison, you have been a great friend and tremendous support since you started in the lab. Thanks for always being there to help me out, or cheer me up. I will definitely miss our ELISA days.

I'd like to thank my assessors, Prof Rob Nibbs and Prof Hugh Willison. Rob, you have given me tons of advice and guidance over the last few years and you're (occasionally brutal) honesty is something that I have always appreciated. In addition, for many reasons, I am extremely grateful to Prof Allan Mowat. Big Al, thanks for giving me advice, reading my thesis and allowing me to vent in your office. Also, thanks for taking pity on me and occasionally driving me to work in

the rain. I'm sorry if I tend to show my appreciation by being infuriatingly cheeky. I'd also like to thank Rajeev Krishnadas and Simon Milling. Rajeev, thanks for your endless wisdom. Simon thanks for putting up with all my annoying science questions over the past couple of months. Hopefully these will subside now that I have submitted (but no promises)...

In addition to the vast amount of support and friendship I have received from everyone in the lab, I have also had an incredible amount of moral support from all of my friends. Massive thanks to Felix and Pam. It has always been a comfort to know that we've all been in this together. Special thanks go to team 'AT GANI', thanks for all the climbing, camping, snowboarding and drinking adventures along the way, especially those involving Alpine play parks. Special thanks go to Karen, Jo, Sonia, Lindsay and Dave. You have always been there for me, no matter what, and I couldn't ask for better friends. To Mark, I won't subject you to anything cheesy, but thanks for being such an excellent [insert appropriate insult here]. In particular though, I'd like to say a huge thank you to Brian. You know fine well that you've been a great mate over the years so I won't get sappy with you either. That's not what we're about. All I will say is that it takes a true friend to call your mum a *****.

For his charming cheek and ridiculous banter, I'd also especially like to thank my Pete (The Hat). Pete, thank you for all your counselling and support. Also, thank you for putting up with me over the last few months of thesis writing and (most importantly) for bringing me cheese and beer. I love you.

Finally, I would not have gotten anywhere if it hadn't been for my family. My wonderful parents have given me unwavering love and support (both moral and financial) throughout my entire existence, and believe me; this has not always been deserved! You are both such incredibly smart people and the best role models I could ever have asked for. Also, I'd like to thank my brother Ewan and his lovely fiancée Jo. You are both such a huge support and wonderful friends into the bargain. Thank you for being there.

List of abbreviations

A		DAVID	Database for annotation, visualisation and integrated discovery
ACTH	Adrenocorticotrophic hormone		
APC	Antigen presenting cell	DC	Dendritic cell
aRNA	Amplified ribonucleic acid	dH ₂ O	Distilled water
		DNA	Deoxyribonucleic acid
B		E	
BBB	Blood brain barrier	EAE	Experimental autoimmune encephalomyelitis
BCSFB	Blood cerebrospinal fluid barrier	EDTA	Ethylenediaminetetraacetic acid
BDNF	Brain-derived neurotrophic factor	ELISA	Enzyme-linked immunosorbent assay
BCSFB	Blood spinal cord barrier	ERK	Extracellular signal-regulated kinase
BM	Bone marrow	EtOH	Ethanol
C		F	
Ca ²⁺	Calcium	FU	Fluorescence units
CAM	Cellular adhesion molecule	G	
cDNA	Complementary deoxyribonucleic acid	GABA	γ-aminobutyric acid
CNS	Central nervous system	GAF	IFNγ-activated factor
COX	Cyclooxygenase	GAPDH	Glyceraldehyde 3-phosphate
CRF	Corticotrophin releasing factor	GAS	IFNγ-activated site
cRNA	Carrier ribonucleic acid	gDNA	Genomic deoxyribonucleic acid
CSF	Cerebrospinal fluid	GFP	Green fluorescent protein
CT	Cycle threshold	GO	Gene ontology
CVO	Circumventricular organ	GPCR	G protein-coupled receptor
D			
DAMP	Damage-associated molecular pattern		
DAT	Dopamine transporter		

GR	Glucocorticoid receptor	KYN	Kynurenine
H		L	
HPA	Hypothalamic-pituitary-adrenal	LN	Lymph node
		LPS	Lipopolysaccharide
I		LTA	Lipoteichoic acid
ICAM	Intracellular adhesion molecule	M	
IDO	Indoleamine 2,3 dioxygenase	M1	Classically-activated macrophages
IFN	Interferon	M2	Alternatively activated macrophages
IFNAR	Interferon- α/β receptor	MadCAM	Mucosal addressin cellular adhesion
IFNGR	Interferon- γ receptor		
IFNLR	Interferon- λ receptor	MAPK	Mitogen-activated protein kinase
IL	Interleukin	MHC	Major histocompatibility complex
IL-1R	IL-1 receptor	MHV	Mouse hepatitis virus
IL-1ra	IL-1 receptor antagonist		
iNOS	Inducible nitric oxide	mPGES	Microsomal prostaglandin E synthase
IP	Intraperitoneal	MPO	Myeloperoxidase
IPA	Ingenuity pathway analysis	mRNA	Message ribonucleic acid
IRF	Interferon regulatory factor	MS	Multiple sclerosis
ISG	Interferon stimulated gene	MTC	Multiple testing correction
ISGF	IFN-stimulated gene factor		
ISRE	IFN-stimulated response element	N	
I.V.	Intravenous	NADPH	Nicotinamide adenine dinucleotide phosphate
IVT	<i>In vitro</i> transcription	NET	Neutrophil extracellular traps
J		NK	Natural killer
JAK	Janus activated kinase	NLR	Nod-like receptors
K		NMDA	N-methyl-D-aspartate
KA	Kynurenic acid	NO	Nitric oxide

		RMA	Robust multichip average	
O				
	OAS	2',5' oligoadenylate	RLR	Rig-like receptors
	OVA	Ovalbumin	RNA	Ribonucleic acid
			ROS	Reactive oxygen species
P			RQ	Relative quantification
	PAMP	Pathogen associated molecular pattern	RT	Reverse transcriptase
	PBL	Peripheral blood leukocytes	RTE	Relative transcript expression
	PBMC	Peripheral blood mononuclear cell	S	
	PBS	Phosphate buffered saline	SEM	Standard error of the mean
	PC	Principle components	SERT	Serotonin transporter
	PCA	Principle component analysis	SSRI	Selective serotonin reuptake inhibitor
	PCR	Polymerase chain reaction	STAT	Signal transducer and activator of transcription
	PGE ₂	Prostaglandin E ₂	T	
	PGES	Prostaglandin E synthase	TAE	Tris-acetate EDTA
	PM	Perfect match	TBP	TATA binding protein
	Poly(I:C)	Polyinosinic: polycytidylic acid	T _{CM}	Central memory T cell
	PSGL	P-selectin glycoprotein ligand	TE	Tris-EDTA
	PRR	Pattern recognition receptor	Treg	T regulatory cell
	PVM	Perivascular macrophage	T _{EM}	Effector memory T cell
	PVN	Paraventricular nucleus	Th	T helper
			TLDA	TaqMan low density arrays
			TLR	Toll-like receptor
			TNF α	Tumour necrosis factor
Q			TNFR	Tumour necrosis factor
	QPCR	Quantitative polymerase chain reaction	tRNA	Transfer ribonucleic acid
	QUIN	Quinolinic acid		
R				
	RIN	RNA integrity number		

V

VCAM Vascular-associated
adhesion molecule

W

WNV West-Nile virus

1 Introduction

1.1 The Immune Response

Our bodies are constantly under threat from a multitude of opportunistic microorganisms which occupy every square inch of our environment, our skin and our mucosal surfaces. Fortunately, we are shielded from this potentially pathogenic environment by physical epithelial barriers. However, these barriers can be breached and consequently our bodies must be armed with effective counter-defence strategies in order to rapidly deter invading pathogens and heal damage so that we don't succumb to infection. To this end, the immune system acts as our internal armed forces. Fortified with an arsenal of inflammatory mediators and anti-microbial agents, it is well equipped to combat the vast majority of threats it encounters in a lifetime. It is constantly vigilant. Some leukocyte populations act as sentinels, continuously surveying the extracellular environment for any signals alluding to danger. Others act as scouts, circulating between lymphoid organs in their search for foreign antigen. Upon detection of damage or pathogenic invasion, waves of leukocytes are rapidly recruited to the site of injury whilst reinforcements are deployed from the bone marrow. The first battalion of leukocytes that arrive at an inflamed site are those affiliated with the innate immune system. The innate immune system constitutes the immediate and non-specific arm of the immune response. During an infectious insult, whilst it battles to control the spread of pathogens, an antigen-specific adaptive response is primed in nearby lymph nodes (LNs). Not only do leukocytes of the adaptive immune system act as reinforcements in the attack against pathogens but they generate immunological memory which protects the host from subsequent infections of the same nature. The immune system is intricate, dynamic and extremely well coordinated. A complex interplay exists between the innate and adaptive arms of the immune response, and the antigen-specific host-defence mechanisms, utilized by the adaptive immune system, very much complement the highly specialised effector functions of the innate immune response. Innate and adaptive immunity will now be discussed in more detail, with particular emphasis on some of the key effector mechanisms adopted by both systems to provide host protection.

1.1.1 Innate Immunity

Activation of the innate immune system is promptly triggered with the generic release of a multitude of inflammatory signalling molecules following any physical or pathogenic insult to the body. However, in order to execute an appropriate counter-offensive, the innate immune system must first recognise when it is injured or under attack. To this end, the innate immune system has evolved a myriad of cellular receptors which enable it to recognise different pathogenic components, termed pathogen-associated molecular patterns (PAMPs), or endogenous molecules that are associated with cell death or injury, termed damage-associated molecular patterns (DAMPs). These receptors, referred to as pattern-recognition receptors (PRRs), are highly specific for different molecular patterns from different sources. They therefore allow immune cells to tailor their effector responses according to different types of infection or injury. The best characterised of the PRRs are the members of the Toll-like receptor (TLR) family which reside within cellular membranes. TLRs can therefore recognise PAMPs or DAMPs that are present in either the extracellular environment or within membrane-bound vesicles. Humans and mice have 10 and 13 functioning TLRs respectively¹. Although TLRs 1-9 each have a distinct specificity, the ligands for human TLR10 and murine TLRs 11-13 have yet to be defined. TLR ligation triggers an intracellular signalling cascade which culminates in the transcription of numerous genes encoding relevant inflammatory mediators such as cytokines and chemokines¹. Complementing the action of TLRs, Nod-like receptors (NLRs) reside within the cytoplasm where they are strategically positioned to recognise intracellular PAMPs and DAMPs and, depending on the receptor, generate an appropriate transcriptional response or activate the inflammasome^{1,2}. Activation of the inflammasome contributes to the inflammatory response by cleaving certain cytokines, including IL-1 β ; transforming them to an active state. Like NLRs, Rig-like receptors (RLRs) also reside in the cytoplasm. This family of PRRs predominantly recognise virally-derived PAMPs and therefore their ligation is typically associated with the induction of anti-viral mediators such as interferons (IFNs)^{1,2}. The broad-spectrum release of inflammatory mediators that occurs as a result of PRR ligation is one of the initiating steps in a cascade of events which shapes innate and adaptive immune responses and triggers the four cardinal features of acute inflammation; heat, redness, swelling and pain.

Amongst their various actions, inflammatory mediators induce activation and vasodilation of nearby blood vessels³. Not only does this increase blood flow to the site of injury, but activated endothelial cells upregulate cellular adhesion molecules which facilitate interactions between circulating leukocytes and the endothelium. Activation of the vasculature also stimulates the release of clotting factors and platelet aggregation which, depending on the nature of the injury, can either minimise blood loss or prevent the spread of pathogens to the blood stream³. The induction of an acute inflammatory insult promptly triggers a wave of innate leukocyte populations to infiltrate and accumulate within the inflamed site³. Leukocyte infiltration is initiated, coordinated and maintained by inflammatory mediators such as cytokines (Section 1.1.4) and chemokines (Section 1.1.6). Inflammatory mediators also play a role in blood vessel dilation³. Within dilated blood vessels, although blood flow increases, its velocity decreases. This leads to an increased number of leukocytes passing slowly through the inflamed vasculature and is therefore the cause of two of the classical features of acute inflammation; redness and heat³. Interactions between chemokines and their receptors enable leukocytes to adhere to activated endothelial cells and extravasate from the blood to the inflamed tissue (Section 1.1.6). During acute inflammatory responses, the permeability of the vasculature increases resulting in swelling, or oedema³. In addition to permitting the ingress of protective plasma proteins from the circulation, this expedites the infiltration of leukocytes. Neutrophils, a short-lived population of innate granulocytes, are the first leukocytes to arrive on the scene³. Due to their multifaceted approach to host defence, neutrophils play a pivotal role in acute inflammatory responses. They have numerous strategies for clearing pathogens from an infected site. Not only are they skilled at phagocytosis, but they are armed with a battery of cytokines, chemokines and highly-reactive anti-microbial peptides contained within intracellular granules⁴. These granules are rapidly deployed to the plasma membrane and their contents released following neutrophil activation. Within the cell, phagosomes containing engulfed microorganisms fuse with granules to form phagolysosomes⁵. This triggers the formation of the nicotinamide adenine dinucleotide phosphate (NADPH) oxidase enzyme complex, subsequently generating reactive oxygen species (ROS) within phagolysosomes⁵. Pathogens are therefore exposed to anti-microbial agents within a highly-oxidative environment which culminates in their inactivation and

their subsequent death. When activated, neutrophils can also rapidly release ROS into the extracellular environment⁶. Although this can contribute to pathogen clearance, it may also lead to bystander tissue damage and therefore amplify local inflammation. Moreover, neutrophils release structures known as neutrophil extracellular traps (NETs)⁵. Composed of a web-like complex of nuclear components and anti-microbial granular proteins, these NETs trap, neutralise and destroy extracellular microorganisms. Neutrophils can also be activated to produce a number of inflammatory cytokines and chemokines which amplify local inflammatory responses and promote further leukocyte infiltration, particularly the infiltration of 'inflammatory' monocytes⁷ (Section 1.1.6.2). Once in the tissue, monocytes rapidly differentiate into macrophages and monocyte-derived dendritic cells (DCs). Therefore, not only are neutrophil effector functions important for pathogen clearance, but they drive the immune response forward by attracting macrophages and monocyte-derived DCs to the site.

Like neutrophils, macrophages are proficient phagocytes. During steady state conditions, their basal duty is to clear cell debris, erythrocytes and apoptotic cells⁸. This they do efficiently. However, macrophages are equipped with a whole spectrum of PRRs² which makes them one of the primary sensors of pathogenic insults or mechanical injuries to the host. Macrophages are a highly plastic population of leukocytes. Upon recognition of danger signals, they rapidly change morphology and differentiate into classically-activated (M1) macrophages⁸. By secreting an abundance of cytokines, chemokines and inflammatory agents, these can both contribute to innate host defence and shape adaptive immune responses. One of the main characteristics of M1 macrophages is their ability to activate NADPH oxidase and to produce the inducible form of nitric oxide synthase (iNOS)⁹. These result in the synthesis of ROS and nitric oxide (NO), which both play an integral role in host defence, allowing M1 macrophages to mount an effective antimicrobial defence. ROS and NO can function within the cell, to combat intracellular pathogens, or may be released into the extracellular environment along with other microbicidal agents that contribute to host defence¹⁰. During the resolution of inflammatory responses, macrophages differentiate into alternatively activated macrophages and contribute to wound healing and suppression of the inflammatory milieu⁸.

As DCs can also phagocytose microbes and produce inflammatory cytokines, they too contribute to innate immune responses. However DCs are best known for their key role in transporting antigen to the lymph nodes (LNs) where they can present it to naïve lymphocytes in order to prime and shape adaptive immune responses (Section 1.1.2). Another cell population that plays a role in innate immune responses are natural killer (NK) cells. NK cells are rapidly recruited to sites of inflammation where they become activated by inflammatory cytokines and other danger signals¹¹. During infection they live up to their name by targeting and killing infected cells. Furthermore they produce inflammatory cytokines that enhance the microbicidal actions of macrophages⁸. Therefore, a number of innate effector cells are sequentially recruited to sites of infection or injury. Via a complex interplay, these cell populations cooperate in the induction, maintenance and resolution of inflammatory responses and in the clearance of invading pathogens. In addition, a number of these innate leukocytes contribute to inducing and shaping the appropriate adaptive immune response (Section 1.1.2).

Amongst the repertoire of inflammatory agents that are produced during acute inflammatory responses are complement components and lipid mediators such as prostaglandins. The complement system is integrally involved in host defence. Complement components bind to pathogenic or apoptotic cell surfaces to trigger a cascade of proteolytic events which ultimately lead to opsonisation of their targets¹². Opsonised cells or pathogens can be readily cleared from the environment by phagocytosis. Prostaglandins are immune modulators which are involved both in the induction phase and in the resolution phase of immune responses¹³. They can be rapidly synthesised from membrane-released arachidonic acid by a number of cell types following a pathogenic insult or trauma. This requires the sequential induction of cyclooxygenase (COX) enzymes followed by prostaglandin synthases¹³. Prostaglandins have a diverse range of functions. They contribute to the inflammatory response by promoting vasodilation, vascular permeability and subsequent oedema¹⁴. In addition, prostaglandins play a role in inducing fever (Section 1.4.2.2) and pain¹⁵, one of the cardinal features of inflammation. During the course of an inflammatory response, prostaglandins gradually induce the expression of anti-inflammatory lipid mediators which promote the resolution of inflammation¹⁶.

Inflammation also leads to systemic effects that contribute to host defence. Inflammatory chemokines can recruit mature leukocytes from the bone marrow thus increasing their numbers in the circulation^{17,18}. In addition, an acute phase response is stimulated in the liver. A vast number of acute phase proteins can be secreted from the liver into the circulation¹⁹. These have an assortment of functions which collectively promote host defence. Acute phase proteins include: opsonins, such as C-reactive protein, serum amyloid A and various complement components; coagulation factors, such as fibrinogen and von Willebrand factor; and factors such as ferritin and transferrin, which sequester free iron¹⁹. In summary, following a pathogenic insult or mechanical trauma, the concerted action of a host of inflammatory mediators, innate leukocytes and antimicrobial peptides function both locally and systemically to aid host defence.

1.1.2 Adaptive Immunity

Adaptive immunity is a lymphocyte-dependent antigen-specific response to invading pathogens. Antigen uptake in the presence of danger signals causes tissue-resident DCs to alter their surface marker expression and migrate through lymphatic vessels to the draining LNs³. Free antigen can also travel to draining LNs through the lymphatics²⁰. It then filters through the subcapsular sinus and, depending on its size, into the LN conduit system. In the T cell zones of LNs, small antigen is continuously sampled from conduits by LN-resident DCs²⁰. To initiate adaptive immune responses, mature antigen-loaded DCs must first present their antigen to T cells and provide the relevant signals required for T cell priming^{3,21}. Once they encounter DCs bearing their cognate antigen, T cells undergo clonal expansion and differentiate into an assortment of effector T cells, memory T cells and follicular helper cells. Effector T cells promptly migrate to the site of infection to carry out their appropriate host-defence functions, whereas follicular helper cells remain in the LN and travel to the follicle/T cell zone boundary to prime antigen-specific B cell responses²². Simultaneously, within the follicles of the LN, B cells can acquire certain kinds of antigen from a specialised population of subcapsular sinus macrophages which scavenge particulate antigen from the lymph^{23,24}. Following specific antigen uptake, B cells migrate towards the T cell zones and present antigen to follicular helper cells²⁵. Only when an antigen-experienced T cell encounters its cognate

antigen on the B cell surface will full B cell priming occur. Primed B cells then clonally expand, differentiating into memory B cells or antibody-secreting plasma cells, which migrate to the spleen and bone marrow and secrete large amounts of antibodies into the circulation.

The effector T cell population that is generated during an adaptive immune response is diverse. Depending on the cytokine repertoire present during T cell priming, effector CD4⁺ T cells can adopt one of a variety of possible phenotypes. For example, Th1 cells, primed in response to interleukin (IL)-12, produce vast amounts of IFN γ and contribute to the immune response against intracellular bacterial infection²⁶, whereas Th2 cells, primed in response to IL-4, produce IL-4, IL-5 and IL-13 and contribute to the host-response against helminths²⁶. In addition to these well characterised CD4⁺ T cell populations are Th9 cells, Th17 cells and Th22 cells²⁷. Whilst Th17 cells have been associated with the immune response against extracellular pathogens, such as bacteria and fungi, both Th9 cells and Th22 cells are newly described and any roles these cell populations might have, outside a general contribution to tissue inflammation, have yet to be established²⁷. In contrast, the phenotypic outcome for a primed CD8⁺ T cell is less ambiguous. Once activated, CD8⁺ T cells transform into cytotoxic killing machines which target infected, cancerous or damaged cells for programmed cell death^{3,28}.

In addition to producing an antigen-specific effector response, the priming of adaptive immunity generates immunological memory. Following a primary exposure to antigen, the frequency of lymphocytes that are specific for this antigen increases dramatically. Although the majority of these lymphocytes are short-lived effector cells, a proportion of them, known as clonally expanded memory lymphocytes, can persist in the body for a lifetime²⁹. Different populations of memory lymphocytes include CD8⁺ memory T cells, CD4⁺ effector memory T cells (T_{EM}), CD4⁺ central memory T cells (T_{CM}) and memory B cells. Aside from T_{EM} cells, all of these memory cells express lymphoid tissue homing molecules, such as CCR7^{29,30} (Section 1.1.6.2). Like naïve lymphocytes, these cell populations circulate between secondary lymphoid organs scouting for antigen. However, during recall responses, they expand much more rapidly than naïve lymphocytes following an initial pathogen encounter³¹. In contrast, T_{EM} cells do not retain a lymphoid tissue homing phenotype. Instead they express

inflammatory chemokine receptors and integrins which enable them to rapidly infiltrate inflamed tissues²⁹. In addition to a faster response, memory lymphocytes respond to antigen with greater potency than naïve or effector lymphocytes³¹. Therefore due to their long lifespan, their enrichment in the circulation and their heightened ability to respond to pathogens, memory lymphocytes protect the host against subsequent infections with the same pathogen following an initial exposure.

1.1.3 Cytokines: an intercellular communication system

The cytokine superfamily encompasses a large number of small protein moieties which collectively provide a network of communication between virtually every cell type of the body. These cellular communication molecules have a highly diverse range of physiological functions. Amongst their multitude of roles in immune system communication, cytokines are critically involved in the organogenesis of secondary lymphoid organs, the induction and resolution of inflammation, the modulation of host defence mechanisms and the coordination of leukocyte migration (Section 1.1.6). As this thesis is exclusively focused on immune and nervous system responses during experimental inflammatory models, only the cytokines that are relevant to this work are discussed in more detail below. These include cytokines which have a role in modulating inflammation and host defence, such as IFNs and inflammatory cytokines, and chemokines, which coordinate leukocyte migration.

1.1.4 Inflammatory cytokines

'Inflammatory cytokines' is an umbrella term covering a range of inducible cytokines which are known to amplify inflammatory responses. Three prototypical inflammatory cytokines released early after infection or tissue damage are tumour necrosis factor- α (TNF α) and two members of the interleukin (IL) family, IL-1 β and IL-6. The release of these proteins is triggered following a physical or pathogenic insult to the body. By acting in an autocrine and paracrine manner, inflammatory cytokines stimulate a cascade of events leading to local inflammation. IL-1 β , IL-6 and TNF α share the capacity to induce activation, vasodilation and permeabilisation of nearby blood vessels³. This increases blood flow to the site of injury, contributes to the influx of plasma

proteins to the tissue and enhances the release of clotting factors from the endothelium³. In addition, inflammatory cytokines, particularly TNF α , are potent activators of tissue macrophages². By inducing further cytokine and NO production, this amplifies the local inflammatory response. Thus inflammatory cytokines are rapidly induced in response to tissue damage or pathogen detection. As part of a protective host response, these cytokines act locally to contribute to the four characteristic hallmarks of inflammation: heat, redness, swelling and pain.

IL-1 β , IL-6 and TNF α also function in an endocrine manner. Acting at sites distal to their production, these inflammatory cytokines trigger a number of systemic effects that augment the host response to infection. For example, they can stimulate the production of acute phase proteins from hepatocytes in the liver, thus contributing to the acute phase response³. Furthermore, inflammatory cytokines induce fever and a number of behavioural symptoms that are associated with sickness (Section 1.4.1). There are several ways in which fever can aid host defence. As some pathogens are thermosensitive, an increase in body temperature may help curtail their replication³². Furthermore, hyperthermia can enhance many metabolic processes involved in the effector mechanisms of both the innate and the adaptive immune response³²⁻³⁴. Inflammatory cytokine-induced behavioural changes, such as fatigue and social withdrawal, are also beneficial to the host as they promote energy conservation and reduce the risk of exposure to further dangerous stimuli³⁵. Therefore inflammatory cytokines, such as IL-1 β , IL-6 and TNF α , have a combination of local and systemic effects which ultimately promote leukocyte migration to the site of injury, aid pathogen clearance and prevent the spread of infection.

1.1.5 Interferons

First named for their ability to interfere with viral replication, IFNs comprise a panel of cytokines that are integrally involved in host defence. IFNs can bind to one of three types of IFN receptor and are therefore classified accordingly. Those that bind to the ubiquitously expressed IFN- α/β receptor (IFNAR) are termed type I IFNs. In mammals there are approximately 20 members of this IFN subfamily. These include, but are not limited to, various types of IFN α (13 in humans and 14 in mice) and usually a single IFN β . The recently discovered type

III IFNs engage the IFN λ receptor (IFNLR)³⁶. To date, there are 3 known members of this subfamily; IFN λ 1 (IL-29), IFN λ 2 (IL-28A) and IFN λ 3 (IL-28B)³⁷. Unlike the type I IFNAR, the type III IFN receptor is expressed predominantly by epithelial cells in certain tissues, such as the kidney and the brain³⁸. The only known type II IFN, IFN γ , binds to the widely distributed IFN γ receptor (IFNGR). Through similar signal transduction pathways, the ligation of these IFN receptors can induce the expression of thousands of IFN-stimulated genes (ISGs)³⁹ (Figure 1.1).

Up until relatively recently, the general dogma regarding type I and II IFN responses stated that ISGs induced by type I IFNs had a prominent role in combating viral infections, whereas those induced by type II IFNs were part of the host response against intracellular microbes. This view is supported by a battery of evidence to suggest that antiviral and antimicrobial responses are profoundly impaired in IFNAR- and IFN γ -deficient rodents respectively⁴⁰⁻⁴⁸. Furthermore, ISGs associated with type I IFNs often encode proteins with antiviral properties. For example, their induced protein repertoire includes a number of 2',5' oligoadenylate synthases (OAS), which block the spread of infections by degrading viral RNAs⁴⁹. They also induce members of the Mx family of GTPases, which suppress replication by inhibiting the intracellular transport of viral proteins (Reviewed in Ref 50). In contrast, type II ISGs often encode proteins with microbicidal properties, such as iNOS⁵¹, a crucial enzyme involved in the synthesis of NO. These reports confirm a pivotal role for type I and type II IFNs in mediating antiviral and antimicrobial responses respectively. Like type I IFNs, the type III IFN subfamily are also inducible following viral infections⁵². Although less is known about this particular IFN category, they have been shown to activate similar signalling pathways to type I IFNs^{36,52,53} (Figure 1.1), and thus induce a similar ISG expression profile. Furthermore, type III IFNs can modulate host responses to certain viral infections *in vivo*^{52,54}.

Taken together, the data above have led to the general view that type I and type III IFNs induce an antiviral immune response whereas type II IFNs mediate responses to intracellular bacteria. However, whilst this may be true, to distinguish IFN subfamilies purely based on these physiological functions is too simplistic. In fact, there is a considerable degree of overlap between the ISG repertoires that are induced by these different classes of IFNs³⁹. It is likely this is at least partially due to the ability of type I and type III IFNs to stimulate

transcription of type II ISGs⁵⁵ (Figure 1.1). The similar transcriptional profile shared by the three IFN subtypes, suggests that type I and/or type III IFNs may share some of the same physiological functions as the type II IFN subfamily. In support of this, type II IFNs are produced during certain viral infections. Studies using IFN γ -deficient mice have demonstrated the involvement of type II IFNs in modulating a proportion of antiviral responses^{43,56-58}. Furthermore, the induction of type I and type III IFNs has been described during a number of intracellular bacterial infections⁵⁹⁻⁶³. By suppressing bacterial growth or replication, type I IFNs appear to have a supportive role in host defence during a variety of intracellular microbial infections^{60,62-65}. However, the role of type I IFNs in antimicrobial immunity is not clear-cut. By suppressing the innate immune system and sensitising infected cells to bacterial-induced apoptosis, the production of type I IFNs can have a deleterious effect during certain other bacterial infections, such as *Listeria monocytogenes* and *Francisella tularensis*⁶⁶⁻⁶⁹. Due to the similarities in the signalling pathways utilized by both type I and type III IFNs, it could be predicted that type III IFNs also have similar complex roles in modulating specific antimicrobial responses. However, as this cytokine subfamily has only recently been described, their role in bacterial infection is yet to be established *in vivo*. In summary, these findings imply that it may be inaccurate to pigeonhole IFN subfamilies as being either antiviral or antimicrobial. IFNs of all categories are produced in response to a wide array of pathogenic stimuli and depending on the cell populations involved, or the nature of these stimuli, specific IFN subtypes might function cooperatively or individually to induce the relevant host defence mechanisms.

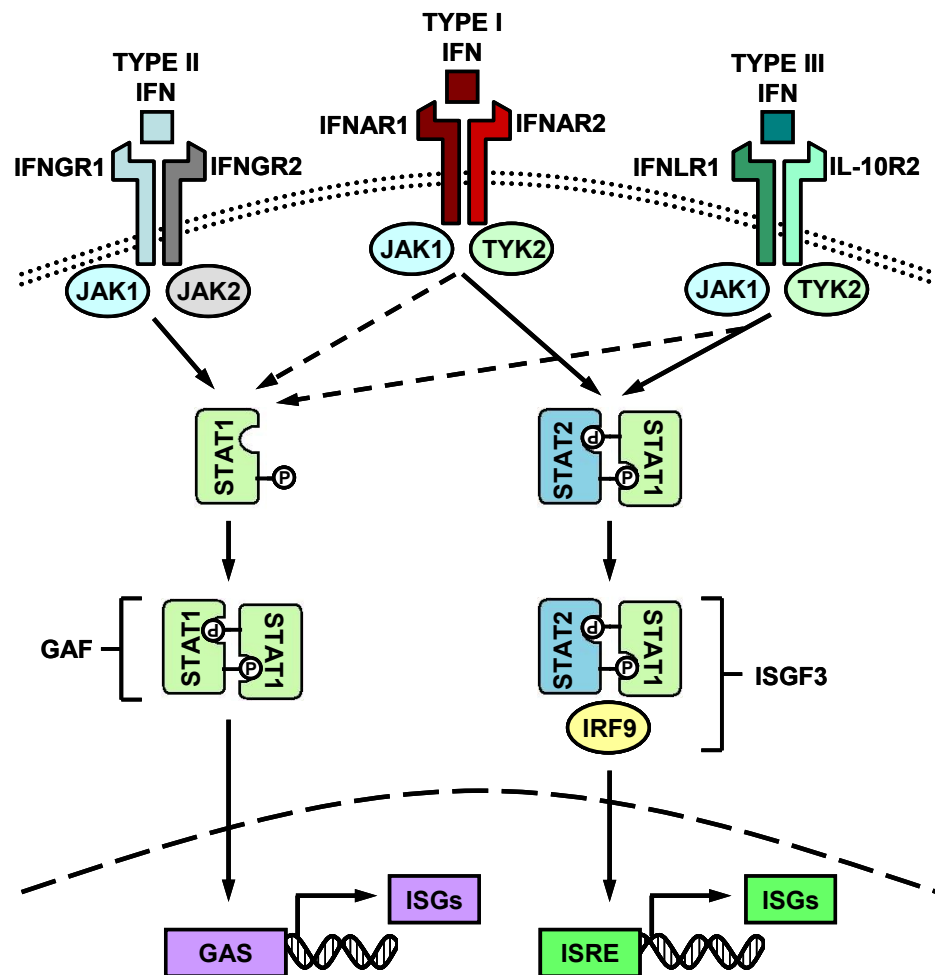


Figure 1.1 IFN receptor signalling pathways.

Interferons (IFNs) bind to one of three heterodimeric IFN receptors. The only known type II IFN, IFN γ , binds to the IFN γ receptor. This receptor is composed of an IFNGR1- and an IFNGR2-chain which associate intracellularly with the Janus activated kinases (JAKs), JAK1 and JAK2. Receptor ligation leads to the downstream phosphorylation and homodimerisation of signal transducer and activator of transcription (STAT) 1 molecules. Activated STAT1 homodimers form a transcription factor known as the IFN γ -activated factor (GAF). GAF subsequently translocates to the nucleus and stimulates the transcription of IFN-stimulated genes (ISGs) that contain an IFN γ -activated site (GAS) in their promoter region. The type I IFN receptor, which consists of the two subunits; IFNAR1 and IFNAR2, and the type III IFN receptor, which is comprised of IFNLR1 and IL-10R2, both associate with JAK1 and tyrosine kinase (TKY) 2. Ligation of either receptor triggers the phosphorylation of STAT1 and STAT2. This results in the formation of the IFN-stimulated gene factor 3 (ISGF3), a transcription factor complex which comprises a STAT1:STAT2 heterodimer and an associated IFN regulatory factor, IRF9. ISGF3 stimulates the transcription of ISGs by binding to the IFN-stimulated response element (ISRE). In addition to activating ISGF3, ligation of either the type I or the type III IFN receptor can lead to the formation of GAF and the subsequent transcription of GAS-associated ISGs.

1.1.6 Chemokines

Chemokines, or chemotactic cytokines, are small, diverse proteins with a key role in inducing the directed migration of target leukocytes. They can be categorised into four subfamilies: CXC/ α chemokines, CC/ β chemokines, XC/ γ

chemokines and CX_3C/δ chemokines⁷⁰. Intramolecular di-sulphide bonds between conserved cysteine residues dictate both the tertiary structure of chemokines and their subsequent nomenclature^{70,71} (Figure 1.2). With 28 and 16 members respectively, CC- and CXC-chemokines represent the largest of the chemokine families. Both XC- and CX_3C -chemokine sub-groups contain only a single member known to-date⁷¹. Although chemokines have a multitude of functions *in vivo*, their best characterised role is to orchestrate leukocyte migration, both during homeostasis and inflammation.

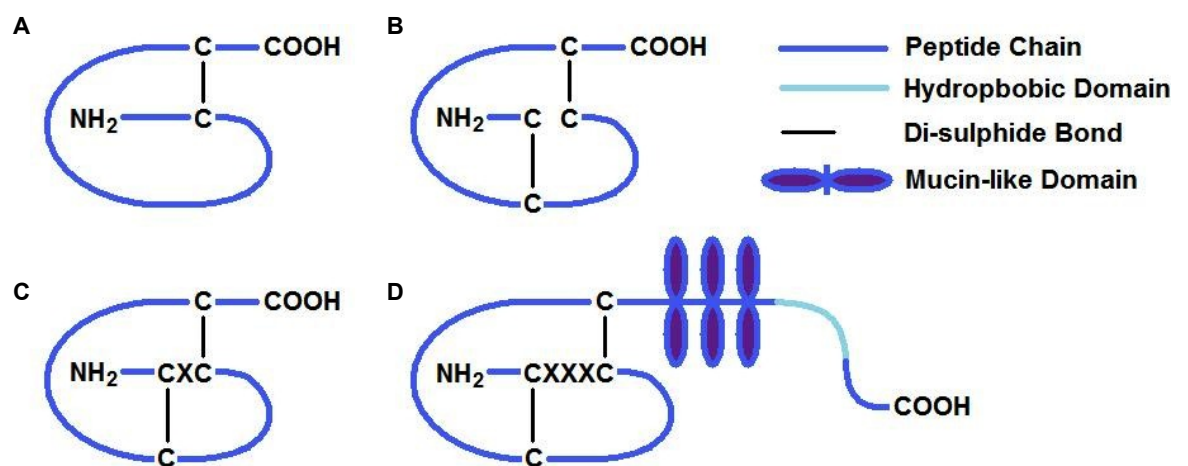


Figure 1.2 Conserved Structures of the Four Chemokine Families.

Chemokines are classified according to the assembly of cysteine residues located near the amino-terminus (-NH₂). (A) The sole member of the XC chemokines, XCL1, has one cysteine residue near the amino terminus. (B) CC chemokines have two adjacent cysteine residues near the amino terminal. (C) CXC chemokines have two cysteine residues at the amino-terminus which are separated by a non-conserved amino acid residue. (D) The only known member of the CX_3C family, CX_3CL1 (fractalkine), has two cysteine residues at the amino-terminus which are separated by three non-conserved amino acid residues. CX_3CL1 and CXC family member CXCL16, have an adhesive mucin-like domain, a membrane-spanning hydrophobic α -helix and a short cytoplasmic tail. CX_3CL1 and CXCL16 are the only transmembrane chemokines that have been discovered.

Chemokines exert their functions by binding to 7 transmembrane-spanning G protein-coupled receptors (GPCRs), activating a cascade of downstream signalling pathways. These chemokine receptors are classified according to the chemokine ligands to which they bind. There are 10 known CC receptors and 6 known CXC receptors⁷². CX_3C and XC receptor families both consist of one known member⁷². Leukocytes express specific chemokine receptor profiles which will

depend on each cell's lineage and activation state⁷³. This receptor profile will dictate where each cell has the capacity to migrate to *in vivo*. The majority of CC chemokine receptors and 3 out of the 6 known CXC receptors have more than one chemokine ligand (Table 1.1). Likewise, many of the CC and CXC chemokines can bind to more than one receptor^{71,72}. Not only does this promiscuity allow many of the chemokine systems to adopt an element of redundancy⁷⁴, but it enable chemokines to finely tune immune responses.

Receptors	Ligands
CC Receptors	
CCR1	CCL3, CCL3L1, CCL5, CCL7, CCL8, CCL13, CCL14, CCL15, CCL16, CCL23
CCR2	CCL2, CCL7, CCL8, CCL13, CCL16
CCR3	CCL5, CCL7, CCL8, CCL11, CCL13, CCL15, CCL24, CCL26, CCL28
CCR4	CCL17, CCL22
CCR5	CCL3, CCL3L1, CCL4, CCL4L1, CCL5, CCL8
CCR6	CCL20
CCR7	CCL19, CCL21
CCR8	CCL1
CCR9	CCL25
CCR10	CCL27, CCL28
CXC Receptors	
CXCR1	CXCL6, CXCL8
CXCR2	CXCL1, CXCL2, CXCL3, CXCL5, CXCL6, CXCL7, CXCL8
CXCR3	CXCL9, CXCL10, CXCL11
CXCR4	CXCL12
CXCR5	CXCL13
CXCR6	CXCL16
CX₃C Receptor	
CX ₃ CR1	CX ₃ CL1
XC Receptor	
XCR1	XCL1

Table 1.1 Chemokine receptors and their specific ligands.

1.1.6.1 Coordinating leukocyte migration

Chemokines are best known for their role in inducing chemotaxis, the process whereby the directed migration of cells is dictated by a chemical gradient. By ligating chemokine receptors and thus activating G protein-mediated signalling pathways, these chemotactic cues trigger a series of conformational and molecular changes within leukocytes to promote their directed mobility⁷⁵. Despite the fact that leukocytes migrate towards soluble chemokine gradients *in vitro*, the evidence to suggest that this phenomenon occurs *in vivo* is sparse.

A prototypical example of chemokine function *in vivo* is their role in facilitating leukocyte recruitment to tissues. Rather than involving a chemokine gradient, this particular function is dependent on immobilised chemokines, presented on the surface of the endothelium⁷⁶. All leukocytes express a specific combination of cellular adhesion molecules and chemokine receptors. This combination of surface molecules forms a site-specific molecular “postcode” which governs leukocyte entry to tissues both in homeostasis and inflammation. To enter a tissue from the circulation, leukocytes must first cross the vascular wall. Leukocyte recruitment is a complex and tightly controlled process which, for the sake of simplicity, can be broken down into a series of generalised stages (depicted in Figure 1.3). Leukocytes begin by rolling along the endothelium. Initial contact is generally mediated by transient interactions between selectins on the endothelial surface and glycosylated ligands on the leukocyte membrane⁷⁷. If they express the appropriate chemokine receptor, leukocytes will receive signals from immobilised chemokines that are presented on the surface of the vascular endothelial cells. Via G protein mediated signalling pathways, chemokine receptor ligation triggers conformational changes within a leukocyte to induce integrin clustering and activation⁷⁷. Activated integrins bind to cellular adhesion molecules from the Ig superfamily with high affinity, thus triggering the firm arrest of leukocytes to vascular endothelial cells. This is followed by their diapedesis across endothelial cell junctions and into tissues⁷⁷. Therefore, the recruitment of circulating leukocytes to tissues follows a specific sequence of tightly controlled events that is dependent on the expression of adhesion molecules, by both leukocytes and endothelial cells, and the presentation of chemokines on the surface of the endothelium.

Much less is known about how chemokines control the migration of leukocytes once they have entered a tissue. Studies using chemokine receptor deficient rodents have highlighted the fundamental role of specific chemokine systems in the positioning and retention of leukocytes within tissues. An example of this is the role of the CCR7 ligands, CCL19 and CCL21, and the CXCR5 ligand, CXCL13, in the positioning of lymphocytes within specific LN microenvironments (discussed in Section 1.1.6.2). In 2005, Okada *et al.* demonstrated a CCL21 gradient in the LN, extending from the T cell zone towards the follicles²⁵. This was the first time a chemokine gradient had been visualised *in vivo*. Using intravital microscopy, Okada *et al.* also showed that B cells migrated in a random manner within LN follicles. Following antigen encounter, B cells upregulated the CCL21 receptor, CCR7, which promoted their directed migration towards the follicle/T cell zone boundary²⁵. This indicates that a functional CCL21 gradient may exist within the LNs. Due to the constitutive movement of fluids within tissues, a soluble chemokine gradient would be difficult to maintain *in vivo*. Chemokines are often bound and “presented” by sulphated residues on cell surfaces or within the extracellular matrix⁷⁶. It therefore remains to be established whether chemokine receptor ligation induces the random motility of leukocytes (chemokinesis), or whether the directed migration of leukocytes is triggered by immobilised chemokine gradients (haptotaxis). In support of the latter, Weber *et al.* demonstrated that interstitial gradients of immobilised CCL21 extend from the lymphatic endothelium into the skin⁷⁸. This gradient was shown to be functional as it was essential for the directed migration of DCs into lymphatic vessels, as demonstrated using intravital microscopy. Thus, leukocytes respond to chemokines *in vivo*, but it is unclear whether their movement is dictated by a process of chemotaxis, chemokinesis or haptotaxis. What is clear is that chemokines and their receptors are crucially involved in inducing leukocyte motility and in the strategic positioning of leukocytes within tissues.

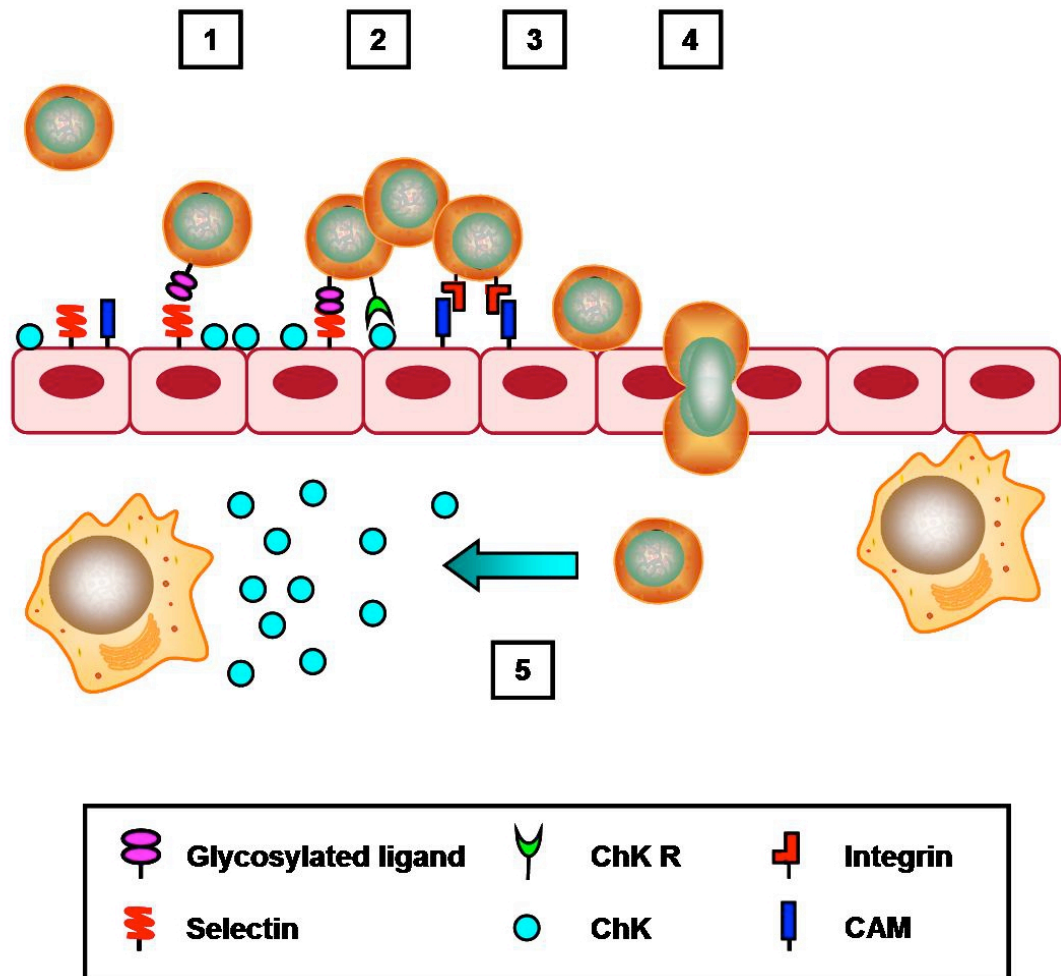


Figure 1.3 Leukocyte recruitment to tissues.

Migration of leukocytes to tissues occurs in a series of stages. (1) Transient interactions between selectins and glycosylated ligands facilitate the rolling of leukocytes along the activated endothelium. (2) Chemokines (ChKs), displayed on the surface of the endothelium, bind to leukocyte chemokine receptors (ChK Rs) to activate integrins. (3) Activated integrins bind to cellular adhesion molecules (CAM) to induce firm adhesion of leukocytes to the endothelial surface. This is followed by diapedesis (4) across inter-endothelial junctions. Once in the tissues, chemokines govern the directed migration of leukocytes to their target location. This may be facilitated by chemokine gradients.

1.1.6.2 Chemokines during homeostasis and inflammation

Chemokines coordinate leukocyte migration during both homeostatic and inflammatory conditions. Thus, depending on their role *in vivo*, chemokines can be classified as being ‘homeostatic’ or ‘inflammatory’. However, it is important to note that this rule is not absolute. A degree of overlap exists between these sub-categories. For example, the production of a number of ‘homeostatic’ chemokines can be enhanced during inflammatory conditions and many of the chemokines considered ‘inflammatory’ have a key role during homeostasis⁷¹.

Under steady state conditions, ‘homeostatic’ chemokine production is constitutive and strictly regulated. These chemokines are expressed in discrete regions within specific tissues to facilitate the targeted migration of patrolling leukocytes throughout the body. An ideal example of this cell- and tissue-specific phenomenon is the highly synchronised action of the homeostatic chemokines, CCL19, CCL21 and CXCL13. CCL19 and CCL21 function through the chemokine receptor CCR7^{79,80}. CCR7 ligation is involved in the recruitment of naïve T cells to the LNs and in the targeting of T cells to specific LN microenvironments⁸¹. Furthermore, CCR7 and its ligands play a role in the homing of DCs through the lymphatics to T zones of the LNs, where they will encounter patrolling T cells^{21,81}. B cells also utilise CCR7 to enter the LN. However, upon entering the LN, B cells migrate to specific B cell follicles. This is dependent on interactions between CXCR5, expressed on the surface of B cells, and its ligand CXCL13 which is produced within follicles⁸². Thus, in the steady state, CCL19, CCL21 and CXCL13 collectively coordinate a finely tuned series of events leading to the specific positioning of leukocytes within specialised LN microenvironments.

One of the most important homeostatic chemokines, particularly in terms of development, is CXCL12 which functions primarily by binding to CXCR4. CXCL12 was the first chemokine to evolve. It is highly conserved across many species, including lower vertebrates^{83,84} and is hence considered the ‘primordial chemokine’. Moreover, both CXCL12- and CXCR4- deficiencies have proven to be perinatally lethal in mice due to abnormalities, particularly in haematopoiesis and cerebellar formation⁸⁵⁻⁸⁷. Thus CXCL12 is crucial for both immune system and brain development. The CXCL12/CXCR4 axis also plays a number of prominent roles during adult life. For example CXCL12 is intrinsically involved in the homing to and retention of haematopoietic stem cells in the bone marrow⁸⁸. In addition, CXCL12 may have a number of roles in the central nervous system (CNS) during steady-state conditions. These are described in detail in Section 1.3.2.1.

As the name suggests, ‘inflammatory’ chemokines are highly inducible following virtually any pathogenic insult. Their primary function is to recruit the appropriate leukocyte populations to sites of inflammation. Many inflammatory chemokines exist. As they are of particular relevance to this thesis, the actions

of CCL2, CCL3, CCL5, CXCL1, CXCL2, CXCL9 and CXCL10 will now be discussed. Both CXCL1 and CXCL2 are rapidly induced during acute inflammatory responses. These molecules exert their chemotactic functions by ligating CXCR2, a receptor predominantly expressed by neutrophils⁸⁹⁻⁹¹. In addition to promoting chemotaxis, CXCR2 ligation is thought to contribute to other aspects of neutrophil activation, including degranulation and cytokine production⁹². By activating endothelial cells in nearby blood vessels, proteins released during degranulation can induce the secretion of CCL2 from the endothelium⁹⁰. CCL2 is a potent chemoattractant for circulating 'inflammatory' monocytes which express CCR2^{93,94}. Thus, neutrophil recruitment to inflamed tissues generally precedes the infiltration of 'inflammatory' monocytes.

In addition to CCR2, 'inflammatory' monocytes have been reported to express CCR1⁹³. Like CCR5 (discussed below), CCR1 responds to the chemokines CCL3 and CCL5. However, the ability of CCL3 to attract 'inflammatory' monocytes *in vitro* has been shown to be considerably weaker than that of CCL2, suggesting that CCR2 may be the predominant chemokine receptor involved in the recruitment of this monocyte subpopulation⁹⁵. Circulating monocytes can rapidly differentiate into macrophages once they reach an inflamed tissue. This is associated with an upregulation of chemokine receptors CCR1 and CCR5 and a downregulation of CCR2^{95,96}. As both CCR1 and CCR5 respond to the shared ligands, CCL3 and CCL5, this paradigm shift means that differentiated macrophages are more susceptible to the chemoattracting actions of both of these chemokines, and less susceptible to CCL2⁹⁵. CCL3 and CCL5 also have the capacity to attract 'resident' monocytes, which are known to express CCR5⁹⁴.

CXCL9-11 are IFN-inducible chemokines which are commonly induced during Th1 cell-mediated immune responses⁹⁷⁻⁹⁹. Whilst their shared receptor, CXCR3, is expressed mainly by activated T cells, it can also be found on a number of other leukocyte populations, including NK cells⁹⁹⁻¹⁰¹. In addition to CXCR3, activated T cells, particularly Th1 cells and T_{EM} cells, also generally express CCR1 and CCR5, enabling them to migrate towards both CCL3 and CCL5. Thus, relevant leukocyte populations can be rapidly recruited to inflamed tissues following the elevated secretion of specific combinations of inflammatory chemokines.

1.2 Immune Components of the CNS

The brain and the spinal cord collectively make up the CNS. Under normal homeostatic conditions, these organs are largely isolated from the peripheral immune system. The CNS lacks conventional lymphatic drainage¹⁰², contains very few ‘professional’ antigen presenting cells (APCs)¹⁰³ and is separated from the periphery by seemingly impenetrable cellular barriers fortified by complex tight junctions¹⁰⁴. The blood-cerebrospinal fluid barrier (BCSFB) separates the circulation from the cerebrospinal fluid (CSF) while the blood-brain barrier (BBB) and blood-spinal cord barrier (BSCB) demarcate the vasculature feeding the brain and spinal cord parenchyma respectively. These barriers serve to protect the CNS parenchyma from plasma components and inflammatory leukocytes. As a result of this apparent isolation from the peripheral immune system, until very recently the CNS was considered to be an ‘immune-privileged’ site.

Within the CNS a number of different, highly specialised cell populations harmoniously coexist. Ensheathed in myelin, neurons relay sensory information to discrete brain regions which subsequently command the appropriate motor response. Oligodendrocytes provide the myelin-rich membrane which insulates neuronal axons. This sheath speeds up action potential propagation along each axon. Further protection and support is provided by astrocytes and microglia (discussed below). Collectively these cell types constitute a crucial and vastly complicated cellular network. Neurons are postmitotic and are therefore not capable of self-renewal¹⁰⁵. Thus, a degree of separation between the immune system and the CNS is an evolutionarily advantageous strategy as it protects these critical and non-renewable neuronal circuits from the collateral damage that could arise as a result of peripheral inflammation. However, the notion that the CNS is completely isolated from the immune system is too simplistic. The brain and spinal cord are important organs, and in fact many immunological mechanisms, both innate and adaptive, act in parallel to enable the CNS to mount an appropriate response to infection. Thus the term ‘immune-specialised’ is arguably a more apt description of the immune-components that protect the CNS. The mechanisms that mediate innate and adaptive immunity in the CNS will now be discussed. As it is of particular relevance to this thesis, this discussion will predominantly focus on immune responses in the brain.

1.2.1 Innate components

Microglia and astrocytes constitute the principal innate responders of the CNS. Both cell types are endowed with a number of PRRs and so can respond to pathogenic insults with the induction of numerous inflammatory mediators¹⁰⁶⁻¹¹⁵. However, whereas microglial exposure to pathogenic stimuli culminates in the production of many inflammatory cytokines, chemokines and reactive oxygen species, astrocyte stimulation results in a more finely tuned chemokine response which may lead to the selective recruitment of appropriate leukocyte populations to sites of CNS injury.

1.2.1.1 Microglia

Microglial cells are generally considered the tissue macrophages of the CNS parenchyma. Their haematopoietic origin differentiates them from other CNS-derived cells. Microglia are generated from yolk sac-derived myeloid precursors early in development¹¹⁶ and constitute between 5 and 20% of the glial cell population in the CNS¹¹⁷. Rather than being continually replenished from bone marrow-derived myeloid progenitor cells, as was once proposed, their population is sustained by the self-renewal of the CNS-resident progenitor cells that enter the brain during embryogenesis¹¹⁶.

Microglia have a number of functions and differ in morphology depending on their activation state. Under physiological conditions, 'resting' microglia perpetually extend, retract and remodel highly motile cellular processes¹¹⁸. These dynamic processes continuously sample the extracellular space scouting for pathogens. Microglial processes are also known to interact with neuronal synapses but the functional significance of this remains unclear¹¹⁹. Microglia are the principle innate effector cells of the CNS. During steady state, their morphology closely resembles that of immature myeloid cells¹²⁰. However, microglia have the capacity to respond to a large array of pathogens and inflammatory agents. Consequently, microglial activation is a classic hallmark of virtually all CNS pathologies. Microglia express numerous cytokine receptors and PRRs. In addition to the TLRs discussed below, they have been reported to express the mannose receptor and mRNA encoding the cytoplasmic NLRs, NOD1 and NOD2¹²¹⁻¹²³. These receptors are involved in the phagocytosis of pathogens

and the intracellular recognition of bacterial components respectively. This receptor profile allows microglia to sense and respond to cytokines, PAMPs and DAMPS. Following pathological stimuli, microglia rapidly transform into activated effector cells. Now capable of enhanced phagocytosis^{124,125}, antigen presentation (Section 1.2.2.3) and inflammatory mediator production^{108,109,126,127}, 'activated' microglia are more akin in morphology to mature myeloid cells such as activated macrophages.

Several studies have been carried out to characterise the full repertoire of PRRs that are expressed by microglial cells and their functional significance. Of the 13 known TLRs, TLRs 1-9 are expressed by primary microglial cells, isolated from humans, primates and rodents¹⁰⁶⁻¹⁰⁹. A number of these receptors have been shown to be functional *in vitro*. For example, treating primary cultured microglia with ligands specific for TLR2, TLR3, TLR4 and TLR9 induce the expression of a host of inflammatory mediators^{108,109,126,127}. TLR3 recognises viral double-stranded RNA and TLR9 recognises CpG motifs from both viral and bacterial DNA, whereas TLR2 and TLR4 respond to gram-positive and gram-negative bacterial components respectively¹. Therefore, microglia have the capacity to respond to viral and bacterial pathogens. Stimulating microglia using PAMPs induces a similar inflammatory response regardless of the nature of the pathogenic insult. For example, following ligation of either antiviral or antimicrobial TLRs, microglia have been shown to upregulate the expression of a wide variety of inflammatory cytokines, including IFN β , IL-1 β , IL-6, IL-12 and TNF α ^{108,109,126,127}. Furthermore, they produce reactive oxygen species, such as NO via the upregulated expression of iNOS^{109,126}. TLR2-, TLR3- or TLR4-ligation of microglia also upregulates the expression of inflammatory chemokines, including CCL2, CCL3, CCL5 and CXCL10^{108,109,127} enabling the potential recruitment of activated CD4⁺ Th1 cells, T_{EM} cells, CD8⁺ cytotoxic T cells and NK cells, as well as monocytes and macrophages. Collectively, the above leukocyte populations are well equipped to respond to either a viral or a bacterial infection. Therefore, microglial cells, stimulated by TLR ligands *in vitro*, produce a large number of inflammatory cytokines in addition to various chemokines. Although potent, this inflammatory response is more generalised when compared to that of astrocytes (Section 1.2.1.2), as microglia produce inflammatory mediators that are comparable regardless of the immune stimuli.

Although microglia are therefore capable of initiating a wide range of inflammatory responses *in vitro*, they are maintained in a quiescent state in the normal CNS *in vivo* through neuronal interactions. Neurons express both the glycoprotein CD200, and the chemokine CX₃CL1 which interact with their corresponding receptors, CD200R and CX₃CR1, found on the surface of microglia¹²⁸⁻¹³⁰. These interactions exert a potent restraining influence and their disruption leads to elevated microglial activation and neurotoxicity¹²⁸⁻¹³⁰. Therefore, the absence of these *in situ* interactions needs to be considered when interpreting the effects of activating isolated microglia with TLR ligands *in vitro*. There have however been some investigations into microglial TLR responses *in vivo*. Intraperitoneal injection of lipopolysaccharide (LPS), a TLR4 agonist, leads to an upregulation of TLR2 and CD14 mRNA by microglial cells in a TLR4-dependent manner¹³¹. Furthermore, microglial TLR4 expression is necessary for leukocyte recruitment to the cerebral vasculature following intracerebral LPS injection¹³². These results suggest that microglial cells do express functional TLR4 *in vivo*. TLR2 and TLR3 may also be functional on microglial cells *in vivo* as a number of groups have demonstrated that microglial responses are impaired in TLR2- and TLR3-deficient rodents¹³³⁻¹³⁵. Therefore, TLR-expression by microglia may play important roles *in vivo*.

1.2.1.2 Astrocytes

Astrocytes are the most abundant cell type in the CNS. Their primary functions include maintenance of the BBB, uptake and metabolism of excess glutamate and γ -aminobutyric acid (GABA), regulation of extracellular potassium levels and the production of several trophic and survival factors (reviewed in Ref 136). However, they also play a part in innate immune responses of the CNS.

Like microglia, primary cultured astrocytes have been reported to express a number of PRRs and can respond to a variety of PAMPs by producing inflammatory mediators. However they may not possess as wide a repertoire of TLRs as microglia and there are conflicting data on the precise TLR profile they may express. This may be due to species-specific differences in TLR expression. Indeed, a report by McKimmie *et al.* demonstrated a differential TLR repertoire in the CNS of three different mouse strains¹³⁷. As most reports show that astrocytes express TLR3¹¹⁰⁻¹¹³, astrocytes have been implicated in antiviral

responses^{110,113}. However, as will be discussed below, astrocytes also appear to express a number of functional antimicrobial PRRs and therefore express the appropriate receptors to recognise either viral or bacterial pathogens.

Stimulation of astrocytes with the TLR3 ligand, polyinosinic:polycytidylic acid (poly(I:C)), results in the upregulation of TNF α and a number of chemokines, particularly CXCL10, CCL5, and to a lesser extent, CCL2^{110,112,113}. One report also noted the upregulation of IFN α and IFN β ¹¹³. A similar response is seen following TLR9 activation of astrocytes using CpG, which leads to the production of inflammatory cytokines and the chemokines CCL2, CCL3, CCL4 and CXCL10^{114,115}. CCL5 and CXCL10 attract activated T cell populations and NK cells which are integral in the host response against viral infection. Monocyte recruitment is also a common feature in the virus-infected brain, and accordingly, the chemokine profile expressed by astrocytes following poly(I:C) or CpG stimulation includes the expression of a number of monocyte chemoattractants, namely CCL2, CCL3, CCL4 and CCL5. Therefore, by expressing inflammatory and antiviral cytokines and by producing the chemokines necessary to attract the relevant antiviral leukocyte populations to the site of injury, astrocytes may play a pivotal role in modulating antiviral responses in the CNS.

There is increasing evidence to suggest that astrocytes may also be able to respond to bacterial PAMPs *in vitro* as they have been reported to express TLR2, TLR4 and the cytosolic NLR, NOD2. Although the expression of TLR4 is not detected consistently^{110,138}, many reports show that astrocytes are capable of responding to LPS *in vitro*^{111,113,139,140}. The astrocytic response to either TLR2 or TLR4 ligation is remarkably similar, involving a production of the monocyte chemoattractants, CCL3, CCL5 and in particular, CCL2^{112,113,141,142}. Both TLR2 and TLR4 ligands also induce a potent upregulation of TNF α . In addition, LPS has also been reported to induce iNOS expression and the production of neutrophil chemoattractants, such as CXCL1 and CXCL2^{112,113,141}. Thus, the chemokine profile that is induced in astrocytes in response to TLR2 and TLR4 ligation is ideally suited to attract an influx of neutrophils and monocytes into the CNS. As these cell types play a pivotal role in antimicrobial responses, this would undoubtedly contribute to the host response against bacterial infection in the CNS. Furthermore, the upregulation of iNOS may lead to enhanced NO synthesis. NO is crucial in the host response against a number of bacterial infections

(reviewed in Ref 143). Although NOD2 expression has also been shown to contribute to inflammatory cytokine induction in astrocytes¹⁴⁴; its role in chemokine induction has yet to be established. Consequently, by attracting antimicrobial effector cells from the periphery and by inducing the expression of antimicrobial agents, astrocytes may also play a role in the central immune response against bacterial pathogens.

The ability of astrocytes to modulate innate immune responses in the CNS, may depend on the extracellular milieu. In inflammatory conditions or following TLR ligation, astrocytes can upregulate the expression of a number of TLRs, making them more efficient in their ability to recognise and respond to pathogens^{111,113,139}. In addition, inflammatory cytokines have been shown to trigger the induction of intracellular adhesion molecule-1 (ICAM-1) and vascular-associated adhesion molecule-1 (VCAM-1) on astrocytes¹¹³. As astrocytic processes ensheath the cerebral vasculature to form the glia limitans, which constitutes a barrier to restrict the exchange of cells and molecules between the CNS and the periphery¹⁴⁵, enhanced adhesion molecule expression at this location may facilitate the ingress of infiltrating inflammatory leukocytes to the CNS parenchyma from the perivascular spaces.

Although the role of astrocytes in pathogen recognition has been relatively unexplored *in vivo*, it is apparent that astrocytes have the potential to contribute to innate immune responses in the CNS by recognising a combination of viral and microbial pathogens and inducing an appropriate inflammatory response. Furthermore, by upregulating adhesion molecule expression and tailoring their chemokine induction, astrocytes may attract the relevant leukocyte populations into the brain to suit the pathological stimuli.

1.2.2 Adaptive components in the CNS

Recent evidence suggests that the CNS can mount successful adaptive responses against local antigens. As will be discussed below, antigen can be transported from the brain to the cervical LNs where it can be presented by APCs to naïve T cells. A proportion of the T cells which are primed in the cervical LNs home to the brain¹⁴⁶, possibly by adopting a specific brain-homing phenotype. These may enter the CNS across one of the cellular barriers that protect it from the

periphery. Once in the CNS, T cells encounter strategically positioned APCs which may propagate a CNS-targeted immune response.

1.2.2.1 Antigen drainage

Although the CNS is devoid of conventional lymphatic vessels, there is evidence to suggest that CNS-derived antigen in the CSF and interstitial fluid of the parenchyma can drain from the brain to the cervical LNs. These pathways have been determined using radiolabelled and fluorescently labelled antigen. CSF passes through the subarachnoid space where it drains to the cervical LNs via the nasal lymphatics¹⁴⁷. Interstitial fluid appears to drain from the brain along perivascular pathways, flowing along the basement membranes of capillaries and arteries sequentially until reaching the cervical LNs¹⁰². Although antigen can travel to the cervical LNs, whether or not brain-derived APCs can travel to LNs to present antigen remains controversial. The evidence for this will be discussed in Section 1.2.2.3.

Once antigen reaches the LNs, it is presented by LN-resident APCs to elicit an adaptive immune response. A well established animal model of CNS autoimmunity is the immunisation of rodents with myelin-derived antigens emulsified in adjuvant to induce experimental autoimmune encephalomyelitis (EAE)¹⁴⁸. This is generally associated with an infiltration of leukocytes across the BSCB and the subsequent development of inflammatory, demyelinating lesions in the spinal cord. Focally damaging the cerebral hemisphere seven days post-inoculation has been shown to cause a 6-fold increase in cerebral inflammation¹⁴⁹. The importance of this pathway for the initiation of immune responses in the brain is shown by the fact that the cerebral lesions occurring during EAE are markedly reduced by the removal of the cervical LNs¹⁵⁰.

The cervical LNs have also been implicated in driving brain-specific B cell responses. Injecting human albumin into the brain or CSF of rats has been shown to induce an antibody response in the cervical LNs; an effect that was abolished by cervical LN obstruction¹⁴⁷. Together these observations suggest that antigen is drained from the brain to cervical LNs where it can induce antibody responses and activate brain-homing lymphocytes.

1.2.2.2 Immune Surveillance

In the steady state, a limited number of leukocytes constitutively patrol the CNS; a phenomenon known as immune surveillance. Leukocytes entering the CNS to sample brain-derived antigen must first combat either the BCSFB, the BBB or BSCB. The best characterised route of leukocyte entry to the healthy brain is via the choroid plexus, a richly vascularised site on the ventricles of the brain where CSF is secreted and where endothelial fenestrations and intercellular gaps facilitate an easy migration of molecules and cells into the perivascular space¹⁵¹. The CSF of healthy individuals contains approximately 150 000 T cells¹⁵², the majority of which are T_{CM} cells that have presumably been recruited from the bloodstream^{152,153}. P-selectin recruits circulating T cells to the choroid plexus stroma whilst epithelial cells constitutively express leukocyte extravasation-associated adhesion molecules P- and E-selectin, ICAM-1 and VCAM-1 on their apical surface^{153,154}. Not only is T cell entry to the CNS impaired in P-selectin null mice¹⁵⁵ but P-selectin glycoprotein ligand-1 (PSGL-1), a ligand for both P- and E-selectin, is expressed by all CD4⁺ T_{CM} cells in the CSF of patients with non-inflammatory neurological conditions¹⁵⁶. Once across the BCSFB, T_{CM} cells circulate in the CSF for several hours, scanning the surface of central APCs for antigen before returning to the bloodstream^{152,153}. However, upon encounter with their cognate antigen in the CNS, T_{CM} cells initiate a massive inflammatory response that often culminates in the invasion of inflammatory leukocytes.

T_{CM} cells may also cross the BBB to patrol the perivascular regions of the brain parenchyma where they will potentially encounter antigen displayed by perivascular macrophages (PVMs). Due to a network of tight junctions, trans-endothelial migration across the BBB is severely restricted and occurs only at post-capillary venules¹⁵². The adhesion molecules involved in facilitating this migration in the steady state have not been clearly defined. It is known however, that non-inflamed BBB endothelium expresses CD34, ICAM-2 and to a lesser extent ICAM-1, but not P-selectin, E-selectin or VCAM-1¹⁵⁷. As a result, the initial adherence of leukocytes to the vasculature may involve interactions between CD34 on the endothelium and L-selectin on the surface of T_{CM} cells. Thus by a series of interactions with the highly specialised barriers that separate the CNS from the periphery, peripherally activated T cells with varying

specificities continuously enter central compartments to sample CNS-derived antigen.

1.2.2.3 Professional and 'amateur' APCs of the CNS

The non-inflamed brain contains relatively few professional APCs, although monocyte-derived DCs have been reported in the choroid plexus and the meninges^{103,158}. The presence of BBB-associated DCs has also been reported in the healthy mouse brain¹⁵⁹. These APCs may act as sentinels, strategically localised to interact with and present antigen to surveying T cells as they enter the CNS. Observations made by Greter *et al.* support this hypothesis. When T cells enter the CNS during EAE, they require reactivation signals from MHC class II-expressing APCs to induce pathology¹⁵⁹. By crossing MHC class II-deficient mice with mice that express MHC class II under the control of the CD11c promoter (CD11c-H2-Ab1/H2-Ab1^{-/-}), Greter *et al.* demonstrated that MHC class II-expressing CD11c⁺ DCs were sufficient to restore pathology to mice that lacked all other MHC class II-expressing cell types¹⁵⁹. As only activated T cells can enter the brain¹⁶⁰, CNS-derived DCs may be intrinsically involved in restimulating T cells as they enter from the periphery. Following this response, a wave of leukocytes can rapidly infiltrate the CNS from the periphery. This leukocyte infiltrate has been reported to include blood-derived DCs which, once in the CNS, can potentiate the presentation of brain-derived antigen to infiltrating T cells¹⁶¹.

An additional role for CNS-resident DCs may be the transportation of antigen from the CNS to the draining LNs. DCs in the cervical LNs have been shown to present myelin-derived antigen during EAE and the demyelinating autoimmune disease, multiple sclerosis (MS)¹⁶². It is not clear whether these DCs migrated to the LNs from the brain, or whether free antigen was taken up by LN-resident DCs after draining through the lymphatic system. However, following microinjection of the protein antigen ovalbumin (OVA) into the brain, labelled DCs rapidly accumulate at the injection site before migrating to the cervical LNs to induce a robust T cell response¹⁴⁶. The resulting fully primed, OVA-specific T cells then adopted a CNS-homing phenotype and subsequently travelled to the brain. These studies suggest that DC trafficking from the brain to the cervical LNs should not

be ruled out as a possible mechanism of priming adaptive CNS-specific cellular responses.

In addition to the classical APCs of the CNS, microglia, PVMs and astrocytes all share the capacity to upregulate MHC class II molecules in an inflamed environment. Thus, these cell types may also have a role in activating T cell responses *in vivo*. Encapsulated by the basement membrane on the abluminal side of the BBB, PVMs constitutively express MHC class II molecules and the costimulatory molecules required for antigen presentation and T cell activation¹⁶³. Due to their strategic location these macrophages may be able to restimulate activated T cells as they cross the BBB. Selective depletion of PVMs after an intraventricular injection of chlodronate liposomes resulted in a delayed onset of EAE accompanied by a reduction of disease severity, suggesting a role for PVMs in antigen presentation *in vivo*¹⁶⁴.

The role of microglia in antigen presentation *in vivo* has long been debated. In addition to upregulating MHC class II molecules^{109,165}, activated microglia upregulate costimulatory molecules, such as CD40, CD80 and CD86^{109,165}. As described in Section 1.2.1.1, they also produce a number of cytokines and chemokines, which could shape T cell effector functions. Many studies have described the ability of activated microglia to prime naïve T cells and to reactivate effector T cells¹⁶⁵⁻¹⁶⁸. However, these studies focus on microglial functions *in vitro*. Activated microglia have also been shown to be able to cross-present exogenous antigen *in vivo* after naïve CD8+ T cells were injected into the brain¹⁶⁷. There is evidence to suggest that naïve T cell priming by microglia may be atypical. For example, although microglial-activated T cells upregulate the activation marker CD25 and target cells in an antigen-specific manner, they do not proliferate^{169,170}. In fact, antigen presentation by microglia may act as a method of limiting T cell responses in the CNS by inducing the apoptosis of antigen-specific T cells¹⁶⁹. The *in vitro* studies are limited as removing microglia from the constraints of their microenvironment can have a profound impact on their behaviour (see Section 1.2.1.1). In addition, naïve T cells are not known to enter the CNS. As a consequence, it is unclear whether these reports are biologically relevant. Nevertheless, microglia expressing MHC class II and costimulatory molecules have been detected in inflammatory lesions during MS

and EAE¹⁷¹⁻¹⁷³ and therefore these cells may have a role in the secondary activation of effector T cells during pathology.

Unlike microglia and PVMs, astrocytes are generally considered to be poor activators of T cell responses. Although they typically express very low levels of MHC class I, MHC class II and costimulatory molecules, several reports demonstrate that these surface molecules are inducible following IFN γ -stimulation *in vitro*¹⁷⁴⁻¹⁷⁶. These reports, however, are not always consistent as some studies note a lack of costimulatory molecule (CD80 or CD86) induction following IFN γ treatment^{165,177}. Furthermore in mice that overexpressed IFN γ , the induction of MHC class I or class II molecules could be detected in microglia but not astrocytes¹⁷⁸. It has been demonstrated *in vitro*, that the induction of MHC molecules can be inhibited by the presence of other cytokines, such as TNF α or IL-1 α ^{179,180}. Therefore, the induction of these molecules *in vivo* may depend on the exogenous cytokine milieu. Many studies have attempted to investigate whether IFN γ -treated astrocytes are capable of priming T cell responses. These studies have yielded highly variable results and almost exclusively focus on cultured astrocytes. For example, Constantinescu *et al.* demonstrated the capacity of cultured, IFN γ -stimulated astrocytes to induce the proliferation of myelin-specific T cells¹⁸¹. In contrast, in a similar set of experiments, Weber *et al.* showed an induction of cytotoxic T cell activity but an absence of proliferation¹⁸¹. Taken together, these studies show that whilst IFN γ may endow astrocytes with the ability to prime T cell responses *in vitro*, their ability to do so *in vivo* requires further clarification. It is unlikely that antigen presentation by astrocytes plays a major role in driving CNS-specific T cell responses.

1.3 Chemokines in the CNS

It is becoming increasingly clear that chemokines play a role in CNS responses. Not only are they induced in the CNS following injury or pathogenic insult, but a limited repertoire of chemokines and their receptors are constitutively expressed in discrete regions of the CNS and thus may be involved in neuronal

and/or glial cell communication. The involvement of relevant chemokine systems in homeostasis and inflammation will now be discussed below.

1.3.1 Chemokines in CNS disorders

Chemokines are induced in the brain following several CNS disorders. Often this is accompanied by the infiltration of leukocytes from the periphery. Although leukocyte infiltration can be beneficial to the host, for example in the clearance of pathogens from the CNS, it can also be detrimental. Infiltrating leukocytes produce a variety of inflammatory mediators which can lead to tissue damage and enhanced morbidity. Also, during autoimmune diseases such as MS, autoreactive lymphocytes can directly target CNS-derived self antigen resulting in demyelinating lesions and neuronal damage. Understanding the functional relevance of the chemokine systems that are induced in the brain during different CNS disorders is highly important in order to delineate those that are pivotal to host defence and those which contribute to pathogenesis.

1.3.1.1 Chemokines in viral encephalitis

Viral encephalitis is typically associated with a substantial induction of chemokines within the CNS. These chemokines recruit leukocytes from the periphery which mount an antiviral immune response. Although this is often required for viral clearance, as mentioned above, the effects can also be deleterious. Two examples of viruses that can cause encephalitis in rodents are West-Nile virus (WNV) and mouse hepatitis virus (MHV). The key chemokine systems that are involved in host defence and neuropathology following CNS infection with either of the aforementioned viruses have been well characterised and as a result, the involvement of the relevant chemokine systems has been described below.

WNV is a mosquito-borne arbovirus. Due to its global distribution, it is now considered an endemic pathogen. Fortunately, patients who contract WNV are often asymptomatic and the vast majority of patients who do experience symptoms are merely burdened with flu-like symptoms. However, a small proportion of patients experience severe neurological symptoms, such as meningitis or encephalitis, as a result of CNS infection¹⁸². This can be lethal and

the majority of survivors of neuroinvasive WNV experience persistent neurological deficits for months to years after the infection resolves. Several studies using mouse models of WNV indicate that survival of WNV-induced CNS disease is largely dependent on the chemokine-mediated recruitment of leukocytes to the CNS. This is at least partially translatable to human pathology. For example, it has been well established that CCR5 plays a key role in modulating anti-viral responses in both humans and mice infected with WNV. Leukocyte recruitment to the CNS is fundamental for viral clearance and survival¹⁸³⁻¹⁸⁵. Genetic depletion of CCR5 is associated with a significant reduction of CD4⁺ and CD8⁺ T cells, NK cells and macrophages and increased viral load in the CNS following WNV infection¹⁸³. Moreover, all CCR5-deficient mice succumbed to infection, compared with only 35% of wild-type mice, suggesting that CCR5-dependent leukocyte infiltration of the CNS is fundamental for successful anti-viral defence in this model. This can be reversed by the adoptive transfer of CCR5⁺ splenocytes¹⁸³. Interestingly, the fraction of leukocytes expressing CCR5 in the CNS of wild-type mice was not large enough to account for the substantial reduction of leukocytes observed in the CNS of CCR5-deficient mice. Therefore, the accumulation of CCR5-bearing leukocytes in the CNS may trigger further leukocyte recruitment in a CCR5-independent manner. This is likely to be at least partially dependent on interactions between CXCR3 and one of its ligands CXCL10, which is highly upregulated in the CNS of WNV-infected mice¹⁸⁶⁻¹⁸⁸. Blocking the effects of CXCL10, either using neutralising antibodies, CXCL10- or CXCR3-deficient mice, led to impaired CD8⁺ T cell trafficking to the CNS, failure to control viral replication and subsequently reduced survival rates^{187,188}. The CCL2/CCR2 axis also appears to play a role in anti-viral CNS responses to WNV as a reduction in infiltrating monocytes was noted in the CNS of virally-infected CCR2-deficient mice¹⁸⁶. However, this observation was shown to be a result of monocytopenia in the blood rather than a defect in monocyte recruitment to the CNS. Impaired monocyte accumulation in the CNS was associated with increased viral burden and mortality. Therefore, chemokines, produced in the brain and in the periphery, are pivotal in coordinating leukocyte levels in the blood and their subsequent recruitment to the CNS. Chemokine-mediated accumulation in the CNS is required for the host to mount a successful anti-viral response following WNV infection.

Complementing the data derived from the murine models of WNV, a role for CCR5 has also been established in human pathology. This was determined by genotyping cohorts of Caucasian patients with symptomatic WNV to compare the frequency of the CCR5 loss-of-function allele, CCR5 Δ 32, with that of the general population. Unsurprisingly, the frequency of individuals homozygous for the CCR5 Δ 32 allele was markedly higher in symptomatic WNV patients than in the general population¹⁸⁹. In one cohort, homozygosity for this allele was significantly linked to fatality. Therefore, consistent with the data from murine models, CCR5 deficiency is a major risk factor for symptom presentation following WNV infection.

Chemokines are also required for mice to successfully clear MHV infection in the CNS. However, in some cases, chemokine production in the CNS can lead to excessive tissue damage. MHV is a corona virus. When injected intracranially, neurotropic strains of MHV trigger an acute encephalomyelitis followed by chronic demyelinating disease that is phenotypically similar to the human autoimmune disease, MS¹⁹⁰. One of the chemokine axes shown to be pivotal in coordinating the host response against MHV is the CCL2/CCR2 axis. CCL2 is rapidly induced in the brain following MHV infection¹⁹¹. In the absence of its receptor, CCR2, mice were unable to clear the virus from the CNS and therefore all succumbed to infection¹⁹¹. This was associated with a significant decrease in CD4⁺ T cell and macrophage infiltration and a reduction in IFN γ production in the CNS. Therefore, CCL2 induction in the CNS, and the subsequent recruitment of CCR2-expressing macrophages, is required for the successful clearance of MHV from the CNS.

Within a day of viral administration, CXCL10 can be detected in the brain colocalised with viral infection¹⁹². As the infection disseminates throughout the CNS parenchyma, so does the expression of CXCL10, produced predominantly by astrocytes. CXCL10 plays a major role throughout the course of the disease. In the acute stages of MHV infection, this role is beneficial. CXCL10 is involved in recruiting CD4⁺ and CD8⁺ T cells to the CNS, both of which are required for anti-viral defence. In the absence of CXCL10, this process is markedly reduced, resulting in impaired viral clearance and increased mortality^{193,194}. CXCL10 expression is also required for the induction of CXCL9 and CCL5 in the CNS^{190,193}. The majority of T cells infiltrating the brain during MHV infection express the

chemokine receptor CXCR3, and unsurprisingly, CXCL9 has also been shown to contribute to T cell recruitment to the CNS¹⁹⁵. Although they are crucial for survival, infiltrating T cells contribute to a progressive accumulation of macrophages in the CNS. Macrophages are the end-stage effector cells in demyelinating diseases. By producing inflammatory mediators which generate bystander tissue damage, macrophages amplify demyelination. One of the key chemokine axes responsible for their recruitment is the CCL5/CCR5 axis. CCL5 expression is triggered by the CXCL10-induced infiltration of CD4⁺ T cells¹⁹⁰. This has no benefit to the host as blocking the effects of this axis using CCR5-deficient mice had no effect on viral clearance¹⁹⁶. In fact, blocking the CCL5/CCR5 axis, either using CCL5-specific neutralising antibodies or CCR5-deficient mice, led to a clear reduction of macrophage infiltration, demyelination and subsequent disease severity^{197,198}. Therefore, by recruiting virus-specific CD4⁺ and CD8⁺ T cells to the brain during MHV infection, the acute induction of CXCL10, followed by CXCL9 plays a crucial role in anti-viral defence. However, one caveat to the induction of CXCL10 in the brain is that recruited CD4⁺ T cells trigger CCL5 production, inevitably leading to the destructive infiltration of CCR5-expressing macrophages.

Thus, a number of chemokines are induced in the CNS following viral infection. The data described above suggest that the induction of chemokines targeting the receptors CXCR3, CCR2 and CCR5 play an important role in the recruitment of T cells, NK cells and macrophages from the circulation. Depending on the nature of the insult, the infiltration of these cell populations can be beneficial to the host, promoting viral clearance from the CNS, or deleterious, leading to bystander tissue damage.

1.3.1.2 Chemokines in MS and EAE

MS is a chronic, inflammatory autoimmune disease of the CNS. It is characterised by accumulation of autoreactive and inflammatory leukocytes which form demyelinating lesions within the CNS parenchyma. Many studies have attempted to analyse and interpret the involvement of specific chemokine systems in MS pathology and much of our current understanding of these systems is derived from observations made using rodent models of demyelinating diseases, like EAE. In terms of immune cell components, MS is primarily a T cell- and macrophage-

mediated pathology. Three chemokine receptors that are considered highly important in mediating the recruitment of these leukocyte populations to the CNS during multiple other pathologies are CCR2, CCR5 and CXCR3^{183,186-188,191,193,194,197,198}. Interestingly, CCR5 expression has been described on monocytes and lymphocytes in the CSF and lesions of MS patients^{156,199-201}, and elevated levels of CCL3 and CCL5 have been observed both in lesions and in the CSF of MS patients during relapse²⁰²⁻²⁰⁴. In addition, increased expression of CCL3 and CCL5 has been reported in the CSF of animals with EAE²⁰⁵⁻²⁰⁷. However, neither CCL3- or CCR5-deficient mice are resistant to EAE²⁰⁸, nor is there an association with CCR5Δ32 allele homozygosity and protection against MS²⁰⁹. This suggests that CCR5 is not essential for MS or EAE pathogenesis, possibly as a result of the high level of redundancy in chemokine systems. In the absence of CCR5, the chemokines CCL3 and CCL5 may recruit CCR1-expressing leukocytes to the CNS. In support of this, CCR1-deficient mice exhibit a reduction in both severity and incidence of EAE²¹⁰. Furthermore, CCR1 antagonism ameliorated disease phenotype in a rat model of EAE²¹¹. As a result, CCR1 blockade was considered a potential treatment target in MS patients. Disappointingly, the CCR1 antagonist did not prove beneficial in clinical trials²¹².

The majority of CD4⁺ T cells that patrol the CSF of patients with MS and non-inflammatory neurological diseases express CXCR3^{156,213}. However, the same is true for T cells in the CSF of patients with no neurological diseases²¹⁴. Therefore, although CXCR3 may mediate T cell entry to the CSF, this does not appear to require neuroinflammation. Interestingly, during MS relapses, an increased proportion of CD4⁺ T cells have been reported to express CXCR3 in both peripheral blood and CSF compared to that of patients in remission^{202,213}. In both studies, this was associated with increased disease activity. In addition, proximal to demyelinating lesions, the majority of T cells in perivascular cuffs were reported to express CXCR3²¹⁴. Moreover, CXCL10 expression was shown to be elevated both in demyelinating lesions²¹⁴ and in the CSF of MS patients during attacks²⁰⁰. Although these observations suggest that CXCR3 ligands may be involved in recruiting T cells to the brain during MS, the involvement of this chemokine axis has been difficult to confirm in EAE models. Blocking the actions of either CXCL10 or its receptor CXCR3 using neutralising antibodies has had variable effects on the incidence and severity of EAE²¹⁵⁻²¹⁸. However, studies

using CXCL10- or CXCR3-deficient rodents consistently suggest that this chemokine axis is not essential for the recruitment of mononuclear cells to the CNS^{216,218-220}. In fact, most studies agree that EAE is exaggerated in animals lacking either molecule^{216,218,220}. It has been reported that glial cells produce CXCR3 ligands in response to IFN γ ²²¹. Therefore, during MS and EAE, the expression of CXCR3 on infiltrating T cells and the induction of CXCR3 ligands in the CNS may represent an epiphenomenon that occurs as a result of IFN γ -producing encephalitogenic T cells accumulating in the CNS in response to other mediators.

The CCL2/CCR2 axis has a fundamental role in the induction of EAE and is therefore likely to contribute to MS pathology. In MS patients, CCL2 is highly expressed by reactive astrocytes within demyelinating lesions and in the surrounding parenchyma^{204,222}. Surprisingly, the concentration of CCL2 is consistently depleted in the CSF of MS patients compared to patients with other inflammatory diseases^{200,223}. This has been hypothesised to occur as a result of increased CCL2 uptake by infiltrating CCR2⁺ monocytes²²⁴. Although central CCL2 production is assumed to facilitate the specific recruitment of CCR2-expressing mononuclear cells from the periphery, an explicit role for this chemokine and its receptor in contributing to MS pathology has not yet been verified. In addition to being expressed in MS lesions, CCL2 is also expressed by astrocytes nearby inflammatory foci in the CNS of animals with EAE^{225,226}. Confirming a major involvement of this chemokine system in EAE pathogenesis, it has been reported that EAE is either markedly attenuated or completely absent in mice lacking either CCL2 or CCR2²²⁷⁻²²⁹. Although this provoked the development of CCR2 antagonists for the treatment of MS, these inhibitors failed to show any improvements in clinical trials²³⁰.

These studies highlight a number of chemokines and chemokine receptors that play a role in the recruitment of mononuclear cells to the CNS during MS and EAE. However, these represent only a few of the many chemokine systems that are potentially involved. For example, CCR7 is expressed on the majority of T_{CM} cells in the CSF of MS patients and on infiltrating DCs in MS lesions. Its ligands, CCL19 and CCL21 have also been characterised on the luminal surface of the BBB during EAE^{231,232}. In addition, there may be a role for the CCL20/CCR6 axis in the trafficking of T cells to the CNS across the choroid plexus epithelium during the

initial stages of EAE²³³. A number of other chemokine systems have also been implicated in MS and EAE pathogenesis. These have been reviewed extensively in Ref 234. Despite the characterisation of the chemokine profile present in lesions and CSF of MS patients and the identification of the chemokine systems that are crucial for the induction of EAE, the key chemokines responsible for MS pathogenesis remain poorly defined. This is at least partially because the knowledge gained from EAE models does not always accurately translate across species. Another major issue in deciphering the involvement of specific chemokine axes in MS is that the therapeutic use of chemokine receptor antagonists has so far failed to show any benefits in clinical trials. It is unclear whether the observed lack of improvement in these trials is due to chemokine redundancy or a failure in the efficacy of the receptor antagonists. As a result, there have been very few advances in this field in the past decade.

1.3.1.3 Central chemokine induction in response to systemic inflammation

Very little has been published relating to chemokine induction in the brain following systemic inflammation. The majority of the research in this area focuses on central chemokine responses following the systemic administration of TLR ligands in experimental rodent models of inflammation. In these models, systemic LPS-induced inflammation is commonly associated with a central upregulation of the neutrophil chemoattractants, CXCL1 and CXCL2, and a number of CC and other CXC chemokines²³⁵⁻²³⁸. These include CCL2, CCL5 and CXCL10, which are known for their role in the infiltration of leukocytes to the CNS during viral encephalitis (Section 1.3.1.1). A similar chemokine repertoire has also been reported following peripheral administration of poly(I:C)^{239,240}. However these studies are primarily focused on transcriptional data. Thus, systemically stimulating mice with certain TLR ligands can lead to an induction of chemokines in the brain.

Although many different chemokines are induced in the brain following systemic TLR3- or TLR4-induced inflammation, the function of these chemokines remains largely unexplored. The upregulation of CXCL1 and CXCL2 in the brain following high systemic doses of LPS has been associated with an influx of neutrophils to the CNS^{236,237}. Although it is not required for neutrophil rolling and adhesion to the cerebral vasculature, CXCR2 expression was shown to be necessary for

neutrophils to invade the brain parenchyma²³⁷. The remainder of the chemokines, induced in the brain in response to LPS, are known to recruit T cells, NK cells and monocytes/macrophages to sites of inflammation (Section 1.1.6). However, to my knowledge, there have been no reports of any of these cell populations infiltrating the brain following systemic LPS challenge. Although a similar phenomenon has yet to be described during systemic LPS-induced inflammation, the central upregulation of CCL2 has been shown to recruit monocytes to the brain in an experimental murine model of hepatic inflammation²⁴¹. Therefore, depending on the context, central chemokine expression triggered in response to systemic inflammation can result in the recruitment of inflammatory leukocytes to the brain.

The chemokines CCL3 and CCL5 have been described as endogenous pyrogens. Both are induced in the brain in response to systemic LPS challenge²³⁸, thus their production in the brain may play a contributing role in the development of fever. In rats, microinjection of CCL5 into the hypothalamus induced a febrile response^{242,243}. This was ameliorated by pretreating rats with either a microinjection of CCR5-specific monoclonal antibodies into the same site or an intravenous injection of the CCR1/CCR5 antagonist, Met-CCL5. Met-CCL5 also suppressed the febrile response in rats following intravenous LPS injection²⁴³, suggesting that CCR1 and/or CCR5 ligands contribute to LPS-induced fever in rats. In addition to the *de novo* expression of inflammatory chemokines in the brain, it has been recently demonstrated that systemic LPS-induced inflammation results in the reduced expression of CX₃CR1²⁴⁴; a chemokine receptor which plays a prominent role in maintaining CNS homeostasis (1.3.2.2). This effect, which is particularly pronounced in aged mice, results in microglial hyperactivation. In a study using CX₃CR1-deficient mice, overt microglial activation following systemic LPS challenge lead to prolonged social withdrawal²⁴⁵. This was associated with elevated microglial expression of IL-1 β and indoleamine 2,3 dioxygenase (IDO), both of which are implicated in the development of inflammation-induced behavioural changes (Section 1.4.3). These data suggest that, in response to systemic inflammation, the central modulation of chemokines and their receptors may have downstream implications on neuroinflammation and the subsequent development of sickness behaviours.

1.3.2 Chemokines in CNS homeostasis

In addition to their role in CNS disorders, it has been suggested that chemokines may be intrinsically involved in CNS homeostasis. Both neurons and glial cells constitutively express a number of chemokines and their receptors in spatially specific regions of the adult brain. However, the functional significance of this expression remains largely unclear. Often, the neuroanatomical distribution of chemokines and their specific receptors overlap giving rise to the hypothesis that these chemokines may have a role in basal communication between neurons and glia.

1.3.2.1 Chemokines as neuromodulators

It has been suggested that chemokines may function as a class of neuromodulator; being released at nerve endings and having pre- and post-synaptic effects, both directly and indirectly by modulating the activity of 'classical' neurotransmitters. The chemokines that have been most widely studied in this field are CXCL12 and CCL2. The involvement of these chemokines and their receptors in CNS homeostasis will be summarised below, including any evidence supporting the potential involvement of chemokines in modulating synaptic transmission.

CXCL12 and its receptor, CXCR4, are highly expressed throughout the brain during embryogenesis and the CXCL12/CXCR4 axis is a critical component in orchestrating brain development. However, high levels of constitutive expression, of both ligand and receptor, persevere into adulthood in highly regionalised areas of the brain^{246,247}. As well as being expressed by microglia and astrocytes, both ligand and receptor are expressed by neurons. Anatomically mapping CXCL12 and CXCR4 expression in the adult rat brain revealed that serotonergic neurons in the dorsal raphe nucleus, cholinergic neurons in the substantia innominata and dopaminergic neurons in the substantia nigra expressed both receptor and ligand²⁴⁶⁻²⁴⁸. CXCL12 and CXCR4 are also both expressed in hypothalamus and the posterior pituitary^{247,249}. Interestingly, in the latter sites, both CXCL12 and CXCR4 were colocalised with vasopressin in presynaptic nerve terminals indicating the possibility that CXCL12 may be released at neuronal synapses²⁴⁹.

Although it is generally considered to be an inflammatory chemokine, animal studies have shown that CCL2 is also constitutively expressed in the brain, along with its receptor, CCR2^{250,250-252}. As with CXCL12 and CXCR4, neuroanatomical mapping of CCL2 and CCR2 has demonstrated the presence of both receptor and ligand on cholinergic, dopaminergic and vasopressin-expressing neurons^{250,252}. As a result, several studies have attempted to investigate the potential involvement of CXCL12/CXCR4 axis and the CCL2/CCR2 axis in modulating neuronal transmission.

Electrophysiological recordings, using whole cell patch clamp, have demonstrated that exposing neuronal subtypes from the relevant brain regions to CXCL12 can modulate neuronal membrane potential, often triggering action potentials. For example, CXCL12 has been shown to have depolarising effects on serotonergic neurons from the dorsal raphe nucleus²⁴⁸. This was attributed to the presynaptic release of both glutamate and GABA. CXCL12 also enhanced GABA-induced inhibitory currents in dopaminergic neurons from the substantia nigra²⁵³. In contrast, CXCL12 was shown to have an inhibitory effect on the firing of vasopressin neurons²⁴⁹. Electrophysiological experiments have also demonstrated that CCL2 can affect neuronal membrane potential. CCL2 was shown to enhance the excitability of hippocampal neurons and dopaminergic neurons in the substantia nigra^{254,255}. The subsequently increased neuronal firing that was observed in the hippocampus was attributed to elevated glutamatergic transmission. CCL2 can also induce calcium (Ca^{2+}) transients in primary cultured neurons isolated from a number of other different brain regions²⁵⁰. Chemokine-induced changes in membrane potential may have downstream consequences on the release of neurotransmitters or neurohormones. Indeed following-up the electrophysiological experiments with *in vivo* studies have shown that injecting CXCL12 into the third ventricle inhibits the release of vasopressin into the blood²⁴⁹. Moreover, injecting either CXCL12 or CCL2 into the substantia nigra stimulated a rapid release of dopamine into the striata^{255,256}. In either case this was accompanied by enhanced locomotor function. Collectively, these data suggest that chemokines may have the capacity to modulate neuronal transmission. This appears to occur indirectly through the modulation of neurotransmitter release, specifically glutamate and/or GABA.

Although intriguing, these studies are limited as they invariably involve exposing the brain, or brain slices, to high concentrations of the relevant chemokines. There is no literature to suggest that this is representative of what occurs under physiological conditions *in vivo*. From the described experiments, it is unclear whether CXCL12 or CCL2 act directly on neurons to modulate the release of neurotransmitters or whether they function primarily on glial cells to govern neurotransmitter uptake. Moreover, it is worth noting that chemokines, particularly inflammatory chemokines such as CCL2, induce the expression of a number of other mediators. Thus, when interpreting observations derived from injecting a chemokine into the brain, it is difficult to delineate between the direct effect of the chemokine and the potential indirect effects of inducible agents. Taken together, these observations demonstrate that, under experimental conditions, chemokines have the capacity to indirectly impact neuronal membrane potential resulting in altered neuronal transmission. By doing so, chemokines may be able to modulate neuroendocrine functions and neurotransmitter release in steady state conditions. However, this remains to be clarified *in vivo*.

1.3.2.2 Maintaining microglial quiescence

CX₃CL1 is the exclusive member of the CX₃C chemokine family. It is constitutively expressed by neurons in spatially specific regions of the brain^{257,258}. Although the exact function of CX₃CL1-expressing neurons remains to be established, the CX₃CL1 receptor, CX₃CR1, is constitutively expressed throughout the brain by microglial cells^{257,258}. As a result, much research has gone into elucidating the role of the CX₃CL1/CX₃CR1 axis in the brain. A fundamental tool that has been widely beneficial in accelerating these studies has been the replacement of *Cx3cr1* with a green fluorescent protein (GFP) reporter gene. Creating a CX₃CR1 null locus, the generation of CX₃CR1^{gfp} mice has enabled phenotypic comparisons between CX₃CR1^{+/+}, CX₃CR1^{gfp/+} and CX₃CR1^{gfp/gfp} mice²⁵⁹. Analyses of these mice have identified a number of phenotypes resulting from the lack of CX₃CR1 signalling. For example, CX₃CL1 has been shown to exert a potent restraining influence on microglia *in vivo*. Using CX₃CR1 deficient mice, several groups have described elevated microglial activation, often accompanied with increased cytokine production following the induction of CNS diseases or systemic LPS challenge^{128,245,260-262} (Section 1.3.1.3)

Although these observations relate to microglial responses during neuroinflammatory and neurodegenerative disorders, microglia are constitutively exposed to CX₃CL1. Therefore, CX₃CR1 ligation may have a physiological role in maintaining microglial quiescence in steady state conditions.

Supporting the concept described above, impaired signalling through CX₃CR1 has been shown to enhance microglial activation in the hippocampus of healthy rodents^{130,263}. In the adult brain, microglia have been shown to shape hippocampal neurogenesis through the phagocytosis of apoptotic neuroblasts²⁶⁴. Two separate studies have demonstrated that disrupting CX₃CL1-mediated signalling in rodents, by either administering CX₃CR1-specific monoclonal antibodies or using CX₃CR1-deficient animals, resulted in impaired hippocampal neurogenesis^{130,263}. In both studies, reduced neurogenesis was accompanied by enhanced hippocampal microglial activation and elevated levels of hippocampal IL-1 β . Rodgers *et al.* also noted impaired synaptic plasticity and cognitive function in CX₃CR1 deficient rodents¹³⁰. Interestingly, the described deficits could be reversed in either study by infusion of the IL-1 receptor antagonist (IL-1ra)^{130,263}. Not only do these studies highlight a potential role for IL-1 β in modulating adult neurogenesis, but they implicate the CX₃CL1/CX₃CR1 axis in suppressing microglial activation and inflammatory cytokine production during physiological conditions.

1.4 Peripheral inflammation and behaviour

Although the immune system was once considered autonomous, there is now considerable evidence to suggest that immune responses are in part conducted by the sympathetic nervous system and the hypothalamic-pituitary-adrenal (HPA) axis (reviewed in Ref 265). The immune system responds in kind. Through the release of inflammatory mediators, the immune system rapidly alerts the brain to peripheral inflammation, ultimately invoking an appropriate behavioural response. Thus the immune system and the nervous system are intimately interlinked. This bi-directional interplay is essential in mounting a successful response to pathogens.

1.4.1 Evidence of inflammation-induced behavioural changes

It is well established that systemic infection or inflammation can have marked effects on mood and behaviour. These behavioural changes, termed sickness behaviours, include fever, somnolence, loss of appetite, social withdrawal, anhedonia, malaise and impaired motor and cognitive function^{266,267}. Sickness behaviours are highly conserved, occurring in many mammalian species as a result of numerous types of infection²⁶⁸. By promoting energy conservation and minimising heat loss, they represent a sound strategy designed help an organism overcome infection. As will be described below, sickness behaviours also occur during chronic inflammatory diseases. In these instances, what should be a beneficial, self-limiting system can become dysregulated. This can lead to a maladaptive behavioural response characterised by prolonged depression and anxiety. In the remainder of this section, the evidence backing the immune system as a key contributor to the behavioural symptoms of sickness will be discussed, as will the routes of immune-to-brain communication and the potential mechanisms of inflammation induced sickness behaviours.

1.4.1.1 Cytokine-induced behavioural changes

Acute or chronic exposure to cytokines or potent inflammatory agents, such as LPS, induces a variety of behavioural symptoms in both humans and rodents. Thought to be mediated by the actions of inflammatory cytokines TNF α , IL-1B and IL-6, these behavioural phenotypes often markedly resemble symptoms of major depression.

In the last 15 years, a number of human studies have been aimed at investigating the impact of peripheral endotoxin-induced inflammation on mood and cognition. In a study using healthy volunteers, the administration of LPS elicited an acute behavioural response characterised by significantly elevated depression and anxiety within the first few hours following treatment²⁶⁹. These behavioural phenotypes were significantly correlated with elevated plasma levels of TNF α and IL-6. Furthermore, inducing low-grade inflammation by injecting healthy volunteers with a *Salmonella typhi* vaccination has been shown to negatively affect mood and cognitive function²⁷⁰⁻²⁷². These symptoms correlated with elevated levels of circulating IL-6. Thus, in humans, elevated levels of

circulating cytokines may guide the behavioural response by transmitting peripheral inflammatory signals to the brain.

Although intriguing, the findings described above are limited as they focus on a highly acute inflammatory insult. Under physiological conditions, most inflammatory pathologies will be more chronic in nature. In addition the correlation between depression and elevated peripheral cytokines may represent an epiphenomenon. There are however several lines of evidence linking chronic inflammatory stimulus and specific cytokines to profound changes in mood and behaviour. The manifestation of major depressive disorders is a common comorbidity associated with chronic inflammatory diseases. Strikingly, approximately 50% of patients with multiple sclerosis will present with a psychiatric illness during their lifetime, with major depression being the most common²⁷³. This association is not limited to inflammatory diseases of the CNS. Patients with peripheral chronic inflammatory disorders, such as rheumatoid arthritis, psoriasis and inflammatory bowel disease, are also at a greater risk of developing major depression than the general population²⁷⁴⁻²⁷⁶.

Although once considered of psychosocial aetiology, the manifestation of major depressive disorders in patients with chronic inflammatory diseases may occur through the direct effects of peripheral inflammatory cytokines. Supporting this hypothesis are the results of a phase III clinical trial in which patients with moderate to severe psoriasis were treated with soluble TNF α receptor Etanercept. Neutralisation of TNF α caused a reduction in depression which preceded a reduction in disease severity²⁷⁶. Further supporting the notion of cytokine-induced depression; patients receiving chronic IFN α or IL-2 therapy face a significant risk of experiencing neuropsychiatric side effects during treatment^{277,278}. Both recombinant cytokines are used therapeutically to treat chronic hepatitis C and various malignancies. Occurring in approximately one third of patients²⁷⁹, IFN α -induced depressive symptoms markedly resemble symptoms of idiopathic major depression. Moreover, these symptoms can be prevented by pre-treatment with anti-depressant medication^{277,278}. Less predictable are the neuropsychiatric side effects induced by IL-2 which have been reported to include belligerence, gross disorientation and possible psychosis²⁸⁰.

Supporting these clinical data, it is well established that injecting rodents with inflammatory cytokines or cytokine-inducing agents induces a myriad of sickness behaviours. Using animal models to investigate sickness behaviours and depression-like behaviours has been widely beneficial in developing our understanding of the underlying mechanism behind inflammation-induced behavioural changes. Specifically it has confirmed the importance of specific inflammatory cytokines in transmitting information to the brain. For example, injecting rodents systemically with LPS, a potent inducer of IL-1 β , IL-6 and TNF α , triggers the full spectrum of sickness behaviours, including fever, anorexia, decreased motor activity and activation of the HPA axis²⁸¹⁻²⁸⁵. Inflammatory cytokines are thought to be the principle mediators of LPS-induced sickness behaviours as similar behavioural symptoms occur in response to centrally or systemically administered recombinant IL-1 β or TNF α ²⁸⁶⁻²⁹¹. Indeed blocking IL-1 β signalling, either using IL-1 receptor deficient mice or by administering IL-1ra, can ameliorate many of the behavioural phenotypes induced by LPS²⁹²⁻²⁹⁵.

It is worth noting that a number of LPS- or cytokine-induced sickness behaviours strikingly resemble the clinical symptoms of depression, such as anhedonia and social withdrawal²⁶⁶. In addition, a number of LPS-induced sickness behaviours can be treated with conventional antidepressants²⁹⁶⁻²⁹⁸. These observations have led to attempts to form a distinction between sickness behaviours and so-called depression-like behaviours. This is no easy task. The idea that rodents experience “depression” is controversial. Moreover considerable overlap exists between sickness and depression-like behaviours. Despite these complexities, a study by Frenois *et al.* demonstrated that 24 hours following systemic LPS injection, long after mice had recovered from the potentially confounding influence of reduced motor activity and loss of appetite, mice presented with behaviours resembling depressive symptoms²⁹⁹. These were characterised by a prolonged duration of immobility during the forced-swim test, understood to represent behavioural despair, and a decreased preference for sucrose which is thought to be a sign of anhedonia. Thus, although symptoms of sickness and depression may be difficult to distinguish in rodents it is possible that, in the hours following LPS injection, a distinct fraction of depressive-like behaviours persevere after other sickness behaviours resolve.

Overall, the evidence to suggest that cytokines can have a negative impact on mental wellbeing is compelling. The mechanisms by which cytokines, and cytokine inducing agents such as LPS, transmit signals to the brain and the downstream effect this is thought to have on neural circuitry will be discussed in detail in Sections 1.4.2 and 1.4.3.

1.4.1.2 Depression and inflammatory cytokines

Not only have inflammatory cytokines been shown to contribute directly to symptoms of depression but medically healthy patients with major depression often present with elevated levels of inflammatory mediators in their circulation. These include inflammatory cytokines, such as IL-1 β , IL-2, IL-6, IFN γ and TNF α , the soluble IL-6 receptor, sIL-6R and the IL-1 receptor antagonist³⁰⁰. Although the specific association of individual cytokines, and soluble cytokine receptors/receptor antagonists, with major depression has been variable between reports, the underlying theme of enhanced immune activation has been constant. To combat the variability between individual reports, a meta-analysis, performed by Dowlati *et al.* confirmed the significant elevation of both IL-6 and TNF α in patients with major depression³⁰⁰. Thus major depression is consistently associated with enhanced immune activation and the inflammatory cytokines IL-6 and TNF α may be reliable biomarkers in pathology.

The immune dysfunction that accompanies major depression is likely to be of clinical importance as inflammatory mediators may contribute to pathology (Section 1.4.3). As described above, anti-inflammatory agents have proven beneficial in ameliorating depressive symptoms in patients with chronic inflammatory diseases. Furthermore, several studies have shown that treating medically healthy depressed patients with immune-targeted therapy, specifically COX inhibitors, in combination with antidepressants showed greater efficacy in combating depression than antidepressants alone³⁰¹⁻³⁰³. In a study by Mendlewich *et al.* patients treated with COX inhibitors in combination with antidepressants showed remission despite being initially unresponsive to antidepressant therapy alone³⁰³. Cyclooxygenases are the rate-limiting enzymes in the synthesis of prostaglandins. Prostaglandins have a role in modulating inflammatory responses in the periphery (Reviewed in Ref13) and are implicated in the transmission of immune signals across the BBB (see Section 1.4.2.2). As a result, the beneficial

effects of COX inhibition are likely due to the subsequent impairment of these processes. Thus, prostaglandin-induced responses are likely to contribute to the pathogenesis of major depression.

1.4.2 Routes of immune-to-brain communication

Under normal homeostatic conditions, the CNS is protected from the changeable and potentially pathogenic milieu of the periphery by the BCSFB and the BBB. Due to the delicacy of the CNS and the danger of intrathecal swelling, the entry of immune cells and inflammatory mediators is tightly regulated. However, the brain must be able to respond to changes in the peripheral inflammatory environment otherwise the behavioural phenotypes that accompany infection, chronic peripheral inflammation and cytokine therapy would not be seen. The precise mechanisms by which these peripheral immune challenges are communicated to the brain to induce sickness behaviours remain to be fully clarified. Several pathways, which will be discussed below, have been implicated in this immune-to-brain interplay. These are assumed to primarily involve the intermediary action of inflammatory cytokines and cytokine-induced secondary messengers, such as prostaglandins. Using animal models, it has been demonstrated that most sickness behaviours can be induced by peripheral or central administration of either IL-1 β or TNF α ²⁸⁶⁻²⁹¹. Furthermore, a number of the central responses to peripheral inflammation, and the resulting behavioural phenotypes, can be attenuated by blocking the effects of IL-1 β (discussed in Section 1.4.3). Although not a requisite for any of the psychiatric symptoms, IL-6 is required for the induction of a fever response²⁸¹. Thus, from these studies it is abundantly clear that cytokines may play a crucial role in immune-to-brain communication and sickness behaviour induction.

1.4.2.1 Active cytokine transport

The BBB is an endothelial lining of the cerebral vasculature. Its specialised transport systems severely restrict the transcellular exchange of molecules between the periphery and the CNS. Inflammatory cytokines, such as IL-1 α , IL-1 β , IL-6 and TNF α , are amongst the repertoire of proteins and peptides that can be actively transported across the BBB³⁰⁴⁻³⁰⁷. Several studies have demonstrated that peripherally administered radiolabelled cytokines have the capacity to

enter the CNS³⁰⁴⁻³⁰⁷, even when the BBB remains intact. This unidirectional influx can be inhibited by the administration of excess unlabelled cytokines, indicating the presence of cytokine-specific, saturable active transport systems. The function of these receptors may be modulated in pathological settings. For example, activity of the TNF α transporter is increased following spinal cord injury or stroke^{307,308}. Interestingly, LPS has been shown to modulate the active transport of insulin and amyloid- β across the BBB^{309,310}. However, the effect of LPS on the transport of inflammatory cytokines remains to be established.

Cytokine transporters function at a low capacity and are quickly saturated. Whilst a role for active cytokine transport in the induction of sickness behaviours, particularly in memory processing, has been inferred³¹¹, the evidence supporting active transport as a key route of immune-to-brain communication is minimal.

1.4.2.2 Humoral routes of communication

Peripheral inflammatory mediators and cytokine inducers, such as LPS, can signal to the brain via several humoral routes of communication. Both cytokines and LPS can activate the brain endothelium, thus relaying signals across the BBB. In addition, blood-borne inflammatory agents may activate certain brain regions directly.

In general, the BBB protects the brain from the periphery. However, there are small specialised brain regions surrounding the margins of the cerebral ventricles, termed the circumventricular organs (CVOs), which lack a conventional BBB. In these regions, which possess a fenestrated endothelium, neurons and microglia may be exposed to circulating inflammatory mediators. Supporting this, the expression of the immediate-early gene c-Fos, a classic indicator of neuronal activation, is induced in sensory CVOs of the rat brain following the intraperitoneal administration of LPS or the intravenous injection of IL-1 β , IL-6 or TNF α ³¹²⁻³¹⁴. Furthermore, IL-1 β , IL-6 and TNF α mRNA is rapidly induced in these regions in response to systemic LPS, but not in response to the intravenous injection of inflammatory cytokines^{312,313,315}. This suggests that LPS may have a direct role activating cells in the CVOs, as well as an indirect role via the induction of inflammatory cytokines. Indeed, TLR4 is widely expressed

throughout the CVOs³¹⁶. In addition to neuronal activation, characterised by c-Fos induction, systemic administration of LPS triggers a wave of microglial activation that is dependent on the paracrine effects of TNF α ³¹⁷⁻³¹⁹. Beginning mainly in the CVOs, but also in the choroid plexus and the leptomeninges, this response extends to adjacent brain structures and after high doses of LPS, spreads throughout the parenchyma. Thus, circulating cytokines and LPS have the capacity to induce neuronal activity in the CVOs. In addition, systemic LPS challenge can induce local inflammation and microglial activation in the CVOs. Via the paracrine effects of TNF α , this culminates in the activation of microglia throughout the parenchyma.

A more defined route of immune-to-brain communication is the activation of the BBB by blood-borne inflammatory agents. Via a complex interplay between endothelial cells and perivascular macrophages (PVMs), this leads to the synthesis of prostaglandins. In turn, prostaglandins can freely diffuse into the parenchyma and activate discrete brain regions. In fact, a number of brain responses to peripheral inflammation, such as fever and HPA axis activity, are at least partially dependent on prostaglandins, particularly prostaglandin E₂ (PGE₂)^{320,321}. This demonstrates the pivotal role of BBB activation in transmitting peripheral immune signals to the brain.

Cytokines stimulate cells associated with the BBB endothelium by signalling through cytokine receptors to activate the inflammatory transcription factor NF κ B. In support of this, intravenous IL-1 β or TNF α administration triggers a rapid and transient induction of I κ B- α throughout both large and small vessels of the brain vasculature and in scattered parenchymal microglia^{312,320}. Not only is NF κ B a potent inducer of I κ B- α but it is also a positive regulator of COX-2 transcription³²². Indeed, COX-2 is highly induced throughout the vasculature in response to either cytokine^{312,323}. Co-staining for COX-2 protein and specific cell markers revealed that, in response to IL-1 β , COX-2 was produced predominantly by PVMs³²⁴. As it is the rate-limiting enzyme in prostaglandin synthesis, enhanced COX-2 production could potentially result in the elevated release of these soluble mediators from cells associated with the endothelium. The terminal enzyme in the synthesis of PGE₂, microsomal prostaglandin E synthase (mPGES), is also induced in the cerebral vasculature following intravenous IL-1 β challenge^{324,325}. COX-2 and mPGES are typically expressed in a concomitant

manner³²⁶ and unsurprisingly, virtually all COX-2 positive vascular cells co-expressed mPGES³²⁵. Thus, cytokine-mediated activation of the cerebral vasculature and associated PVMs leads to the rapid induction of the necessary enzymatic components required for PGE₂ synthesis. Subsequently, PGE₂ was shown to be synthesised in PVMs following IL-1 β challenge³²⁴.

In a similar manner to inflammatory cytokines, intraperitoneal LPS injection induces the transcription of I κ B- α , COX-2 and mPGES mRNA in the BBB endothelium. In addition, I κ B- α expression extended to microglial cells of the parenchyma³²⁷. Again, COX-2 and mPGES were co-localised³²⁸. The induction of these genes occurs rapidly. However, in contrast to the transient response that is induced by circulating cytokines, induction of I κ B- α , COX-2 and mPGES following LPS injection is comparatively prolonged^{320,323}. As expected, the enhanced expression of COX-2 protein and mPGES mRNA was accompanied by increased PGE₂ production; this time by both endothelial cells of the cerebral vasculature and associated PVMs³²⁴. Using brain endothelial monolayers, Moore *et al.* demonstrated that four times more PGE₂ was released from the abluminal side of a cultured endothelial cell layer than the luminal side³²⁹. Therefore, PGE₂ would appear to be released into the parenchyma in a polarised fashion. In addition to inducing inflammatory cytokine production in the periphery, which in itself contributes to endothelial cell activation, LPS can activate the BBB vasculature directly. In support of this, inducing tissue specific, sterile inflammation using intramuscular turpentine injection, induced a similar pattern of BBB activation as injecting inflammatory cytokines³²⁷. This was completely blocked in IL-1 β -deficient mice; however, BBB activation in response to systemic LPS injection remained intact³²⁷. Consequently, although IL-1 β is capable of activating cells associated with the cerebral endothelium, it is not essential for BBB activation in response to LPS.

The distinct action of IL-1 β and LPS on the cerebral vasculature is highlighted in an elegant study by Serrats *et al.* This group demonstrated that ablation of PVMs, using chlodronated liposomes, completely abolished COX-2 and mPGES expression by cells associated with the cerebral vasculature in response to intravenous IL-1 β injection³²⁴. In contrast, PVM ablation markedly potentiated the expression of both molecules in response to intraperitoneal LPS injection, leading to heightened PGE₂ production in the brain³²⁴. This implies a bi-

directional interaction between endothelial cells and PVMs whereby, in response to IL-1 β , activation of PVMs and subsequent PGE₂ production occurs downstream of endothelial cell activation. However, PVMs would appear to exert a potent inhibitory effect on endothelial cell activity which is partially overcome by LPS leading to the production of PGE₂ by endothelial cells. Whether produced in response to IL-1 β or LPS, elevated PGE₂ production was associated with enhanced activation of the HPA control circuitry, characterised by increased c-Fos expression in the catecholaminic neurons that project onto the hypothalamus. HPA axis activation subsequently leads to the increased production of stress hormones³²⁴. This is likely to be mediated by PGE₂ as intracerebral PGE₂ injection is sufficient to induce the same response³³⁰. The impact that enhanced HPA axis activity has on behaviour will be discussed in Section 1.4.3.1.

Activated endothelial cells may also perpetuate the immune response by secreting cytokines into the brain and into the periphery. In support of this, LPS has been shown to stimulate cytokine production, including IL-6 and TNF α , in brain endothelial monolayers³³¹. Whilst cytokines were secreted from both the luminal and abluminal sides of the monolayers, IL-6 production was 2-fold greater on the abluminal side, suggesting that IL-6 might be released into the brain in a polarised manner. In addition to enhanced cytokine production, activated endothelial cells upregulate cytokine receptor expression in response to intravenous inflammatory cytokine administration or intraperitoneal LPS injection. This has been documented for both TNF α receptor subtypes, TNFR1 (p55) and TNFR2 (p75), and both components of the IL-6 receptor, IL-6R and gp130^{312,313}. Upregulation of cytokine receptor expression is likely to enhance the ability of endothelial cells to respond to circulating cytokines. This may result in increased activation of the cerebral vasculature and thus enhanced transduction of immune signals into the brain.

Taken together these reports suggest that, via different mechanisms, LPS and inflammatory cytokines, particularly IL-1 β , can activate cells associated with the cerebral vasculature. By inducing COX-2 and mPGES expression, this leads to elevated PGE₂ production. In turn, PGE₂ activates the HPA axis, thus mediating the transduction of inflammatory signals across the BBB. In parallel, activated endothelial cells of the BBB produce cytokines whilst simultaneously increasing

cytokine receptor expression. This is likely to perpetuate endothelial cell activation and enhance immune signal transduction from the periphery to the brain.

1.4.2.3 Leukocyte infiltration

As described in Section 1.2.2.2, a steady flow of leukocytes migrate from the blood to patrol the brain. To do this they must cross one of the two cellular barriers that protect the brain from the periphery; the BBB or the BCSFB. During homeostatic conditions, this process is highly exclusive (briefly described in Section 1.2.2.2). However, following inflammatory insult, either peripheral or central, the restrictions that govern leukocyte entry to the brain become more relaxed. The consequences, which range from enhanced adhesion of leukocytes to the cerebral vasculature to mass immune cell invasion of the CNS, depend on the nature of the inflammatory insult.

Following an inflammatory insult to the CNS, the expression of adhesion molecules is upregulated by cerebral vasculature endothelial cells. This phenomenon is best characterised in neuroinflammatory disorders in which leukocyte infiltration of the CNS plays a prominent role, such as ischemic stroke and MS. Ischemic stroke triggers an inflammatory response in the brain. The central production of cytokines and chemokines results in the activation of the cerebral vasculature and the subsequent recruitment of neutrophils and monocytes from the peripheral blood. Amongst the adhesion molecules that are upregulated by the cerebral vasculature in response to ischemic stroke are P- and E- selectin and Ig superfamily member, ICAM-1³³². These adhesion molecules play a crucial role in pathology as their neutralisation leads to a reduction in infarct volume, and mortality rate, whilst improving neurological outcome³³². ICAM-1 induction is thought to be mediated by IL-1 β . In support of this, ICAM-1 expression following cerebral ischemia is reduced in mice which overexpress IL-1 α ³³³. The firm adhesion of ICAM-1 to integrins, present on the surface of leukocytes, requires chemokine-mediated G α_i signalling pathway activation. The presence of a number of chemokines on the BBB endothelium has been well documented in response to ischemic stroke. Of note is the presence of CXCL8, CCL2 and CCL3 which have all been implicated in the recruitment of monocytes and neutrophils to the brain during pathology³³². Thus, stroke-induced

inflammation leads to elevated adhesion molecule expression and chemokine presentation by the cerebral vasculature.

Leukocyte infiltration of the brain is also a cardinal feature of both MS and EAE. Current dogma suggests that MS is initiated by autoreactive T cells which enter the immune-specialized CNS under the pretext of immunosurveillance^{153,156,232,332}. As described in Section 1.2.2.3, these T cells most likely encounter their cognate antigen displayed by APCs in the CSF. This leads to a robust inflammatory response which subsequently facilitates T cell infiltration across the BCSFB and the BBB. PSGL-1 is expressed by most encephalitogenic T cells in the CNS of mice with EAE. It has the capacity to bind to P-, E- or L-selectin³³⁴ thus may be involved in lymphocyte tethering to the BBB during MS. In support of this, immunohistochemical analysis has identified the expression of E selectin in the cerebral vasculature associated with MS lesions³³². In addition, CD4+ T cells from MS patients express elevated levels of PSGL-1 and have an enhanced ability to cross an *in vitro* model of the inflamed BBB³³². ICAM-1 and VCAM-1 are also associated with MS lesions³³⁵. Moreover, the ligands for these adhesion molecules, integrins lymphocyte function-associated antigen 1 (LFA-1) and very late antigen 4 (VLA-4) respectively, are expressed by infiltrating inflammatory leukocytes³³⁵. Activation of these integrins undoubtedly involves interactions between chemokine receptors on the leukocyte cell surface and one of the many chemokines that are upregulated in the brain during pathology. A brief outline of some of the chemokine systems that have been implicated in MS pathology has been given in Section 1.3.1.2. During MS, inflammatory leukocytes also infiltrate the CSF across the BCSFB. The precise mechanisms governing this recruitment remain to be defined. However, within the choroid plexus, inflammatory conditions have been shown to upregulate epithelial expression of both ICAM-1 and VCAM-1 and also to induce *de novo* mucosal addressin cellular adhesion molecule (MadCAM-1) expression¹⁵¹. Therefore central inflammation, induced by autoreactive T cells, leads to elevated adhesion molecule expression on both the BCSFB and the BBB. This, coupled with a massive central induction of inflammatory chemokines leads to immune cell invasion of the CSF and the brain parenchyma.

Elevated adhesion molecule expression and enhanced recruitment of leukocytes to the BBB endothelium can often be a feature of CNS disorders. However, the

same has been reported following peripheral inflammatory insults. Systemic administration of LPS can activate the BBB endothelium leading to an upregulation of ICAM-1 and P- and E-selectin³³⁶⁻³³⁸. This enhances the rolling and tethering of activated lymphocytes to the vasculature^{339,340}. Activation of the BBB endothelium, characterised by enhanced expression of VCAM-1, has also been documented in a mouse model of hepatic inflammation²⁴¹. BBB activation was associated with enhanced rolling and adhesion of monocytes to the cerebral vasculature and subsequent parenchymal invasion. Thus, activation of the BBB endothelium and recruitment of leukocytes to the brain is not a phenomenon that is limited to CNS disorders.

Inflammatory cytokines are implicated at various stages of leukocyte recruitment to the brain. As described above, IL-1 β induces ICAM-1 expression during cerebral ischemia. In addition, intraventricular IL-1 β injection has been shown to induce ICAM-1 protein, and CCL2 mRNA expression, in the cerebral vasculature which lead to the central recruitment of monocytes and neutrophils³⁴¹. Adhesion molecules such as ICAM-1 and VCAM-1, and inflammatory chemokines, can also be induced by TNF α . As described in Section 1.3.1.3, following the induction of hepatic inflammation, TNF α was shown to play a role in central CCL2 production and subsequent monocyte recruitment²⁴¹. Furthermore, inflammatory cytokines, such as TNF α , IL-1 β and IL-6, have been shown to disrupt BBB integrity²⁴¹. Thus, cytokines have an intrinsic role in enhancing adhesion molecule expression, increasing chemokine production and increasing BBB permeability. These effects relax the conditions required for leukocyte recruitment to the brain.

By enhancing the production of inflammatory mediators, infiltration of leukocytes into the CNS will likely potentiate the central inflammatory response. This may have downstream implications on behaviour. In support of this, Pollack *et al.* demonstrated that the transient sickness behaviours that are associated with EAE preceded neurological deficits but coincided with the leukocyte infiltration of the brain, the central induction of inflammatory cytokines and the hypothalamic production of PGE₂³⁴². Furthermore, blocking leukocyte recruitment to the brain prevented the induction of sickness behaviours that are associated with hepatic inflammation²⁴¹. The mechanisms by which inflammatory cytokines impact behaviour are described in Section 1.4.3. Taken together,

these reports demonstrate that during inflammatory CNS diseases, and some peripheral inflammatory diseases, adhesion molecules are upregulated by endothelial cells of the cerebral vasculature. This, in association with the enhanced production of chemokines in the CNS, culminates in leukocyte recruitment across the BBB. Furthermore, the elevated production of cytokines in the brain that accompanies inflammatory cell invasion may have a potent impact on behaviour.

1.4.2.4 Neuronal transmission

The vagus nerve extends from the brain and innervates the viscera. Not only does it play an integral role in modulating responses in the periphery, but afferent projections carry information from the viscera to the nucleus of the solitary tract²⁶⁶. Secondary projections in turn relay this information to a number of different brain regions. Secondary projection sites include regions of the brain that are relevant to behaviour, including the paraventricular nucleus of the hypothalamus, which has a role in the activation of the HPA axis (see Section 1.4.3.1), and the central amygdala which has a role in fear conditioning and social behaviour^{266,343}. The role of the vagus nerve in transmitting immune signals to the brain became apparent when it was demonstrated that intraperitoneal administration of LPS led to neuronal activation, characterised by activation of the transcription factor Fos (protein product of c-Fos), in both primary and secondary projection areas of the vagus nerve²⁶⁶. Since then a number of studies have been aimed at identifying the functional significance of this peripherally-induced neuronal activation, with particular relevance to its effect on sickness behaviours.

Vagotomy experiments have been repeatedly used to determine the role of the vagus nerve in LPS or IL-1 β -induced sickness behaviours. Several groups have reported that the fever response to IL-1 β or LPS is attenuated in vagotomised rodents^{287,344,345}. However, the results of these studies have been highly variable with a number of other groups reporting that the LPS- or IL-1 β -induced fever response is unaffected in vagotomised rodents^{289,346,347}. General dogma suggests that the effect of vagotomy on IL-1 β - or LPS-induced fever may be dose-dependent. In IL-1 β - or LPS-challenged mice, vagotomy has been shown to attenuate the monophasic fever induced by low doses of either stimulus,

whereas the biphasic fever induced by high doses was unaffected^{345,346}. However, this rule has not been consistent as a separate study demonstrated that vagotomy had no effect on fever regardless of the administered dose of IL-1 β ²⁸⁹. Several other consequences of vagotomy have been described, such as an attenuation of hyperalgesia³⁴⁸ and activation of the HPA axis³⁴⁹ following peripheral LPS or cytokine challenge, despite having no effect on central IL-1 β production³⁵⁰. Moreover, the reduction of social exploration that occurs following peripheral IL-1 β administration was attenuated in vagotomised rats²⁸⁹. To summarise, by relaying immune signals to the brain, the vagus nerve plays a role in mediating LPS- or cytokine-induced CNS responses. However, this role appears to be partial and most likely occurs in parallel to other routes of immune-to-brain communication.

1.4.3 Mechanisms of cytokine-induced behavioural changes

Once peripheral immune signals are transmitted to the brain, they can have a profound effect on neural circuitry, leading to activation of the neuroendocrine system and altered neural transmission and plasticity. Individually, each of these actions has the capacity to impact mood and behaviour, as will be discussed below. However, in reality, these actions are likely to occur in parallel. In addition, to a certain extent, each of the effects described below will have an impact on each other. The relative induction of each will probably depend on the nature and duration of the inflammatory insult. Thus, a number of mechanisms exist whereby peripheral inflammation can alter brain function to promote sickness behaviours or in extreme cases, depression or anxiety.

1.4.3.1 HPA axis activation

The complex network of interactions between the hypothalamus, the pituitary gland and the adrenal glands collectively constitute the HPA axis. By modulating a major part of the neuroendocrine system, the HPA axis coordinates the body's response to stress. Both physical and 'psychological' stress trigger the production of corticotrophin releasing factor (CRF) from the paraventricular nucleus (PVN) of the hypothalamus³⁵¹. CRF subsequently stimulates the release of adrenocorticotrophic hormone (ACTH) from the anterior pituitary gland into the circulation. In turn, circulating ACTH induces the secretion of glucocorticoids

(cortisol in humans or corticosterone in rodents) from the adrenal glands³⁵¹. By binding to glucocorticoid receptors (GRs), situated in various tissues throughout the body, these hormones exert a multitude of effects on the periphery and the brain. Not only do glucocorticoids control metabolism, modulate the growth of bone and muscle and suppress the immune system but they also act as neuromodulators, impacting neuronal survival, proliferation, excitability and signalling³⁵¹. GRs are widely expressed throughout the brain, particularly in regions which are known to govern mood, behaviour and cognition, such as the dorsal raphe nucleus, the hippocampus and other regions of the limbic system³⁵¹. It is therefore unsurprising that aberrant activation of the HPA axis is associated with neuropsychiatric disorders like depression and anxiety.

Under steady state conditions, the HPA response is rapid and short-lived. Various feedback mechanisms exist which dampen HPA axis activity. Not only do glucocorticoids exert potent anti-inflammatory effects on the immune system but they reduce further CRF release from the PVN and subdue ACTH secretion from the pituitary³⁵². When these negative feedback mechanisms are impaired, it can lead to an exaggerated HPA axis response. This is assumed to occur in a proportion of patients with major depression who consistently present with elevated levels of cortisol in their plasma, urine and CSF³⁵². Interestingly, a significant literature indicates that GR expression and function is impaired in depressed patients^{353,354}. Furthermore, cortisol production could not be suppressed by the administration of a GR agonist, dexamethasone³⁵⁴. These data suggest that this group of depressed patients develop glucocorticoid resistance as a consequence of altered GR function and expression. By leading to impaired negative feedback of the HPA axis, this is at least partially responsible for the exaggerated HPA axis responses that are associated of major depression.

In a proportion of depressed individuals, antidepressant therapy has been shown to restore GR expression and function^{353,354}. In doing so, antidepressants restore the intrinsic negative feedback mechanisms of the HPA axis, thus normalising its activity. This has led to the hypothesis that hyperactivation of the HPA axis may in fact contribute to pathology. Ridder *et al.* have subsequently corroborated this using genetically manipulated mice which underexpress the glucocorticoid receptor. Mimicking the impaired receptor function observed in depressed individuals, these mice are significantly more prone to depressive-like symptoms

than their wild type littermates when exposed to environmental stressors³⁵⁵. Therefore, as well as being associated with depression, hyperactivation of the HPA axis might also play a role in pathology.

Inflammatory cytokines are strongly implicated in influencing various stages of HPA axis activation in response to either physical or psychological stress. There is evidence demonstrating that immune challenge, whether as a result of bacterial or viral infection or exposure to recombinant cytokines or LPS, triggers the activation of the HPA axis in both patients and rodents³⁵⁶. Ultimately, this leads to elevated levels of ACTH and glucocorticoids in the circulation. Although many cytokines have been implicated in inducing HPA activity, IL-1B is generally considered to be the most potent. Unlike other inflammatory cytokines, IL-1B activates the HPA axis consistently across models and species³⁵⁶. In fact, in many cases, immune-induced activation of HPA axis can be abrogated in IL-1 receptor (IL-1R)-deficient mice, or by administration of IL-1ra³⁵⁷. However, blocking IL-1B activity has variable effects on HPA axis activation in rodents following systemic LPS injection. For example, numerous reports suggest that IL-1B has a pivotal role in triggering the HPA response to endotoxin^{284,356-358}. However, Dunn *et al.* and Ebusui *et al.* demonstrated that blocking the effects of IL-1B, using IL-1ra, had no significant effect on HPA axis activation following the systemic administration of LPS^{359,360}. Furthermore, Kozak *et al.* showed a normal rise in circulating corticosterone in IL-1B-deficient mice in response to LPS²⁸². Thus, IL-1B may not be the sole, or indeed the principle mediator of HPA responses following LPS injection. These conflicting findings are likely dependent on a number of variables, such as; the species or strain of rodent used in the experimental model, the dose and strain of LPS that was administered, the route of LPS administration or the time elapsed following injection. For example, Perlstein *et al.* demonstrated that, following LPS challenge, IL-1B, IL-6 and TNF α acted synergistically to activate the HPA axis³⁶¹. However, the predominance of each cytokine in triggering an ACTH response depended on the dose of LPS administered and the time point at which ACTH concentrations were assessed following LPS injection. Taken together, these reports suggest that, although cytokines have a fundamental role in activating the HPA axis following inflammatory insult, the precise involvement of individual cytokines may depend on the nature of the immune challenge.

Cytokines, particularly IL-1 β , also play a role in modulating HPA axis activation in response to psychological stress. Numerous rodent stress models have been shown to induce IL-1 β expression and subsequent protein production in a variety of brain regions (Reviewed in Ref 357). Included in these brain regions are the hypothalamus and the pituitary where IL-1 β secretion has been shown to occur rapidly following inescapable footshock³⁶². IL-1 β is also implicated in the stress response in humans. Many studies utilising various forms of stressful stimuli have demonstrated that IL-1 β production in the periphery is enhanced in response to stress³⁵⁷. The importance of this cytokine in modulating the body's stress circuitry has been defined by blocking its action in rodent stress models. For example, Shintani *et al.* established that central administration of IL-1ra prior to the induction of immobilisation stress led to a dampening of the HPA response³⁶³. Moreover, Goshen *et al.* demonstrated that activation of the HPA axis was impaired in IL-1RI-deficient mice following exposure to mild stress³⁶⁴. In contrast, following the induction of severe stress, HPA axis activation in IL-1RI-deficient mice was comparable to that in wild-type mice³⁶⁴. Consequently, although signalling through the type I IL-1R plays a key role in modulating the HPA axis in response to certain stressors, it is not the sole mediator of HPA axis activation following severe stress.

The main mechanism of inflammatory cytokine-induced HPA axis activation is arguably the hypothalamic induction of CRF. Intraperitoneal IL-1 β -injection has been shown to enhance the secretion of both CRF from the hypothalamus and ACTH from the pituitary. However, IL-1 β -induced ACTH production has been shown to be dependent on hypothalamic CRF as it can be ameliorated by administering CRF-specific antibodies^{365,366}. HPA activation may also be partially mediated by the direct effect of cytokines on the pituitary gland. Although there have been conflicting reports regarding the ability of pituitary cells to secrete ACTH in response to cytokines *in vitro*³⁶⁵⁻³⁶⁷, an *in vivo* study by Kariagina *et al.* demonstrated that systemic LPS injection could induce ACTH and corticosterone production in CRF deficient mice³⁶⁸. This response was coupled with increased IL-1 β , IL-6 and TNF α expression in the pituitary and thus may have been initiated by the action of these cytokines on ACTH-secreting pituitary cells. A direct effect of inflammatory cytokines on the adrenal glands has also been

proposed³⁵⁶. Although this has been substantiated by *in vitro* studies, it is not clear to what extent this occurs *in vivo*.

Finally, cytokines have been shown to affect the negative feedback mechanisms of the HPA axis. Via a number of different inflammatory signalling pathways, various cytokines have been shown to interfere with the function of the glucocorticoid receptor and its translocation to the nucleus³⁶⁹. In doing so, these cytokines can contribute to glucocorticoid resistance which, as described above, may have an impact on behaviour and depressive symptoms. Thus, not only do cytokines induce activation of the HPA axis but they can also impair the negative feedback mechanisms that are employed by glucocorticoids. By leading to an exaggerated HPA axis response, prolonged exposure to cytokines could potentially contribute to depressive symptoms.

1.4.3.2 Neurotransmitter modulation

Monoamine neurotransmitters, such as serotonin and dopamine, play a pivotal role in modulating emotion, behaviour and cognition. Consequently, dysregulated monoamine transmission is proposed as a component of the pathophysiology of neuropsychiatric disorders. Both serotonin and dopamine have been linked to major depression. As a result, selective serotonin reuptake inhibitors (SSRIs), which modulate serotonin transmission, are the most common and effective drugs used to combat depression. In addition to major depression, altered serotonin transmission is also associated with anxiety and obsessive compulsive disorder (Reviewed in Ref 370), whereas altered dopamine transmission is commonly associated with attention-deficit hyperactivity disorder, schizophrenia and psychosis³⁷¹⁻³⁷³. Indeed the majority of anti-psychotic drugs target dopamine receptors³⁷². Intriguingly, monoamine transmission can be modulated on a number of levels by inflammation. As a result, through its impact on both the serotonergic and dopaminergic systems, the central upregulation of inflammatory cytokines, which occurs as a result of peripheral inflammation, may have a profound impact on mood and behaviour.

A number of mechanisms control monoamine transmission, one of which involves high affinity monoamine reuptake at neuronal synapses. With regards to serotonin and dopamine, this is mediated by the serotonin transporter (SERT)

and the dopamine transporter (DAT) respectively. Inflammation is one of many factors which can regulate the activity and expression of these transporters. Treatment of both neurons and astrocytes with inflammatory cytokines, such as IL-1 β and TNF α , results in elevated SERT expression and significantly enhanced reuptake activity^{374,375}. This is thought to occur through cellular activation of the p38 mitogen-activated protein kinase (MAPK) signalling pathway. In a proof of concept study, directly linking peripheral immune activation to elevated SERT activity, Cavanagh *et al.* used single positron emission computed tomography to demonstrate that blocking TNF α in patients with rheumatoid arthritis led to a 20% reduction in SERT activity³⁷⁶. Furthermore, injecting mice systemically with LPS has been shown to increase both DAT and SERT activity^{377,378}. The latter effect led to enhanced symptoms of behavioural despair in an IL-1RI-dependent manner³⁷⁸. Increased DAT expression has also been reported in patients with major depression³⁷³. Thus, peripheral inflammation has been shown to modulate the activity of monoamine transporters; an effect that may have a direct impact on behaviour.

In parallel to their effect on SERT and DAT activity, inflammatory cytokines can also impact the biosynthesis of monoamines. This occurs indirectly. Dopamine biosynthesis is impaired as a result of IFN α -induced NO production in the brain³⁷⁹. The effects of inflammatory cytokines on serotonin biosynthesis occur via activation of IDO, the rate-limiting enzyme in the degradation of tryptophan (Figure 1.4). Not only is tryptophan an essential amino acid, but it is a precursor for the biosynthesis of serotonin. Both LPS and IFN γ have been shown to activate IDO. LPS-induced IDO activation is dependent on the p38 MAPK signalling pathway and involves the intermediary and synergistic effects of inflammatory cytokines IL-1 β , IL-6 and TNF α ³⁸⁰. However, IFN γ enhances IDO expression and activity in a manner dependent on the transcription factors, signal transducer and activation of transcription (STAT)-1 and IFN regulatory factor (IRF)-1³⁸¹. By converting the available tryptophan into kynurenine, IDO activation is thought to have a negative impact on the levels of serotonin biosynthesis and may thus impact mood. Indeed blocking IDO has been shown to attenuate LPS-induced depression-like behaviours in mice³⁸¹.

In addition to reducing tryptophan availability, cytokine-induced IDO activation leads to the generation of a number of neuroactive metabolites which may also

contribute to depressive symptoms. In support of this, peripheral administration of kynurenine, the breakdown product of IDO-induced tryptophan catabolism, was sufficient to induce depression-like behaviours in mice³⁸¹. In the CNS, kynurenine will either be converted to quinolinic acid (QUIN) by microglia or kynurenic acid (KA), by astrocytes (Figure 1.4). QUIN and KA agonise and antagonise N-methyl-D-aspartate (NMDA) receptors respectively and thus have opposing effects on glutamate release (for review see Ref 382). QUIN is excitotoxic, stimulating glutamatergic activity whilst simultaneously inducing oxidative stress. Cytokine-induced excitotoxicity may have an impact on neural plasticity. This will be discussed in more detail in Section 1.4.3.3. In contrast, by inhibiting glutamate release, KA is neuroprotective³⁸². However, as dopamine release is partially regulated by glutamate³⁸³, elevated KA may lead to a dampening of dopamine transmission.

Although QUIN-mediated excitotoxicity can be neurotoxic, a defined link between neurotoxicity and depressive symptoms has yet to be established. However, recent clinical evidence suggests that glutamate may have a role to play in the pathophysiology of depression. Elevated levels of glutamate have been observed in the serum of depressed patients, and in regions of the brain associated with the limbic system^{384,385}. This may be due to enhanced glutamate release³⁸⁶, decreased metabolism³⁸⁷ or reduced uptake³⁸⁸. Importantly, targeting glutamatergic transmission, either using the NMDA antagonist ketamine^{389,390}, or riluzole which inhibits glutamate release³⁹¹, can have potent and rapid antidepressive effects. Therefore QUIN-mediated glutamate production, as a result of increased IDO activity, may play a role in inflammation-induced behavioural deficits. However, the putative behavioural effects of enhanced IDO activation may be dependent on the relative induction of neuroprotective KA versus the neurotoxic QUIN.

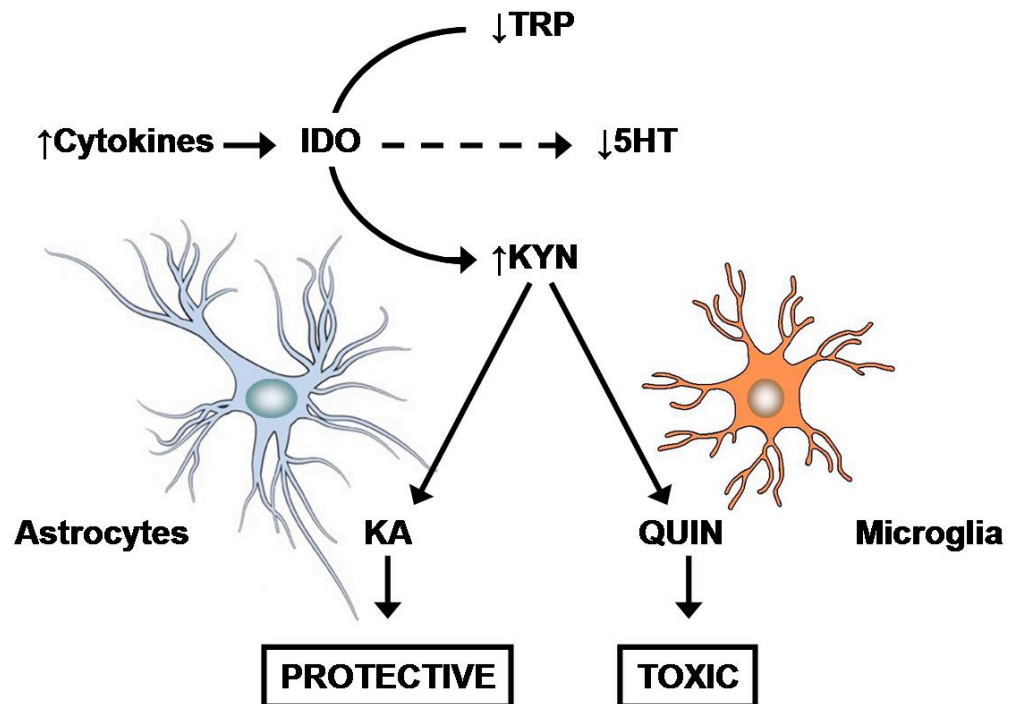


Figure 1.4 The kynurenine pathway.

Tryptophan (TRP), the essential amino acid precursor for serotonin (5-HT), is oxidised through the enzymatic action of indoleamine 2,3 dioxygenase (IDO). This process can be modulated by inflammatory cytokines, which induce the activity of IDO. By enhancing TRP oxidation, cytokine-induced IDO activity may limit 5HT biosynthesis. Furthermore, enhanced IDO activity will increase levels of kynurenine (KYN), the major metabolite of TRP degradation. KYN can be further metabolised in glial cells to generate one of two neuroactive metabolites; kynurenic acid (KA) in astrocytes or quinolinic acid (QUIN) in microglia. KA is an N-methyl-D-aspartate (NMDA) receptor antagonist and is thus neuroprotective. However, as an NMDA receptor agonist, QUIN can induce glutamatergic activity. In addition, the breakdown of KYN to QUIN is associated with reactive oxygen species. Glutamatergic activity and oxidative stress can collectively lead to CNS excitotoxicity making QUIN neurotoxic.

Taken together, these reports suggest that inflammatory cytokines, produced in the brain in response to systemic inflammation, can affect both the biosynthesis of monoamines and their reuptake at the synapse. By leading to impaired monoamine transmission, these collective effects are likely to adversely affect mood and behaviour.

1.4.3.3 Cytokines modulate neural plasticity

Like chemokines, inflammatory cytokines, such as IL-1 β , IL-6 and TNF α , and their receptors are constitutively expressed at low levels in the brain. However, following a pathogenic insult, the levels of cytokines in the brain increase dramatically. Under homeostatic conditions, these cytokines are thought to play a role in modulating synaptic plasticity by regulating neurotrophic support, regulating neurogenesis and controlling the balance of excitatory glutamatergic activation and inhibitory GABAergic activation. Through these actions, alterations to central cytokine concentrations as a result of inflammation, may impact neuronal firing patterns causing behavioural anomalies.

The hippocampus is part of the limbic system and plays a major role in memory formation³⁹². It is one of two regions of the brain where neurogenesis persists into adulthood. A proportion of patients with major depression have reduced hippocampal volume³⁹³. Moreover, antidepressants have been shown to enhance neurogenesis both in humans and in animal models³⁹⁴⁻³⁹⁶. This has led to the hypothesis that impaired hippocampal neurogenesis may contribute to the pathophysiology of depression. In agreement with this, hippocampal neurogenesis was required for the behavioural effect of antidepressants in mice³⁹⁷. Many factors are thought to influence the rate of neurogenesis, including stress and inflammation. For example, reports have demonstrated that systemic administration of IFN α or LPS markedly reduced hippocampal neurogenesis in rodents, as did exposure to chronic stressors³⁹⁸⁻⁴⁰¹. These effects can be ameliorated by blocking the effects of inflammatory cytokines. Decreased neurogenesis induced by IFN α or chronic stress was attenuated by blocking the effects of IL-1 β ^{398,400}. Following systemic LPS injection, neurogenesis was restored via the administration of a non-steroidal anti-inflammatory agent, indomethacin³⁹⁹. These reports suggest a causative role of inflammatory cytokines in reducing hippocampal neurogenesis.

A number of mechanisms have been proposed to account for the observed cytokine-induced reduction in neurogenesis. Not only is the IL-1RI expressed by hippocampal neurons *in vivo*, but hippocampal neural progenitor cells proliferate *in vitro* in response to IL-1 β ³⁹⁸. This suggests a potential direct effect of IL-1 β on hippocampal neurons. IL-1 β can also dampen neurogenesis indirectly via

activation of the HPA axis (Section 1.4.3.1). There is considerable evidence linking HPA axis activation and impaired neurogenesis. For example, Goshen *et al.* demonstrated that the elevated HPA axis activation and simultaneous reduction in neurogenesis that typically occurs in response to stress, does not occur in IL-1RI-deficient mice⁴⁰¹. Moreover, the administration of corticosterone was sufficient to cause a reduction in neurogenesis in both wild type and IL-1R deficient mice. This implies that IL-1 at least partially mediates its effects on neurogenesis via activation of the HPA axis. Contrary to the inhibitory effects that HPA axis activation has on neurogenesis, suppressing neurogenesis in animal models has been shown to result in increased activation of the HPA axis⁴⁰². Thus, a negative feedback mechanism may occur, which perpetuates the simultaneous enhancement of HPA axis activation and reduction of neurogenesis. Increased activation of the HPA axis could account for the proposed impact that reduced neurogenesis may have on behaviour (Section 1.4.3.1).

Another mechanism that may contribute to a cytokine-induced reduction in neurogenesis is reduced levels of hippocampal brain-derived neurotrophic factor (BDNF). BDNF is a neurotrophic regulatory factor which is downregulated in the hippocampus of rodents in response to IL-1 β or LPS administration⁴⁰³ and in the circulation of patients treated with IFN α ⁴⁰⁴. BDNF has a multitude of functions. In addition to controlling neuronal survival, differentiation, transmission and plasticity, BDNF has a role in promoting neurogenesis⁴⁰⁵. Therefore, inflammatory cytokines or LPS may adversely affect neurogenesis by causing a decrease in hippocampal BDNF production.

Due to its pleiotropic nature, a sustained decrease in BDNF levels might negatively affect neuronal function in a number of ways other than neurogenesis. As BDNF promotes survival, neuronal viability may be impaired. Supporting this, the loss of dopaminergic neurons in response to peripheral LPS injection was prevented by BDNF infusion into the striatum⁴⁰⁶. It is unclear what impact, if any, these effects have on behaviour. Patients treated with IFN α presented with reduced circulating BDNF levels regardless of whether they developed depression⁴⁰⁴. However, an allelic variant of the BDNF gene, that causes reduced BDNF production, is associated with depression levels following IFN α -therapy⁴⁰⁴. Consequently, a cytokine-induced reduction in BDNF levels can

affect neural plasticity via a number of different mechanisms and this, in turn, may have a downstream impact on behaviour.

Inflammatory cytokines have been shown to elevate the expression of glutamate receptors whilst at the same time reduce the expression of GABA receptors at the synapse⁴⁰⁷. In addition, cytokines can further enhance glutamatergic activity by increasing glutamate release and decreasing glutamate reuptake via the downregulation of glutamate transporter expression in a manner that would appear to be dependent on NO production⁴⁰⁸⁻⁴¹⁰. Thus, prolonged or excessive inflammation could tip the excitatory/inhibitory balance in favour of excitatory glutamatergic transmission. In combination with an IDO-induced breakdown of kynurenine to QUIN (Section 1.4.3.2), these effects could potentially induce CNS excitotoxicity. Damage to highly sensitive neurons and oligodendrocytes in regions of the brain associated with emotions, behaviour and cognitive function may contribute to some of the effects of cytokine-induced psychiatric disorders.

To summarise, inflammatory cytokines, induced in the brain in response to systemic inflammation, can impact neural plasticity through a number of mechanisms. These effects which lead to dampened neurogenesis, diminished neurotrophic support and elevated glutamatergic transmission, may collectively increase activation of the HPA axis, reduce neurogenesis, adversely effect neuronal viability and trigger CNS excitotoxicity. However, the downstream impact that altered neural plasticity has on mood and behaviour following peripheral inflammation remains to be fully established.

1.5 Thesis aims

The immune system and the nervous system are not as distinct as was once thought. Both systems utilise cytokines and chemokines as a method of communication and they appear to interact in a bidirectional manner. Inflammation in the periphery has been shown to have an impact on mood and behaviour. Furthermore, there is evidence to suggest that depressive disorders could influence the levels of inflammatory mediators in the periphery.

As described above, the brain can become sensitised to the occurrence of a peripheral inflammatory response by a number of mechanisms which act in

parallel. However, the biological pathways that culminate in the onset of neuropsychiatric symptoms remain to be fully defined. *The overall aim of this thesis was to establish a more in-depth understanding of the bidirectional relationship, and communication pathways, that exist between the immune system and the nervous system.* In doing so, I sought to identify potential mechanisms that could account for inflammation-induced behavioural changes.

1. The aim of Chapter 3 was to determine what impact an acute exposure to systemic LPS had on neurological transcriptional modulation.
2. The aim of Chapter 4 was to use different sterile, and TLR-dependent, models of peripheral inflammation to investigate the molecular mechanisms involved in modulating of gene expression in the brain following peripheral LPS injection.
3. Employed by both the immune system and the nervous system, chemokines are prime candidates for orchestrating inter-system communication. Thus the aim of Chapter 5 was to establish whether chemokine transcription was induced in the brain following a series of systemic LPS injections. Due to their well characterised role in coordinating leukocyte migration, an additional aim of this chapter was to determine whether chemokine induction triggered an influx of leukocytes to the brain following systemic LPS exposure.
4. Having highlighted a number of chemokines that could potentially mediate leukocyte recruitment to the brain following systemic LPS challenge, the aim of Chapter 6 was to optimise a protocol that would enable these chemokine systems to be compared to those involved in MS.

2 Materials & Methods

2.1 General Reagents & Buffers

2.1.1 Materials & Reagents

Unless otherwise specified, all chemicals, kits and reagents were purchased from Life Technologies.

All plastics were purchased from BD Biosciences unless stated otherwise.

2.1.2 Buffers

0.5M EDTA (pH8): 186.1g ethylenediaminetetraacetic acid (EDTA) (Sigma Aldrich) and 20g NaOH (Sigma Aldrich) was dissolved in 900ml distilled H₂O (dH₂O), adjusted to pH8 using HCl (Sigma Aldrich) and then made up to 1L using dH₂O.

MACS Buffer: 500ml phosphate-buffered saline (PBS), 2ml 0.5M filter sterilised EDTA and 10ml foetal calf serum.

PEA Buffer: 500ml PBS, 1ml 0.5M filter sterilised EDTA and 2.5ml 4.5% human albumin (Bio Products Laboratory).

Tris-acetate EDTA (TAE) Buffer: A 50x stock solution of TAE buffer was made by dissolving 242g Tris base (Sigma Aldrich) in 750ml dH₂O. 57.1ml glacial acetic acid (Sigma Aldrich) and 100ml 0.5M EDTA was then added and the buffer was made up to 1L with dH₂O. Before use, stock buffer was diluted 1:50 in dH₂O.

10mM Tris-EDTA (TE) Buffer: 1M Tris-EDTA buffer (Sigma Aldrich) was diluted 1:100 with nuclease-free H₂O before use.

2.2 In Vivo Procedures

2.2.1 Animal welfare

All animals were housed within the Biological Services Central Research Facility and Joint Research Facility at the University of Glasgow. Animals were maintained in specific pathogen-free conditions and given access to food and

water *ad libitum*. All experiments received ethical approval and were performed under the auspices of a UK Home Office Licence.

2.2.2 Mice

6-7 week old, male C56BL/6 mice were purchased from Harlan laboratories. Before experimental procedures were carried out, mice were given a week to acclimatise. After procedures, mice were culled using a recognised schedule 1 technique.

2.2.3 Induction of systemic inflammation using LPS

2.2.3.1 Acute model

Systemic inflammation was induced in 8 week old C57BL/6 mice by intraperitoneal (I.P.) injection of LPS (*Escherichia Coli*, serotype 055:B5; Sigma Aldrich). 100µl of 1mg/ml LPS, or an equivalent volume of vehicle (sterile PBS), was injected into the peritoneal cavity. Mice were culled 6 hours, 12 hours or 48 hours after LPS, or vehicle, challenge.

2.2.3.2 'Chronic' endotoxin tolerance model

To induce endotoxin tolerance, C57BL/6 mice were injected (I.P.) with a single 100µl dose of 0.5mg/ml LPS, or an equivalent volume of vehicle (sterile PBS), daily for 2, 5 or 7 consecutive days. Mice were culled 24 hours after final injection.

2.2.4 Induction of systemic inflammation using TNFα

Systemic inflammation was induced in 8 week old C57BL/6 mice by intravenous (I.V.) injection of recombinant murine TNFα (Peprotech). 100µl of 10µg/ml TNFα, or the equivalent volume of vehicle (sterile dH₂O), was injected into the tail vein at 0 and 24 hours. Mice were culled 6 hours or 24 hours after final injection.

2. 90% EtOH	1 hour
3. 95% EtOH	1 hour
4. 100% EtOH	3 x 2 hours
5. Xylene	3 x 2 hours
6. Paraffin wax	2 x 4 hours

2.3.3.2 Tissue embedding

Processed brain tissue was divided into 3 coronal sections using a brain slicer. Coronal sections were orientated appropriately and embedded into wax blocks using the Histocentre 3 (Thermo Scientific, Massachusetts, US). Blocks were stored at room temperature until required for further sectioning.

2.3.3.3 Tissue sectioning

Embedded tissue blocks were cut into 5µm sections using a microtome. Sections were mounted onto charged frosted microscope slides (Superfrost Plus, VWR) and stored at room temperature until required for histological analysis.

2.3.4 Preparation of brain samples for gene expression analysis

Brains were dissected from mice as described above and cut in half (sagittally) through the interhemispheric fissure using a scalpel. Right hemispheres were placed in cryovials (Alpha Laboratories) and snap frozen in liquid nitrogen. Frozen tissue was stored at -80°C to maintain RNA integrity until required for RNA purification.

2.3.5 Isolation of plasma from peripheral blood

Mice were culled by a recognised schedule 1 technique. Blood was collected from the right atrium, in 20µl EDTA, with a 1ml syringe. Blood was transferred to 1.5ml eppendorf tubes (Greiner) and plasma was separated from blood cells by centrifugation for 10 minutes at 300g. The plasma was then transferred to 1.5ml eppendorf tubes and centrifuged at 3000g for 5 minutes to pellet remaining

platelets. Platelet-free plasma was collected as the supernatant and stored at -80°C until required for protein expression analysis.

2.3.6 Isolation of leukocytes from peripheral blood

Mice were culled by a recognised schedule 1 technique. Blood was collected from the right atrium in 20µl EDTA with a 1ml syringe. Blood was transferred to 1.5ml eppendorf tubes and blood cells were pelleted by centrifugation for 10 minutes at 300g. After removing the plasma, pelleted blood cells were added to a 15ml falcon tube with 5ml 1x red blood cell lysis buffer (Miltenyi) and incubated for 7 minutes at room temperature. 10ml of PBS was added to each sample and the cells were pelleted by centrifugation for 7 minutes at 300g. The supernatant was decanted and pelleted cells were washed with 15ml PBS. Cells were centrifuged as before, resuspended in 1ml PBS and transferred to 1.5ml eppendorf tubes. Cells were pelleted by centrifugation for 5 minutes at 600g. The supernatant was aspirated and the cell pellets were lysed in 700µl RLT buffer (Qiagen). Lysed samples were homogenised by centrifugation through a Qias shredder column (Qiagen) for 2 minutes at 13 000g and stored at -80°C to maintain RNA integrity until required for RNA purification.

2.3.7 Isolation of bone marrow

Mice were culled by a recognised schedule 1 technique and perfused. Skin, tendons and muscle tissue were stripped from the hind legs and the tibia and femur were dissected from mice by cutting through the connective tissue above the tibia and below the femur at the ankle joint. The bones were cleaned of excess muscle tissue then cut at the top and the bottom using surgical scissors. Using a 23G needle and a syringe, Bone marrow was flushed from the bones with PBS and then pushed through a 70µm cell strainer, using the plunger from a 5ml syringe, to create a single cell suspension. Cell number and viability was determined by staining cells with Trypan blue and counting them using a haemocytometer. Cells were pelleted by centrifugation for 7 minutes at 300g. The cell pellet was washed in PBS and then centrifuged as before. Cells were resuspended to a concentration of 5×10^6 cells/ml. 1ml of each cell sample was transferred to 1.5ml eppendorf tubes. Cells were pelleted by centrifugation for 5 minutes at 600g. Cell pellets were lysed in 700µl RLT buffer. Lysed samples were

homogenised by centrifugation through a Qiasredder column for 2 minutes at 13 000g and stored at -80°C to maintain RNA integrity until required for RNA purification.

2.3.8 Generation of single-cell suspension from brain digests

Mice were culled by a recognised schedule 1 technique and perfused. Brains were dissected from the mice as described above and then kept on ice in HBSS prior to digestion. Brain tissue was finely diced using a scalpel and then each brain was digested in 10ml of digestion cocktail, pre-warmed to 37°C. The cocktail consisted of; 6µg/ml Liberase TM (Roche), 5U/ml DNaseI and 25mM HEPES buffer diluted in HBSS. Samples were shaken at 750rpm for 45 minutes at 37°C. Following digestion, cell suspensions were passed through a 70µm cell strainer. Cells were washed twice with 2mM EDTA in HBSS and centrifuged after each wash at 300g for 10 minutes at 4°C. Cell pellets were then washed in MACS buffer and resuspended in 1.8ml MACS buffer. 200µl of Myelin removal beads (Miltenyi) was added to each sample and samples were incubated at 4°C for 15 minutes. Cells were then washed in MACS buffer, centrifuged as before and resuspended in 2ml MACS buffer. Myelin was removed using the AutoMACS (Miltenyi) programme, DepleteS. Myelin-depleted cells were eluted from the AutoMACS columns in 4ml MACS buffer. Cells were pelleted as before and resuspended in 1ml MACS buffer. Cell number and viability was determined by staining cells with Trypan blue and counting them using a haemocytometer.

2.4 Human Primary Cell Procedures

2.4.1 Patients & clinical samples

Buffy coats were obtained from the NHS as surplus from Scottish National Blood Transfusion Service. All donors gave informed consent and ethics were obtained from the relevant local ethics committee.

2.4.2 Isolation of mononuclear cells from peripheral blood

PBMCs were separated from buffy coats using a density gradient. Blood taken from buffy coats was diluted 1:1 with PEA buffer. 10ml of the diluted mixture was layered on top of 4ml histopaque 1077 (Sigma Aldrich) in a 15ml falcon tube.

Tubes were spun for 20 minutes at 500g with no brake, separating the blood into 4 distinct phases. Peripheral blood mononuclear cells (PBMCs) which collect at the interphase between the plasma and the histopaque were transferred into a 15ml falcon tube using a sterile pasteur pipette. Cells were washed twice with ice-cold PEA, centrifuging for 5 minutes at 350g and decanting the supernatant after each wash. Washed cells were resuspended in PBS to a concentration of 1×10^6 cells/ml.

PBMCs were serially diluted 10-fold to get concentrations of 1×10^5 and 1×10^4 cells/ml. These were transferred to 1.5ml eppendorf tubes into aliquots of 500, 1×10^3 , 5×10^3 , 1×10^4 , 5×10^4 and 5×10^5 cells. PBMCs were pelleted by centrifugation at 600g for 5 minutes. The supernatant was removed and the PBMCs were lysed in RLT buffer. Cells were vortexed in RLT to aid lysis and then stored at -80°C to maintain RNA integrity until required for RNA purification.

2.5 Gene Expression Analysis

2.5.1 RNA purification

2.5.1.1 RNA extraction from cells using silica-membrane technology

RNA was extracted following the RNeasy Mini Kit protocol (Qiagen) and the RNeasy Micro Kit protocol (Qiagen) as described by the manufacturers.

As described previously, cells were lysed in RLT buffer, homogenised using a QiaShredder and stored at -80°C until required for RNA purification. The volume of RLT buffer used depended on cell number:

$<1 \times 10^5$ cells	70 μl RLT
1×10^5 to 5×10^6 cells	350 μl RLT
$>5 \times 10^6$ cells	600 μl RLT

Where specified, 200ng *E. coli* transfer RNA (Sigma Aldrich) was added to the RLT prior to cell lysis.

RNA was precipitated by adding 1 volume of 70% EtOH in nuclease-free H_2O . RNA from each sample was collected by centrifugation through an RNeasy spin

column (Mini Kit) or an RNeasy MinElute spin column (Micro Kit). Spin columns were washed several times to remove any protein impurities and then air dried. Unless specified otherwise, genomic DNA was digested on-column between washes as described in the protocol. RNA was eluted from the RNeasy spin columns into 1.5ml nuclease-free eppendorf tubes (Life Technologies) in 30-100µl nuclease-free H₂O and in approximately 12µl from the RNeasy MinElute spin columns. This was quantified using a nanodrop (Nanodrop 1000, Thermo Scientific) and stored at -80°C to maintain RNA integrity until required for cDNA synthesis.

2.5.1.2 RNA extraction from cells using Trizol

Cells were lysed by vortexing with 800µl of Trizol reagent and the lysate incubated for 5 minutes at room temperature. Where specified, 200ng *E. coli* total RNA was added to the lysate. 160µl of chloroform:Isoamyl alcohol (1:24) (Sigma-Aldrich) was added to each sample, vortexed and incubated for 3 minutes at room temperature. Samples were then spun at 13 000g for 15 minutes at 4°C to separate the mix into 3 distinct phases. The upper aqueous phase of each sample was transferred into 1.5ml nuclease-free eppendorf tubes and the RNA precipitated with 400µl 100% isopropanol (VWR). Samples were incubated for 2 hours at -20°C before being centrifuged at 13 000g for 10 minutes at 4°C. The RNA pellet was then washed with 75% EtOH in nuclease-free H₂O. This was centrifuged at 13 000g for 5 minutes at 4°C and the supernatant discarded. RNA pellets were air-dried and then dissolved in 12µl nuclease-free H₂O.

2.5.1.3 RNA extraction from tissues using Trizol

‘Snap-frozen’ brain tissue was disrupted using a Qiagen TissueLyser. Brain tissue was shaken in 2ml nuclease-free eppendorf tubes, containing 1ml Trizol and a 5mM stainless steel bead (Qiagen), for 10 minutes at 50 oscillations per second. The disrupted tissue and Trizol mixture was then divided between 2x 2ml nuclease-free eppendorf tubes. 500µl Trizol was added to each eppendorf tube. Samples were vortexed and incubated for 5 minutes at room temperature. 200µl of chloroform:Isoamyl alcohol was added to each eppendorf tube, vortexed and incubated at room temperature for 3 minutes. Samples were then spun at 13

000g for 15 minutes at 4°C to separate the mix into 3 distinct phases. The upper aqueous phase of each sample was transferred into 1.5ml nuclease-free eppendorf tubes and the RNA precipitated with 500µl 100% isopropanol. Samples were incubated for 10 minutes at room temperature before being centrifuged at 13 000g for 10 minutes at 4°C. The RNA pellet was then washed with 75% EtOH in nuclease-free H₂O. This was centrifuged at 13 000g for 5 minutes at 4°C and the supernatant aspirated. RNA pellets were air-dried and then dissolved in 50µl nuclease-free H₂O. RNA from each sample was re-combined to give a final volume of 100 µl.

2.5.1.4 Genomic DNA digest using DNA-free™

Where specified, contaminating genomic DNA was removed from RNA samples using a DNA-free™ kit, as described by the manufacturers. Briefly, 1µl of 10x DNase I buffer and 1µl recombinant DNase I was added to 10µl of RNA sample. Reactions were incubated for 20 minutes at 37°C. 1.2µl of DNase Inactivation Agent was added to stop the reactions. Samples were centrifuged and the RNA was then aspirated from pelleted genomic DNA and stored at -80°C until required for cDNA synthesis.

2.5.1.5 RNA clean-up

RNA extracted from tissue was purified using a Qiagen RNeasy Mini kit as described by the manufacturers. 350µl RLT buffer was added to each 100µl sample and mixed by inverting. RNA was precipitated by adding 250µl of 100% EtOH. RNA from each sample was collected by centrifugation through an RNeasy spin column. Spin columns were washed several times to remove impurities and then air dried. Genomic DNA was digested on-column between washes as described in the protocol. RNA was eluted from the RNeasy spin columns in approximately 100µl nuclease-free H₂O. This was quantified using a nanodrop (Nanodrop 1000, Thermo Scientific) and stored at -80°C to maintain RNA integrity until required for cDNA synthesis.

2.5.2 Assessment of RNA integrity

The quality of RNA was assessed by the University of Glasgow Polyomics Facility. Assessment was performed using a 2100 Bioanalyzer (Agilent) on a Nano chip or

Pico chip in accordance with manufacturer's instructions. All chips and reagents used were supplied in the RNA 6000 Nano kit (Agilent) or the RNA 6000 Pico kit (Agilent).

RNA was diluted in nuclease-free H₂O to the required concentration.

Pico chip

Total RNA	50-5000 pg/ml
mRNA	250-5000 pg/ml

Nano chip

Total RNA	5-500 ng/ml
mRNA	25-250 ng/ml

65µl of gel matrix was mixed with 1µl of a nucleotide-specific dye. To prime the chips, 9µl of the gel-dye mix was applied to the appropriate wells. Pressure was applied using a priming syringe (supplied) to disperse the gel-dye mix throughout the microfluidics of the chip. 9µl was also applied to an additional 2 wells as described in the protocol.

After priming, 5µl of RNA 6000 marker was applied to each of the sample wells and also the ladder well of each chip. 1µl of ladder was then pipetted into the ladder well and 1µl of each diluted RNA sample was added to each of the sample wells. Chips were vortexed briefly to mix contents and then RNA was separated in a microchannel according to size using the 2100 Bioanalyzer.

2.5.3 Microarrays

Microarrays were run at the University of Glasgow Polyomics Facility. Prior to array, the quality of purified RNA was verified as described above. Purified RNA was sent to the Glasgow Polyomics Facility where it was amplified by *in vitro* transcription (IVT) and converted to sense-strand cDNA using an Ambion WT Expression kit (Life technologies). cDNA was then fragmented and labelled using a GeneChip WT Terminal Labelling kit (Affymetrix). Fragmented cDNA was then loaded and run on GeneChip mouse gene 1.0 ST arrays (Affymetrix). All procedures were carried out as described by the manufacturers.

2.5.4 Microarray analysis

Raw data from the microarray study were provided by the University of Glasgow Polyomics Facility and analysed using Parkek Genomics Suite v6.5 and Genespring GX software v10. Details of the analyses are described in detail in the text (Chapter 3).

2.5.4.1 DAVID Bioinformatics

Gene ontology terms were assigned to differentially expressed genes using the Database for Annotation, Visualization and Integrated Discovery (DAVID) Bioinformatics Resources v6.7 (<http://david.abcc.ncifcrf.gov/>). Analysis was performed in accordance with two protocols outlined by Huang *et al.*^{411,412}. Significance of enrichment was determined using a modified Fisher's Exact test and a Benjamini-Hochberg multiple testing correction was used to correct for the rate of type I errors. Co-expression of a gene cluster was considered significant if it satisfied a p-value cut-off of 0.05.

2.5.4.2 Ingenuity pathway analysis

Genes were grouped into canonical pathways using Ingenuity Pathway Analysis software (Ingenuity® Systems, www.ingenuity.com). Significance of differentially altered pathways was determined using a Fisher's Exact test and a Benjamini-Hochberg multiple testing correction was used to correct for the rate of type I errors. Enrichment of a pathway was considered significant if it satisfied a p-value cut-off of 0.05.

2.5.4.3 Interferon signature analysis

The potential of different IFN subtypes to regulate differentially expressed ISGs was determined using the Interferome database v1.0 (<http://interferome.its.monash.edu.au/interferome/home.jsp>). Interferome is a database of ISGs, established from a compilation of data from microarray and proteomic experiments in which cells or tissues have been treated with different types of IFNs⁴¹³.

2.5.5 cDNA Synthesis

Unless otherwise stated, cDNA was synthesised using Quantitect Reverse Transcription kit (Qiagen). cDNA required for applications involving TaqMan gene expression assays was synthesised using the High Capacity RNA-to-cDNA kit. When stated, the SuperScript III Reverse Transcription kit was used as a potential alternative to the High Capacity kit.

Regardless of the method used, for each experimental group, cDNA synthesis reactions were accompanied by 2 control reactions:

1. -RT control: Reverse transcriptase (RT) was substituted for nuclease-free H₂O to control for genomic DNA contamination.
2. No template control: Template RNA was substituted for nuclease-free H₂O to control for contamination of reagents.

2.5.5.1 Quantitect

To first eliminate contaminating genomic DNA (gDNA) from the RNA template, the following DNase-digests were set up in 0.2ml nuclease-free PCR tubes:

Template RNA ($\leq 1\mu\text{g}$)	$\leq 12\mu\text{l}$
7x gDNA Wipeout Buffer	2 μl
Nuclease-free H ₂ O*	
Total volume	<u>14μl</u>

*Reaction made up to 14 μl in H₂O.

The contents were mixed by pulse centrifugation. To eliminate gDNA, reactions were incubated at 42 °C for 2 minutes before being placed on ice to stop the reaction.

To perform the reverse transcription reaction, the following master mix was assembled and then added to the contents of each tube to give a final reaction volume of 20 μl :

Quantiscript RT*	1µl
5x Quantiscript RT Buffer	4µl
RT Primer Mix	1µl
Total volume	<u>6µl</u>

*Substituted with 1µl nuclease-free H₂O in -RT control reactions.

Tubes were pulse centrifuged to mix. The RT reaction was carried out in a thermocycler set for the following programme:

1. 42 °C 15 minutes
2. 95 °C 3 minutes
3. 4 °C Forever

cDNA was diluted 1:5 in nuclease-free H₂O and stored at -20 °C until required for gene expression studies.

2.5.5.2 High Capacity RNA-to-cDNA

To perform reverse transcription using the High Capacity RNA-to-cDNA kit, the following components were assembled in 0.2ml nuclease-free PCR tubes:

Template RNA (≤2µg)	≤9µl
2x RT Buffer	10µl
20x RT Enzyme Mix*	1µl
Nuclease-free H ₂ O†	
Total Volume	<u>20µl</u>

*Substituted with 1µl nuclease-free H₂O in -RT control reactions.

†Reaction made up to 20µl in H₂O.

Contents were mixed by pulse centrifugation. Reverse transcription was carried out in a thermocycler set for the following programme:

1. 37°C 60 minutes
2. 95°C 5 minutes
3. 4°C Forever

cDNA was stored neat at -20°C until required for gene expression studies.

2.5.5.3 SuperScript III

Prior to reverse transcription, the following reactions were set up in 0.2ml nuclease-free PCR tubes:

Template RNA (<500ng)	≤8μl
Random Hexamers (50 ng/μl)	1μl
dNTP Mix (10mM)	1μl
Nuclease-free H ₂ O*	
Total volume	<u>10μl</u>

*Reaction made up to 10μl in H₂O.

After mixing contents by pulse-centrifugation, tubes were incubated at 65°C for 5 minutes in a thermocycler, to denature RNA, and then placed on ice for at least 1 minute.

A master mix was prepared, containing the following reagents:

10x First Strand Buffer	2μl
MgCl ₂ (25mM)	4μl
DTT (0.1M)	2μl
RNaseOUT (40 U/μl)	1μl
SuperScript III RT (200 U/μl)	1μl
Total Volume	<u>10μl</u>

*Substituted with 1μl nuclease-free H₂O in -RT control reactions.

10µl of master mix was added to each reaction to create a total reaction volume of 20µl. Contents were mixed by pulse centrifugation. Reverse transcription occurred in a thermocycler set for the following programme:

1. 25°C 10 minutes
2. 50°C 50 minutes
3. 85°C 5 minutes
4. 4°C Forever

cDNA samples were collected by pulse centrifugation. After the addition of 1µl RNaseH (2 U/µl), samples were incubated for 20 minutes at 37°C in a thermocycler.

cDNA was stored neat at -20°C until required for gene expression studies.

2.5.6 Polymerase chain reactions

Polymerase chain reactions (PCRs) were performed using pre-made red PCR master mix (Roalab) as described below:

Red PCR mastermix	45µl
Forward primer	0.5µl
Reverse primer	0.5µl
Template cDNA	1-2µl
Nuclease-free H ₂ O*	
Total Volume	<u>50µl</u>

*Reaction made up to 10µl in H₂O.

PCR reactions were run in a thermocycler set for the following programme:

1. 95°C 3 minutes

2. 95 °C	15 seconds	} 35-40x cycles
3. 60 °C	15 seconds	
4. 72 °C	45 seconds	
5. 72 °C	5 minutes	
6. 4 °C	Forever	

2.5.6.1 Electrophoresis of PCR products

Electrophoresis was used to separate the PCR products according to size through a 2% agarose gel containing ethidium bromide. To form a 2% agarose gel, the appropriate weight of agarose (Sigma-Aldrich) was added to TAE buffer and heated in the microwave until dissolved. Ethidium bromide was then added and the melted agarose was poured into a gel cassette. Combs were inserted into the cassette and the agarose gel was left to cool and set. Gels containing PCR products were run in TAE buffer for 45-60 minutes at 100 volts. To verify that the products were the correct size, they were compared to a DNA ladder. Hyperladder IV (Bioline) was used for products <1000 bp whereas Hyperladder I (Bioline) was used for products <10kb. The visualisation of PCR products was performed under UV light using an Alpha 2200 Digital UV-Visphoto Imager (Alpha Innotech).

2.5.7 Quantitative real-time PCR

2.5.7.1 Primer design

To perform quantitative real-time PCR (QPCR), a set of specific primers had to be designed to amplify each target gene. The design of these primers had to adhere to a stringent set of conditions to ensure the accuracy and efficiency of the reaction. In addition to designing primers for use in the QPCR reaction, an additional set of primers had to be designed in order to create PCR products to act as standard templates.

All primers were designed using Primer3 Input software version 0.4.0 (<http://frodo.wi.mit.edu/>).

Specification for QPCR primers:

Primer size	18 to 24 base pairs (bp) (20 bp optimal)
Melting temperature (T _m)	59.5 °C to 61 °C (60 °C optimal)
GC content	40% to 65% (50% optimal)
Max self complementarity	3 (≤2 optimal)
Max 3' complementarity	1
Amplicon size	≤150bp

To create standard templates for each target gene, standard primers were designed that would amplify the region in which the QPCR primers would bind. These primers were designed using similar parameters as outlined above; however, the size of the amplicon could vary between 100bp and 2000bp and if the software did not return any suitable results, the maximum self complementarity could be increased to 5. Standard primers were designed to flank the amplicon targeted by the relevant QPCR primers and the adjacent 20bp on either side.

All primers were synthesised by Integrated DNA Technologies. The specificity of the primer sequences (Table 2.1 & Table 2.2) was first assessed using the free online bioinformatics resource, Basic Local Alignment Search Tool (<http://blast.ncbi.nlm.nih.gov/Blast.cgi>). Following acquisition of the primers, their specificity was confirmed by running a PCR reaction using any cDNA containing the transcript of interest. Primers were considered specific if they amplified a single product of the appropriate size.

Gene Name	Forward Primer (5' - 3')	Reverse Primer (5' - 3')
Apobec3	TTC ACC CGT CTC CCT TCA	AGC GTG GAT GTT GTC CTT GT
C4	TGA CTG CCT TCG TGC TGA	TGC TCT GTG GAT GAC TGG AC
Ccl2	CTC ACC TGC TGC TAC TCA TTC A	CCA TTC CTT CTT GGG GTC A
Ccl3	CAG CCA GGT GTC ATT TTC CT	CAG GCA TTC AGT TCC AGG TC
Ccl5	CTA CTG CTT TGC CTA CCT CT	ACA CAC TTG GCG GTT CCT T
Ccr1	GCC CTC ATT TCC CCT TCA A	CGG CTT TGA CCT TCT TCT CA
Ccr3	GAT TGC CTA CAC CCA CTG CT	CGG AAC CTC TCA CCA ACA A
Ccr5	TTT GTC CTG CCT TCA GAC C	TTG GTG CTC TTT CCT CAT CTC
Ctsc	AGG CCA CAC AGC TAT CAG TT	TTG CCA ACA AAG CAA GCC CA
Cxcl1	GCT TGC CTT GAC CCT GAA	TGT CTT CTT TCT CCG TTA CTT GG
Cxcl2	AAG TTT GCC TTG ACC CTG AA	TCT CTT TGG TTC TTC CGT TG
Cxcl10	GCT CAA GTG GCT GGG ATG	GAG GAC AAG GAG GGT GTG G
Cxcr2	TGT CTG CTC CCT TCC ATC TT	CCA TTT CCT CTC CTC CAC CT
Cxcr3	AGT GCT TGT CCT CCT TGT AGT TG	GGT GTT GTC CTT GTT GCT GA
Fcgr4	CGT GGC ATC AAA TCA CAT TC	CCG CAC AGA GAA ATA CAG CA
Gbp2	CCA AGC GAG ATG CCT TTA TC	TTC TTC TTC CAG GGG TCC A
Gbp3	AGT TCC AGA AGA AGC TGG TGG TCA	AGT TCA GCC TGG CAG TGA CGA ATA
Gbp4	CCT CCT TCC TCT TTC TTC TTC CTT T	GTG TTT CTA TGG GGG TGT GG
Gbp6	AAA CAC ACT CCC TCT CCC AGT	TGA AGC CAG TCA ACA TCC AG
Ifit1	GAC AAG GCA ATC ACC CTC TAC T	TCT TTC AGC CAC TTT CTC CAA
Ifitm3	CGC TCC ATC CTT TGC CCT TCA GTG	GCC CCC ATC TCA GCC ACC TCA T
Igrm1	AGT TCA GCA GGT AGC CCA GA	TCA GCC TCA GTT TCC ACT CC
Il1b	CGC TCA GGG TCA CAA GAA AC	GAG GCA AGG AGG AAA ACA CA
Il2rg	CGG AAG CCT GAA CAT CAA TC	CCA AGG TGA GTA GGG GAG GT
Il6	TTC CAT CCA GTT GCC TTC TT	ATT TCC ACG ATT TCC CAG AG
Irf7	GAA GAG GCT GGA AGA CCA ACT	AGA TAA AAC GCC CTG TGC TG
Lcn2	TGA ATG GGT GGT GAG TGT GGC TGA	TCC TTG GTA TGG TGG CTG GTG GG
Lgals3bp	ATT CCT GTG TCC CCT CCT TC	GTG AGT GCT GGC TGA AAC CT
Ly6a	ACC TCC ACC CTT GTC CTT TT	GAG CAC CTA CCT ACC CAG CA
Oasl2	AGC GAG CGA GGG ATG TTC AGG T	TGG GGC TGT AGG GGT TTG TCC AG
Pglyrp	TCT GGA ATG TGG GGG TGT CTC	TTT GGA TGA CCT GAT AGA GTT GG
Rtp4	GCA TCT TTG GGT GAG AAG AT	ATG GGG AGG AAC TCT TTG GT
Saa3	TCT TCC TGT TGT TCC CAG TCA	CCC AGT AGT TGC TCC TCT TCT C
Serpina3n	ACA GCC TGG AGG ATG TCC TTT CAA	TGG TTC CTG TGA TTG CAG ACA GGT
Sp100	CAT CAT TTT CCT TGG CTG GT	CAT TTT GGT TGG TCC TTG CT
Stat1	GAA AAA CGC TGG GAA CAG AA	CGA CAG GAA GAG AGG TGG TC
Tbp	TGC TGT TGG TGA TTG TTG GT	AAC TGG CTT GTG TGG GAA AG
Tnfa	CAC CAC CAT CAA GGA CTC AA	GAG GCA ACC TGA CCA CTC TC

Table 2.1 QPCR primer sequences

Gene Name	Forward Primer (5' - 3')	Reverse Primer (5' - 3')
Apobec3	GGA CCA TTC TGT CTG GGA TG	GGA GGG TGA GGG GAG ATA AA
C4	GAG CCC TTC TTG TCC TGT TG	AGT TTG CCT TGG TGA TGG AG
Ccl2	CAC CAG CAC CAG CCA ACT	GCA TCA CAG TCC GAG TCA CA
Ccl3	CCA CGC CAA TTC ATC GTT	TAT GCA GGT GGC AGG AAT GT
Ccl5	CCC TCA CCA TCA TCC TCA CT	TCA GAA TCA AGA GGC CCT CTA TCC
Ccr1	ACT TTG GCA TCA TCA CCA G	CTC AGA TTG TAG GGG GTC CA
Ccr3	GCC ATC CGT CTT ATT TTT GTT G	ATT TCT TGC TCC CCA GTT GA
Ccr5	ACC CAT TGA GGA AAC AGC AA	CTT CTG AGG GGC ACA ACA AC
Ctsc	GCT TTC TCT GCC ATC TGC TC	CTT CCA CCA CCC CAA AAT C
Cxcl1	CTG GGA TTC ACC TCA AGA ACA	CTT TTC GCA CAA CAC CCT TC
Cxcl2	CGC CCA GAC AGA AGT CAT AG	ACT CAC CCT CTC CCC AGA AA
Cxcl10	CGA TGG ATG GAC AGC AGA GAG CCT	GAC AAG GAG GGT GTG GGG AGC A
Cxcr2	CGG GGT TCC TTC TTG TCT TT	TGC TAT GTT CCT GTG TGA GG
Cxcr3	TGG GGT CTC TGT CTG CTC TT	TTT GCC TCT CCC TCT TCT CA
Fcgr4	AAC GGC AAA GGC AAG AAG T	TGG GGC AGA GAA AGT GTA AAA
Gbp2	TTT GTG GGC TTC TTT CCA AC	CTT TGC TGC CTC TGT GAG TG
Gbp3	CCC CAG AGA GGA CAA AGT GA	ACC CCC CAG GAA CAG AGA AAG
Gbp4	TTG GTT TTG TGA GGG CAT TT	ATC CAG TAA GGG GAG GCA GT
Gbp6	GTC TTC TCT TCC CCC ACC TC	GGC TCC CAA TAA AAC CGC AC
Ifit1	GCA AGA GAG CAG AGA GTC AAG GCA	GCA GGG TTC ATT TCC CCA GTG AGC
Ifitm3	TCT GAG AAA CCG AAA CTG CCG CA	TGT AGG GAG GGG CAA GGA GGG A
Igrm1	CTG CTC CAC TAC TCC CAA C	CTC TCC AGC CCA AAA ACA AA
Il1b	CAC TCA TTG TTG CTG TGG AG	ATG TGC TGG TGC TCA TTC A
Il2rg	CCA GAG AAA GAA GAG CAA GCA	GAA AGA GGG CAA GGG ACA C
Il6	TCC AGA AAC CGC TAT GAA GT	CTC CAG AAG ACC AGA GGA AA
Irf7	CTG TGA CCC TCA ACA CCC TAA	GAG CCC AGC ATT TTC TCT TG
Lcn2	TTC CGG GGC AGG TGG TAC GTT	AAG ACA GGT GGA TGG GGA GTG CTG
Lgals3bp	TGG TCA TAC GCC CCT TCT AC	CAC AGG AAA TCC CAC AGG AC
Ly6a	GGA GGC AGC AGT TAT TGT GG	ACT CAA CAG GGG GAC ATT CA
Oasl2	AGA AAG GGA TGG GAA CAG GTG GCT	GGG TCG GGG ACT AAG CAG GGT T
Pglyrp	TGT TGT TTG CCT GTG CTC TC	CTG AGT CTT TGT TGG GGG TCA A
Rtp4	AGA CAG TGC TTG GCA GGT TC	CTA TGG GGA AGG GCA TTT TT
Saa3	ACC ACT TCC GAC CTG CTG	GCA CAT TGG GAT GTT TAG GG
Serpina3n	TGA CAA TGG GAC ACA ACT GG	AGG GGT AGG GGA CAA GAC AA
Sp100	CCG AAT GGG TCA TCC TTA GA	TCT TTT TCT GCG TCG TTG TG
Stat1	CCT ATG AGC CCG ACC CTA TT	GGA AGC AGG TTG TCT GTG GT
Tbp	GAG TTG CTT GCT CTG TGT GCT G	ATA CTG GGA AGG CGG AAT GT
Tnfa	TCT GTG AAG GGA ATG GGT GT	GGC TGG CTC TGT GAG GAA

Table 2.2 Standard primer sequences

2.5.7.2 Generation of standard templates

In order to quantify expression levels of target genes, a standard curve consisting of PCR signal versus known DNA copy numbers was generated. This was done by performing a PCR reaction using the standard primers to amplify a region of cDNA containing the amplicon of interest. PCR products were separated by gel electrophoresis. The appropriately sized products were cut from the gel and purified using a QIAquick Gel Extraction kit (Qiagen) in accordance with the manufacturer's instructions. The quantity of DNA present in the purified standards was assessed using the nanodrop 1000.

The absolute number of amplicon copies present in each standard was determined using the following calculation:

$$\text{Copies per } \mu\text{l} = \frac{(\text{Concentration (g/}\mu\text{l)}) \times \text{Avogadro's Constant}}{\text{Molecular weight of amplicon}}$$

$$\text{Molecular weight} = \text{Size of amplicon (bp)} \times 660^* \text{ (Daltons)}$$

*Average molecular weight for 1 base paired nucleotide.

Purified standards were diluted 1×10^{-2} in TE buffer and stored at -20°C until required for QPCR.

2.5.7.3 QPCR

cDNA was synthesised as described previously. QPCR amplifications were performed on each cDNA sample in triplicate within wells of either a 96-well PCR plate (Star Lab) or a 384-well PCR plate (Star Lab). A standard curve was generated by serially diluting the purified standards 10-fold in nuclease-free H_2O to obtain dilutions of between 1×10^{-5} and 1×10^{-9} . Each dilution was included on QPCR plates in triplicate.

A master mix containing the following reagents was prepared for each primer pair:

96-Well PCR Plate

SYBR® Green FastMix*	7.5µl
----------------------	-------

Nuclease-free H ₂ O	5.7µl
Forward Primer	0.15µl
Reverse Primer	0.15µl
Total volume	<u>13.5µl</u>

384-Well PCR Plate

SYBR® Green FastMix*	5µl
Nuclease-free H ₂ O	3.8µl
Forward Primer	0.1µl
Reverse Primer	0.1µl
Total volume	<u>9µl</u>

*Purchased from Quanta Bioscience.

Master mix was applied to PCR plates using a multi-channel pipette. 1.5µl of cDNA was added to each well of 96 well PCR plates to create a final reaction volume of 15µl. Alternatively, 1µl of cDNA was added to each well of 384 well PCR plates to create a final reaction volume of 10µl.

QPCR was performed using a Prism® 7900HT Sequence Detection System (Life Technologies) set for the following programme:

1. 95 °C 20 seconds

Then 40 cycles of:

2. 95 °C 3 seconds
3. 60 °C 30 seconds

To confirm the specificity of the QPCR primers a dissociation curve was generated using the following programme:

4. 95 °C 15 seconds
5. 60 °C 1 minute

6. 95 °C 15 seconds

7. 60 °C 15 seconds

2.5.7.4 Determining relative gene expression

Following QPCR, the absolute copy number of QPCR amplicons present in each reaction was calculated from the standard curve. To control for variations in the concentration of RNA used in reverse transcription reactions, data were normalised to the reference gene, TATA binding protein (TBP), as follows:

Normalised copy number = copy number of target gene / copy number of TBP

Fold change values were calculated by comparing the normalised copy number of individual samples to the mean of the control samples.

2.5.7.5 Determining relative transcript expression

When RNA was too low to quantify, relative RNA abundance was assessed by comparing the cycle threshold (CT) values from QPCR amplifications of the reference gene Glyceraldehyde 3-phosphate dehydrogenase (GAPDH). The relative transcript expression (RTE) of GAPDH in each sample was calculated by the following equations:

$$\text{RTE} = 2^x; x = \text{CT}_{\text{Baseline}} - \text{CT}_{\text{GAPDH}}$$

As even slight variations in GAPDH expression levels would skew the results, this method of comparison could only be used when RNA was extracted from the same population of cells.

2.5.8 TaqMan low density array

TaqMan low density arrays (TLDA) were performed using a Prism® 7900HT Sequence Detection System in accordance with manufacturer's guidelines. Array cards were custom-made by Life Technologies to each contain 4 identical panels of 32 different TaqMan assays.

cDNA was synthesised using the High Capacity RNA-to-cDNA kit as described previously. A master mix containing the following reagents was assembled for each sample:

TaqMan Universal Master Mix	100µl
H ₂ O	90µl
cDNA*	10µl
Total volume	<u>200µl</u>

*cDNA reversed transcribed from 1µg RNA.

Using a micropipette, 100µl of sample-specific master mix was loaded into each reservoir of the TLDA cards. Array cards were centrifuged twice at 300g for 1 minute before being sealed using a TLDA sealer provided with the assays. 'Fill reservoirs' were cut from the cards using scissors. The QPCR reactions were then carried out using the following programme:

1. 95 °C 10 minutes

Then 40x cycles of:

2. 97 °C 30 seconds

3. 59.7 °C 1 minute

2.5.8.1 Determining relative gene expression

The relative gene expression of each target gene was then quantified relative to the reference gene TBP using Prism® SDS2.2 software.

The relative gene expression analysis was performed using Prism® SDS2.2 software. The expression of each target gene was first normalised to the reference gene TBP as follows:

$$\Delta CT = CT_{\text{Target gene}} - CT_{\text{TBP}}$$

Then the normalised gene expression in each sample was compared to that of a randomly picked control sample, or calibrator:

$$\Delta\Delta CT = \Delta CT_{\text{Sample}} - \Delta CT_{\text{Calibrator}}$$

Finally the fold change in gene expression, or relative quantification (RQ) value, for each sample, compared to the calibrator, was calculated as follows:

$$RQ = 2^{-\Delta\Delta CT}$$

2.5.9 RNA amplification

RNA was isolated from cells, as described above, and amplified following the SuperScript™ RNA Amplification System protocol, as described by the manufacturers.

First-strand cDNA synthesis

Reactions were set up in 200µl PCR tubes as follows:

Total RNA	<9µl
T7-Oligo(dT) Primers	1µl
DEPC-treated H ₂ O	
Total Reaction Volume	<u>10µl</u>

Contents were mixed by pulse centrifugation. RNA was then denatured by incubating in a thermocycler for 10 minutes at 70°C and then cooled on ice. The following components were then added to each reaction at room temperature:

5X First-Strand Buffer	4µl
0.1M DTT	2µl
10mM dNTP	1µl
RNaseOUT™	1µl
SuperScript™ III RT (200 U/µl)	2µl
Total Reaction Volume	<u>20µl</u>

The tubes were incubated in the thermocycler at 46°C for 2 hours, 70°C for 10 minutes and then placed on ice.

Second-strand cDNA synthesis

The contents from the first strand reaction tubes were added to a 1.5ml microcentrifuge tube along with the following components:

DEPC-treated H ₂ O	91µl
5X Second-Strand Buffer	30µl
10mM dNTP Mix	3µl
DNA Polymerase I (10 U/µl)	4µl
DNA Ligase (10 U/µl)	1µl
Rnase H (2 U/µl)	1µl
Total Reaction Volume	<u>150µl</u>

Tubes were incubated in a refrigerated water bath at 16°C for 2 hours, cooled on ice, then stored at -20°C until required for cDNA purification.

cDNA purification

cDNA was precipitated by adding 500µl of cDNA Loading Buffer and then collected on a silicone membrane by centrifugation through provided spin cartridges. cDNA was then washed with cDNA Wash Buffer, air-dried and then eluted in 100µl DEPC-treated H₂O. The volume of eluate was then reduced to less than 20µl by evaporation using a speed-vacuum centrifuge.

***In vitro* transcription**

DEPC-treated H₂O was added to the purified cDNA to bring the total volume to 23µl. The following components were then added at room temperature:

100mM ATP	1.5µl
100mM CTP	1.5µl
100mM GTP	1.5µl
100mM UTP	1.5µl

10X T7 Reaction Buffer	4µl
T7 Enzyme Mix	7µl
Total Reaction Volume	<u>40µl</u>

After a 16 hour incubation at 37°C, 2µl DNase I was added to each tube. The tubes were then incubated for a further 30 minutes to digest template cDNA.

aRNA purification

Amplified RNA (aRNA) was precipitated by adding 160µl of RNA Binding Buffer followed by 100µl of 100% EtOH. It was then collected on a spin cartridge silicon membrane by centrifugation. RNA was then washed twice with 500µl RNA Wash Buffer, air-dried and eluted in 100µl DEPC-treated H₂O. Purified aRNA was stored at -80°C.

2.6 Protein Analysis

2.6.1 ELISA

Murine plasma cytokines were analysed using DuoSet enzyme-linked immunosorbent assay (ELISA) Development System kits (R&D Systems). As ELISA reactions were performed in half-area 96 well ELISA plates, all the volumes of samples and reagents used were half of the recommended volumes. Otherwise, ELISAs were performed as described in the manufacturer's instructions. All reactions were performed in duplicate.

2.6.2 Flow Cytometry

The relative proportion of cell populations was determined by staining cells for relevant surface antigen. The expression of surface antigen was assessed using a MACSQuant Analyzer (Miltenyi).

A single cell suspension was generated from mouse brains as described in Section 2.3.8. PBL were isolated from whole blood (Section 2.3.6), and strained through nitex mesh. Cells were counted using a haemocytometer. 1×10^6 cells from each sample were transferred to FACS tubes and washed in 2ml MACS buffer. These were then resuspended in 100µl MACS buffer and labelled with fluorochrome-

conjugated antibodies. To prevent non-specific binding, Fc receptors were first blocked by adding 1µl FcR block (Miltenyi) per 1×10^6 sample. Cells were incubated for 10 minutes on ice. To label surface antigen, fluorochrome-conjugated antibodies, as described in Table 2.3, were added to each sample.

Antigen	Fluorochrome	Clone	Dilution	Company
CD3	PE	145-2C11	1/25	eBioscience
CD8	FITC	53-6.7	1/100	BioLegend
CD11b	APC	M1/70	1/100	eBioscience
F4/80	PerCP	BM8	1/100	BioLegend
CD45*	VB	30/F11	1/100	BioLegend
CD45**	AF450	30/F11	1/100	eBioscience

Table 2.3 Fluorescently-conjugated antibodies used for flow cytometry

*Used to identify CD45-expressing cells on days 2 and 5 of LPS time course.

**Used to identify CD45-expressing cells on days 2 and 5 of LPS time course.

5µl of each antibody was added to the cells and cell samples were incubated on ice for 20 minutes in the dark. Labelled cells were washed in 3ml MACS buffer and pelleted by centrifugation at 300g for 10 minutes. Supernatant was decanted and the cells resuspended in 200µl MACS buffer. To discern live from dead cell populations, 1µl of Draq7 (Abcam) was added to each sample.

The surface antigen expression of individual cells from each sample was immediately assessed using a MACSQuant analyzer (Miltenyi) as described by the manufacturers.

2.6.3 Histology

Histology was performed on brain tissue sections by the Veterinary Diagnostic Services Laboratory, a core facility within the University of Glasgow. The primary antibodies used are listed in Table 2.4. These were used with horseradish peroxidase-conjugated anti-rabbit and anti-mouse secondary antibodies from Envision+ System-HRP labeled polymer kits (DAKO).

Antigen	Host Species	Clone	Dilution	Company
CD3	Rabbit	SP7	1/30	Vector
MPO*	Rabbit	GA511	1/1000	Dako
Calprotectin	Mouse	MAC387	1/500	Dako

Table 2.4 Primary antibodies used for immunohistochemistry.

*MPO: Myeloperoxidase

3 Transcriptional profiling of CNS following systemic inflammation

3.1 Introduction and aims

As previously described, systemic infection or inflammation can have a profound effect on the CNS, manifesting in a number of autonomic and behavioural adaptations and increased neuroendocrine activation. These behavioural phenotypes, termed sickness behaviours, occur during acute bacterial or viral infections, but also during chronic inflammatory diseases²⁷⁴⁻²⁷⁶. In the latter case, what would be a beneficial, self-limiting system can become dysregulated. The prolonged depression and anxiety that ensues represents a major burden to patients, not least because these detrimental co-morbidities lead to a poorer clinical outcome.

It is becoming increasingly evident that inflammatory cytokines play a pivotal role in triggering a number of sickness behaviours. This has been discussed in detail in Section 1.4.1. Moreover patients with major depressive disorders, that are otherwise medically healthy, often present with elevated levels of inflammatory cytokines both in their circulation and their CSF²⁷⁶. Thus it would appear that a bi-directional interplay exists between the immune system and the nervous system. The extent to which this inter-system communication impacts the normal functioning of the brain is currently under much scrutiny and a great deal of progress has been made into deciphering neuroimmune communication pathways. However, the precise effect immune activation has on neural circuitry remains unclear. One well characterised model of systemic inflammation which has been used repeatedly to explore routes of neuroimmune communication, involves injecting mice, intraperitoneally, with LPS. Renowned for inducing a multitude of sickness behaviours, LPS-induced inflammation has become a key model in establishing how the brain responds to changes in the peripheral inflammatory milieu.

In the immediate hours following a single injection of LPS, the response in the brain is well characterised. Therefore, the main aim of this chapter was to establish what prolonged impact LPS-induced systemic inflammation had on transcriptional modulation in the brain. To this end, C57BL/6 mice were injected intraperitoneally with a high dose of LPS. Whole brain RNA profiles, 48 hours after injection, were compared to a vehicle injected control group using Affymetrix microarrays. This is a novel approach as most studies focus on the

events in the brain that occur within the initial 12 hours following LPS injection. Microarray analysis generated a list of genes that were differentially modulated in the brain in response to systemic LPS. To determine the biological relevance of this, these genes were subsequently grouped into functional categories and pathways. Therefore, in this chapter, transcriptomics were used to investigate the molecular mechanisms by which inflammation originating in the periphery can induce transcriptional modulation in the brain.

3.2 Acute model of systemic LPS-induced inflammation

To induce inflammation systemically, 8 week old male C57BL/6 mice were injected I.P. with 100 µg of LPS or 100µl of vehicle (sterile distilled H₂O). Mice were terminally anaesthetised, and then perfused, either 6 hours, 12 hours or 48 hours after injection.

3.2.1 Model validation

To confirm peripheral inflammation following systemic LPS challenge, the concentration of inflammatory cytokines in the circulation was measured using ELISAs. ELISAs were performed on plasma samples isolated from LPS- and vehicle-injected mice; 6 hours, 12 hours and 48 hours post-injection. Plasma from all mice injected with LPS displayed significantly elevated levels of IL-1β and IL-6, 6 hours following injection (Figure 3.1). Levels IL-1β returned to baseline between 6 and 12 hours following injection and IL-6 levels remained elevated until 48 hours. Although TNFα could not be detected in the circulation at any of the timepoints assayed, it has previously been shown that TNFα levels peak in the circulation of C57BL/6 mice 2 hours following LPS injection (100 µg i.p.) and then rapidly decline⁴¹⁴. Therefore, injecting LPS systemically initiates an inflammatory response in the periphery, with elevated levels of inflammatory cytokines in the plasma for up to 48 hours.

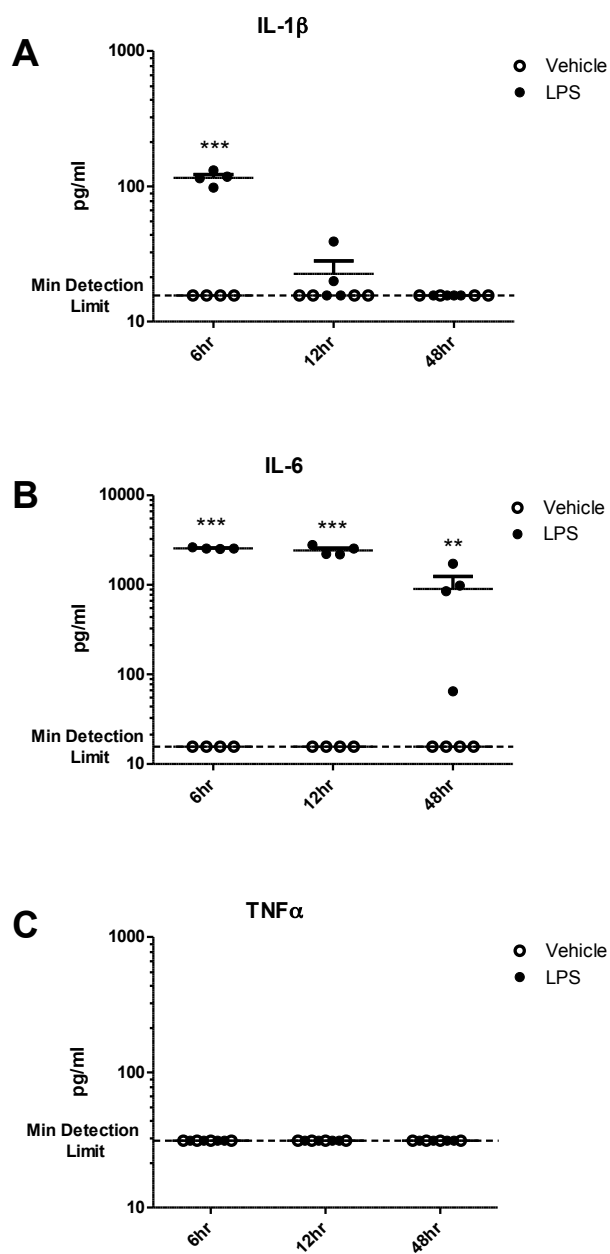


Figure 3.1 Plasma concentration of inflammatory cytokines following systemic LPS injection
 Plasma was isolated from the whole blood of mice; 6 hours, 12 hours and 48 hours following injection with either 100 μ g LPS (I.P.) or an equivalent volume of vehicle. Concentrations of (A) IL-1 β , (B) IL-6 and (C) TNF α in the plasma were determined using ELISA. Data represent the mean \pm SEM. Significance was determined using two-way ANOVA. n = 4/group.

3.2.2 Processing of RNA samples

RNA was extracted from the right brain hemispheres of mice, 48 hours after systemic LPS or vehicle injection. Prior to the microarray analysis, the integrity of extracted RNA samples was assessed using an Agilent 2100 Bioanalyzer. This is a microfluidics-based platform in which nucleotide fragments are separated according to size and evaluated qualitatively using an electropherogram. Using the electropherogram, RNA integrity can be both visually and mathematically assessed using the RNA integrity number (RIN) algorithm. The RIN algorithm screens the electrophoretic trace of each RNA sample and assigns it a RIN score between 1 and 10. This scale, where 10 is perfectly intact and 1 is entirely degraded, is based on the presence or absence of degraded RNA products and the ratio of 28S:18S ribosomal subunit RNA.

Figure 3.2 is an example of an electropherogram exhibiting completely intact RNA. The characteristics of high quality RNA include three distinct peaks; the RNA marker, ribosomal RNA subunit 18S and ribosomal RNA subunit 28S. These are denoted in the electropherogram (Figure 3.2A) by numbers 1, 2 and 3 respectively. Otherwise, there should be very little background noise on the graphs. RNA samples extracted for the microarray study were qualitatively assessed and representative electropherograms from the vehicle-injected and the LPS-injected groups are displayed in Figure 3.2B and Figure 3.2C respectively. The RIN of each sample is listed in Table 3.1. It is recommended that for a sample to be deemed of suitable quality, it should have a RIN of 8 or above. All RNA analysed was of sufficient quality to be used for the microarray study, as exemplified by the high RIN, the clear peaks and the low molecular weight noise visible in the electropherograms.

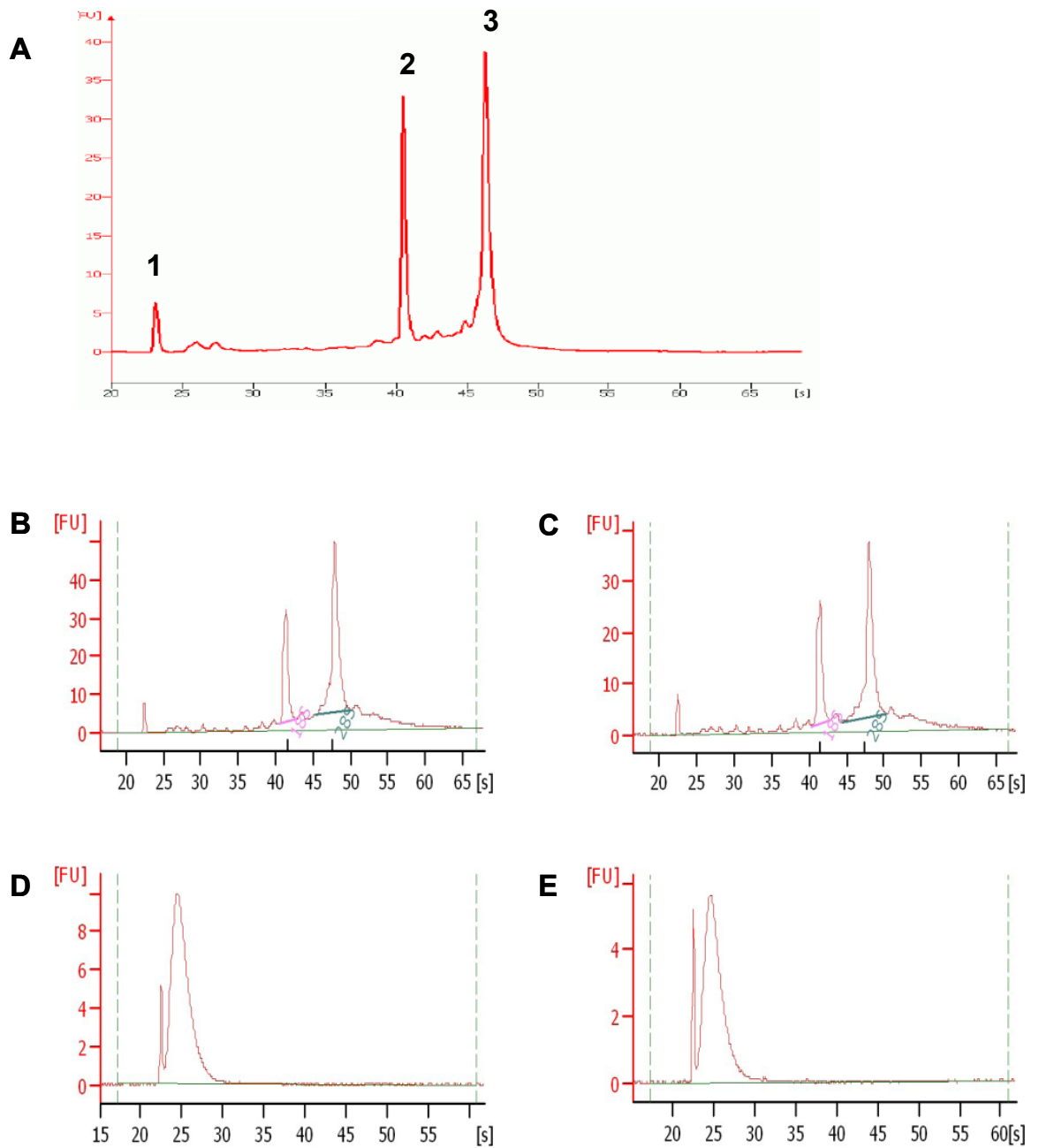


Figure 3.2 Quality of RNA samples and efficiency of DNA fragmentation

RNA was isolated from whole brains, 48 hours after injection with 100 μ g LPS or an equivalent volume of vehicle. Samples were processed for microarray analysis, converted to sense-strand cDNA and then fragmented. Both the quality of the RNA samples and the efficiency of DNA fragmentation were determined using an Agilent 2100 Bioanalyzer. Data are displayed as fluorescence units [FU] over time. (A) Example of high quality total RNA with an RNA integrity value of 10. (B-C) Integrity of whole brain total RNA extracted from; (B) vehicle-injected and (C) LPS-injected mice. (D-E) Fragmented DNA samples from; (D) vehicle-injected and (E) LPS-injected mice. (B-E) Data shown are one representative sample from each group. n = 3/group.

Sample	Ribosomal 28S:18S Ratio	RIN Score
Vehicle 1	1.5	8.9
Vehicle 2	1.4	8.8
Vehicle 3	1.6	9.3
LPS 1	1.7	9.5
LPS 2	1.9	9.5
LPS 3	2.1	9.7

Table 3.1 Integrity of RNA samples

RNA was isolated from whole brains, 48 hours after injection with 100 μ g LPS or vehicle. The ribosomal 28S:18S ratio of each sample was calculated using an Agilent 2100 Bioanalyzer and used to calculate the RNA integrity number (RIN).

Having verified the RNA quality, samples were amplified by in vitro transcription (IVT) and reverse transcribed. The resulting sense-strand cDNA was fragmented and labelled prior to hybridisation. In addition to RNA sample integrity, the efficiency of fragmentation was also checked on the Agilent 2100 Bioanalyzer; this time using a DNA chip. As with the RNA chip, the fragmented DNA was fluorescently labelled and then separated in a microchannel according to size. Fluorescence intensity was measured over time and representative electropherograms from the vehicle-injected and the LPS-injected groups are displayed in Figure 3.2D&E. Each graph exhibits one peak, just adjacent to the DNA marker, suggesting that all DNA fragments, contained in the samples, were of a relatively similar size. It was also apparent that both samples consisted of small DNA fragments, as demonstrated by the short speed at which the fragments moved through the microchannel. Altogether, these data indicate that the RNA samples were of high quality and the fragmentation of the corresponding sense-strand cDNA was successful.

3.3 Determining how systemic LPS injection affects the transcriptional profile of the brain

In order to establish how systemic LPS challenge affects neurological transcriptional modulation, the transcriptional profiles of the brains of three LPS-injected mice were compared to those of three vehicle-injected mice using Affymetrix GeneChip Mouse Gene 1.0 ST arrays. Comprising 764 885 distinct probes, which equates to 28 869 well-annotated gene transcripts, these GeneChips have complete genome coverage. The transcriptome of each sample is interrogated using 25-mer oligonucleotide probes which are specifically

distributed across the entire length of each transcript. Probes are designed for each exon, with a median of 26 probes being specific to each gene transcript. As this system uses probes that anneal to various regions along the length of each gene, these whole-transcript GeneChips are more accurate than the traditional system in which probes localize to the far 3' end of each transcript. As a result, they were an ideal choice of array to use for this study.

3.3.1 Pre-processing of Affymetrix chip data using Partek

Microarrays were performed by the Glasgow Polyomics facility (<http://www.polyomics.gla.ac.uk/>). Data, provided by this core facility, were analysed using Partek Genomics Suite 6.5 software. Prior to analysis, the raw data must be assessed qualitatively and then pre-processed. This occurs in a series of stages, each of which will be described below.

1. Background correction: This corrects for the level of background noise that occurs as a result of non-specific hybridisation.
2. Normalisation: Performed in order to unify the distribution of signal intensities of each chip, thus enabling the comparison and coordinated analysis of data from multiple chips.
3. Summarisation: This first summarises the signal intensities of individual probe sets to exons and then to the corresponding genes; giving each entity a normalised intensity value.

Pre-processing is carried out using an appropriate summarisation algorithm. Although many different summarisation algorithms have been developed, Partek offers only two options; Robust Multi-array Average (RMA) or GCRMA (RMA adjusted for GC content). RMA is considered the most sensitive and specific of the summarisation algorithms and GCRMA is a modified form of RMA. The difference between these two algorithms, which will now be discussed, lies in the background correction step.

3.3.1.1 Background correction of the Affymetrix chips

Background signal intensity is corrected on a chip-by-chip basis. For every set of probes, the observed signal intensity consists of the true intensity, caused by specific hybridisation, and a certain level of background noise, caused by non-specific hybridisation. In order to determine the true intensity, the level of background noise must be established.

The Affymetrix Gene 1.0 ST system uses an innovative design where the background can be determined using 17 000 generic background probes; a comparatively smaller number than previous Affymetrix designs which contain one background probe set to each perfect match (PM) probe set. Instead, these anti-genomic background probes are designed to cover the entire range of GC content. The GCRMA algorithm uses the signal intensities of these probes to determine background. For every transcriptome-interrogating probe set, the GC content is calculated. The background signal, defined as the median signal intensity of all background probes with an equal GC content, is subsequently subtracted from the observed signal of the probe set. The signal that remains is the “true” intensity. In contrast, the RMA summarisation uses a PM only system. Ignoring the background probe intensities, RMA instead takes into account the distribution of the data and applies it to a complex algorithm which models the background signal intensity. This noise level, calculated using RMA, is subsequently subtracted from the observed intensity to obtain the “true” intensity.

The exclusion of background intensities by RMA is thought to reduce noise, however, RMA has the disadvantage that it loses the information that the background probe intensities provide. For that reason, GCRMA was selected to pre-process the dataset.

3.3.1.2 Signal histogram of normalised data

Monitoring of sample hybridisation is an essential step in ensuring the quality of the array data. Whether as a result of user error, or differences in chip manufacturing, variations can occur that affect the reproducibility of the results. Differences in the efficiency of hybridisation can be detected using a set of control transcripts. Prior to hybridisation, fragmented cDNA is added to a

hybridisation cocktail that contains the controls. These consist of standard concentrations of 4 transcripts, bioB, bioC, bioD and cre. BioB is present at a 1.5pM concentration; the detection limit of most arrays. BioC, bioD and cre are present at 5pM, 25pM and 100pM respectively. In order to ensure there are no differences in the efficiency of hybridisation from one chip to the next, the signal intensities of the control transcripts on each chip are plotted on a histogram. Figure 3.3A shows the signal intensities of the 4 hybridisation controls on each of the 6 GeneChips used in the array study. The intensity similarities of each of the controls would suggest that little variation exists between the hybridisation efficiency of each chip.

In addition, the frequency of the signal intensities detected on each microarray chip was also plotted on a signal histogram (Figure 3.3B). After labelled cDNA is hybridised to the chip, signal intensities are calculated for each probe set. The histogram plots the occurring frequency (Y-axis) of a range of signal intensities (X-axis) for all the probe sets on each chip. In addition to controlling for hybridisation quality, this signal histogram controls for other sources of non-biological variation that could affect the results, such as the efficiency of cDNA labelling or starting RNA quantity or quality. Each line on the graph represents a different array chip and these are coloured according to sample grouping. It is clear from the graph that all chips have a similar pattern of signal intensity distribution, therefore ruling out non-biological variables.

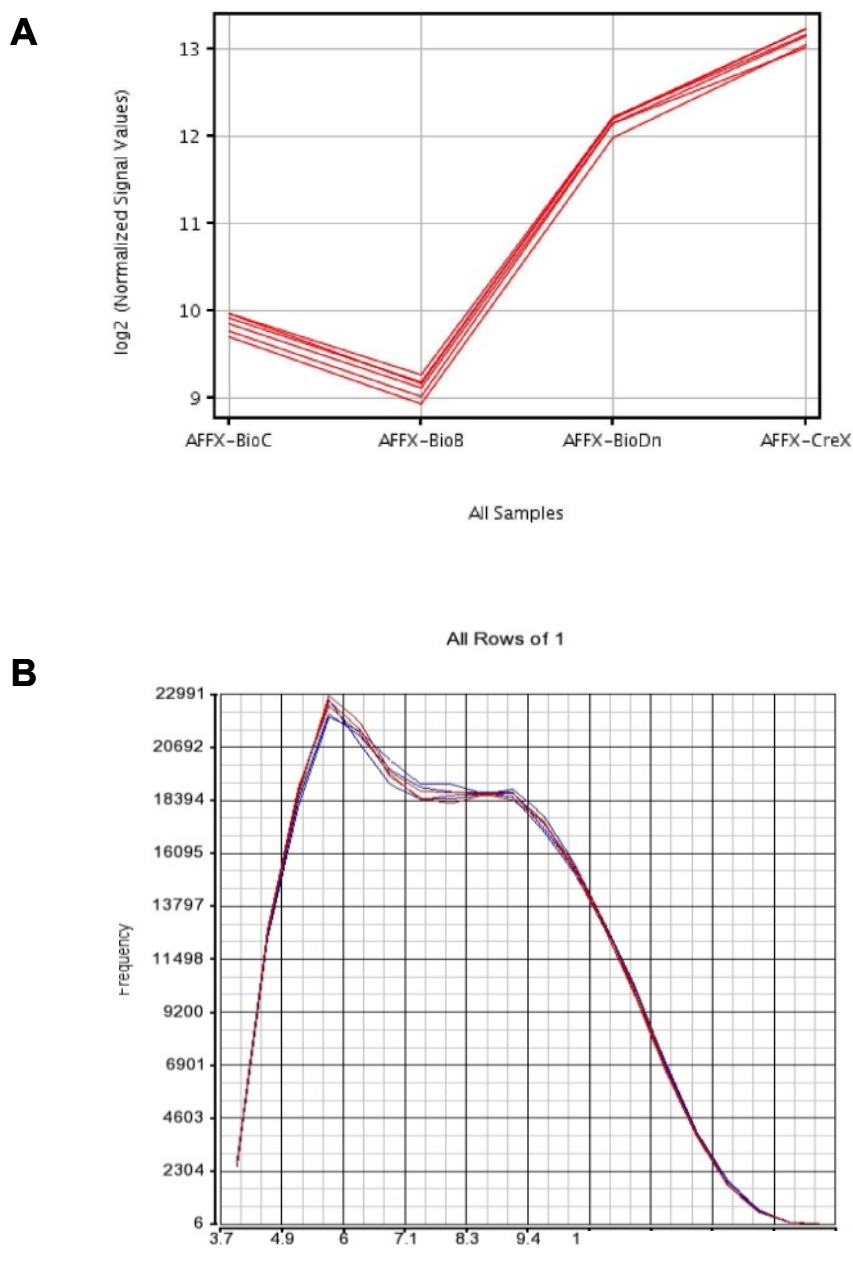


Figure 3.3 Signal histogram of normalised intensity values

A microarray study was performed to compare gene expression in the brains of mice injected with LPS, to a vehicle-injected control group. Labelled sense-strand cDNA was generated from amplified RNA samples and hybridised to each chip along with 4 control transcripts at standard concentrations. Signal intensities of control and sample hybridization were compared between chips using signal histograms. (A) Normalised signal intensities of hybridization controls; bioB, bioC, bioD and cre. Each line on the histogram represents an individual GeneChip. (B) The occurring frequency of signal intensities for all probe sets on each chip. Each line represents an individual GeneChip and thus an individual sample. Lines are coloured according to experimental grouping. Blue represents vehicle-injected control samples and red represents samples taken from LPS-injected mice. $n = 3/\text{group}$.

3.3.1.3 Principle component analysis

Prior to gene expression analysis, principle component analysis (PCA) was performed to check the quality of the data. PCA is a mathematical method of reducing the dimensionality of a dataset so that trends in the data can be easily visualised. Useful for datasets with large numbers of variables, PCA functions by applying a new set of variables to the data. These variables, less in number than those of the original dataset, are termed the principle components (PC) and are designed to retain as much of the variance of the original variables as possible. PC1 represents the variable with the greatest variance and subsequent components are numbered in ascending order with decreasing significance. The Affymetrix dataset was subject to PCA and each sample was plotted according to the top 3 most significant PC components.

A plot displaying the PCA scores of all of the GeneChip data is shown in Figure 3.4. When grouped in this manner, samples with a similar transcription profile should cluster together. This allows the distinction between different groups of data to be visualised and also highlights any outliers in a particular group. The points on the graph represent the samples from each group, clustered around an additional centroid circle. These are coloured according to their experimental grouping. The vehicle-injected mice were more tightly clustered than the LPS-injected group, suggesting that more transcriptional variation exists between the brains of the LPS-injected mice. In spite of this variation, there is a clear distinction between the group of LPS-injected mice and the group of control mice.

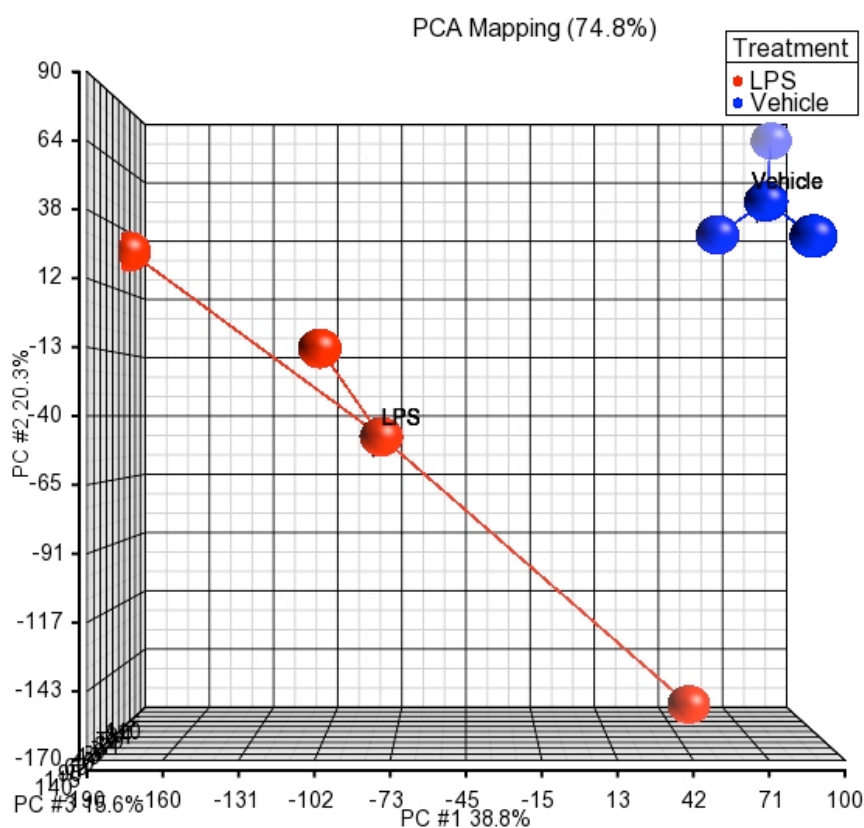


Figure 3.4 Principle component analysis of microarray samples

A microarray study was performed to compare gene expression in the brains of mice injected with LPS to a vehicle-injected control group. The 3 largest principle components of the array study were compared using a principle component analysis (PCA) plot. Each circle on the graph represents data from individual GeneChips, and therefore individual samples, clustered around a centroid circle. The more tightly clustered a group of circles are, the more they are transcriptionally similar. Samples are coloured according to experimental grouping. Blue represents vehicle-injected control samples and red represents samples taken from LPS-injected mice. n = 3/group.

3.3.2 Gene expression analysis of Affymetrix chips using Partek

The quality control measures, outlined above, have systematically ruled out sources of variation, such as differences in RNA quality, the labelling of samples or the quality of sample hybridisation. As a result, it can now be assumed that any differences observed between the two groups of samples are a result of genuine shifts in their transcriptional profiles. In order to determine which of the observed transcriptional changes are likely to be biologically meaningful, normalised intensity values, established using the GCRMA algorithm, were subject to statistical analysis.

3.3.2.1 Genes identified by Partek as being differentially expressed in the brains of LPS challenged mice

In order to assess which genes were differentially expressed in the brains of LPS-injected mice compared to the vehicle-injected controls, a one-way ANOVA was performed on the data, along with a Benjamini-Hochberg multiple testing correction (MTC) with a false discovery rate (FDR) of 0.1.

MTCs are a statistical method of reducing the rate of type I errors, i.e. the rate of wrongfully rejecting the null hypothesis. The rate of type I errors rises in magnitude when multiple hypotheses are simultaneously tested from a single dataset. For that reason, accurately testing the hypotheses derived from a microarray study, with tens of thousands of variables, can prove problematic. Based on a set of observations, the p-value is the probability that the null-hypothesis is true. The more often a p-value is calculated from a single dataset, the greater the probability is of generating a false positive, or type I error. For example, in a microarray study, for every 1000 genes that have a p-value of 0.05, probability suggests that 50 of these (1000×0.05) will, by chance, be false positives. MTCs increase the stringency of statistical analysis tests, thereby reducing the rate of type I errors. Subsequently, MTCs should always be applied to datasets containing large numbers of variables, such as those generated from microarray studies.

One of the drawbacks of MTCs is that whilst reducing the occurrence of false positives, they increase the chance of false negatives. Benjamini-Hochberg is the least stringent of the MTCs utilized by Partek, making it the ideal MTC to use for such a small study. The Benjamini-Hochberg method ranks all entities according to their p-value; from most to least significant. A corrected p-value is calculated from the equation below where N = total numbers of entities and r = rank:

$$\text{Corrected p-value} = \text{p-value} * (N/N-r)$$

The stringency of the MTC can be controlled by setting the FDR value. This is the expected proportion of incorrect rejections. By setting the FDR to 0.1, every entity with a corrected p-value of less than 0.1 was considered significant. This set the unadjusted p-value cut-off to 0.00036562. 131 entities satisfied this significance threshold. Of these significant entities, those that were

differentially expressed by at least 1.5-fold are displayed in Table 3.2. The table has been sub-divided into the 55 entities that were upregulated 2-fold or more and the additional 30 entities that were differentially expressed by at least 1.5-fold. Although significant, the remaining 46 entities that were not differentially expressed as much as 1.5-fold were not included in further analyses as they are unlikely to be biologically relevant.

Genbank Accession	Gene Symbol	Gene Name	Fold Change	P-value
Fold Change ≥ 2				
NM_008491	Lcn2	Lipocalin 2	29.29	2.61E-05
NM_011315	Saa3	Serum amyloid A3	11.60	2.56E-04
NM_016850	Irf7	Interferon regulatory factor 7	6.08	1.1E-04
NM_011854	Oasl2	2'-5' Oligoadenylate synthetase-like 2	5.44	1.01E-04
BC150711	AI607873	Interferon activated gene 204 homologue	4.93	3.74E-05
NM_023386	Rtp4	Receptor transporter protein 4	4.75	1.21E-04
NM_025378	Ifitm3	Interferon induced transmembrane protein	4.22	1.30E-05
NM_011579	Tgtp1	T-cell specific GTPase 1	3.79	3.64E-04
NM_008620	Gbp4	Guanylate binding protein 4	3.76	1.39E-04
NM_013563	Il2rg	Interleukin 2 receptor, gamma chain	3.71	9.29E-05
NM_023065	Ifi30	Interferon gamma inducible protein 30	3.64	9.95E-05
NM_144559	Fcgr4	Fc receptor, IgG, low affinity IV	3.57	4.23E-06
NM_194336	Gbp6	Guanylate binding protein 6	3.54	5.68E-06
NM_009252	Serpina3n	Serine (or cysteine) peptidase inhibitor, clade A	3.52	3.12E-04
NM_001082960	Itgam	Integrin alpha M	3.41	2.45E-04
NM_001033767	Gm4951	Predicted gene 4951	3.36	4.14E-05
---	N/A*	---	3.35	2.71E-05
NM_011150	Lgals3bp	Lectin, galactoside-binding, soluble, 3 binding protein	3.31	7.93E-05
NM_001001892	H2-K1	Histocompatibility 2, K1, K region	3.24	3.11E-04
NM_008331	Ifit1	Interferon-induced protein with tetratricopeptide repeats	3.23	3.50E-05
NM_009780	C4b	Complement component 4B (Childo blood group)	3.13	2.78E-04
NM_011905	Tlr2	Toll-like receptor 2	3.09	1.74E-05
---	Rnf213**	Ring finger protein 213	3.09	1.22E-04
AK173199	Rnf213	Ring finger protein 213	3.07	5.21E-06
NM_010260	Gbp2	Guanylate binding protein 2	3.02	8.62E-05
NM_013673	Sp100	Nuclear antigen Sp100	3.02	1.8E-04
NM_145545	Gbp7	Guanylate binding protein 7	2.86	3.04E-05
---	Rnf213**	Ring finger protein 213	2.74	1.15E-04
NM_010130	Emr1	EGF-like module containing, mucin- like, hormone receptor-li	2.72	1.74E-04
---	Rnf213	Ring finger protein 213	2.69	1E-04

---	N/A*	---	2.69	2E-04
NM_011693	Vcam1	Vascular cell adhesion molecule 1	2.68	1.11E-04
NM_018734	Gbp3	Guanylate binding protein 3	2.66	6.62E-05
NM_009402	Pglyrp1	Peptidoglycan recognition protein 1	2.56	1.89E-05
NM_010738	Ly6a	Lymphocyte antigen 6 complex, locus A	2.55	3.80E-05
NM_009283	Stat1	Signal transducer and activator of transcription 1	2.51	2.41E-04
NM_009982	Ctsc	Cathepsin C	2.47	3.09E-06
NM_153197	Clec4a3	C-type lectin domain family 4, member a3	2.46	2.91E-04
AK173199	Rnf213	Ring finger protein 213	2.39	2.53E-04
NM_008879	Lcp1	Lymphocyte cytosolic protein 1	2.36	1.27E-04
NM_008326	Irgm	immunity-related GTPase family M member 1	2.33	3.25E-04
---	N/A*	---	2.32	1.42E-04
NM_001160415	Apobec3	apolipoprotein B mRNA editing enzyme	2.32	1.86E-04
NM_031195	Msr1	Macrophage scavenger receptor 1	2.29	4.58E-05
---	Rnf213**	Ring finger protein 213	2.26	1.29E-05
NM_011708	Vwf	Von Willebrand factor homolog	2.26	3.89E-05
NM_031376	Pik3ap1	phosphoinositide-3-kinase adaptor protein 1	2.21	1.41E-04
NM_021384	Rsad2	Radical S-adenosyl methionine domain containing 2	2.18	2.37E-04
---	N/A*	---	2.13	1.4E-04
NM_001163522	Emcn	Endomucin	2.12	1.34E-04
NM_001037713	Xaf1	XIAP associated factor 1	2.09	1.74E-04
NM_001113356	C1rb	Complement component 1, r subcomponent B	2.09	1.99E-04
NM_013690	Tek	Endothelial-specific receptor tyrosine kinase	2.06	1.37E-04
NM_012054	Aoah	Acyloxyacyl hydrolase	2.04	3.06E-04
NM_001039530	Parp14	Poly (ADP-ribose) polymerase family, member 14	2.02	7.28E-05
Fold Change ≥ 1.5 and < 2				
NM_013805	Cldn5	claudin 5	1.97597	8.43E-05
---	Rnf213**	Ring finger protein 213	1.91996	1.46E-04
NM_172479	Slc38a5	Solute carrier family 38, member 5	1.86936	8.83E-05
NM_001081215	Ddx60	DEAD (Asp-Glu-Ala-Asp) box polypeptide 60	1.8692	1.33E-05

NM_010833	Msn	Moesin	1.85669	1.59E-04
NM_010741	Ly6c1	lymphocyte antigen 6 complex, locus C1	1.84075	1.33E-04
NR_030719	Gm8979	very large inducible GTPase 1 pseudogene	1.83413	8.11E-05
BC023105	BC023105	cDNA sequence BC023105	1.81633	5.22E-05
NM_025992	Herc5	hect domain and RLD 5	1.80396	2.4E-04
NM_009868	Cdh5	cadherin 5	1.80082	1.62E-05
NM_010493	Icam1	intercellular adhesion molecule 1	1.79505	1.36E-04
---	N/A*	---	1.76818	1.63E-04
---	Rnf213**	Ring finger protein 213	1.763	3E-04
NR_003507	Oas1b	2'-5' oligoadenylate synthetase 1B	1.75542	1.55E-04
NM_010104	Edn1	endothelin 1	1.74503	1.66E-04
NM_028261	Tmem173	transmembrane protein 173	1.73832	2.27E-05
NM_010225	Foxf2	forkhead box F2	1.71563	7.39E-05
NM_007609	Casp4	caspase 4, apoptosis-related cysteine peptidase	1.70807	1.29E-04
NM_031181	Siglece	sialic acid binding Ig-like lectin E	1.69006	1.7E-04
NM_009888	Cfh	complement component factor h	1.64032	2.28E-04
NM_001037298	Fam38a	family with sequence similarity 38, member A	1.62396	9.95E-05
NM_019963	Stat2	signal transducer and activator of transcription 2	1.60841	1.01E-04
NM_030253	Parp9	poly (ADP-ribose) polymerase family, member 9	1.59804	1.17E-04
NM_001111059	Cd34	CD34 antigen	1.59774	8.42E-05
---	N/A*	---	1.58439	1.27E-04
NM_025659	Abi3	ABI gene family, member 3	1.54831	1.42E-04
---	N/A*	---	1.52005	3.61E-04
NM_028195	Cyth4	cytohesin 4	1.5195	1.00E-04
NM_183168	P2ry6	pyrimidinergic receptor P2Y, G-protein coupled, 6	1.51848	3.49E-04
NM_007705	Cirbp	cold inducible RNA binding protein	-1.5643	3.09E-04

Table 3.2 Differentially expressed entities identified using Partek

Microarrays were analysed using Partek Genomics Suite. These data show the fold change and significance of the entities that were upregulated ≥ 2 -fold, and additional entities that were differentially expressed ≥ 1.5 -fold but < 2 -fold, in the brains of mice injected with 100 μ g LPS compared to vehicle. Significance was calculated using one-way ANOVA.

*Probe sets do not map to annotated genes

**Annotations manually determined using Affymetrix online database, NetAffx

3.3.3 Gene ontology clustering

After a list of differentially expressed genes was generated using Partek Genomics Suite, it was then subject Gene ontology clustering. All genes with a fold change value of 1.5 or greater were analysed using the database for annotation, visualisation and integrated discovery (DAVID) Bioinformatics Resources 6.7 (<http://david.abcc.ncifcrf.gov/>). DAVID is a free online software system that systematically maps lists of relevant genes according to their biological function. This applies biological relevance to a dataset, by determining which groups of functionally related genes are significantly enriched. Significance of enrichment is determined using a modified Fisher's Exact test and a Benjamini-Hochberg MTC was used to correct for the rate of type I errors involved in performing multiple comparisons. Co-expression of a gene cluster was considered significant if it satisfied a p-value cut-off of 0.05. The top 10 most significantly enriched processes are shown in Figure 3.5.

Amongst the most significantly altered biological groups are the Immune response, Immunity & defence and Macrophage-mediated immunity. This strongly implies the presence of an immune response in the brain following systemic LPS. As macrophages and microglia share many similar characteristics, it is possible that this immune response is linked to microglial activation. Also ranking high in the list of altered processes is Interferon-mediated immunity (Figure 3.5). Therefore, injecting mice systemically with LPS induces an immune response in the brain that may involve microglial activation and the induction of an IFN response.

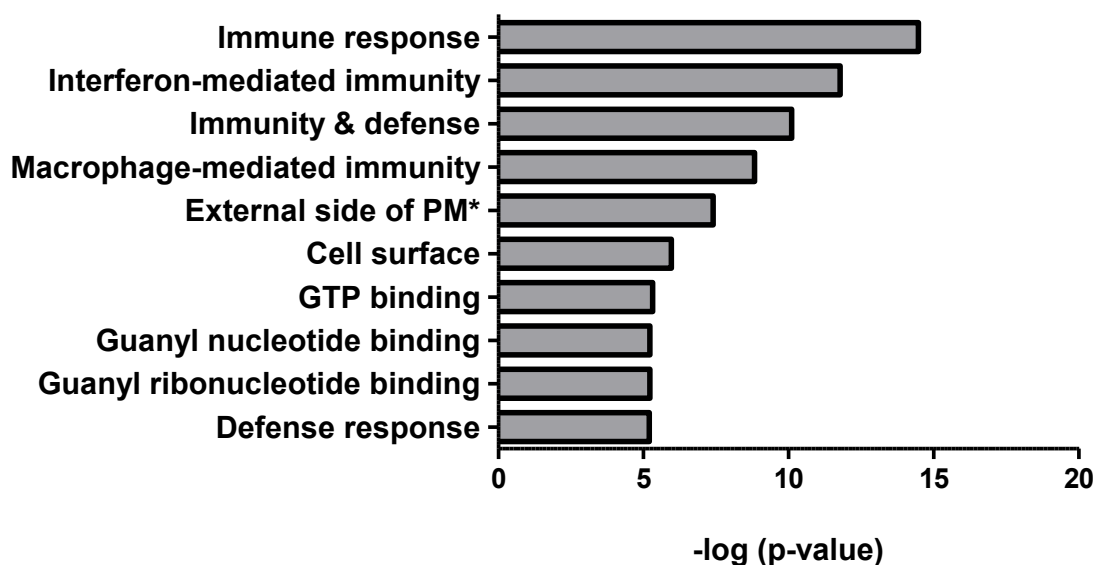


Figure 3.5 Top 10 enriched biological annotations.

Using DAVID bioinformatics software, gene ontology clustering was performed on the list of genes that were identified as being differentially regulated by ≥ 1.5 -fold, in the brains of LPS-challenged mice, compared to a control group. The co-expression of functionally-related gene clusters was rated in order of significance. Significance was calculated using a modified Fisher's Exact test.

*External side of plasma membrane.

3.3.4 Ingenuity Pathway Analysis

To complement and validate the data generated using DAVID, the list of genes were grouped into biological pathways. Pathway analysis, such as that carried out using Ingenuity Pathway Analysis (IPA) software, focuses on the proteins that a list of genes encodes. By investigating the functional relationships and annotated physical interactions between these proteins, as described in the relevant literature, IPA clusters them into molecular networks associated with cellular responses. Rather than providing an accurate representation of which pathways are activated in a given cell type or tissue, this form of data-mining facilitates hypothesis generation only. IPA pathway analysis was performed on significant genes with a fold change of greater-than or equal-to 1.5. Of the 85 entities that satisfied this cut-off, 70 were defined as being well-annotated and "analysis-ready" by the IPA software package. These 70 genes were subsequently grouped into pathways. Significance of differentially altered pathways was determined using a Fisher's Exact test and a Benjamini-Hochberg MTC was used

to correct for the rate of type I errors. The 10 most significantly altered pathways are displayed in Figure 3.6.

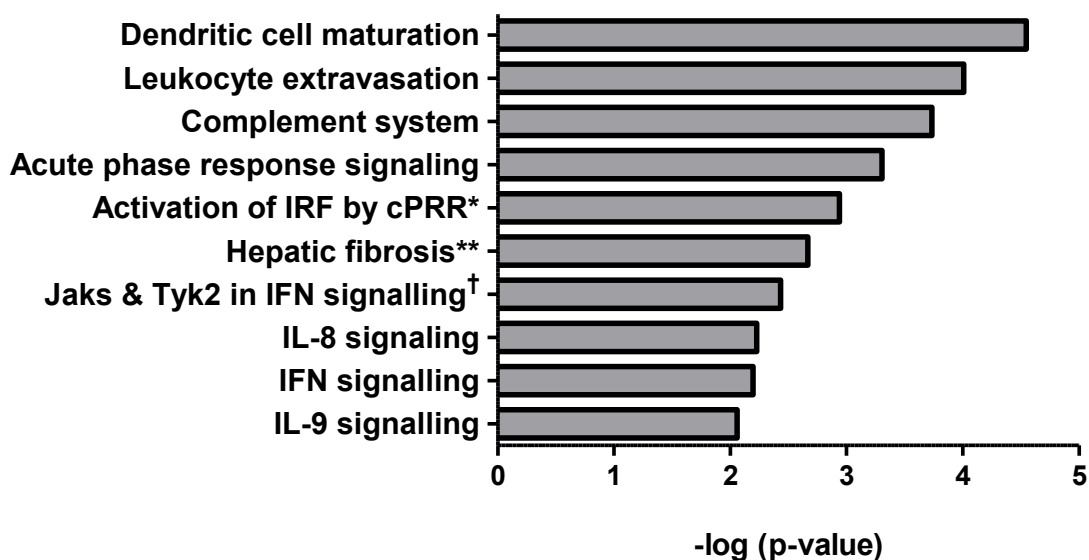


Figure 3.6 Top 10 significantly altered biological pathways.

Using Ingenuity Pathway Analysis software, the list of genes that were identified as being differentially regulated ≥ 1.5 -fold, in the brains of LPS-challenged mice compared to a control group, were grouped into biological pathways. Significance was calculated using a Fisher's Exact test and pathways were ranked accordingly.

*Activation of interferon regulatory factors by cytosolic pattern recognition receptors.

**Hepatic fibrosis/Hepatic stellate cell activation.

†Jak1, Jak2 and Tyk2 in interferon signalling.

The most altered biological pathway was Dendritic cell (DC) maturation. Expression of this pathway appears enhanced due to the upregulation of; *Tlr2*, *H2-K1*, *Icam1*, *Fcgr4*, *Stat1* and *Stat2* (Table 3.2), although the enhancement of most of these genes could be explained by microglial activation. Many of the genes involved in leukocyte extravasation were upregulated in response to peripheral LPS injection. This pathway, illustrated in Figure 3.7, involves the upregulation of a number of genes implicated in both leukocyte rolling and adhesion to the vasculature and subsequent leukocyte transmigration. This may explain the entry of leukocytes to the brain; either across the BBB or across the BCSFB.

Also amongst the top most significant pathways are; Activation of IRF by cytosolic pattern recognition receptors, Jak1, Jak2 and Tyk2 in IFN signalling and IFN signalling. Activation of IRFs by cytosolic pattern recognition receptors,

illustrated in Figure 3.8, involves an upregulation of IRF7, a classic feature of an IFN β response, and upregulation of Stat1 and Stat2; genes that are also involved in IFN signalling (Figure 3.9). The pathway Jak1, Jak2 and Tyk2 in IFN signalling was not shown as it displayed a very similar network of genes as the IFN signalling pathway. Although molecules in IFN-related signalling pathways are transcriptionally enhanced, this does not necessarily equate to post-translational phosphorylation. In addition, it does not appear from the pathway analysis as if there is any of the elevated ISG transcription that would be a characteristic hallmark of signal transduction. In actual fact, the ISGs included in this pathway diagram are only a small fraction of the possible genes that can be modulated by IFNs. IFNs induce the expression of thousands of genes by activating transcription factor complexes that bind to one of two elements in gene promoter regions; the IFN γ -activated site (GAS) or the IFN-stimulated response element (ISRE)⁴¹⁵. As mentioned in more detail below, a high proportion of the genes that are upregulated in the brain in response to LPS are known ISGs. Therefore, not only is the IFN signalling pathway transcriptionally enhanced, but it is also likely to be activated in the brain in response to systemic LPS. These observations provide further evidence of an IFN-response in the brain in response to systemic LPS.

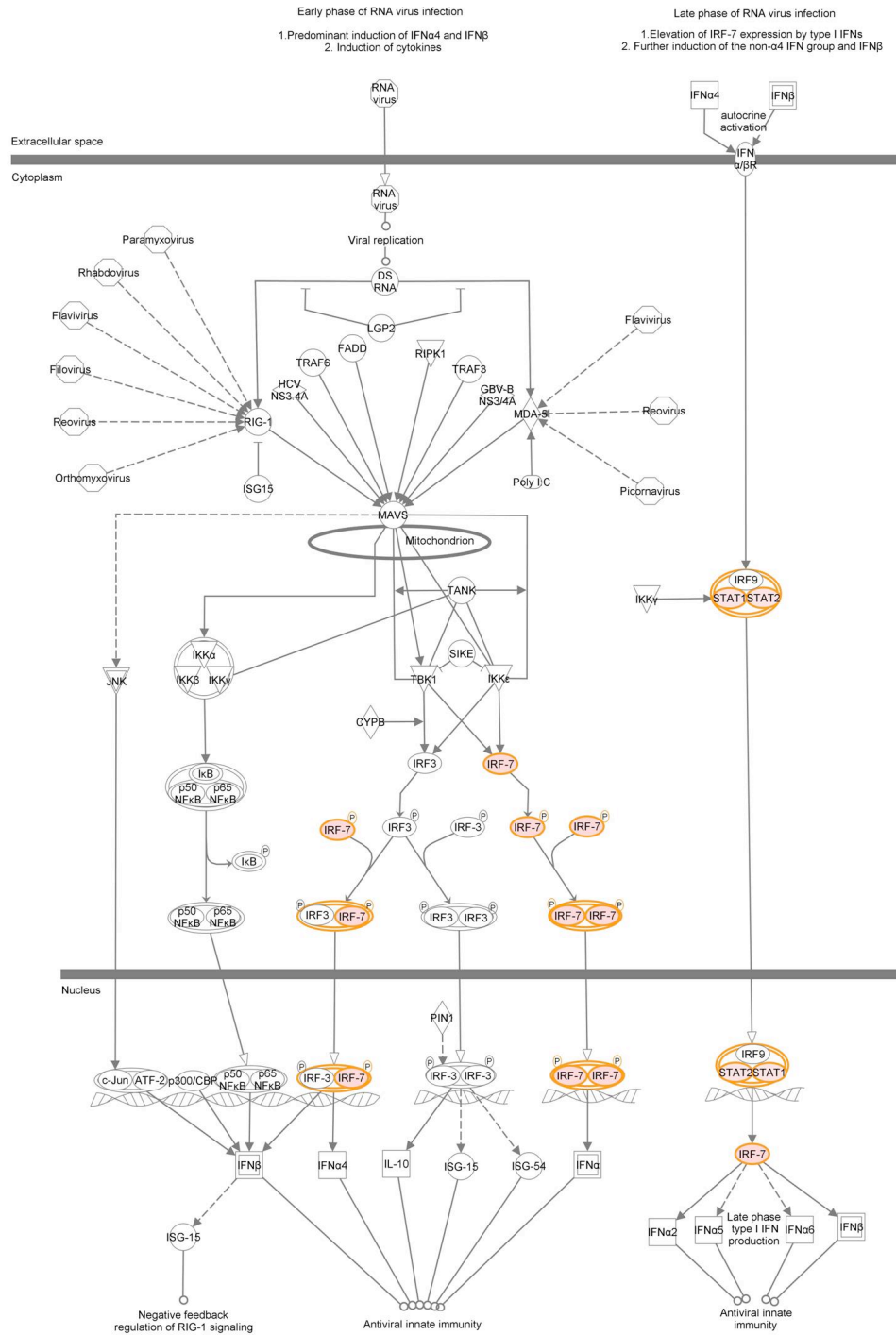


Figure 3.8 The Activation of IRF by cytosolic pattern recognition receptors signalling pathway

This diagram outlines the genes involved in the Activation of interferon regulatory factors (IRFs) by cytosolic pattern recognition receptors signalling pathway: a pathway that was identified using Ingenuity Pathway Analysis (IPA) software as being differentially regulated in response to LPS. Genes that are highlighted red are significantly upregulated by ≥ 1.5 -fold in the brain in response to LPS. Figure was taken from IPA.

Interferon Signaling

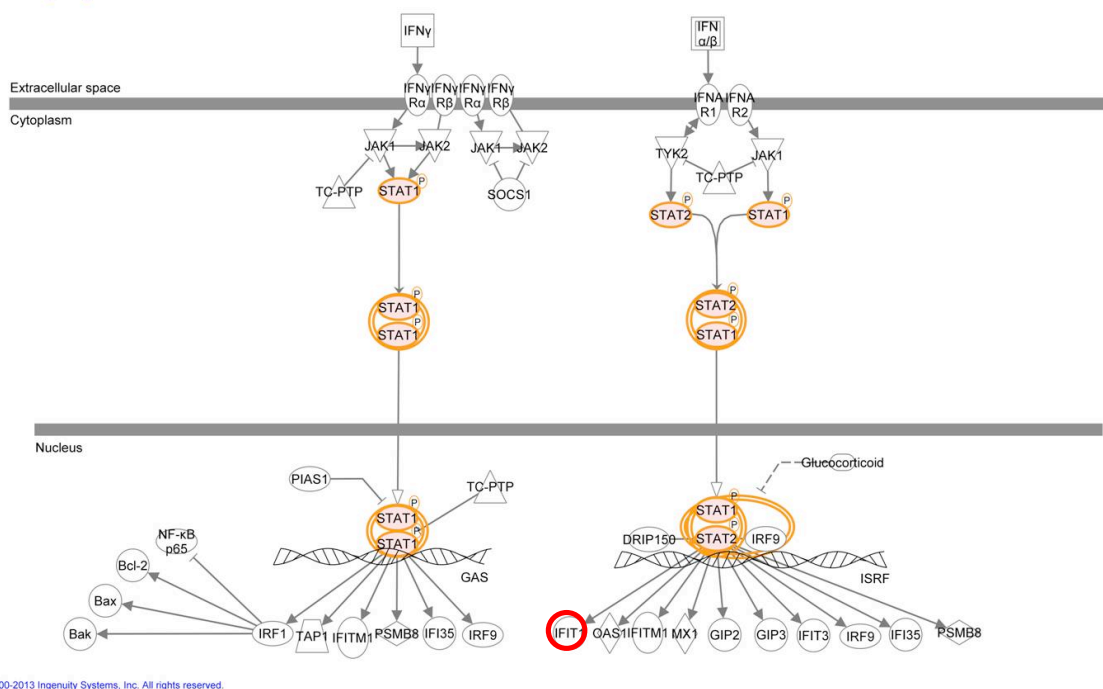


Figure 3.9 The Interferon signalling pathway

Using Ingenuity Pathway Analysis (IPA) software, differential regulation of the interferon signalling pathway was identified as being a downstream effect of peripheral LPS injection. This diagram outlines the genes involved in this pathway, including some of the key interferon stimulated genes that are activated in response. Genes that are highlighted red are significantly upregulated by ≥ 1.5 -fold in the brain in response to LPS. IFIT1 has been outlined in red as although it was significantly upregulated in the brain, it was not deemed “analysis-ready” by IPA and thus excluded from pathway analysis. Figure was taken from IPA.

3.3.5 Re-analysing the Affymetrix data using GeneSpring

Analysing the Affymetrix dataset using Partek Genomics Suite returned a list of 55 differentially expressed entities that satisfied a fold change cut-off of 2. To further validate the microarray, the upregulation of a selection of genes had first to be confirmed using QPCR. With the aim of focusing only on the genes that are most likely to be biologically relevant, the Affymetrix dataset was reanalysed using GeneSpring GX analysis software so that the resulting list of significantly relevant genes could be compared to that generated using Partek.

The Mouse Gene 1.0 ST array data were analysed in GeneSpring using a modified version of RMA, RMA16. This summarisation algorithm conforms to the same 3 steps as RMA; background correction, normalisation and probe summarisation.

However, RMA16 differs from its predecessor in that a value of 16 is added to the normalised intensities calculated using the RMA algorithm. This extra step is for variance stabilisation.

As before, a signal histogram was used to visually assess the efficiency of hybridisation and the separation between the two groups of samples was viewed on a PCA plot. As potential sources of non-biological variability have already been ruled out (Figure 3.3) and the transcriptional variation between groups already been demonstrated (Figure 3.4), the corresponding graphs, generated using GeneSpring, are not shown.

3.3.6 Analysis of Affymetrix data using GeneSpring

To establish a list of significantly relevant genes using GeneSpring GX software, the normalised intensity values created by the pre-processing of the Affymetrix chips were filtered by expression and subject to statistical analysis.

3.3.6.1 Filtering entities on expression

Pre-processing the array chips using RMA16 assigns the 28 869 entities on each chip with a normalised intensity value. In order to eliminate low level background gene expression, each entity had to possess a normalised intensity value that fell within the upper 80% of all the normalised intensity values on that chip. In addition, to be included, each entity had to satisfy this parameter in all three samples of one group. Filtering on expression narrowed the dataset down to 22 927 entities (Figure 3.10A).

3.3.6.2 Genes identified in GeneSpring as being differentially expressed in the brains of LPS challenged mice

To identify differentially expressed genes using GeneSpring, an unpaired t-test was performed on the data, along with a Benjamini-Hochberg multiple testing correction. A profile plot of the normalised intensity values of entities deemed statistically significant is shown in Figure 3.10B. Of the 96 entities that were classified as being significantly different, 89 were upregulated in the brain in response to LPS and 7 were downregulated.

As the aim of reanalysing the array data was to focus only on the genes that were most robustly differentially expressed, a fold change cut-off of 2 was applied to the dataset. 39 entities satisfied this parameter, all of which were upregulated in the brain in response to LPS. The normalised intensity values of these entities are displayed in Figure 3.10C and the relative signal intensities have been displayed in a heatmap (Figure 3.11). The heatmap allows a visual comparison of relative expression to be made; between individual entities, individual samples or groups of samples. The fold change, p-value and gene name (where applicable) of each entity is listed in Table 3.3. Although containing many of the key players that were identified using Partek, this gene list differs to that generated using Partek, both in size and content. In spite of this, genes encoding acute phase proteins lipocalin 2 and serum amyloid A3 were identified in both lists as being the most upregulated (Table 3.2 & Table 3.3). In addition, genes common to both lists were shown to be upregulated by a similar magnitude using either Partek or GeneSpring. A comparison of the two lists will be made below (Section 3.3.7).

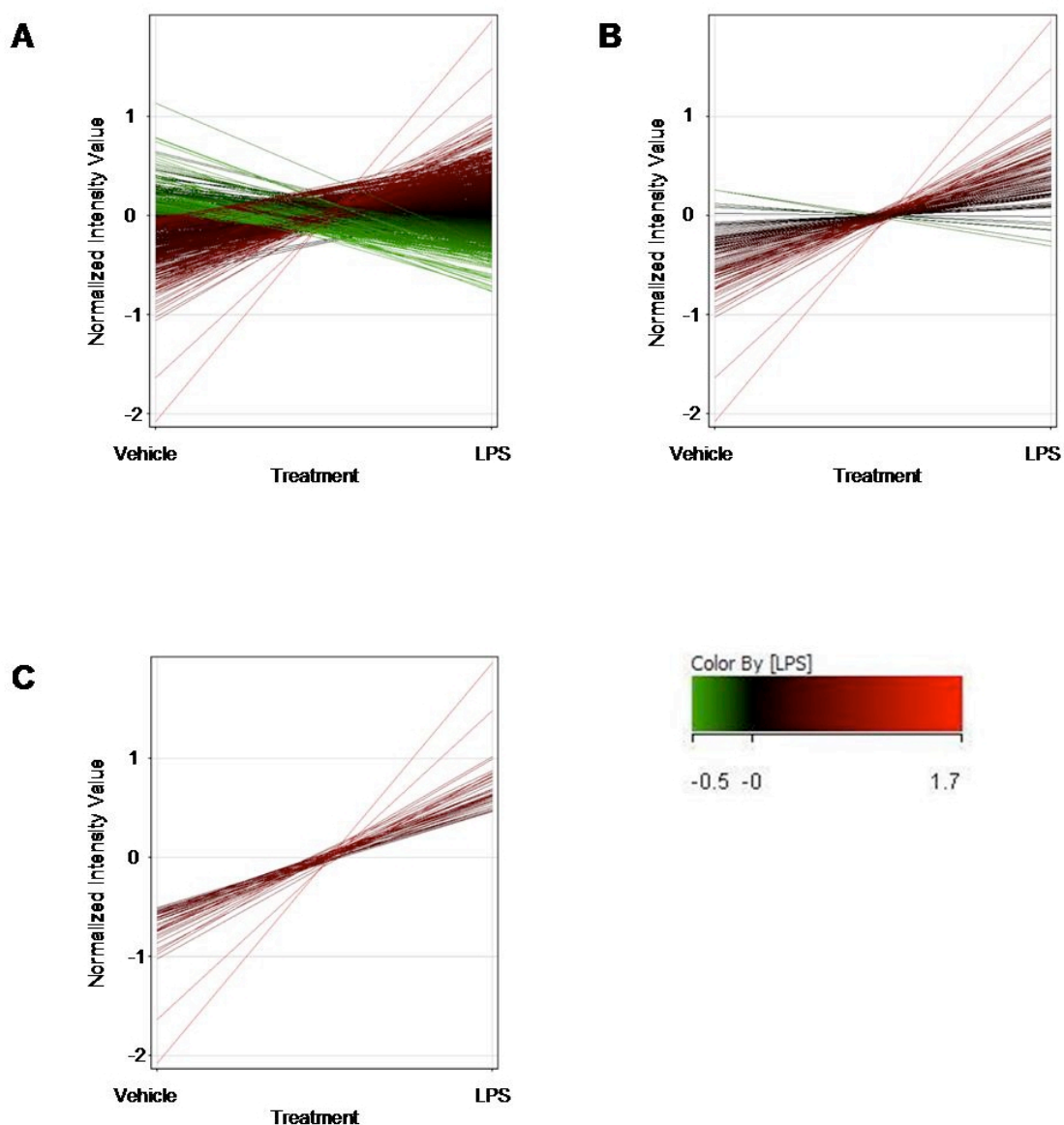


Figure 3.10 Normalised intensity values of individual entities.

Affymetrix gene chips, used to compare gene expression in the brains of LPS- and vehicle-injected mice, were analysed using GeneSpring GX analysis software. These profile plots display the normalised intensity values of (A) all entities after being filtered on expression, (B) all significantly regulated entities (C) All differentially expressed entities satisfying a fold change cut-off of 2. Normalised intensity values were established using the RMA16 summarisation algorithm. Each entity is coloured according to the median normalised intensity value of the LPS-treatment group. $n = 3/\text{group}$.

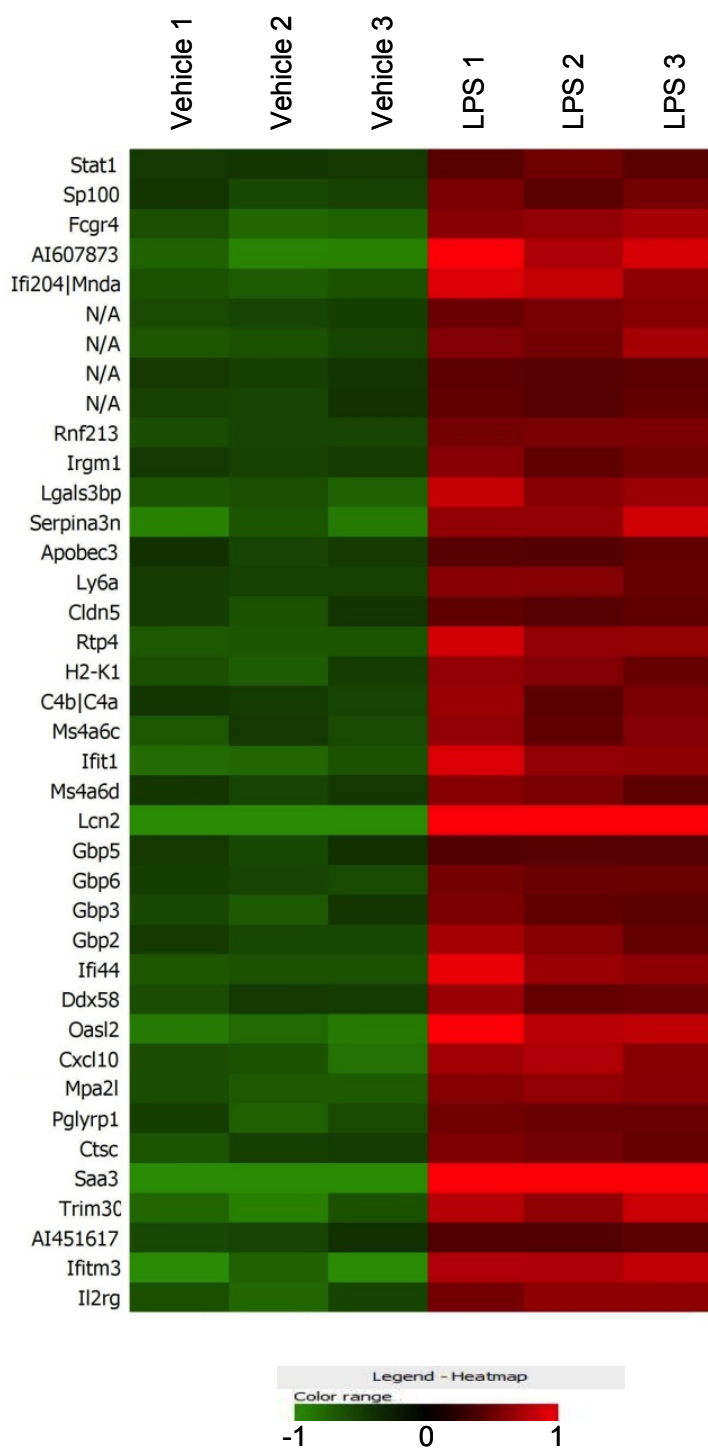


Figure 3.11 Heatmap of the signal intensity of individual entities relative to baseline

This heatmap displays the relative signal intensities of the 39 entities that were classified, by GeneSpring GX software, as being differentially expressed in the brains of LPS-challenged mice compared to vehicle-injected controls. Only entities with a fold change of 2 or greater have been included. Individual entities in each sample are coloured according to their expression level relative to baseline. For ease of visualisation, relative expression values were calculated by mathematically scaling down the normalised intensity values to fit within the range -1 to 1.

Genbank Accession	Gene Symbol	Gene Name	Fold Change	P-value
NM_008491	Lcn2	Lipocalin 2	16.58	8.27E-06
NM_011315	Saa3	Serum amyloid A3	8.69	1.91E-04
BC150711	AI607873	Interferon activated gene 204 homologue	3.93	7.84E-05
NM_011854	Oasl2	2'-5' Oligoadenylate synthetase-like 2	3.91	1.25E-04
NM_025378	Ifitm3	Interferon induced transmembrane protein	3.69	3.91E-05
NM_009252	Serpina3n	Serine (or cysteine) peptidase inhibitor, clade A	3.32	1.65E-04
NM_009099	Trim30	Tripartite motif-containing 30	3.28	9.56E-05
NM_008331	Ifit1	Interferon-induced protein with tetratricopeptide repeats	3.12	1.05E-04
NM_008329	Ifi204	Interferon activated gene 204	3.05	6.68E-05
NM_133871	Ifi44	Interferon activated gene 44	2.94	1.44E-04
NM_023386	Rtp4	Receptor transporter protein 4	2.93	4.51E-05
NM_021274	Cxcl10	chemokine (C-X-C motif) ligand 10	2.91	8.88E-05
NM_144559	Fcgr4	Fc receptor, IgG, low affinity IV	2.90	2.18E-05
NM_011150	Lgals3bp	Lectin, galactoside-binding, soluble, 3 binding protein	2.89	5.40E-05
NM_194336	Gbp6	Guanylate binding protein 6	2.70	4.41E-06
NM_013563	Il2rg	Interleukin 2 receptor, gamma chain	2.64	4.41E-06
---	N/A*		2.60	4.42E-05
NM_00100189 2	H2-K1	Histocompatibility 2, K1, K region	2.49	4.42E-05
NM_010260	Gbp2	Guanylate binding protein 2	2.42	1.13E-04
NM_028595	Ms4a6c	Membrane-spanning 4-domains, subfamily A, member 6C	2.40	1.91E-04
AK173199	Rnf213 LOC6 72511	Ring finger protein 213	2.34	5.92E-07
NM_009402	Pglyrp1	Peptidoglycan recognition protein 1	2.36	8.03E-05
---	Rnf213**	Ring finger protein 213	2.33	1.36E-05
NM_009982	Ctsc	Cathepsin C	2.31	5.42E-05
NM_010738	Ly6a	Lymphocyte antigen 6 complex, locus A	2.29	1.60E-05
NM_018734	Gbp3	Guanylate binding protein 3	2.28	1.60E-04
NM_172689	Ddx58	DEAD box polypeptide 58	2.27	1.26E-04
NM_145545	Gbp7	Guanylate binding protein 7	2.27	3.80E-06
NM_009780	C4b C4a	complement component 4B (Childo blood group) complement 4A (Rodgers blood group)	2.24	1.40E-04

NM_013673	Sp100	Nuclear antigen Sp100	2.22	4.61E-05
NM_026835	Ms4a6d	Membrane-spanning 4-domains, subfamily A, member 6D	2.21	4.36E-05
NM_008326	Irgm	Immunity-related GTPase family M member 1	2.21	2.56E-05
NM_013805	Cldn5	Claudin 5	2.10	1.42E-04
---	Rnf213**	Ring finger protein 213	2.08	2.78E-05
NM_199146	AI451617	Expressed sequence AI451617	2.06	8.85E-05
NM_009283	Stat1	Signal transducer and activator of transcription 1	2.04	5.75E-06
---	Rnf213**	Ring finger protein 213	2.02	2.69E-06
NM_153564	GBP5	Guanylate binding protein 5	2.02	5.17E-05
NM_00116041 5	Apobec3	Apolipoprotein B mRNA editing enzyme	2.02	2.07E-05

Table 3.3 Differentially expressed entities identified using GeneSpring

Microarrays were analysed using GeneSpring GX software. These data show the fold change and significance of the 39 entities that were upregulated ≥ 2 -fold in the brains of mice injected with LPS compared to vehicle. Significance was calculated using an unpaired t-test.

*Probe sets don't map to annotated genes

**Annotations manually determined using Affymetrix online database, NetAffx

3.3.7 Defining the genes commonly identified by both Partek and GeneSpring

As mentioned above, the aim of reanalysing the array data was to focus attention on genes that were highlighted by both software packages as being differentially expressed, thus maximizing scrutiny. The two lists of differentially expressed entities, that satisfied a fold change cut-off of 2, were compared (Figure 3.12). Of the 29 entities that were common to both lists, 24 are known genes. These are grouped according to biological function in Table 3.4. Strikingly, over half of the genes in this list are known ISGs. This supports the hypothesis generated from the Ingenuity pathway analysis; that IFN signalling is induced in the brain following peripheral LPS injection. In addition, a number of genes encoding acute phase reactants are upregulated, as are a variety of genes involved in immunity and defence. Due to their consistency in both datasets, the sub-list of genes, listed in Table 3.4, has subsequently been focused on for the remainder of the study.

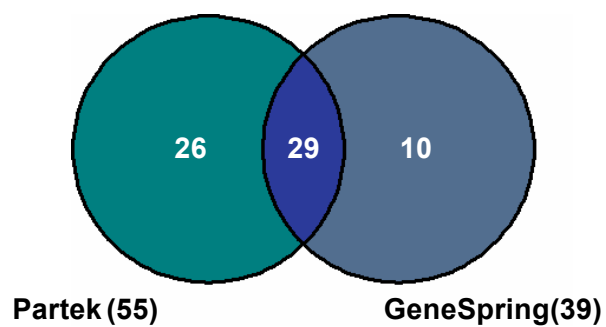


Figure 3.12 Differentially expressed entities identified using Partek and GeneSpring

Affymetrix gene chips were analysed using two software packages: Partek Genomics Suite and GeneSpring GX analysis software. This Venn diagram compares the 55 entities that were identified as being differentially expressed ≥ 2 -fold by Partek, to the 39 entities that were identified by Genespring using the same parameters.

Gene Symbol	Gene Name
Interferon Stimulated Genes	
Ctsc	Cathepsin C
Gbp2	Guanylate binding protein 2
Gbp3	Guanylate binding protein 3
Gbp6	Guanylate binding protein 6
Gbp7	Guanylate binding protein 7
Ifit1	Interferon-induced protein with tetratricopeptide repeats
Ifitm3	Interferon induced transmembrane protein
Igrm1	Immunity-related GTPase family M, member 1
Lgals3bp	Lectin, galactoside-binding, soluble, 3 binding protein
Oasl2	2'-5' Oligoadenylate synthetase-like 2
Rnf213	Ring finger protein 213
Rtp4	Receptor transporter protein 4
Sp100	Nuclear antigen Sp100
Stat1	Signal transducer and activator of transcription 1
Acute Phase Reactants	
Lcn2	Lipocalin 2
Saa3	Serum amyloid A3
Serpina3n	Serine (or cysteine) peptidase inhibitor, clade A
Immunity System Components	
C4b C4a	Complement component 4B (Childo blood group) complement 4A (Rodgers blood group)
Fcgr4	Fc receptor, IgG, low affinity IV
H2-K1	Histocompatibility 2, K1, K region
Pglyrp1	Peptidoglycan recognition protein 1
Cell Surface Molecules	
Il2rg	Interleukin 2 receptor, gamma chain
Ly6a	Lymphocyte antigen 6 complex, locus A
mRNA Editing	
Apobec3	Apolipoprotein B mRNA editing enzyme

Table 3.4 Functional properties of differentially expressed genes, common to both Table 3.2 and Table 3.3.

Affymetrix gene chips were analysed using two software packages: Partek Genomics Suite and GeneSpring GX analysis software. These data show the biological functions of the 24 known genes that were common to both gene lists and upregulated ≥ 2 -fold in the brains of mice injected with LPS compared to vehicle. Genes were clustered according to biological function using the Database for Annotation, Visualization and Integrated Discovery v6.7 (<http://david.abcc.ncifcrf.gov/>).

TLR4 ligation is known to result in the increased production of type I and/or type II IFNs^{55,416}. To determine whether the ISGs were regulated by type I IFNs, type II IFNs or both, the list of ISG was analysed using the Interferome® database. This data mining analysis revealed that all 14 of the ISGs that were common to both array datasets had the potential to be regulated by type I IFNs (Figure 3.13). 8 of these could also be regulated by type II IFNs and 6 of the ISGs could also be regulated by type III IFNs.

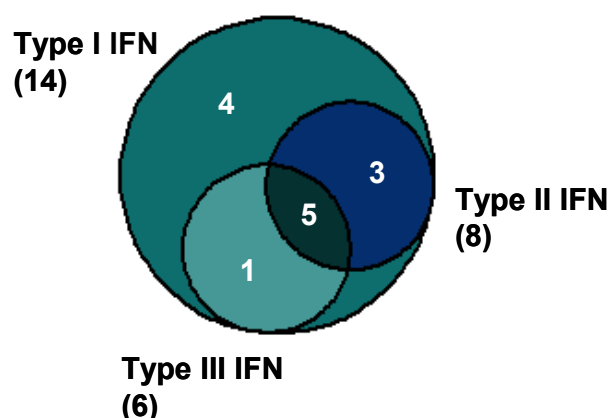


Figure 3.13 Interferon subtype analysis of ISGs induced in the brain

Interferon subtype analysis of the ISGs from Table 3.4 was performed using the Interferome database v1 (<http://vera093.its.monash.edu.au/interferome/>)

In summary, comparing the transcriptional profile of the brains of mice injected with LPS to those injected with vehicle, yielded a list of 85 differentially expressed entities with a fold change of at least 1.5. The known genes in this list were subject to GO clustering and pathway analysis; both of which highlighted the possibility of microglial activation and an IFN response in the brain. In order to focus on the genes that were most robustly differentially expressed, the fold change cut-off was increased. The list of genes satisfying a fold change cut-off of 2 was compared to one generated using a different software package, and thus a different summarisation algorithm. Common to both lists, the resulting sub-list of differentially expressed genes was assumed to be the most meaningful. Determining the biological function of these genes revealed that over half are known ISGs. In short, it would appear that LPS-injection in the periphery may trigger IFN signalling in the brain and a subsequent induction of ISGs.

3.4 QPCR analysis of target genes in the brain, blood and BM of LPS challenged mice

The Affymetrix array dataset has provided a list of genes that were differentially expressed in the brain following intraperitoneal LPS-injection. These were clustered according to biological function and grouped into relevant pathways. Using RNA isolated from an independent experiment, transcriptional changes were then validated by QPCR. To control for the possibility of a contaminating signal coming from the peripheral blood, and to see how the transcriptional response in the brain differed from that of the periphery, the expression of target genes was compared in the brain, PBL and bone marrow of mice, 48 hours after injection with either LPS or vehicle. In addition, QPCR was used investigate gene expression at earlier time points, in order to gain a better understanding of the kinetics of ISG expression.

3.4.1 Validation of differential gene expression using QPCR

In addition to validating the sub-list of genes described in Section 3.3.7, upregulated expression of gene encoding the classic interferon-inducible chemokine, CXCL10 and interferon regulatory factor (IRF) 7 was also validated using SYBR green QPCR, as was the gene encoding the negative regulator of IRF7, guanylate-binding protein (GBP) 4. Designing primers specific to *H2-K1* proved impractical due to the common occurrence of sequence homologies in the MHC gene cluster. Consequently, *H2-K1* was excluded from validation. In addition, due to the relatively high proportion of GBPs in the dataset, *Gbp7* and *Gbp6* were arbitrarily excluded.

With the exception of *Sp100* and *Stat1*, all ISGs assayed were confirmed as being significantly upregulated in the brains of mice challenged with systemic LPS compared to vehicle controls (Figure 3.14), as were the acute phase reactants (Figure 3.15) and all remaining genes aside from *Apobec3* and *C4* (Figure 3.16). Although a few genes, *Lcn2*, *Saa3*, *Il2rg* and *Fcgr4*, showed a markedly greater upregulation when gene expression was measured by QPCR compared to microarray, the induction of the majority of target genes correlated well with the microarray expression data. Therefore, the confirmation of target gene induction using QPCR validates the Affymetrix dataset.

3.4.2 Comparison of central response to peripheral response

With the aim of determining whether the inflammatory response in the brain differs from that of the periphery, and to control for the possibility of a contaminating signal coming from the peripheral blood, gene expression in the brain was compared to that of PBL, 48 hours following systemic LPS challenge. As an additional control, gene expression in the brain was also compared to that of the bone marrow; a highly vascularised peripheral tissue. The fold change of each target gene in both the PBL and the bone marrow was determined using SYBR Green QPCR. QPCR analysis showed a distinct pattern of gene expression in each of the three tissues analysed. Most of the target genes could be separated into three main groups: those that were significantly upregulated in all three tissues, those that were upregulated both in the brain and the PBL or those upregulated only in the brain.

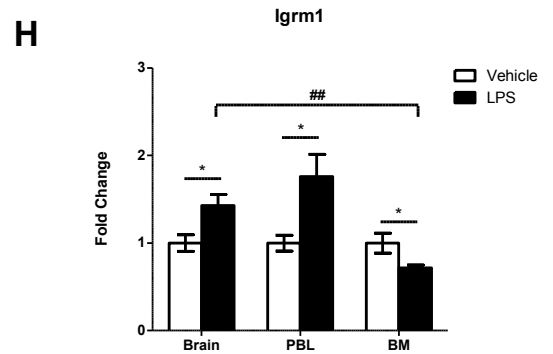
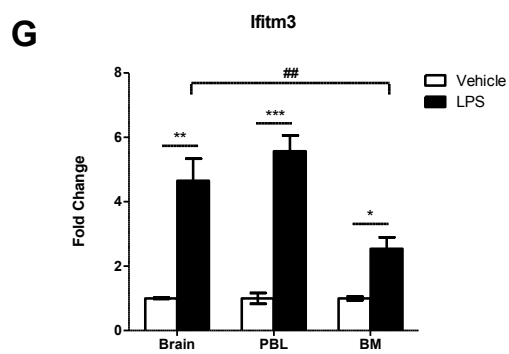
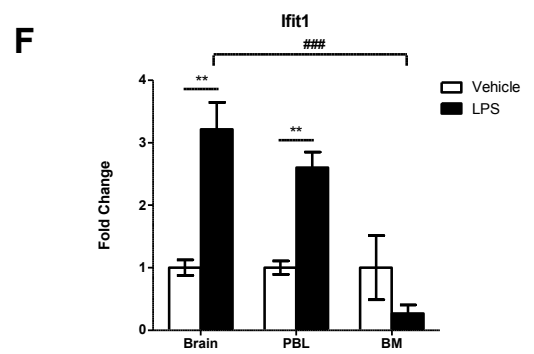
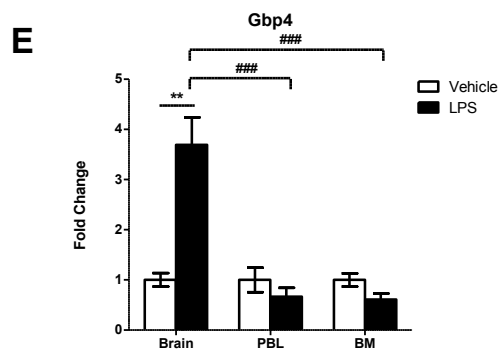
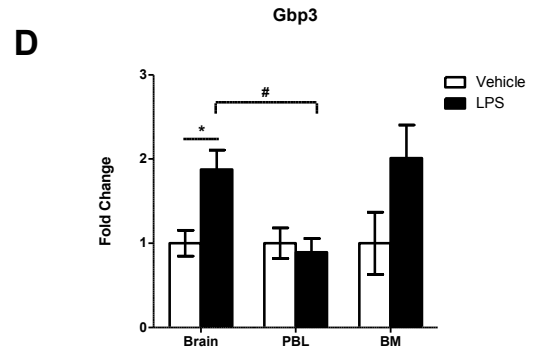
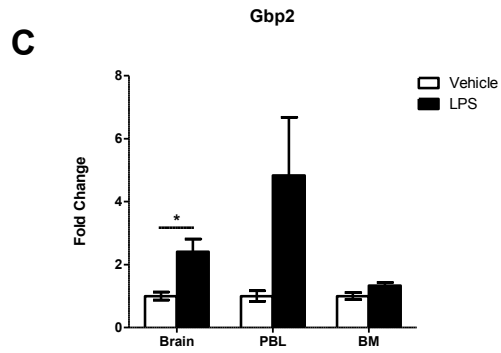
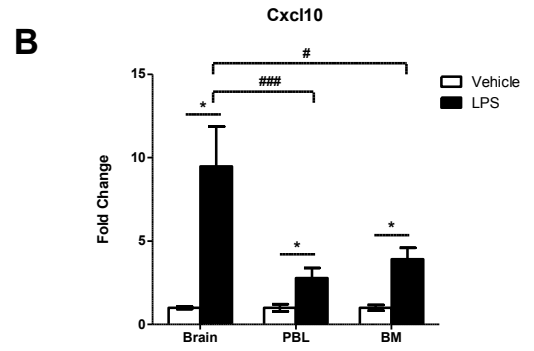
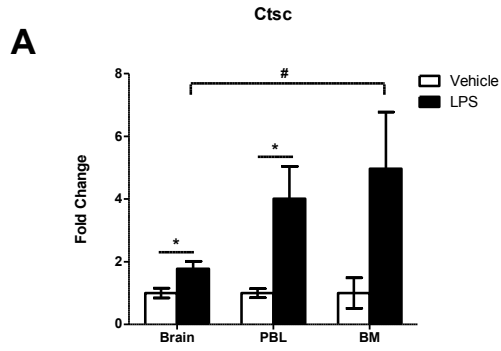
A high proportion of genes were upregulated to a similar extent in both the brain and the PBL. As a result, the enhanced signal observed in the brain following LPS injection, has the potential to be derived from a minute level of blood contamination; despite extensive perfusion. However, by examining gene modulation in multiple tissues, i.e. the brain, blood and bone marrow, it is possible to exclude this possibility. Only two ISGs, *Cxcl10* and *Ifitm3*, were significantly upregulated in the brain, PBL and bone marrow (Figure 3.14). Other genes falling into this category were acute phase reactants; *Lcn2* and *Saa3* (Figure 3.15), and the anti-microbial gene, *Pglyrp1* (Figure 3.16). Significantly upregulated in both the brain and the PBL were ISGs; *Ifit1*, *Igrm1*, *Lgals3bp*, *Oasl2* and *Rtp4* (Figure 3.14) along with an immune response gene; *Fcgr4* (Figure 3.16). Critically, both *Cxcl10* and *Fcgr4* were upregulated to a significantly greater extent in the brain than either of the extra-neural tissues, implying a level of independent modulation in the brain. In contrast, *Pglyrp* and *Saa3* were induced in the brain to a lesser extent than in the PBL, suggesting a greater level of gene regulation in the blood. The bone marrow is highly vascular. As a result, a partial perfusion would likely result in a contaminating signal in all three tissues. Although induced to a similar extent in the brain and the blood, *Ifit1*, *Ifitm3*, *Igrm1*, *Lcn2*, *Lgals3bp*, *Oasl2* and *Rtp4* were upregulated significantly more in the brain than the bone marrow. Taken together, these differences in the fold change of target genes in each tissue are indicative of different levels

of gene regulation. This implies that the observed fold changes in the brain are not a secondary effect of blood contamination.

In further evidence of independent gene regulation in the brain; Type I IFN-regulated ISGs; *Gbp3*, *Gbp4* and *Irf7* were all significantly upregulated in the brain alone (Figure 3.14, Table 3.5), as was cytokine receptor component, *Il2rg* (Figure 3.16). However, *Gbp3* showed a slight trend towards an upregulation in the bone marrow and as a result, the induction observed in the brain was significantly greater than in peripheral blood leukocytes, but not greater than in the bone marrow. Similarly, although IFN γ -regulated gene, *Gbp2*, acute phase reactant, *Serpina3n* and cell surface marker *Ly6a* were significantly upregulated only in the brain (Figure 3.14, Figure 3.15, Figure 3.16 and Table 3.5), these genes also showed a trend towards an upregulation in the PBL. Taken together, these data demonstrate a differential pattern of gene expression in the brain from that of the two peripheral tissues. This is extremely important as it provides evidence of a brain-specific inflammatory response as a result of systemic LPS injection, thus validating the microarray experiment.

Gene symbol	Mean fold change	+/- SEM	P-value
<i>Gbp2</i>	2.41	0.405	0.0160
<i>Gbp3</i>	1.87	0.231	0.0197
<i>Gbp4</i>	3.69	0.545	0.0030
<i>Il2rg</i>	8.95	0.730	< 0.0001
<i>Irf7</i>	4.93	0.561	0.0004
<i>Ly6a</i>	2.61	0.215	0.0003
<i>Serpina3n</i>	2.62	0.439	0.0154

Table 3.5 List of target genes upregulated specifically in the brain



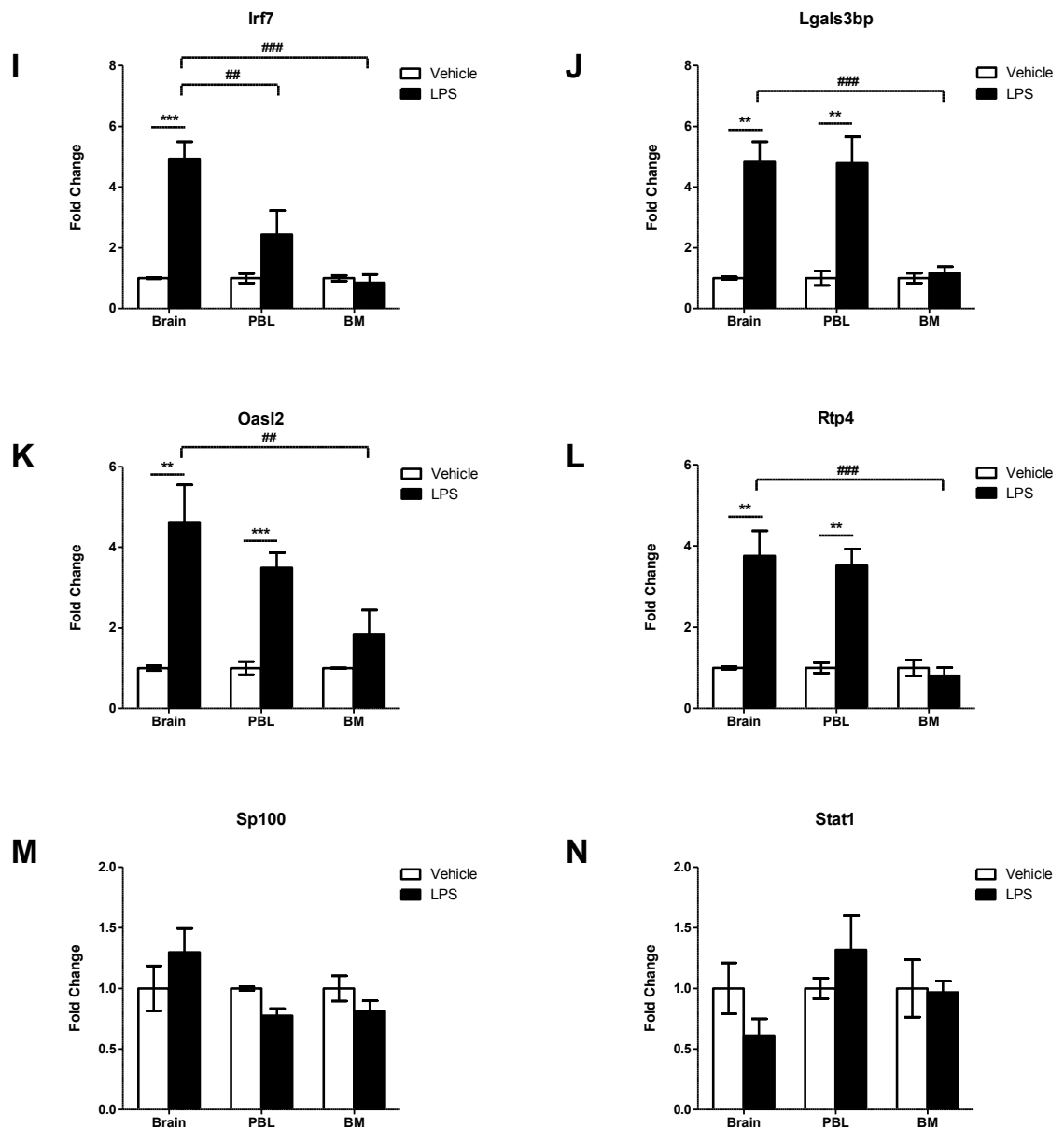


Figure 3.14 Differential ISG expression in the brain, PBL and BM of LPS-treated mice compared to vehicle control group.

RNA was isolated from the brain, peripheral blood leukocytes (PBL) and bone marrow (BM) of mice, 48 hours after injection with 100 μ g LPS or an equivalent volume of vehicle. Gene expression analysis of (A) *Ctsc*, (B) *Cxcl10*, (C) *Gbp2*, (D) *Gbp3*, (E) *Gbp4*, (F) *Ifit1*, (G) *Ifitm3*, (H) *Igrm1*, (I) *Irf7*, (J) *Lgals3bp*, (K) *Oasl2*, (L) *Rtp4*, (M) *Sp100* and (N) *Stat1* was performed using QPCR and normalised to TBP. Data are expressed as fold change in gene expression in the brain, PBL and BM of LPS-injected mice (■) relative to that of vehicle-injected controls (□). Data represent the mean \pm SEM. Significance of each fold change was calculated for individual tissues using an unpaired t-test: * $P \leq 0.05$, ** $P \leq 0.01$, *** $P \leq 0.001$. A statistical comparison was made between the fold induction in the brain and the fold induction in both the PBL and the BM using two-way ANOVA: # $P \leq 0.05$, ## $P \leq 0.01$, ### $P \leq 0.001$. n = 4/group.

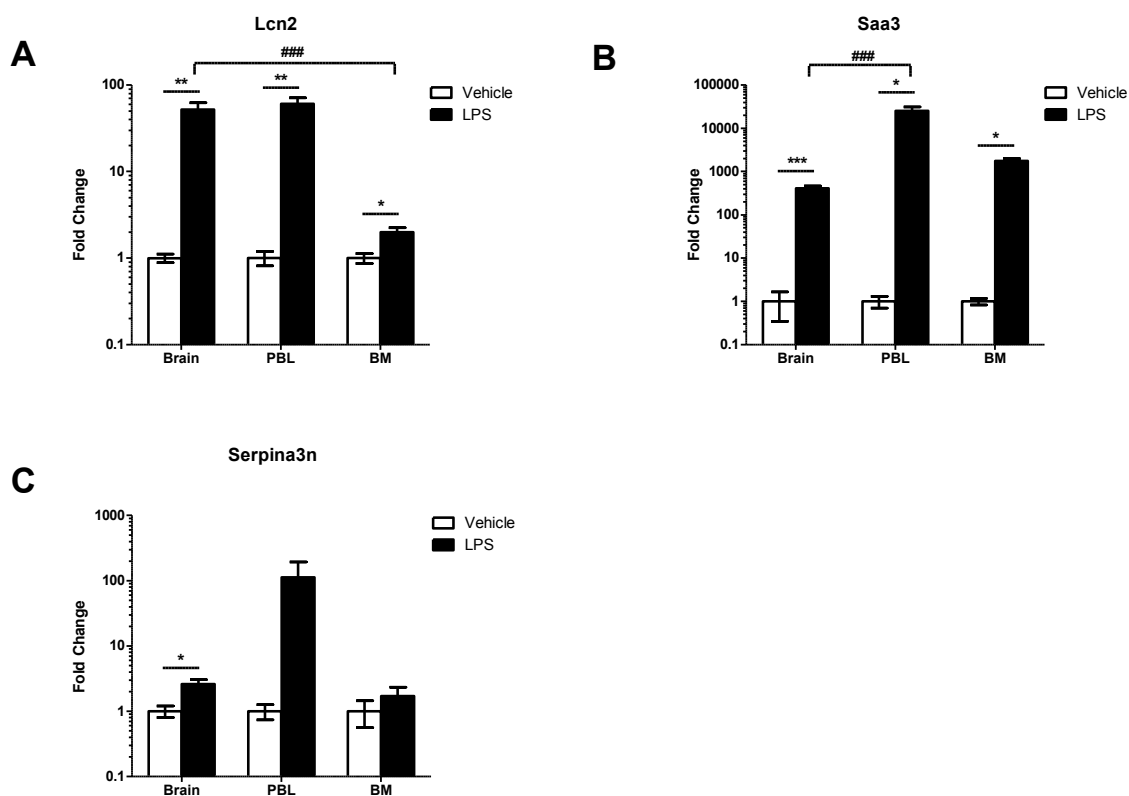


Figure 3.15 Differential expression of acute phase response genes in the brain, PBL and BM of LPS-treated mice compared to vehicle control group.

RNA was isolated from the brain, peripheral blood leukocytes (PBL) and bone marrow (BM) of mice, 48 hours after injection with 100 μ g LPS or an equivalent volume of vehicle. Gene expression analysis of (A) *Lcn2*, (B) *Saa3* and (C) *Serpina3n* was performed using QPCR and normalised to TBP. Data are expressed as fold change in gene expression in the brain, PBL and BM of LPS-injected mice (■) relative to that of vehicle-injected controls (□). Data represent the mean \pm SEM. Significance of each fold change was calculated for individual tissues using an unpaired t-test: * $P \leq 0.05$, ** $P \leq 0.01$, *** $P \leq 0.001$. A statistical comparison was made between the fold induction in the brain and the fold induction in both the PBL and the BM using two-way ANOVA: # $P \leq 0.05$, ## $P \leq 0.01$, ### $P \leq 0.001$. $n = 4$ /group.

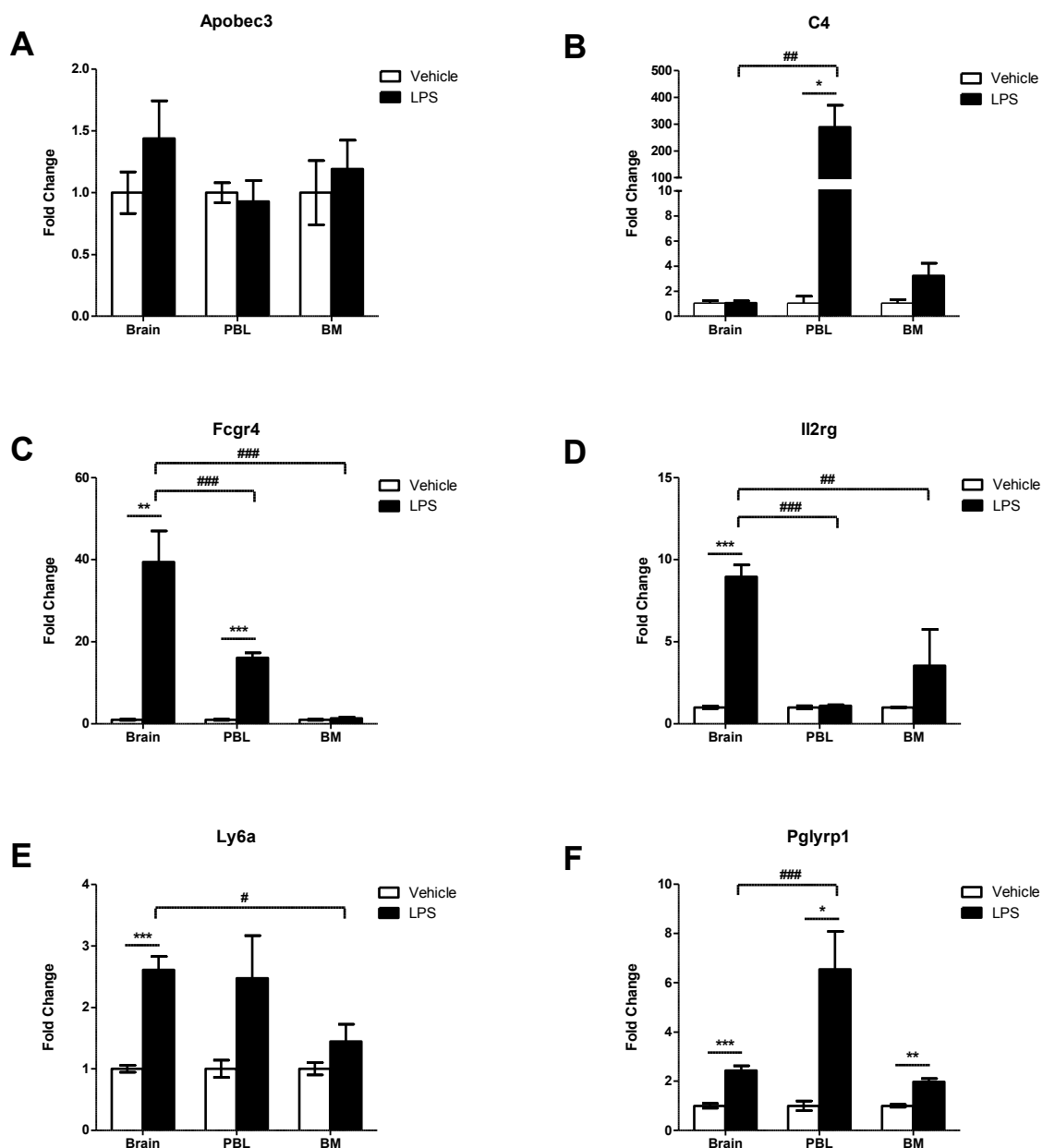


Figure 3.16 Differential expression of remaining target genes in the brain, PBL and BM of LPS-treated mice compared to vehicle control group.

RNA was isolated from the brain, peripheral blood leukocytes (PBL) and bone marrow (BM) of mice, 48 hours after injection with 100 μ g LPS or an equivalent volume of vehicle. Gene expression analysis of (A) *Apobec3*, (B) *C4*, (C) *Fcgr4*, (D) *Il2rg*, (E) *Ly6a* and (F) *Pglyrp1* was performed using QPCR and normalised to TBP. Data are expressed as fold change in gene expression in the brain, PBL and BM of LPS-injected mice (■) relative to that of vehicle-injected controls (□). Data represent the mean \pm SEM. Significance of each fold change was calculated for individual tissues using an unpaired t-test: * $P \leq 0.05$, ** $P \leq 0.01$, *** $P \leq 0.001$. A statistical comparison was made between the fold induction in the brain and the fold induction in both the PBL and the BM using two-way ANOVA: # $P \leq 0.05$, ## $P \leq 0.01$, ### $P \leq 0.001$. $n = 4$ /group.

3.4.3 Determining kinetics of ISGs expression in the brain

In the immediate hours following a single injection of LPS, the response in the brain is well characterised. Largely encompassing an acute phase response, the majority of reported effects in the brain are known to peak within 12 hours following injection^{315,324,417}. To determine whether the upregulation of ISGs, observed 48 hours after LPS injection, is merely a remnant of an earlier response, we looked at expression levels of a selection of ISGs in the brain 6 hours and 12 hours following injection and compared them to the expression levels at 48 hours. With the exception of *Cxcl10*, the expression levels of which are significantly reduced at 48 hours, no significant differences were observed (Figure 3.17). However, in the case of *Gbp4* and *Irf7*, there is a noticeable trend towards a reduction in expression between 12 hours and 48 hours. These data suggest that an IFN response has been initiated in the brain by 6 hours following LPS injection. This response persists until 48 hours after injection, retaining its potency until at least the 12 hour time point.

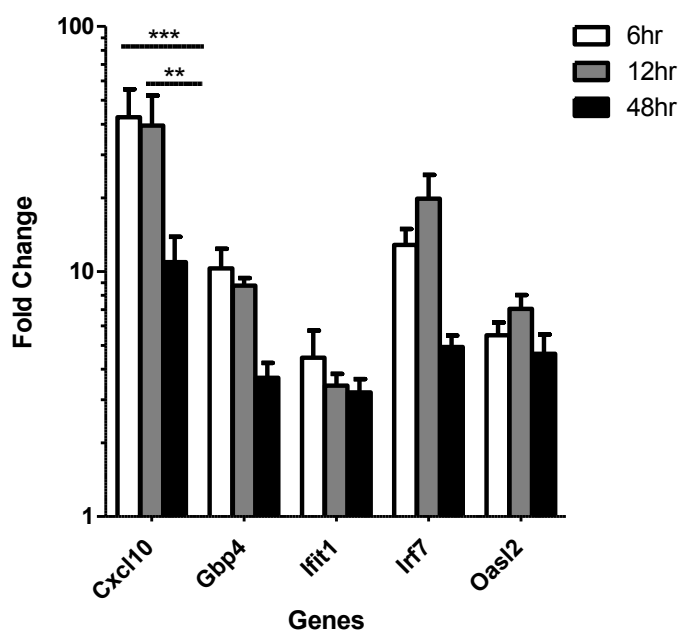


Figure 3.17 Temporal expression of ISGs in the brains of LPS-injected mice

RNA was isolated from the brain, 6, 12 and 48 hours after injection with 100µg LPS or an equivalent volume of vehicle. Relative ISG expression was determined using QPCR and normalised to TBP. Data are expressed as fold change in gene expression in the brain of mice, 6 hours (□), 12 hours (▒) and 48 hours (■) following LPS-injection relative to vehicle-injected controls mouse brains. Data represent the mean ± SEM. A statistical comparison was made between the fold induction at different time points using two-way ANOVA: *P ≤ 0.05, **P ≤ 0.01, ***P ≤ 0.001. n = 4/group.

3.5 Discussion and conclusions

In order to assess what influence LPS-induced systemic inflammation has on gene expression in the brain, microarrays were utilised to compare the transcriptional profile of the brain 48 hours after injection with either LPS or vehicle. The data were subjected to several levels of analysis. A number of transcripts were significantly elevated in the brain 48 hours following LPS injection. These were clustered according to biological function and then grouped into pathways. QPCR analysis was then used to validate the dataset and to compare gene expression in the brain, the PBL and the bone marrow. These further analyses identified a number of key points, the most important being that an innate inflammatory response occurs in the brain in response to LPS. Although this has been characterised previously in the immediate hours following LPS-injection, it is generally assumed that the response resolves within 24 hours^{324,417,418}. From this dataset however, it is apparent that injecting mice with high doses of LPS induces an immune response that lasts in the brain for at least 48 hours. Differing in kinetics and magnitude, this response is distinct from that of the PBL and the bone marrow. This crucial observation supports the validity of the dataset; ruling out the possibility of a contaminating signal coming from the peripheral blood.

The occurrence of an LPS-dependent immune response in the brain was demonstrated when genes were clustered according to their biological function. This method of categorisation revealed that many of the upregulated genes are associated with the “Immune response” and “Immunity and defence”. “Interferon-mediated immunity” and “Macrophage-mediated immunity” also ranked highly in the list of significantly enriched biological processes. Microglia have long been considered the macrophage-like cells of the CNS. They have motile processes which survey the extracellular environment for pathogens or signs of cell damage. Responding accordingly, they play a pivotal role in the innate immune system of the CNS⁴¹⁹. This response is akin to that of tissue macrophages. As microglia also share many structural similarities with their peripheral myeloid-derived counterparts, it can be very hard to distinguish one from the other: so much so that, until recently, it was thought that microglia were derived from the same myeloid precursors as macrophages⁴¹⁹. As a result,

the enrichment of “Macrophage-mediated immunity” could well be an indication of microglial cell-mediated immunity.

Enhanced transcription of genes involved in “Interferon-mediated immunity” is indicative of an IFN-response in the brain. This is certainly backed up by the pathway analysis which shows significant upregulation of the “Activation of IRFs by cytosolic pattern recognition receptors”, “Jak1, Jak2 and Tyk2 in IFN signalling” and the “IFN Signalling” pathways. IFN signalling leads to the downstream activation of an abundance of ISGs. In further support of an IFN response in the brain, the differential transcriptional profile following LPS injection is largely monopolised by the induction of this gene family; with ISGs encompassing over half of the genes believed to be most biologically meaningful.

Crucially, the expression profile in the brain differed from that of peripheral blood leukocytes and from the bone marrow. Target genes were modulated to a different extent in the three tissues analysed. Importantly, ISGs encoding GBP-3, GBP-4 and IRF7 were upregulated independently in the brain, as was the gene encoding the cytokine receptor component, IL-2R γ . In addition, although the genes encoding the interferon-inducible chemokine, CXCL10, and the immunoglobulin receptor, FC γ RIV, were also induced in the periphery, they were upregulated to a significantly greater extent in the brain. Altogether, these data identify a brain-specific response to systemic LPS-induced inflammation. This is extremely important. By ruling out contaminating blood as being a source of the gene expression signal, these observations confirm the brain specificity of the Affymetrix dataset.

Although the mechanism by which ISGs are induced in the brain remains to be examined, the temporal expression patterns of a selection of these genes were demonstrated using QPCR. All ISGs assayed were induced by 6 hours following LPS injection and remained elevated until 48 hours, after the bulk of the acute phase response is known to have resolved⁴²⁰. This implies that early events following peripheral LPS challenge may be responsible for the initiation of ISG expression.

The list of ISGs that are upregulated in response to LPS consists of an assortment of type I, type II and type III IFN-response genes. As IFN γ , the only type II IFN, is known to induce an anti-microbial response⁵⁵, enhanced expression of IFN γ -regulated genes would certainly be expected in the periphery following LPS injection. However, there is no evidence, as yet, to suggest that LPS can enter the brain. Although TLR4 is expressed in the brain, a study with radiolabelled LPS suggested that negligible levels cross the BBB⁴²¹, therefore, it is unclear what has induced the expression of these IFN γ -response genes. IFN γ is known to simulate anti-microbial immunity in a cell-autonomous manner so, although no elevated transcripts encoding IFN γ were detected by the array study, it is possible that IFN γ was produced in the brain at an earlier time point. Certainly in the periphery, IFN γ is thought to be produced approximately 6 hours following intraperitoneal LPS injection^{316,422}. Likewise, the array study detected no elevation of type I IFNs suggesting that any enhanced production of this cytokine family must have also occurred prior to the array if it occurred in the brain at all. Another possibility might be that peripherally produced IFNs have a direct effect on the brain. This will be discussed in more detail below.

The enrichment of type I and type III IFN-regulated genes was a surprising finding as these responses are more readily associated with viral clearance⁵⁵. In spite of this dogma, LPS, and other gram negative bacterial components, can induce IFN β expression downstream of the non-canonical TRIF-dependent signalling pathway⁵⁵. However, for this to be the mechanism accounting for the observed ISG induction either LPS, or LPS-induced IFN β , would have to gain access to the brain. In summary, although both type I and type II ISGs were upregulated in the brain following LPS-injection, the mechanism of their induction remains to be clarified. Further work will be required in order to decipher whether IFN production in the brain occurs following LPS injection and if so, whether systemic LPS can have a direct role in central IFN induction.

If Banks *et al.* are correct in their hypothesis that LPS does not access the brain⁴²¹ one possible explanation, accounting for the central induction of ISGs, is the direct effect of systemic IFNs. A study by Wang *et al.* showed that the brain was highly sensitive to systemic IFN α , delivered by intraperitoneal injection⁴²³. The brain rapidly responded to the recombinant cytokine by increasing ISG transcription. In spite of this, no induction of IFN α 1 or IFN β was detectable in

the brain. Wang *et al.* argue that the direct action of systemic IFN α must therefore be responsible for the central elevation of ISG transcription. Amongst the genes induced in the brain were *Stat1*, and *Gbp3*, both of which appear in the list of target genes that were upregulated in response to systemic LPS. *Cxcl10* transcripts, however, were undetectable following systemic IFN α injection. This conflicts with a previous report by the same group which revealed *Cxcl10* as being one of the main genes to be over-expressed when neurons, either *in vitro* or *in vivo*, were exposed to IFN α ⁴²⁴. Therefore, if systemic IFN α has the capacity to directly access the brain, *Cxcl10* should be detectable following a systemic injection. However, if correct, the hypothesis proposed by Wang *et al.* could account for the induction of ISGs following systemic LPS injection; but only if IFN β and IFN γ also shared the capacity to directly access the brain. Although attractive, this hypothesis requires further evidence to demonstrate that IFN α crossed one of the brain's barriers, or that another IFN α -subtype was not produced in the brain to account for the ISG induction observed by Wang *et al.* An alternative mode of action could be indirect action of peripherally produced IFNs on the CNS, via stimulation of the BBB or afferent nerves.

Of the ISGs upregulated in the brain in response to LPS, CXCL10 had the highest fold change. It was also one of the few genes to be upregulated to a greater extent in the brain than the PBL. CXCL10 has been shown to be induced in the brain following stroke⁴²⁵, West Nile Virus^{187,188} or HIV-associated CNS disease⁴²⁶. It has also been shown to be upregulated by neurons in response to IFN α ; both *in vitro* and *in vivo*⁴²⁴. CXCL10 is an interferon-inducible chemokine which binds CXCR3 to promote leukocyte chemotaxis⁴²⁷. Induction of CXCL10 in the brain following systemic LPS challenge may result in the chemoattraction and subsequent infiltration of CXCR3+ leukocytes. Although there have been previous reports of increased CXCL10 expression in the brain following systemic LPS injection⁴²⁸, CXCR3-mediated leukocyte infiltration to the brain is not a phenomenon that has been reported after peripheral LPS injection. However, 48 hours following LPS injection, CXCL10 is upregulated almost 10-fold, as are a number of genes involved in the leukocyte extravasation pathway. Therefore, leukocyte infiltration is worth investigating as a potential downstream effect of

injecting high doses of LPS peripherally. Chapter 5 will address whether leukocytes infiltrate the brain in response to systemic LPS challenge.

ISGs were not the only genes to remain induced 48 hours after LPS injection. Genes encoding acute phase reactants lipocalin (LCN) 2, serum amyloid A3 (SAA3) and serine-protease inhibitor 3N (Serpina3N) were all amongst the most altered. As a result, “Acute phase response signalling” was highlighted as one of the most significantly enhanced biological pathways. Responsible for activation of the HPA axis and fever, the acute phase response is one of the key features of LPS challenge. Although the liver is considered the principle production site of acute phase proteins, LPS has previously been shown to induce the expression of acute phase reactants in choroid plexus epithelial cells. Utilizing transcriptomics, a study by Marques *et al.* reported a significant induction of a number of genes in the choroid plexus following intraperitoneal LPS injection⁴²⁰. In particular, between 3 and 24 hours, *Lcn2*, *Saa3* and *Serpina3n* were amongst the most upregulated. Therefore, induction of these genes in the choroid plexus is likely to be a contributing factor to the enhanced expression that was detected in the brain 48 hours after systemic LPS injection. Strategically positioned within the cerebral ventricles, the choroid plexus is responsible for cerebrospinal fluid (CSF) production. In addition, it manages molecular and cellular trafficking across the blood-CSF-barrier; acting as an interface between the blood and the CSF. The extra-hepatic release of acute phase proteins into the CSF, in response to the peripheral inflammatory milieu, may represent a defence mechanism employed by the choroid plexus to protect the brain.

In summary, systemic LPS-induced inflammation triggers an immune response in the brain. Observed 48 hours after challenge, the brain has a specific transcriptional signature; characterised by increased ISG expression. ISGs are induced in the brain by 6 hours post-injection and retain their potency for at least 48 hours. However, it has yet to be established whether this induction is a direct effect of central IFN production, or whether peripherally produced IFNs can travel to, or interact with, the brain. Of the ISGs induced in the brain in response to LPS, *Cxcl10* was upregulated most. It was also upregulated to a greater extent in the brain than in the blood. This transcriptional response is indicative of peripherally triggered, interferon-mediated brain inflammation and

the induction of CXCL10 suggests that the brain may be being primed for T cell infiltration.

4 Defining mechanisms of target gene induction in the CNS following systemic LPS challenge

4.1 Introduction and aims

In Chapter 3, it was demonstrated that systemic administration of LPS alters the gene expression profile in the brains of C57BL/6 mice; triggering the induction of a number of inflammatory genes. However, the precise mechanisms accounting for target gene induction in the brain remains to be clarified.

Current dogma suggests that the brain can become sensitised to systemic LPS challenge by a number of mechanisms which act in concert. Described in detail in Section 1.4.2, these comprise neural transmission along with various humoral routes. Circulating inflammatory cytokines, induced in response to LPS, can activate blood vessel endothelial cells to enhance prostaglandin release and thus transmit inflammatory signals across the BBB^{323-325,327}. Supplementing this humoral pathway, afferent neurons innervating regions of inflammation respond to the inflammatory cytokine milieu and relay this information to the brain (Section 1.4.2). Thus, by propagating inflammatory signals from the periphery to the brain, inflammatory cytokines may play a major role in immune-to-brain communication following systemic LPS injection. As a consequence, the initial aim for this chapter was to establish whether elevated circulating inflammatory cytokines were sufficient or indeed necessary to induce a similar transcriptional response as that induced by a single, systemic injection of LPS. To this end, target gene expression was assessed in the brain and matched PBL samples following systemic TNF α -induced inflammation or during LPS-induced endotoxin tolerance, when inflammatory cytokine production is known to be ameliorated in the periphery^{429,430}. Following TNF α -induced inflammation, or LPS-induced endotoxin tolerance, the respective induction or amelioration of circulating cytokines was confirmed by ELISA. Target gene expression in the brain and PBL was then compared to a vehicle injected control group using SYBR Green QPCR.

LPS binds to TLR4 and exerts its effects via one of two downstream signalling pathways (Figure 4.1): activation of the classical MyD88-dependent pathway resulting in inflammatory cytokine induction, or IRF3 activation through the TRIF-dependent pathway triggering IFN β production. The literature surrounding immune-to-brain communication pathways following LPS-induced inflammation almost exclusively focuses on the downstream effects of NF κ B activation as a result of the classical MyD88-dependent pathway. For example, NF κ B activation

is responsible for the induction of inflammatory cytokines which, as described above, can activate the vagus nerve and the BBB endothelium. Furthermore, circulating LPS can activate the brain vasculature directly by ligating TLR4 expressed on the surface of the endothelium (Section 1.4.2.2). By activating NF κ B, this induces COX2 production and enhances prostaglandin synthesis^{324,327,328}. Thus, by activating the MyD88-dependent signalling pathway, LPS can either directly or indirectly propagate inflammatory signals across the BBB.

As these are the most characterised routes of immune-to-brain communication following systemic LPS challenge, it is possible that MyD88-dependent signalling pathway activation is responsible for the central induction of inflammatory target genes. However, as the majority of ISGs upregulated in response to LPS can be regulated by type I IFNs (Section 1.4.2.2), it was hypothesised that they are being expressed downstream of LPS-induced IFN β production via the TRIF-dependent pathway. The secondary aim of this chapter was to explore this hypothesis further by establishing whether target gene induction in the brain occurred following MyD88-dependent pathway activation in the absence of TRIF-dependent signalling. C57BL/6 mice were injected intravenously with the TLR2 ligand, lipoteichoic acid (LTA). TLR2 ligation can only activate NF κ B through the classical MyD88-dependent signalling pathway (Figure 4.1), thereby eliminating the possibility of TRIF-dependent signalling. The expression of target genes in the brain was again compared to a vehicle-injected control group using QPCR. In summary, the expression levels of microarray target genes were investigated in different sterile, and TLR-dependent, models of peripheral inflammation, with the aim of investigating the molecular mechanisms governing the modulation of these genes in the brain following peripheral LPS injection.

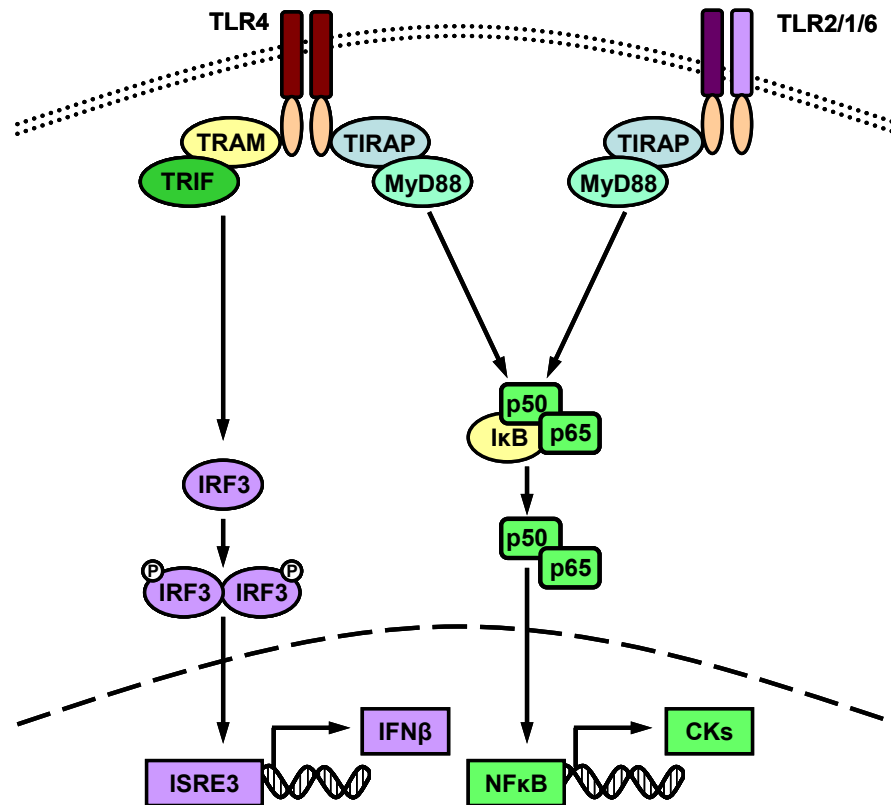


Figure 4.1 TLR-induced signalling pathways.

When activated, toll-like receptors (TLRs) either heterodimerise, such as TLR2 with either TLR1 or TLR6, or homodimerise to induce signalling pathway activation. Signalling is regulated by adaptor molecules. MyD88 is an adaptor used by all TLRs aside from TLR3. TLR7 recruits MyD88 directly, whereas TLR4 and TLR2 recruit MyD88 through bridging adapter TIRAP. MyD88 recruitment ultimately leads to the activation of nuclear transcription factor NFκB by releasing the p50 and p65 subunits from the NFκB inhibitor IκB. Activated NFκB then translocates to the nucleus to induce the expression of inflammatory cytokines. An alternative signalling pathway downstream of TLR4 involves the recruitment of adaptor molecule TRIF through bridging protein TRAM. This ultimately leads to activation of IRF3 and subsequent IFNβ induction (Reviewed in Ref 431).

4.2 Target gene expression following systemic cytokine-induced inflammation

Communication pathways between the immune system and the nervous system are often assumed to involve the intermediary action of inflammatory cytokines. Therefore, to determine whether elevated inflammatory cytokines were sufficient to induce a similar transcriptional profile to systemic LPS, target gene induction was assessed following a sterile, cytokine-induced model of systemic inflammation. 8 week old, male C57BL/6 mice were challenged intravenously with two doses of recombinant murine TNF α (1 μ g at 0 and 24 hours) or an equivalent volume of vehicle (sterile PBS). Mice were terminally anaesthetised, and then perfused, 48 hours after initial injection.

4.2.1 Model validation

To quantify peripheral inflammation following systemic TNF α challenge, the concentration of inflammatory cytokines in the circulation was measured using ELISAs. ELISAs were performed on plasma samples isolated from TNF α - and vehicle-injected mice; 6 hours, 30 hours and 48 hours following initial injection. TNF α and IL-6 were significantly elevated in the circulation 6 hours following a single dose of TNF α (Figure 4.2B&C). 6 hours following the second dose of TNF α (30 hours), TNF α remained slightly but significantly elevated in the plasma, whereas IL-6 had returned to baseline. Surprisingly, no IL-1 β was detected in any of the samples (Figure 4.2A). Therefore, mice challenged systemically with TNF α presented with elevated levels of TNF α and IL-6 in the circulation compared to vehicle-injected controls.

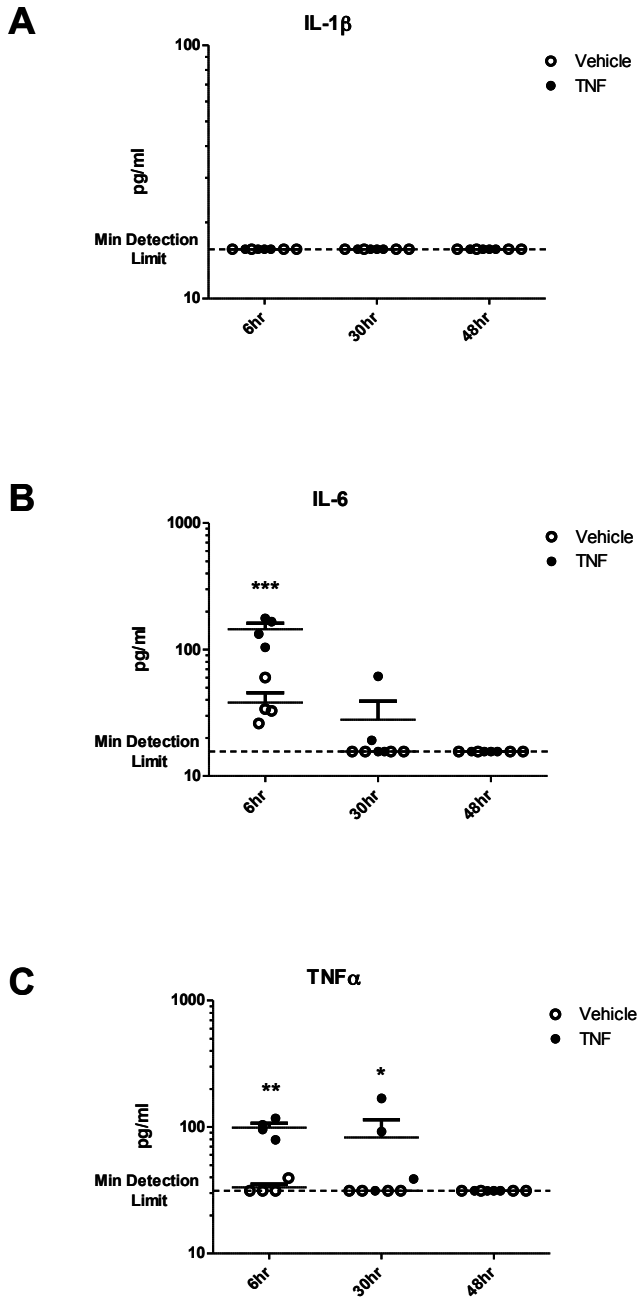
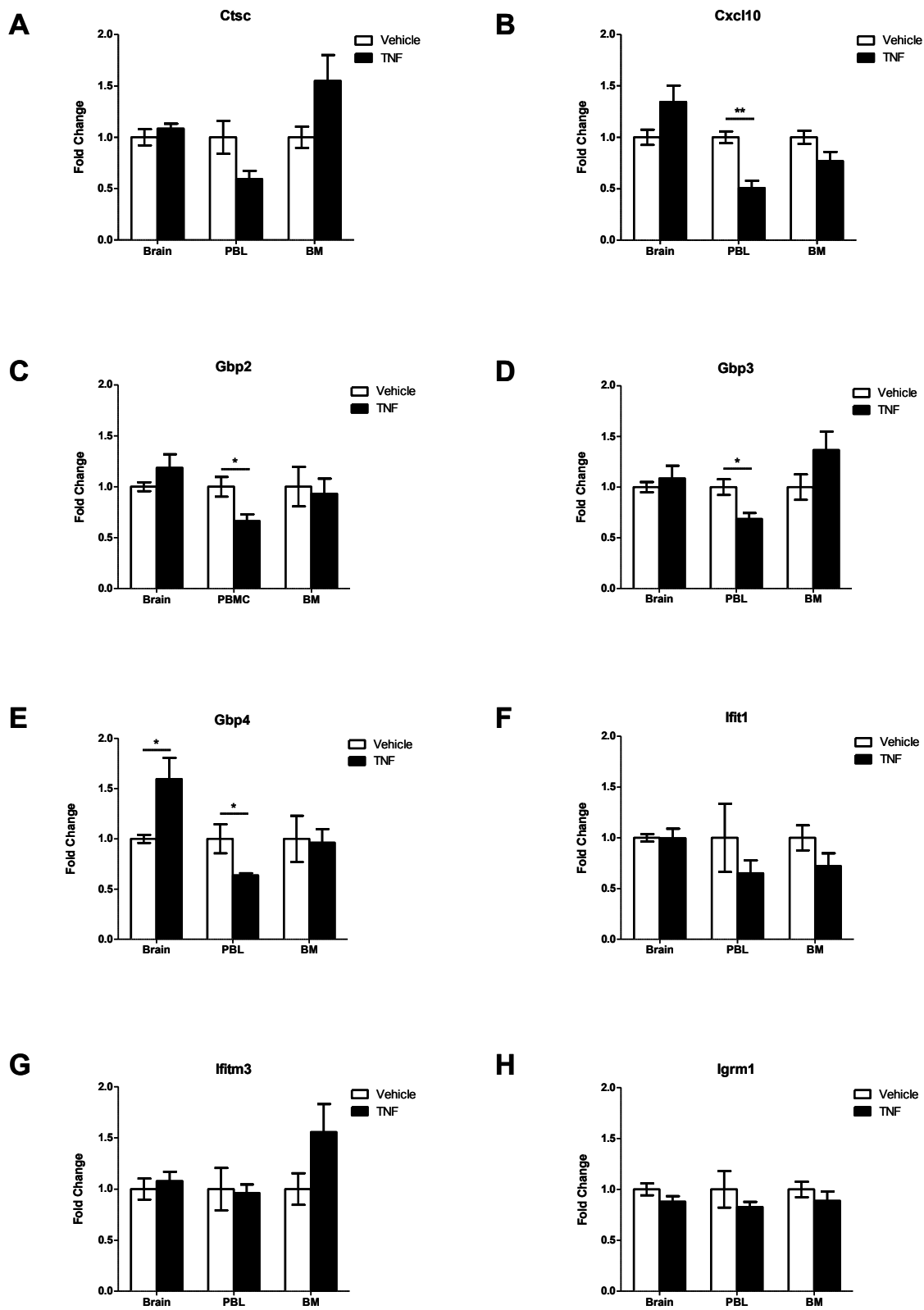


Figure 4.2 Plasma concentration of inflammatory cytokines following systemic TNF α injection

Mice were injected with 1 μ g TNF α (TNF) or an equivalent volume of vehicle at 0 and 24 hours. Plasma was isolated from the whole blood of mice; 6 hours, 30 hours and 48 hours following initial injection. Concentrations of (A) IL-1 β , (B) IL-6 and (C) TNF α (TNF) in the plasma were determined using ELISA. Data represent the mean plus or minus SEM. Significance was determined using two-way ANOVA. n = 4/group.

4.2.2 Target gene modulation in the brain, PBL and BM following systemic TNF α injection

In Chapter 3, using both microarrays and QPCR, a number of genes were identified as being upregulated in the brain in response to a systemic LPS challenge. To establish how these genes were modulated in the brain and periphery following TNF α -induced inflammation, SYBR Green QPCR was used to compare gene expression in the brains, PBL and bone marrow of TNF α - and vehicle-injected mice. Few of the microarray target genes were significantly elevated in the brains of the TNF α -challenged mice. Of the ISGs that were upregulated in the brain in response to LPS, only *Gbp4* was upregulated in the brain in response to systemic TNF α (Figure 4.3). *Stat1* was also upregulated in the brain following intravenous TNF α -injection. Although *Stat1* was included in the list of target ISGs that, following microarray analysis, were identified as being upregulated in the brain in response to systemic LPS (Section 3.3.7), this induction was not confirmed using QPCR. None of the genes encoding acute phase proteins were significantly elevated in the brain following TNF α -injection (Figure 4.4), although there was a trend towards an upregulation of *Saa3* (7.9-fold). Aside from the slight but significant induction of *Gbp4* and *Stat1* (1.59- and 1.26-fold respectively), the only other significantly upregulated genes in the brain were immune response genes, *Il2rg*, *Ly6a* and *Pglyrp1* (Figure 4.5). None of these genes were upregulated more than 2-fold. As a result, it was unclear whether this mild enhancement of gene expression was biologically meaningful.



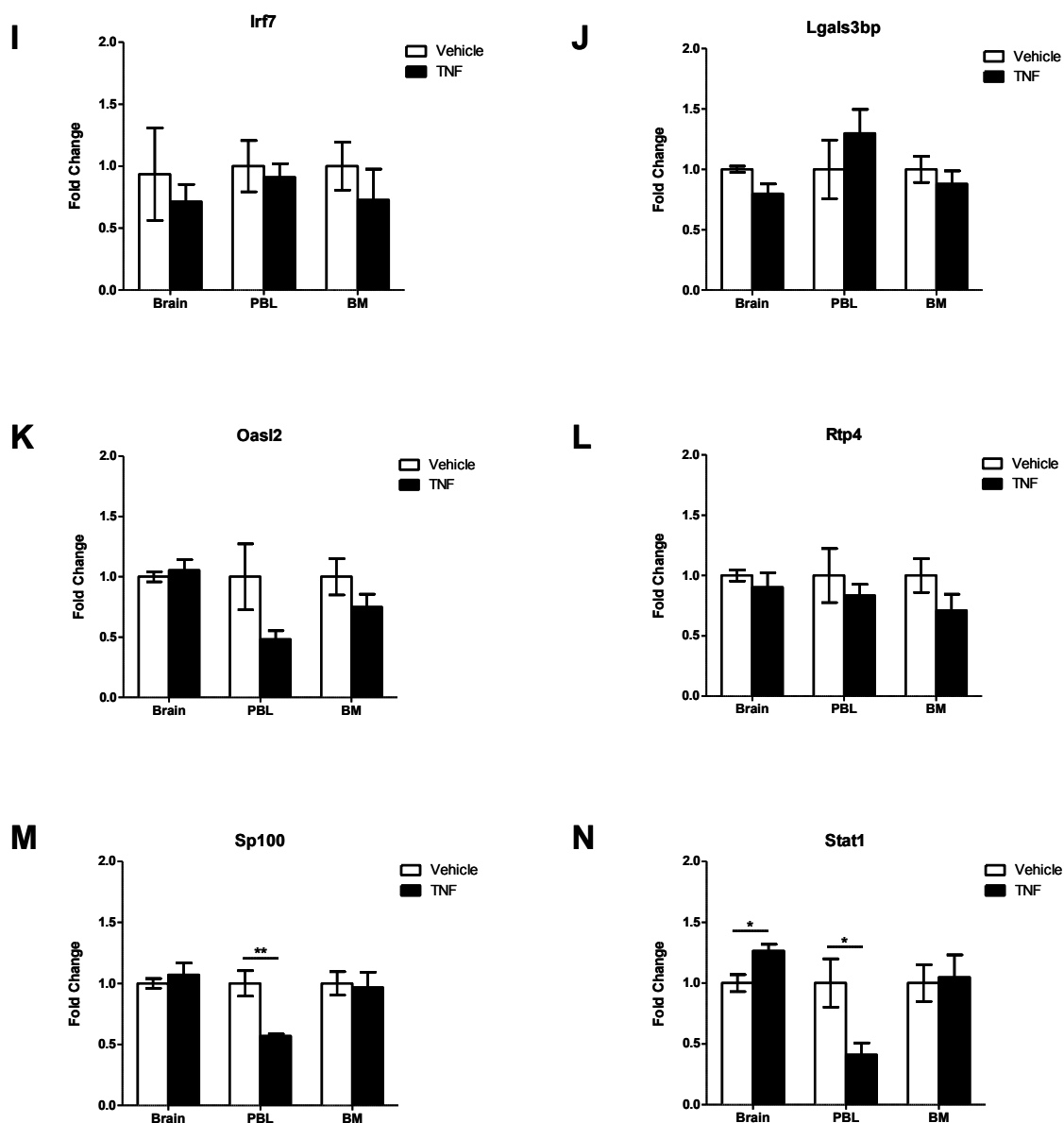


Figure 4.3 Differential expression of ISGs in the brain, PBL and BM of TNF-treated mice compared to vehicle control group.

Mice were injected with 1 μ g TNF α (TNF) or an equivalent volume of vehicle at 0 and 24 hours. RNA was then isolated from the brain, peripheral blood leukocytes (PBL) and bone marrow (BM), 48 hours after initial injection. Gene expression analysis of (A) *Ctsc*, (B) *Cxcl10*, (C) *Gbp2*, (D) *Gbp3*, (E) *Gbp4*, (F) *Ifit1*, (G) *Ifitm3*, (H) *Igrm1*, (I) *Irf7*, (J) *Lgals3bp*, (K) *Oasl2*, (L) *Rtp4*, (M) *Sp100* and (N) *Stat1* was performed using QPCR and normalised to TBP. Data are expressed as fold change in gene expression in the brain, PBL and BM of TNF-injected mice (■) relative to that of vehicle-injected controls (□). Data represent the mean \pm SEM. Significance of each fold change was calculated for individual tissues using an unpaired t-test: * $P \leq 0.05$, ** $P \leq 0.01$, *** $P \leq 0.001$. $n = 4$ /group.

Only two genes were significantly upregulated in PBL; those encoding the acute phase protein SAA3 and the host defence component, PGLYRP1 (Figure 4.4 & Figure 4.5). There was also a trend towards an upregulation of immune response gene, Fcgr4. All three of these genes were also significantly upregulated in the

bone marrow. Not only were no ISGs induced in the blood, but several ISGs, *Cxcl10*, *Gbp2*, *Gbp3*, *Gbp4*, *Sp100* and *Stat1* were significantly downregulated (Figure 4.3), along with immune components, *Apobec3* and *C4* (Figure 4.5). Overall, elevated levels of circulating TNF α were not sufficient to induce the expression of the majority of ISGs, or other target genes, in the brain, PBL or bone marrow. Thus, the central induction of target genes following peripheral LPS challenge is likely to be more than a mere by-product of elevated TNF α or IL-6 in the circulation.

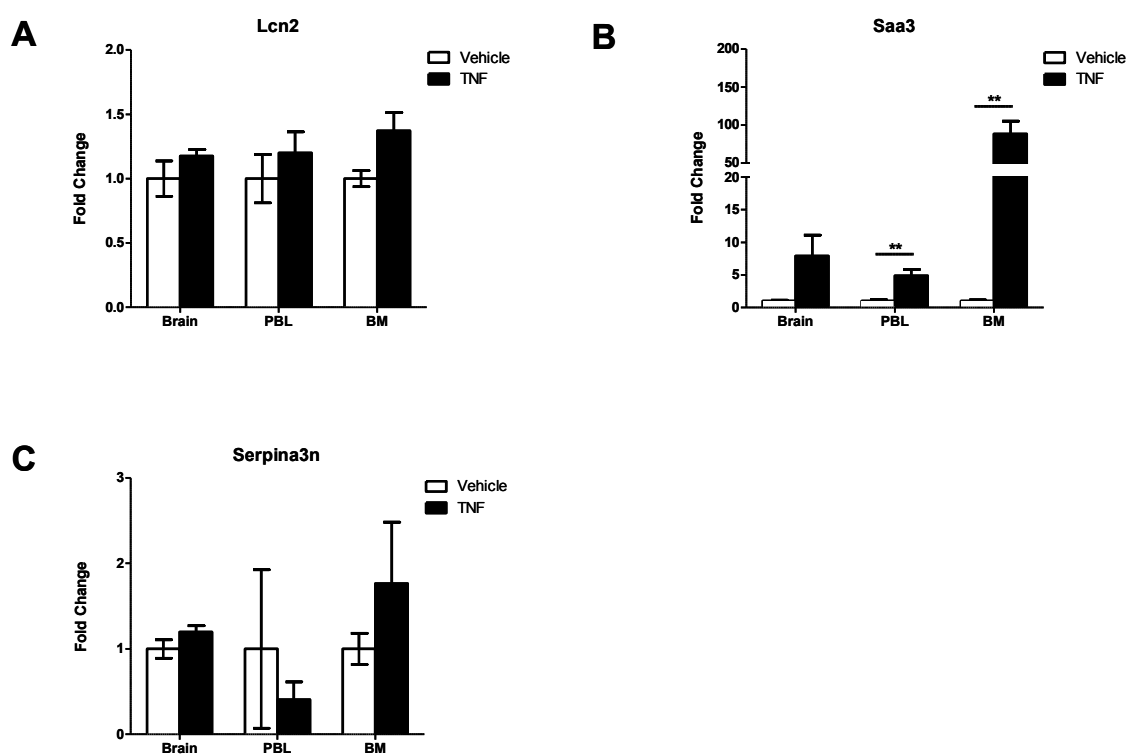


Figure 4.4 Differential expression of acute phase response genes in the brain, PBL and BM of TNF α -injected mice compared to vehicle control group.

Mice were injected with 1 μ g TNF α (TNF) or an equivalent volume of vehicle at 0 and 24 hours. RNA was then isolated from the brain, peripheral blood leukocytes (PBL) and bone marrow (BM), 48 hours after initial injection. Gene expression analysis of (A) *Lcn2*, (B) *Saa3* and (C) *Serpina3n* was performed using QPCR and normalised to TBP. Data are expressed as fold change in gene expression in the brain, PBL and BM of TNF-injected mice (■) relative to that of vehicle-injected controls (□). Data represent the mean \pm SEM. Significance of each fold change was calculated for individual tissues using an unpaired t-test: * $P \leq 0.05$, ** $P \leq 0.01$, *** $P \leq 0.001$. $n = 4$ /group.

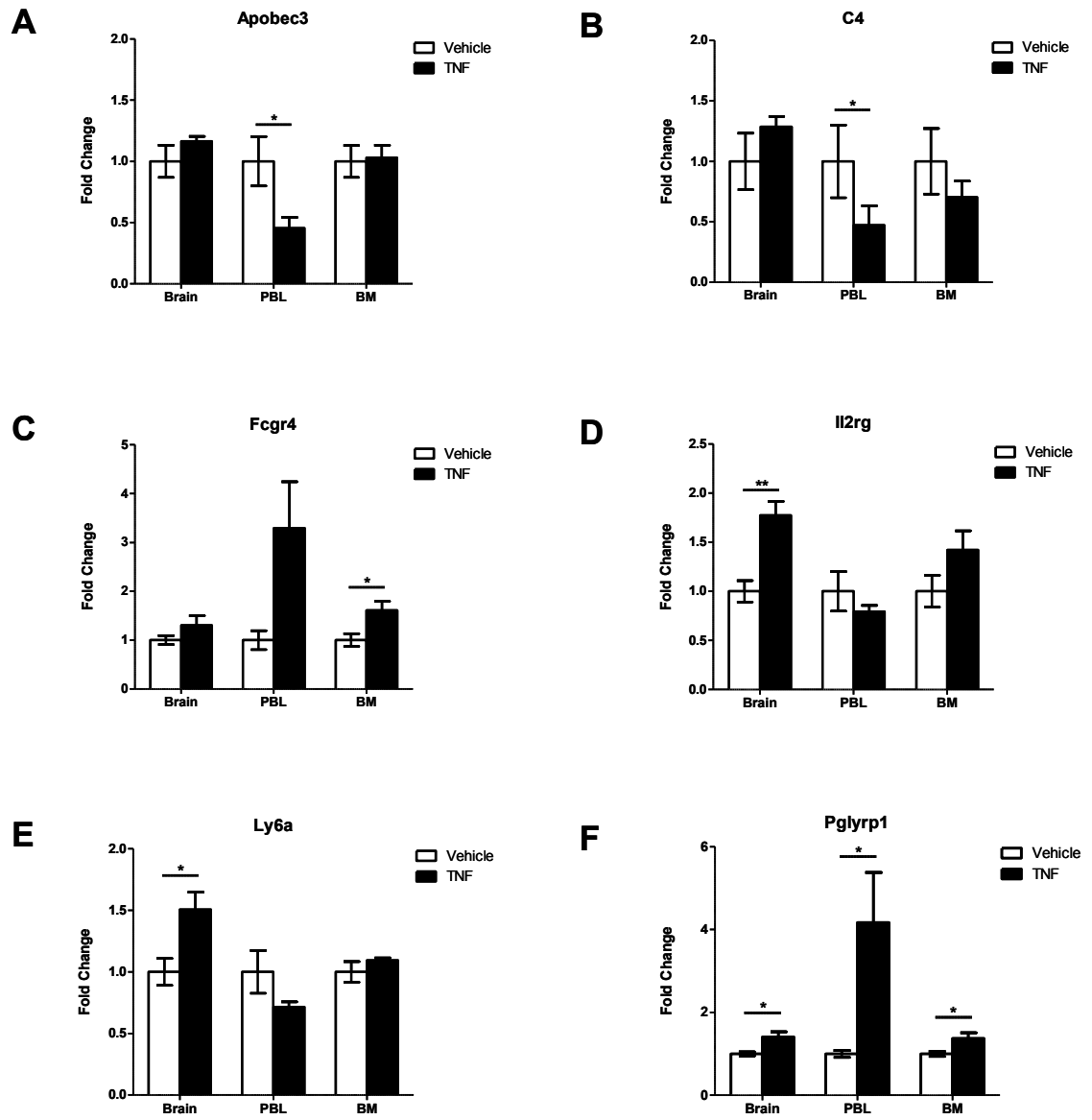


Figure 4.5 Differential expression of remaining target genes in the brain, PBL and BM of TNF α -injected mice compared to vehicle control group.

Mice were injected with 1 μ g TNF α (TNF) or an equivalent volume of vehicle at 0 and 24 hours. RNA was then isolated from the brain, peripheral blood leukocytes (PBL) and bone marrow (BM), 48 hours after initial injection. Gene expression analysis of (A) *Apobec3*, (B) *C4*, (C) *Fcgr4*, (D) *Il2rg*, (E) *Ly6a* and (F) *Pglyrp1* was performed using QPCR and normalised to TBP. Data are expressed as fold change in gene expression in the brain, PBL and BM of TNF-injected mice (■) relative to that of vehicle-injected controls (□). Data represent the mean \pm SEM. Significance of each fold change was calculated for individual tissues using an unpaired t-test: * $P \leq 0.05$, ** $P \leq 0.01$, *** $P \leq 0.001$. $n = 4$ /group.

4.3 Temporal target gene expression in PBL and brain following repeated LPS challenge

Although the majority of target genes were not induced in the brain in response to systemic TNF α -induced inflammation, the above experiments do not rule out the contribution of other inflammatory cytokines which may induce target gene expression in the brain. With the aim of establishing the temporal pattern of target gene expression in the brain and PBL in the context of endotoxin tolerance, when inflammatory cytokine production is known to be ameliorated specifically in the periphery but not in the brain^{429,430,432,433}, mice were exposed to LPS over a prolonged period of time. Endotoxin tolerance is an important defence mechanism designed to protect the host against endotoxic shock. In addition to eliciting expression of a number of proinflammatory genes, initial cellular exposure to LPS triggers the simultaneous downregulation of TLR expression and induction of several inhibitory molecules which negatively regulate TLR signalling⁴³⁴. This culminates in a transient inactivation of various proinflammatory genes by leukocytes in the periphery, including genes encoding the inflammatory cytokines TNF α , IL-1 β and IL-6. At the same time, less potentially pathogenic genes are primed, such as anti-microbial effectors⁴²⁹. As a consequence, repeated exposure to TLR ligands leads to a dampening of the proinflammatory milieu without compromising host defence. Conversely, cytokine expression has been shown to continue in the brain during endotoxin tolerance^{432,433}. To induce endotoxin tolerance, 8 week old, male C57BL/6 mice were injected with a single dose of LPS (50 μ g i.p.) daily for 2, 5 or 7 consecutive days. SYBR Green QPCR was then used to determine the expression of a selection of target genes in the brains and PBL of LPS challenged mice compared to a vehicle injected control group.

4.3.1 Model validation

To verify that the concentrations of inflammatory cytokines are ameliorated in the circulation following prolonged exposure to systemic LPS, plasma levels of IL-1 β , IL-6 and TNF α were measured following a single, systemic, injection of 50 μ g LPS and compared to daily administration of the same dose. 6 hours following a single, intraperitoneal injection, both IL-1 β and IL-6 were significantly elevated in the circulation (Figure 4.6A&B). No TNF α was detected at this time

point (Figure 4.6C). Concentrations of these cytokines are similar, and only slightly lower in magnitude, than what was previously demonstrated following an intraperitoneal injection of 100 μ g LPS (Section 3.2.1). On day 2, after two doses of LPS (on day 0 and day 1) there was still a significant elevation of IL-6 in the circulation of LPS challenged mice, although the concentration was reduced by more than 6-fold from that observed following a single injection. The concentration of IL-6 returned to baseline between days 2 and 5. There was no detectable elevation of TNF α or IL-1 β following multiple LPS challenges at any of the time points analysed. Thus, IL-1 β and TNF α are undetectable in the circulation following multiple LPS challenges. Whilst IL-6 remained significantly elevated after two doses of LPS, it was undetectable for the remainder of the model. In keeping with the literature, this suggests that multiple systemic LPS challenges induce a state of tolerance that is characterised by reduced production of inflammatory cytokines in the periphery.

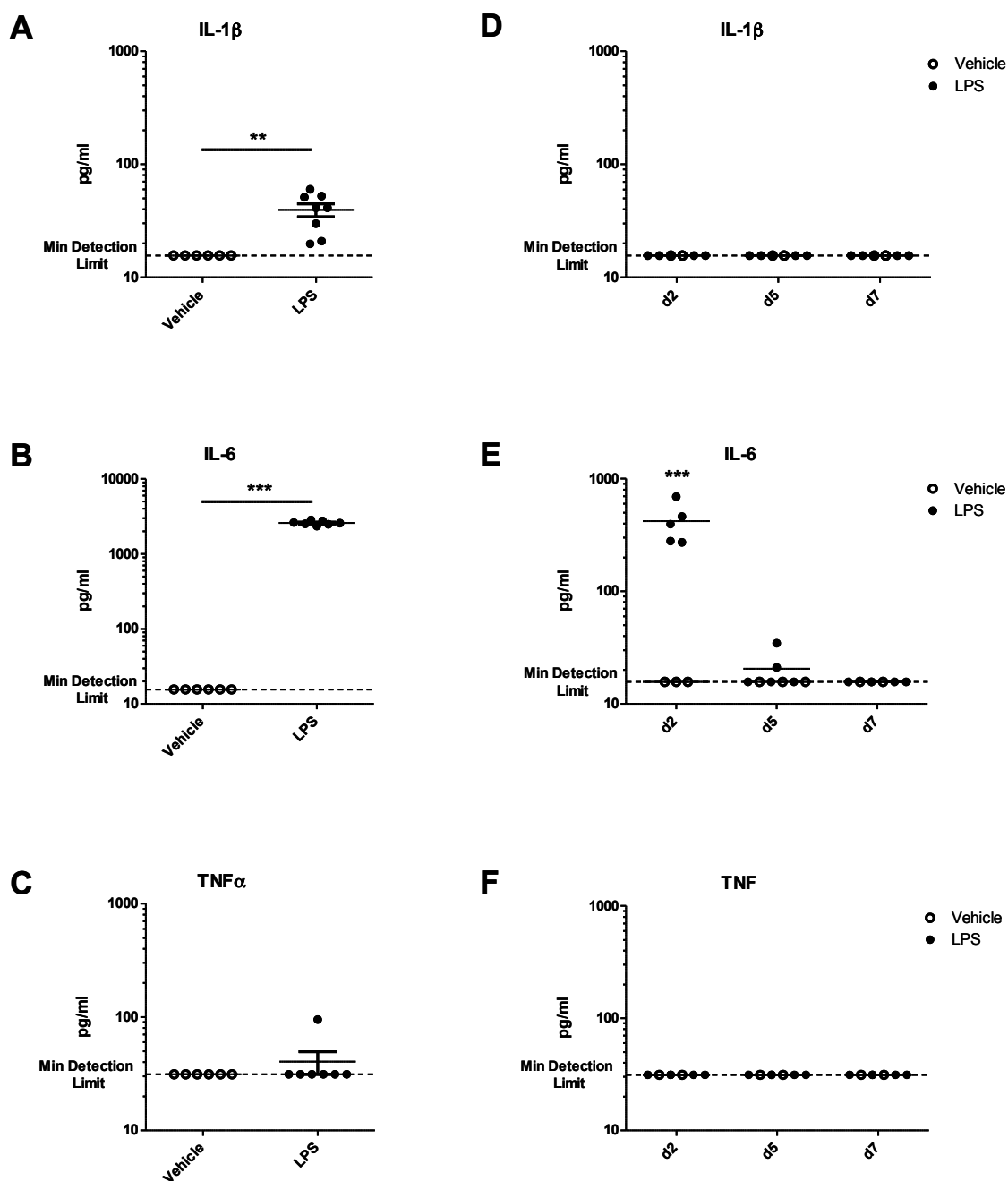


Figure 4.6 Plasma concentration of inflammatory cytokines following acute LPS challenge and during endotoxin tolerance.

(A-C) Concentrations of (A) IL-1 β , (B) IL-6 and (C) TNF α (TNF) in the plasma 6 hours after a single dose of 50 μ g LPS. Significance was determined using an unpaired t-test. n = 6/group (Vehicle), n = 8/group (LPS). (D-E) Mice were injected daily with 50 μ g LPS or an equivalent volume of vehicle. Concentrations of (A) IL-1 β , (B) IL-6 and (C) TNF α (TNF) were measured in the plasma 2 days (d2), 5 days (d5) and 7 days (d7) following initial injection. Significance was determined using two-way ANOVA. n = 3/group (Vehicle), n = 5/group (LPS). All concentrations were determined using ELISA. Data represent the mean plus or minus SEM. *P \leq 0.05, **P \leq 0.01, ***P \leq 0.001.

4.3.2 Comparing cytokine induction in the brain and PBL during endotoxin tolerance

To establish how inflammatory cytokine induction is effected in the brain during endotoxin tolerance, SYBR Green QPCR was performed to compare the transcriptional induction of *Il1b*, *Il6* and *Tnfa* in the brain and matched PBL of LPS injected mice compared to vehicle injected controls. Consistent with previous reports^{432,433}, *Il1b* and *Tnfa* were independently upregulated in the brain following multiple LPS challenges (Figure 4.7). Although *Il1b* expression was reduced in the brain between days 2 and 5, Levels of *Tnfa* transcripts remained significantly elevated throughout the model. As anticipated, under these conditions, inflammatory cytokine transcripts were not induced in PBL (Figure 4.7). Therefore, the brain exhibits a specific cytokine induction in response to multiple LPS challenges. This suggests that the brain may not be subject to the same regulatory mechanisms that dampen cytokine production in the periphery during endotoxin tolerance.

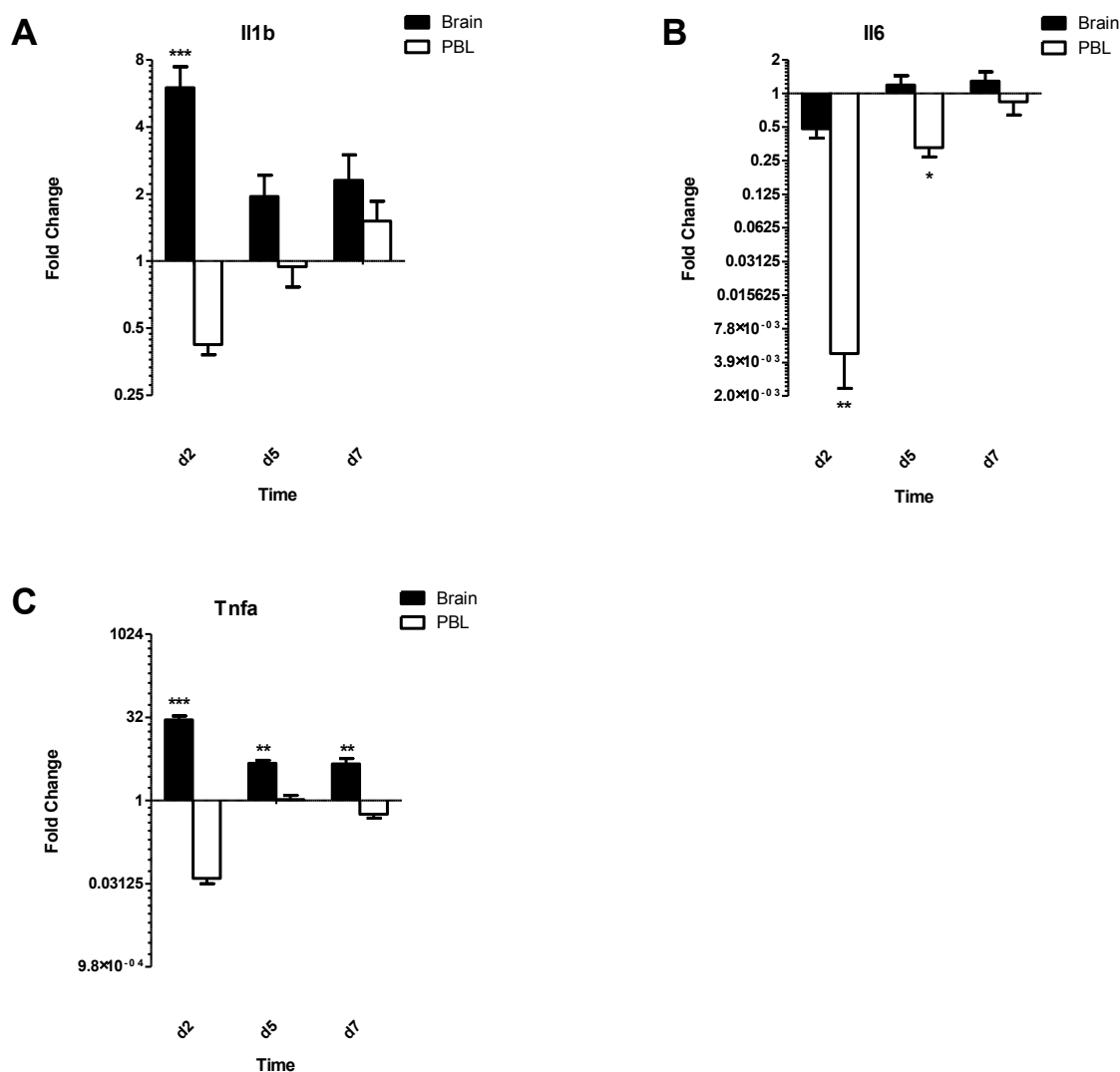


Figure 4.7 Cytokine expression in the brain and in the PBL during endotoxin tolerance.

Mice were injected daily with 50 μ g LPS or an equivalent volume of vehicle. RNA was extracted from brains and peripheral blood leukocytes (PBL), 2, 5 and 7 days following initial injection. Gene expression analysis of (A) *Il1b*, (B) *Il6* and (C) *Tnfa* was performed using QPCR and normalised to TBP. Data are expressed as fold change in gene expression in the brain (■) and PBL (□) of LPS-injected mice relative to vehicle-injected controls. Data represent the mean \pm SEM. A statistical comparison was made, between the fold induction in the brains and PBL of LPS-injected mice and that of vehicle-injected controls, using two-way ANOVA: * $P \leq 0.05$, ** $P \leq 0.01$, *** $P \leq 0.001$. $n = 4$ /group.

4.3.3 Comparing target gene induction in the brain

To determine how target ISG induction is affected during endotoxin tolerance, expression levels of a selection of ISGs in the brain and PBL of LPS-injected mice was compared to those of vehicle-injected mice using SYBR green QPCR. The temporal expression of the ISGs was arbitrarily compared to that of *Il2rg*, a

microarray target gene not regulated by IFNs. At day 2, all ISG were significantly upregulated in the brains of the LPS-challenged mice (Figure 4.8). At the same time point, most ISGs were similarly upregulated in PBL as in brain, with the exception of *GBP4* which was downregulated. On day 5, ISGs remained induced in the brain. All but *Cxcl10* were significantly upregulated at this time point. In contrast, the same genes were significantly downregulated by PBL. By day 7, ISG transcript levels began to return to baseline, with the exception of *Irf7* which remained significantly induced in the brain. In contrast to the temporal expression of ISGs, *Il2rg* displayed a different pattern of expression. *Il2rg* was significantly upregulated in the brain at all time points. The expression levels of this gene did not deviate from baseline in the PBL. These data suggest that whilst ISG expression following repeated LPS challenge is dampened in the periphery, expression continues in the brain, gradually decreasing in potency between days 2 and 7. Subsequently, it would appear that the brain exhibits a specific and prolonged response to repeated LPS challenge. Encompassing ISG induction, this response is distinct from that of the periphery. Not only does this highlight a differential mechanism of gene regulation in the brain from the PBL, but it further verifies that ISG and *Il2rg* expression in the brain is unlikely to be a downstream consequence of elevated peripheral inflammatory cytokines.

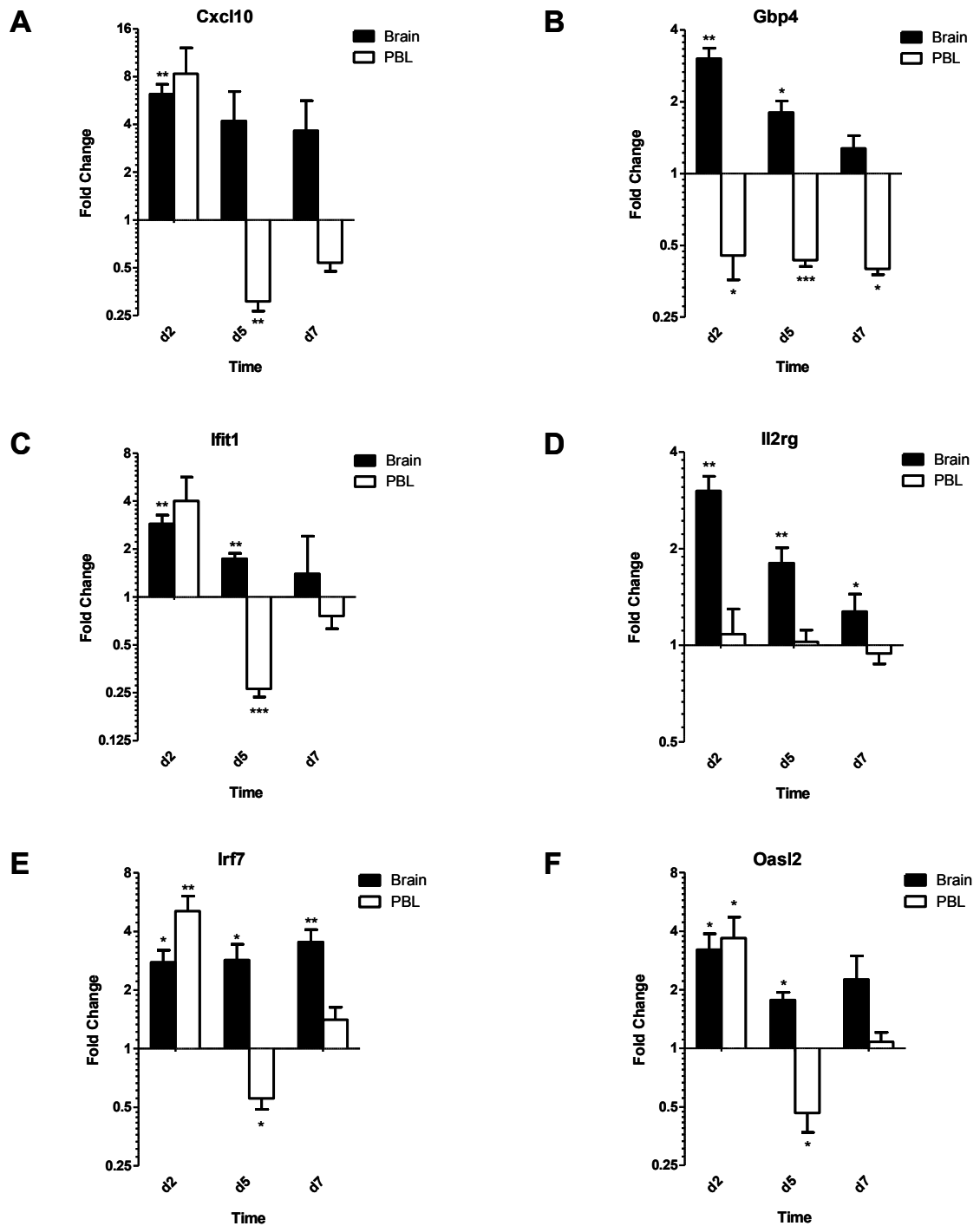


Figure 4.8 Temporal gene expression in the brain and PBL of mice following repeated LPS injections

Mice were injected daily with 50 μ g LPS or an equivalent volume of vehicle. RNA was extracted from brains and peripheral blood leukocytes (PBL), 2, 5 and 7 days following initial injection. Gene expression analysis of (A) *Cxcl10*, (B) *Gbp4*, (C) *Ifit1*, (D) *Il2rg*, (E) *Irf7* and (F) *Oasl2* was performed using QPCR and normalised to TBP. Data are expressed as fold change in gene expression in the brain (■) and PBL (□) of LPS-injected mice relative to vehicle-injected controls. Data represent the mean \pm SEM. A statistical comparison was made, between the fold induction in the brains and PBL of LPS-injected mice and that of vehicle-injected controls, using two-way ANOVA: * $P \leq 0.05$, ** $P \leq 0.01$, *** $P \leq 0.001$. $n = 4$ /group.

4.3.4 Type I IFN induction in the brain

As shown above, ISGs remained induced specifically in the brain and not in PBL following multiple LPS injections. To determine whether this could be a downstream effect of IFN production in the brain, TaqMan low density arrays (TLDA) were used to assess the transcriptional induction of a selection of type I IFNs in the brains of LPS-challenged mice compared to those of vehicle-injected controls. On day 2, only *Ifnh1* was significantly upregulated (Figure 4.9). Transcript levels of the other type I IFN genes remained close to baseline at this time point. All IFN transcripts showed a trend towards an upregulation on day 5. However, *Ifnk* was the only gene to be significantly induced. By day 7, *Ifnk* remained induced in the brain, although this was no longer significant. All other IFN transcripts had returned to levels statistically comparable to baseline. These observations suggest that a mild induction of type I IFNs may occur in the brain following repeated LPS challenges.

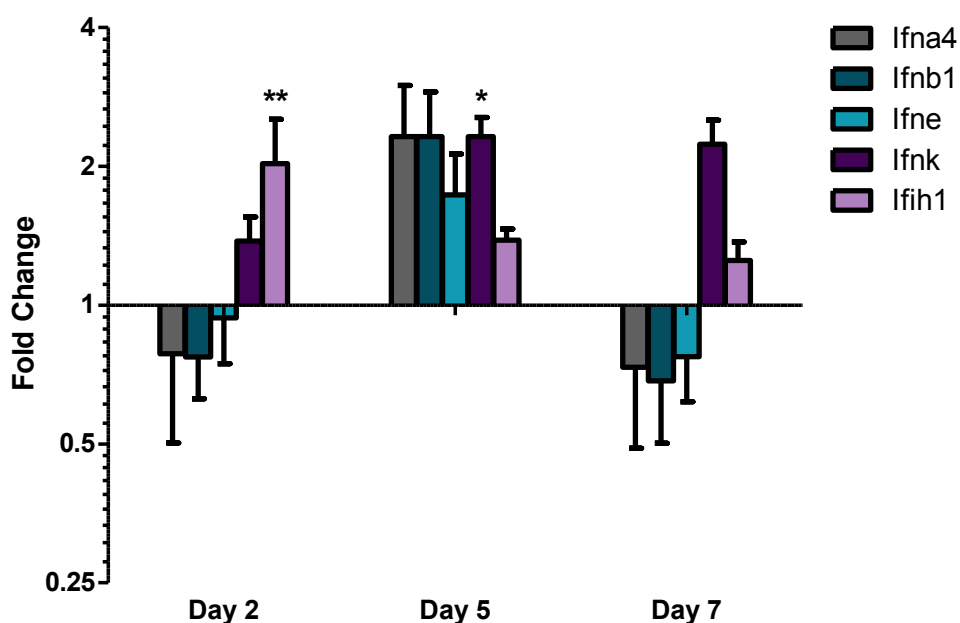


Figure 4.9 Temporal expression of type I IFNs in the brains of mice following repeated LPS injections

Mice were injected daily with 50µg LPS or an equivalent volume of vehicle. RNA was extracted from brains, 2, 5 and 7 days following initial injection. Gene expression analysis of *Ifna4*, *Ifnb1*, *Ifne*, *Ifnk* and *Ifnh1* was performed using TaqMan low density arrays and normalised to TBP. Data are expressed as fold change in gene expression relative to vehicle-injected control mouse brains. Data represent the mean +/- SEM. n = 4-5/group.

4.4 Target gene expression following TLR2-induced MyD88 activation

Elevated ISG expression following systemic LPS injection did not appear to be a downstream by-product of peripheral inflammatory cytokine production as a similar model of sterile inflammation failed to induce the same response. Although this lack of response may have been a result of lower levels of inflammatory cytokines in the circulation, as demonstrated in Section 4.3, expression levels of a selection of target genes remained elevated in the brain following daily LPS injections, long after the cytokine response was dampened in the periphery. Consequently, it is likely that an alternative mechanism is responsible for inducing target gene expression in the brain.

As described previously, LPS can activate two distinct signalling pathways; the MyD88-dependent pathway, or the TRIF-dependent pathway. TLR2 ligand, LTA, however, can only activate the MyD88-dependent pathway (Figure 4.1). As a result, to determine whether the induction of target genes in the brain occurs downstream of TRIF- or MyD88-dependent signalling pathway activation, mice were challenged systemically with LTA. 8 week old, male C57BL/6 mice were injected intravenously with 2 doses (500µg at 0 and 24 hours) or an equivalent volume of vehicle (sterile PBS). Mice were terminally anaesthetised, and then perfused, 48 hours after initial injection.

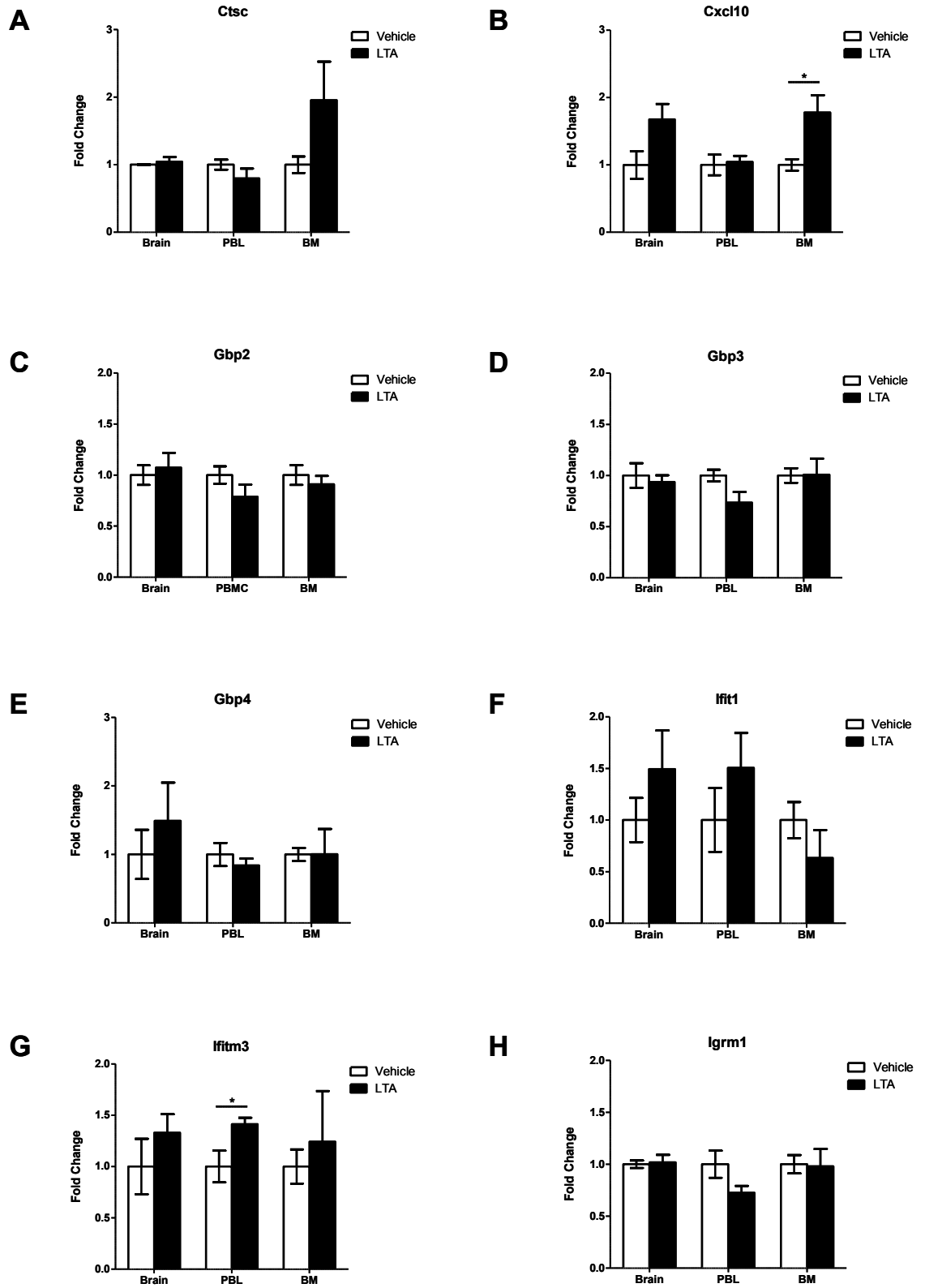
4.4.1 Determining how systemic LTA challenge affects target gene expression in the brain, PBL and BM

To determine whether activation of the MyD88-dependent pathway in the periphery was sufficient to induce a similar transcriptional profile in the brain as induced by systemic LPS, SYBR Green QPCR was used to compare target gene expression in the brains, PBL and bone marrow of mice injected with LTA compared to vehicle-injected controls.

QPCR analysis revealed no significant increase in brain expression of any of the genes shown to be upregulated in response to LPS (Figure 4.10, Figure 4.11 & Figure 4.12). *C4* was the only gene to be significantly upregulated in the brains of mice injected with LTA. Again, although *C4* was one of the target genes that were identified by microarray analysis to be upregulated in the brain in response

to LPS (Section 3.3.7), this upregulation could not be verified by QPCR. Thus, MyD88-dependent activation of NF κ B in the periphery was not sufficient to induce the brain inflammation that occurred downstream of LPS-induced TLR4 activation.

Similar to both the LPS- and the TNF α -challenged mice, *Saa3* was significantly induced in PBL. ISGs, *Ifitm3* and *Lgals3bp* and immune response gene *Fcgr4* were also upregulated by PBL in response to LTA. None of these genes were induced to the same extent as they were by PBL following systemic LPS challenge. A number of target genes; *Cxcl10*, *Sp100*, *Lcn2*, *Saa3* and *Pglyrp1* were significantly induced in the bone marrow of LTA-challenged mice. Of these genes, all but *Sp100* were significantly induced in the bone marrow following systemic LPS challenge. Taken together, these data suggest that although systemic LTA- and LPS-challenge induces the expression of a number of common genes in the periphery, only LPS had the capacity to induce target gene expression in the brain.



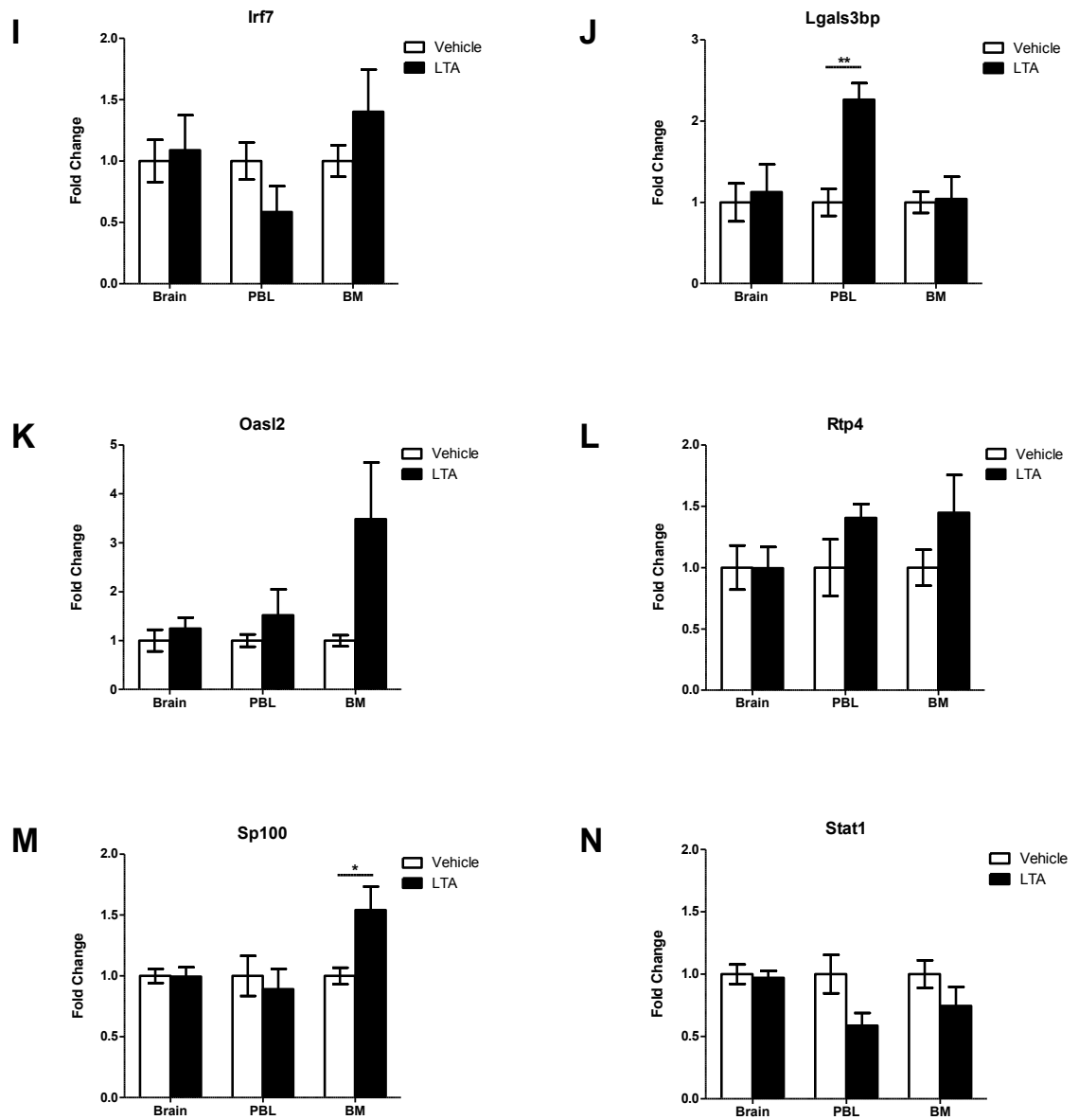


Figure 4.10 Differential expression of ISGs in the brain, PBL and BM of LTA-challenged mice compared to vehicle control group.

Mice were injected with 500 μ g lipoteichoic acid (LTA) or an equivalent volume of vehicle at 0 and 24 hours. RNA was then isolated from the brain, peripheral blood leukocytes (PBL) and bone marrow (BM), 48 hours after initial injection. Gene expression analysis of (A) *Ctsc*, (B) *Cxcl10*, (C) *Gbp2*, (D) *Gbp3*, (E) *Gbp4*, (F) *Ifit1*, (G) *Ifitm3*, (H) *Igrm1*, (I) *Irf7*, (J) *Lgals3bp*, (K) *Oasl2*, (L) *Rtp4*, (M) *Sp100* and (N) *Stat1* was performed using QPCR and normalised to TBP. Data are expressed as fold change in gene expression in the brain, PBL and BM of LTA-injected mice (■) relative to that of vehicle-injected controls (□). Data represent the mean \pm SEM. Significance of each fold change was calculated for individual tissues using an unpaired t-test: * $P \leq 0.05$, ** $P \leq 0.01$, *** $P \leq 0.001$. $n = 4$ /group.

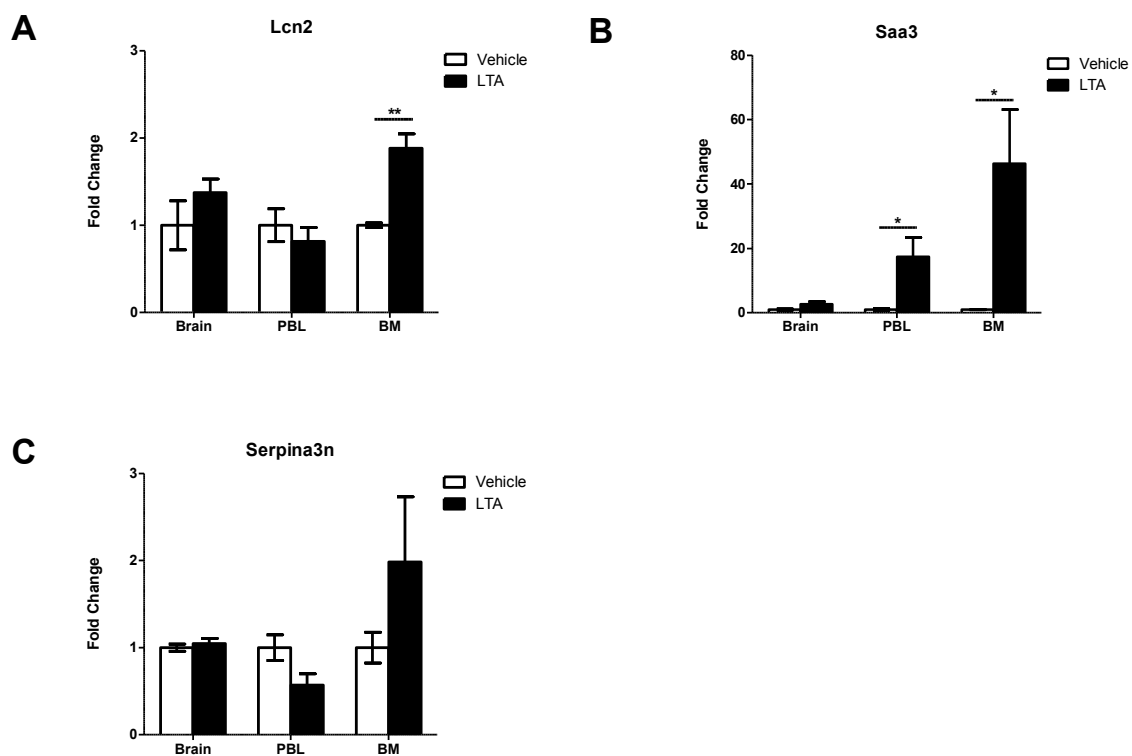


Figure 4.11 Differential expression of acute phase response genes in the brain, PBL and BM of LTA-challenged mice compared to vehicle control group.

Mice were injected with 500 μ g lipoteichoic acid (LTA) or an equivalent volume of vehicle at 0 and 24 hours. RNA was then isolated from the brain, peripheral blood leukocytes (PBL) and bone marrow (BM), 48 hours after initial injection. Gene expression analysis of (A) *Lcn2*, (B) *Saa3* and (C) *Serpina3n* was performed using QPCR and normalised to TBP. Data are expressed as fold change in gene expression in the brain, PBL and BM of LTA-injected mice (■) relative to that of vehicle-injected controls (□). Data represent the mean \pm SEM. Significance of each fold change was calculated for individual tissues using an unpaired t-test: * $P \leq 0.05$, ** $P \leq 0.01$, *** $P \leq 0.001$. $n = 4/\text{group}$.

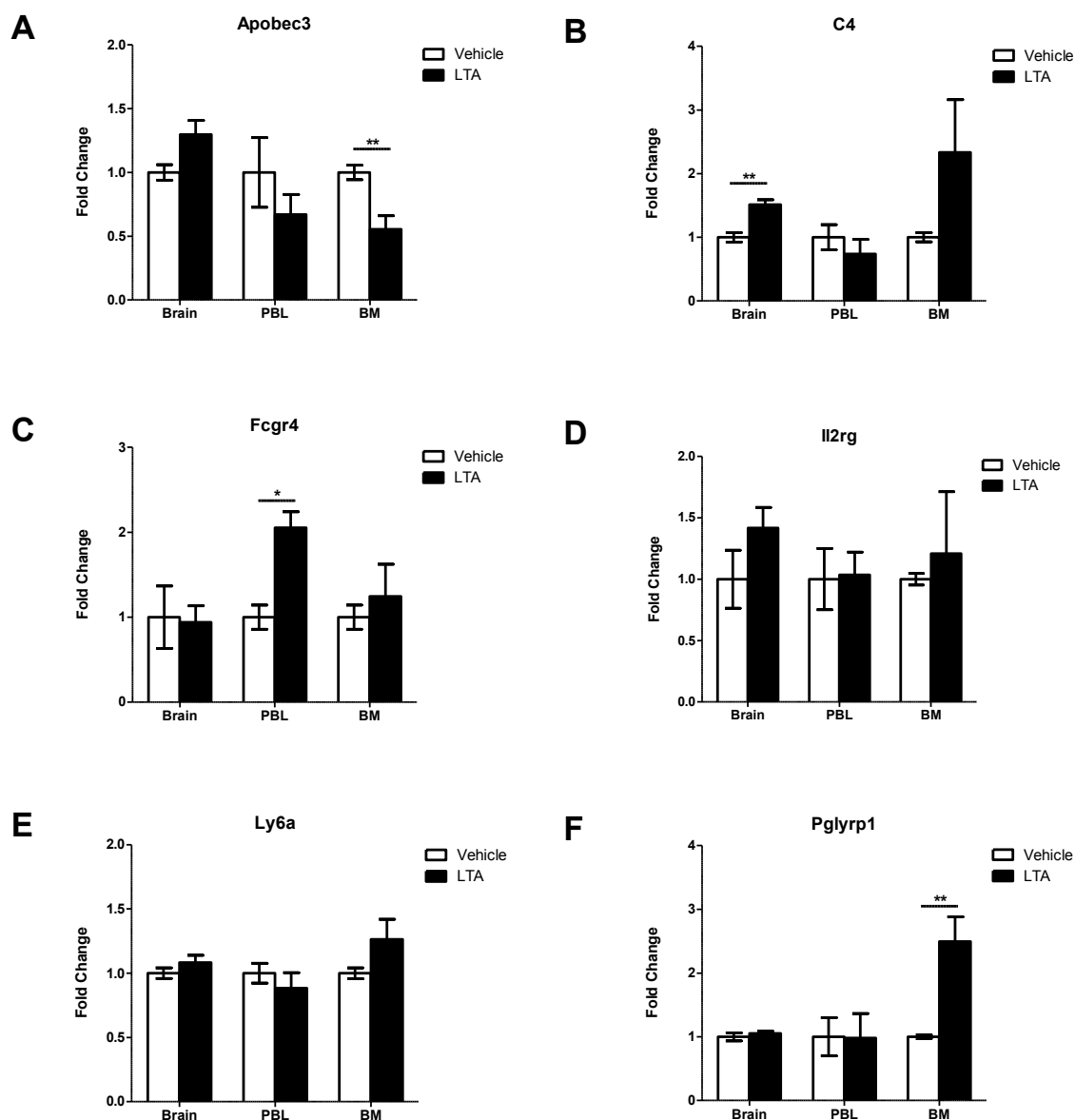


Figure 4.12 Differential expression of remaining target genes in the brain, PBL and BM of LTA-challenged mice compared to vehicle control group.

Mice were injected with 500 μ g lipoteichoic acid (LTA) or an equivalent volume of vehicle at 0 and 24 hours. RNA was then isolated from the brain, peripheral blood leukocytes (PBL) and bone marrow (BM), 48 hours after initial injection. Gene expression analysis of (A) *Apobec3*, (B) *C4*, (C) *Fcgr4*, (D) *Il2rg*, (E) *Ly6a* and (F) *Pglyrp1* was performed using QPCR and normalised to TBP. Data are expressed as fold change in gene expression in the brain, PBL and BM of LTA-injected mice (■) relative to that of vehicle-injected controls (□). Data represent the mean \pm SEM. Significance of each fold change was calculated for individual tissues using an unpaired t-test: * $P \leq 0.05$, ** $P \leq 0.01$, *** $P \leq 0.001$. $n = 4$ /group.

4.4.2 Detecting peripheral inflammation following LTA injection

To assess the extent of peripheral inflammation following systemic LTA challenge, inflammatory cytokines were measured in the circulation and compared to that of a vehicle-injected control group. ELISAs were performed on plasma samples isolated from LTA- and vehicle-injected mice; 6 hours, 30 hours and 48 hours following initial injection. Unexpectedly, very little inflammation was detected in the circulation of mice following systemic LTA challenge. Similar to both the LPS and TNF α models, none of the cytokines assayed were detectable 48 hours after the initial LTA injection (Figure 4.13). 6 hours following initial LTA injection, IL-1 β was significantly elevated in the circulation (Figure 4.13A), however, levels of TNF α and IL-6 were comparable to baseline (Figure 4.13B&C). 30 hours into the model (6 hours after the second injection), elevated IL-6 was detectable in the circulation of two of the four LTA-challenged mice but this was not significant when compared to the vehicle-treated group. These data demonstrate that LTA induces a significant elevation of circulating IL-1 β which returned to baseline between 6 hours and 30 hours. However, at the time points tested, no significant elevation of IL-6 or TNF α could be detected in the circulation of mice that were systemically challenged with LTA compared to vehicle-injected controls.

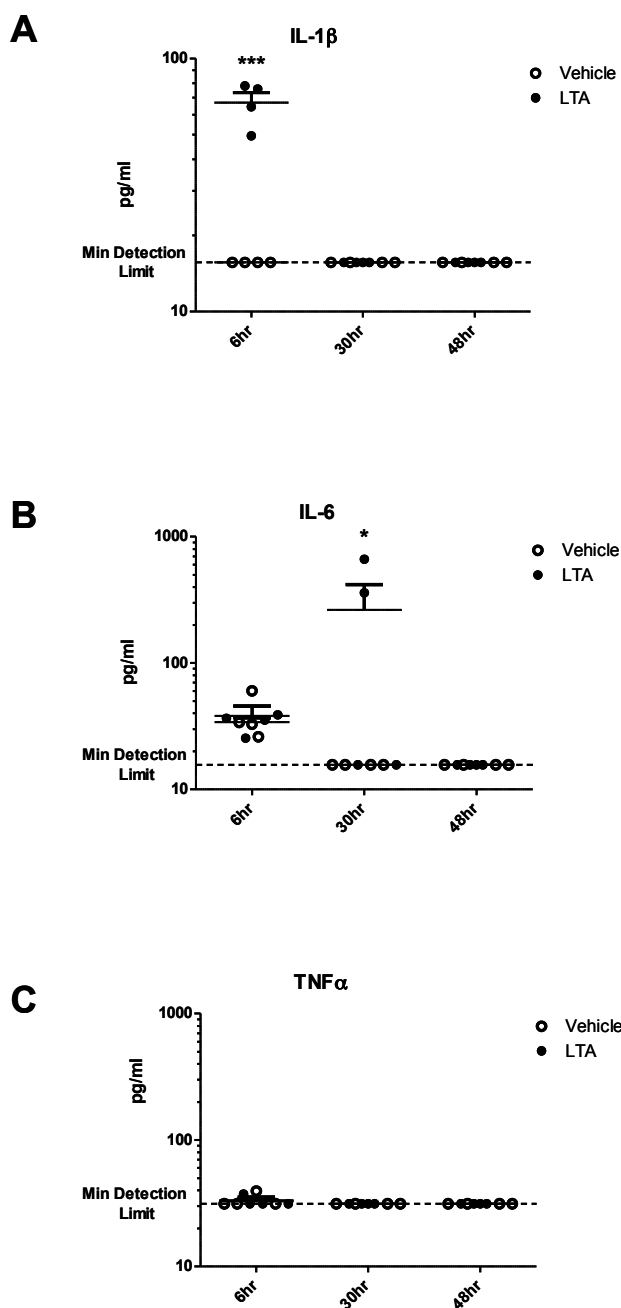


Figure 4.13 Plasma concentration of inflammatory cytokines following systemic LTA injection

Mice were injected with 500 μ g lipoteichoic acid (LTA) or an equivalent volume of vehicle at 0 and 24 hours. Plasma was isolated from the whole blood of mice; 6 hours, 30 hours and 48 hours following initial injection. Concentrations of (A) IL-1 β , (B) IL-6 and (C) TNF α (TNF) in the plasma were determined using ELISA. Data represent the mean plus or minus SEM. Significance was determined using two-way ANOVA. n = 4/group.

4.5 Discussion and conclusions

Transcriptional profiling, utilized in Chapter 3, identified an induction of ISGs and other immune/inflammatory genes in the brains of mice that had been challenged with LPS compared to vehicle-injected controls. To better understand the mechanism behind this induction, the ability of different inflammatory models to modulate target gene expression in the brain was assessed using QPCR.

One of the characterised mechanisms of immune signal transduction across the BBB involves activation of cerebral vascular endothelial cells by circulating cytokines, particularly IL-1 β and TNF α (Section 1.4.2.2). In order to determine whether elevated levels of circulating TNF α were sufficient to induce target gene expression in the brain; mice were challenged intravenously with recombinant murine TNF α . TNF α is the first inflammatory cytokine to be detected in the circulation following systemic LPS challenge and it is thought to play a pivotal role in activating the peripheral cytokine cascade^{414,435,436}. Not only has TNF α been implicated in the development of depression in patients with chronic inflammatory diseases²⁷⁶, but systemic TNF α challenge is known to have an impact on the brain of rodents, subsequently triggering a host of sickness behaviours^{266,286,436}. Gene expression analysis, 48 hours after initial TNF α injection, revealed that, of the genes found to be significantly upregulated 48 hours after LPS challenge, only one was altered in the brain in response to TNF α . These data suggest that target gene induction in the brains of mice injected with LPS may be TLR-specific and not a downstream consequence of sterile inflammation.

Another explanation for the lack of target gene modulation in the brain following systemic TNF α -injection could be that it failed to induce as high a level of systemic inflammation as 100 μ g of LPS. Although TNF α is known to induce an inflammatory cytokine cascade in the periphery and propagate signals across the BBB to induce sickness behaviours, no significant elevation of IL-1 β was detected in the circulation. This may have been an issue with the dose of TNF α used or the time points that were assayed. However, intravenous TNF α challenge significantly enhanced levels of circulating TNF α and IL-6, yet target gene induction in the brain was negligible. Therefore, the central induction of

target genes following LPS challenge is likely to be more than a mere by-product of elevated TNF α or IL-6 in the circulation. Furthermore, injecting mice with the TLR2 ligand, LTA, induced increased levels of circulating IL-1 β . As none of the genes that were induced in the brain in response to LPS were also upregulated in the brain following LTA challenge, central target gene induction does not appear to occur downstream of elevated IL-1 β in the circulation. These observations suggest that circulating inflammatory cytokines do not appear to play a prominent role in inducing ISG transcription, or the expression of other target genes, in the brain. Therefore, the neuroinflammation that is induced in response to LPS is more likely to be a TLR-specific phenomenon and not a generic effect of inflammation. To investigate the role of inflammatory cytokines further, the central induction of target genes could be assessed over time following several different doses of systemic TNF α or following systemic IL-1 β administration. As cytokines often function in synergy, gene expression in the brain could also be measured following the systemic injection of both TNF α and IL-1 β . Alternatively, target gene expression in the brain following systemic LPS injection could be assessed following the neutralisation of TNF α and/or IL-1 β in the periphery using cytokine-specific monoclonal antibodies or soluble cytokine receptors.

To complement the dataset derived from the systemic TNF α -induced model of inflammation, the induction of a selection of target genes, predominantly ISGs, was compared in brain and matched PBL samples, in the context of endotoxin tolerance. It has been well established that endotoxin tolerance leads to a state of hyporesponsiveness in the periphery, characterised by suppression of the inflammatory cytokine milieu^{429,430}. This is certainly supported by the ELISA data which show an absence of any detectable inflammation in the circulation at day 5 or day 7. Only IL-6 was elevated in the circulation at day 2. As mentioned previously, a number of routes exist to sensitise the brain to inflammation in the periphery. As these communication pathways between the immune system and the nervous system often involve the intermediary action of inflammatory cytokines, such as stimulation of the vagus nerve by IL-1 β or endothelium activation by IL-1 β and TNF α (Section 1.4.2), it seems likely that these routes would be impaired in conditions involving endotoxin tolerance. Despite the perceived absence of both TNF α and IL-1 β , ISGs remain induced in the brain

after several peripheral LPS injections. In contrast, the same genes, still induced in the periphery by day 2, are downregulated by day 5, with the exception of *Gbp4* which was downregulated in peripheral blood leukocytes at all time points assayed. As GBP expression has been shown to be directly affected by endotoxin tolerance⁴³⁷, it is possible that *Gbp4* expression would have been silenced after a single injection. Analysing *Gbp4* expression levels at day 1 after a single injection would be required to confirm this. In the periphery, the remaining genes, not directly targeted during endotoxin tolerance, must be negatively regulated between days 2 and 5 by another, as yet unknown mechanism.

What is clear from these observations is that a distinct difference in the expression kinetics of these genes differentiates the brain from the PBL. As mentioned above, previous studies have suggested that the brain continues to secrete cytokines in response to repeated challenge with LPS, even though cytokine production is negatively regulated in the periphery^{432,433}. In keeping with this, QPCR analysis demonstrated a brain-specific induction of *Tnfa* and *Il1b* following multiple LPS injections. Although *Il1b* levels were only significantly induced after 2 LPS injections, *Tnfa* remained significantly induced in the brain throughout the model. In contrast, the same genes were not induced in matched PBL. In addition to *Il1b* and *Tnfa*, the QPCR data demonstrated maintained induction of other immune response genes in the brain that were negatively regulated in the periphery. The mechanism inducing the central induction of these genes in the absence of peripheral cytokines remains to be clarified. However, it is possible that repeated LPS injection causes a breakdown of the BBB allowing LPS to gain access to the brain. Alternatively, phagocytic cells in the CVOs may not have the same regulatory mechanisms as their peripheral counterparts and may therefore continue to respond to repeated LPS challenge. Collectively, these data further imply that circulating inflammatory cytokines are not likely to be responsible for the induction of ISGs or *Il2rg* in the brain following LPS injection.

LPS binds to TLR4 to activate two distinct signalling pathways. IFN β production is a classic hallmark of TLR4-induced IRF3 activation, via the TRIF-dependent signalling pathway (Figure 4.1). As the panel of target genes, which were induced in the brain in response to systemic LPS administration, was highly enriched with type I ISGs (Section 3.3.7), it was hypothesised that a TRIF-

induced IFN β response was accountable for their induction in the brain. To investigate the involvement of TRIF activation in the neuroinflammation induced by systemic LPS injection, mice were challenged with LTA. LTA can only signal through the MyD88-dependent signalling pathway (Figure 4.1). Consistent with previous reports³¹⁸, no response was detectable in the brains of mice following peripheral LTA injection. This lack of response may be due to the inability of TLR2 ligands to stimulate TRIF-dependent signalling and subsequent type I IFN production. Conversely, peripheral stimulation with TLR3 ligands is known to trigger brain inflammation^{239,438}. Similar to the MyD88-independent pathway downstream of TLR4, TLR3 signals through the adaptor molecule TRIF to activate IRF3, ultimately triggering IFN β production⁴³¹. Subsequently, it would appear that IRF activation, whether it occurs in the periphery or the brain, may be a requirement of target gene induction in the brain following systemic administration of TLR ligands.

In further support of this hypothesis, a similar study showed that all target genes were induced in the brain following topical, cutaneous administration of TLR7/8 agonist, Imiquimod (Alison McColl, unpublished data). In this study, Imiquimod was used to create a psoriasis-like skin pathology. This peripheral inflammatory model induced tissue-specific, but not systemic, inflammation and target genes were induced specifically in the brain in the absence of detectable inflammatory cytokines in the circulation. TLR7- and TLR8-ligation both activate IRF7 which then results in the production of IFN α . These findings support the notion that TLR-induced type I IFN production, rather than elevated circulating cytokines, is responsible for target gene modulation in the brain.

To conclusively verify the role of TRIF-dependent signalling in inducing the expression of ISGs and other target genes in the brain following systemic LPS injection, the acute and chronic models of LPS-induced systemic inflammation could be repeated using TRIF- or IRF3-deficient mice. Both TRIF and IRF3 are required for TLR4-induced IFN β expression^{439,440}. Therefore, an absence of target gene expression in the brains of these mice following LPS injection would highlight the importance of MyD88-independent signalling in their induction.

Although these data imply that a TLR-induced type I IFN response is accountable for target gene induction in the brain following systemic LPS challenge, it is still

unclear whether type I IFNs are produced in the brain or whether peripherally produced IFNs act on the brain in an endocrine manner to trigger ISG induction. The TLDA data indicated that transcripts encoding type I IFNs are mildly upregulated following multiple LPS challenges. These data are by no means conclusive and require further investigation. To establish whether any of the observed inductions of type I IFN genes were significant, the TLDA data would first have to be validated by QPCR. Even if the data were validated, it is not clear whether such a slight induction of IFN transcripts would translate to increased protein production. Measuring IFN proteins in brain tissue is technically challenging as IFNs are usually produced in low quantities. Therefore, rather than quantifying IFN levels in the brain, a useful experiment would be to establish whether endotoxin tolerance leads to a dampening of type I IFNs in the periphery. One of the genes that are transiently silenced during endotoxin tolerance is *Ifng*⁴³⁰, however, to my knowledge, it is yet to be determined how type I IFNs respond to repeated LPS challenges. If it were indeed the case that both type I and type II IFNs were silenced in the periphery during this model of endotoxin tolerance, by default this would imply that centrally produced IFNs are more likely to be responsible for ISG induction in the brain than those produced in the periphery. The QPCR data indicate that peripheral type I IFN production may well be dampened during endotoxin tolerance as, following several LPS injections, ISG expression is silenced in PBL but not in the brain. This suggests that type I IFNs may be produced in the brain rather than the periphery during endotoxin tolerance. QPCR analysis of IFN transcript levels in the brain and PBL at different time points, complemented by ELISA assays to quantify protein levels in the brain and blood, would be required in order to confirm this.

In summary, systemic LPS administration induced the transcription of a panel of immune/inflammatory genes in the brain. This transcriptional profile was not induced by the systemic administration of TNF α , nor did it appear to depend on elevated levels of inflammatory cytokines in the circulation. Consequently, the observed induction of target genes in the brain may be dependent on TLR-ligation. In contrast, the same target genes were not induced in the brain following systemic administration of the TLR2 ligand, LTA. TLR2 has a signalling profile that is distinct from that of TLR4 in that it does not activate IRF3

resulting in type I IFN induction. This highlights a potential mechanism of target gene induction in the brain which may be dependent on a TLR-induced type I IFN response.

5 Characterising the chemokine repertoire and leukocyte infiltrate present in the brains of LPS-challenged mice

5.1 Introduction and aims

In Chapter 3 it was established that *Cxcl10* expression was significantly upregulated in the brain following an acute systemic LPS challenge, as was the expression of a number of genes involved in leukocyte extravasation. *Cxcl10* can coordinate the migration of several leukocyte populations, predominantly NK cells, Th1 cells, CD8⁺ cytotoxic T cells and memory T cells^{99-101,441}. It was therefore hypothesised that systemic LPS exposure may result in the infiltration of these leukocytes to the brain. Current literature suggests that systemic LPS injection can result in the recruitment of neutrophils to the cerebral vasculature^{236,237}. Although no other chemokine transcripts, including any encoding neutrophil chemoattractants, were significantly induced in the brain following systemic LPS challenge, transcription was only assessed 48 hours after injection. These data provide a mere snapshot of events occurring in the brain following an I.P. injection of LPS. Therefore, it remains to be determined how systemic LPS exposure modulates the chemokine profile in the brain over time and whether the putative chemokine induction results in leukocyte accumulation within the brain.

The primary aim of this chapter was to establish whether systemic exposure to LPS culminated in the specific recruitment of inflammatory leukocytes to the brain. As there was no way to hypothesise how long leukocytes may take to accumulate within the brain, if indeed they do so at all, it was decided that leukocyte infiltration would be better investigated over a seven day window following daily systemic LPS injections. Although this model leads to LPS tolerance in the periphery, it has the advantage that it may better reflect physiological conditions, such as bacterial infection or septicaemia, than a single dose of LPS. Furthermore, as proof of principle, it was shown in Chapter 4 that *Cxcl10* remained induced in the brain following daily systemic LPS injections.

It has been demonstrated in a variety of settings that different leukocyte populations infiltrate the brain at different time points. For example, following MHV or Semliki Forest virus infection, T cell accumulation in the brain is followed by the infiltration of monocytes^{190,442}. This appears to be dependent on the temporal induction of chemokines within the brain. Therefore, with the aim of assessing which leukocyte populations (if any) were likely to infiltrate the

brain following daily systemic LPS injections, TLDA plates were used to systematically assess the chemokine repertoire in the brain at different time points throughout the LPS model. The induction of chemokine transcripts was compared in LPS- and vehicle-injected mice. The accumulation of target populations of leukocytes within the brains of LPS-challenged mice was then assessed using a combination of immunohistochemistry and flow cytometry.

5.2 Regulation of chemokine and chemokine receptor transcripts following daily systemic LPS injections

Prior to establishing whether leukocytes infiltrated the brains of mice following a series of systemic LPS challenges, gene expression assays were used to assess the repertoire of inflammatory chemokine transcripts that were induced in the brains of the LPS-treated mice. 8 week old C57BL6 mice were exposed to daily injections of LPS (50 µg I.P.) as described in Section 4.3. Mice were culled, and perfused, 2 days, 5 days and 7 days after initial LPS challenge.

5.2.1 Chemokine transcripts are induced in the brain following multiple systemic LPS challenges

To establish how chronic LPS exposure in the periphery regulated chemokine transcripts in the brain, TLDA plates were used to systematically screen for the transcriptional induction of a panel of 17 inflammatory, or brain-related, chemokines in the brains of LPS-injected mice compared to the vehicle-injected control group. On day 2, 48 hours after initial LPS injection, CC chemokine transcripts *Ccl2*, *Ccl5*, *Ccl7*, *Ccl8* and *Ccl11* were significantly upregulated, as were CXC chemokine transcripts, *Cxcl1*, *Cxcl2*, *Cxcl3*, *Cxcl5*, *Cxcl9*, *Cxcl10* and *Cxcl16* (Figure 5.1). Of these, *Ccl2*, *Ccl5*, *Cxcl1*, *Cxcl2*, *Cxcl9* and *Cxcl10* were all upregulated by at least 10-fold. By day 5, the majority of chemokine transcripts did not significantly deviate from baseline, with the exception of *Ccl8*, *Ccl11* and *Cxcl16*. Both *Ccl11* and *Cxcl16* remained significantly elevated in the brain throughout the model. *Cx3cl1* was also significantly upregulated by day 7. Therefore, several genes encoding inflammatory chemokines are significantly induced in the brain following multiple systemic LPS challenges.

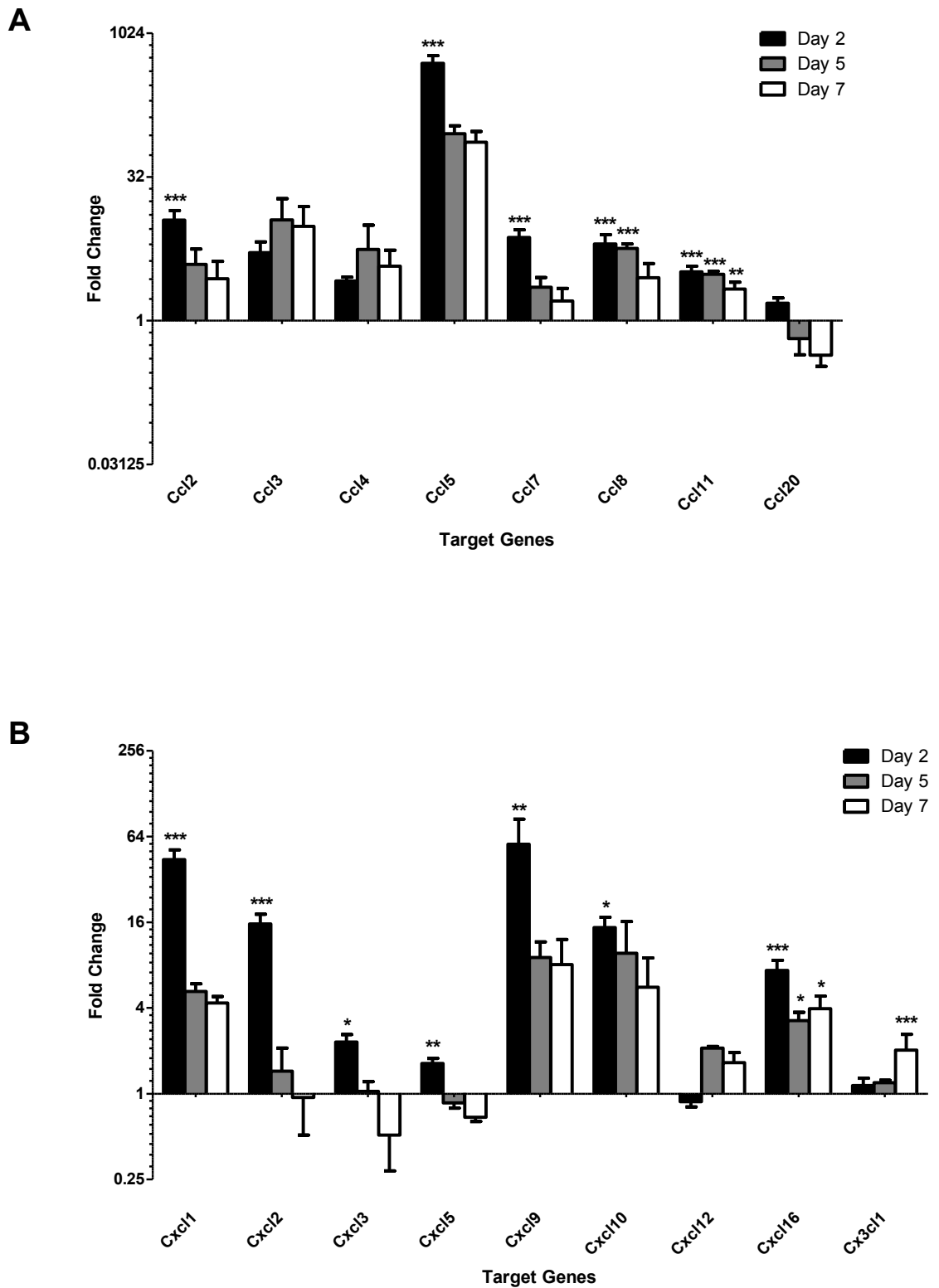


Figure 5.1 Temporal expression of inflammatory chemokines in the brains of mice following repeated LPS injections

Mice were injected daily with 50 μ g LPS or an equivalent volume of vehicle. RNA was extracted from brains, 2, 5 and 7 days following initial injection. Gene expression analysis of (A) CC chemokines and (B) CXC and CX₃C chemokines was performed using TaqMan low density arrays and normalised to TBP. Data are expressed as fold change in gene expression relative to vehicle-injected control mouse brains. Data represent the mean \pm SEM. A statistical comparison was made, between the fold induction in the brains of LPS-injected mice and that of vehicle-injected controls, using two-way ANOVA: * $P \leq 0.05$, ** $P \leq 0.01$, *** $P \leq 0.001$. n = 4-5/group.

To validate the TLDA data, the induction of the majority of the chemokine transcripts that were identified as being upregulated 10-fold or more on day 2 was additionally assessed using SYBR Green QPCR. Consistent with the TLDA data, *Ccl5* was significantly upregulated in the brains of LPS-challenged mice on day 2 (Figure 5.2A). However, the QPCR data also demonstrated that *Ccl5* remained significantly upregulated until at least day 5. Of all the chemokine transcripts assayed, *Ccl5* showed the greatest induction in the brains of the LPS-challenged mice. As a result, attempts were made to confirm this upregulation at a protein level using histology. Unfortunately, due to technical difficulties, this aim was not achieved (data not shown).

CCL3 and CCL5 share similar receptors and are often produced concomitantly, therefore, the transcriptional regulation of *Ccl3* in the brain was also determined by QPCR. Although *Ccl3* expression was statistically comparable to baseline at days 2 and 7, the QPCR data demonstrated that, on day 5, *Ccl3* was significantly upregulated by approximately 23-fold (Figure 5.2A).

The induction of genes encoding neutrophil chemoattractants CXCL1 and CXCL2 was also confirmed for day 2 using QPCR (Figure 5.3A). In addition, *Cxcl2* was shown to be significantly upregulated in the brain until at least day 5. Although the TLDA data demonstrated a significant, approximately 57-fold, induction of the gene encoding IFN-inducible CXCL9, this appeared to be below the detection limit of the QPCR assay and thus could not be validated (data not shown). The significant induction of *Cxcl10* at day 2 of the LPS model was previously confirmed by QPCR in Figure 4.8A. Attempts were also made to establish whether CXCL10 protein was upregulated in the brains of LPS-challenged mice. Unfortunately, due to antibody cross-reactivity, this did not prove possible (data not shown).

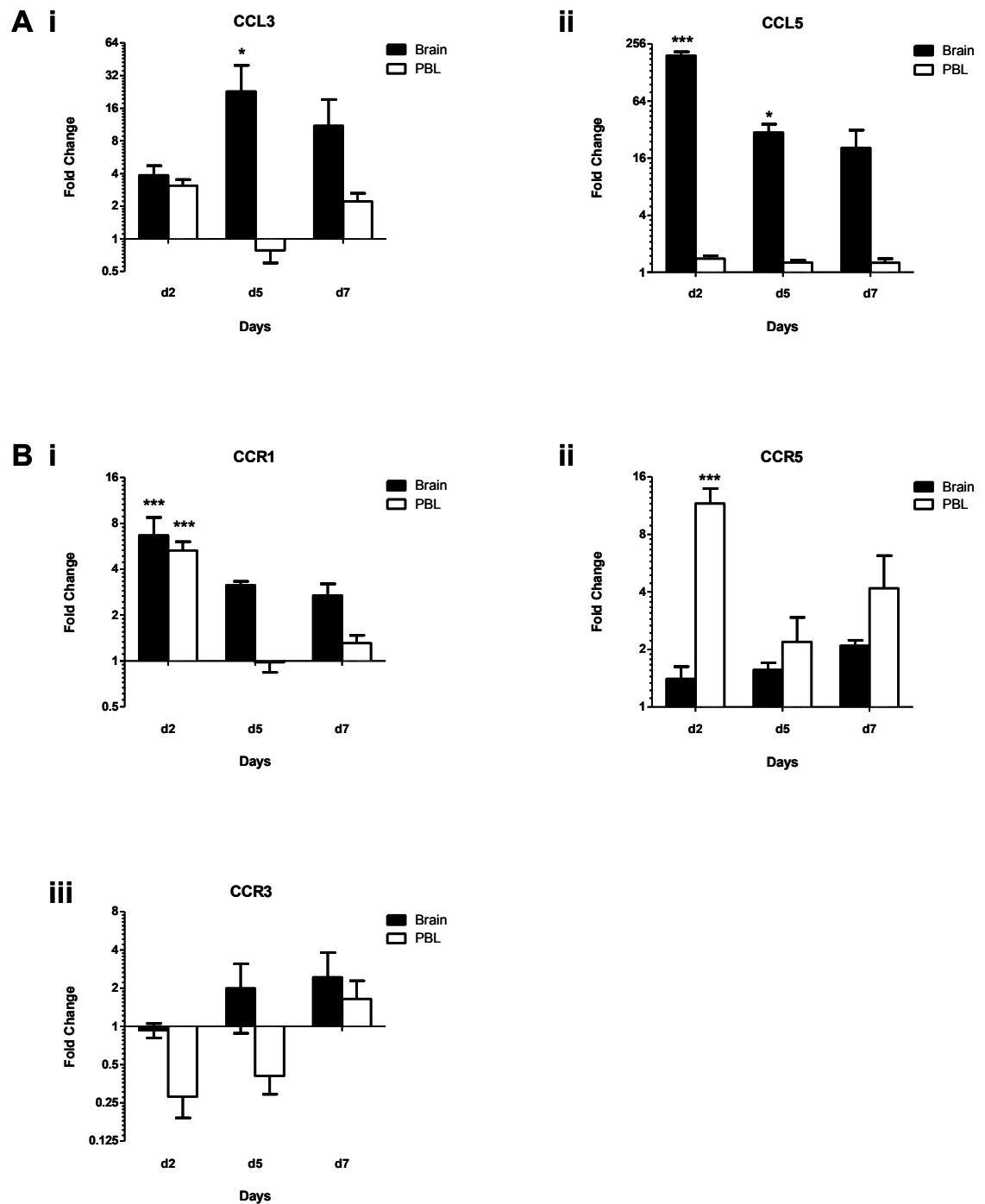


Figure 5.2 Temporal expression of CC chemokine and chemokine receptor in the brain and PBL of mice following repeated LPS injections

Mice were injected daily with 50µg LPS or an equivalent volume of vehicle. RNA was extracted from brains and peripheral blood leukocytes (PBL), 2, 5 and 7 days following initial injection. Gene expression analysis of (A) CC chemokines, (i) *Ccl3* and (ii) *CCL5* and (B) CC chemokine receptors, (i) *Ccr1*, (ii) *Ccr5* and (iii) *Ccr3* was performed using QPCR and normalised to TBP. Data are expressed as fold change in gene expression in the brain (■) and PBL (□) of LPS-injected mice relative to vehicle-injected controls. Data represent the mean \pm SEM. A statistical comparison was made, between the fold induction in the brains and PBL of LPS-injected mice and that of vehicle-injected controls, using two-way ANOVA: * $P \leq 0.05$, ** $P \leq 0.01$, *** $P \leq 0.001$. $n = 4/\text{group}$.

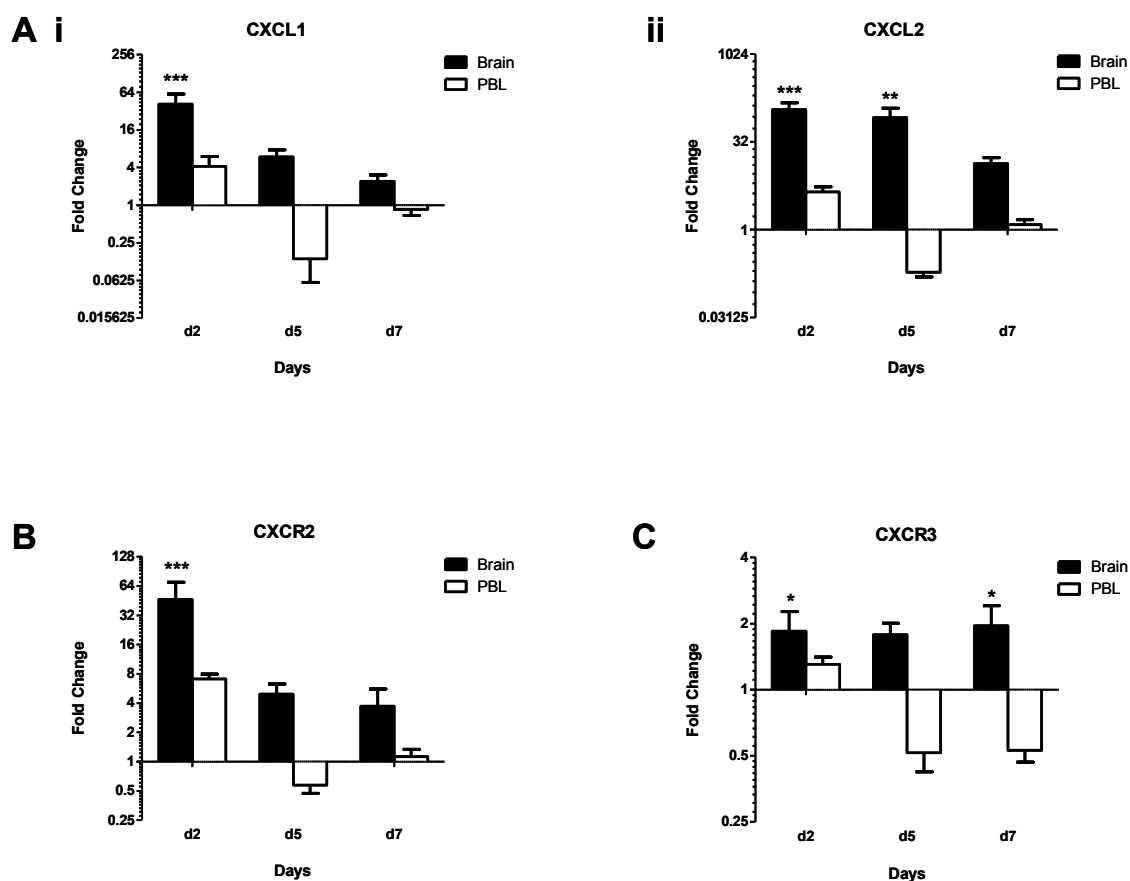


Figure 5.3 Temporal expression of CXC chemokine and chemokine receptor in the brain and PBL of mice following repeated LPS injections

Mice were injected daily with 50 μ g LPS or an equivalent volume of vehicle. RNA was extracted from brains and peripheral blood leukocytes (PBL), 2, 5 and 7 days following initial injection. Gene expression analysis of (A) CXC chemokines, (i) *Cxcl1* and (ii) *Cxcl2* and CXC chemokine receptors, (B) *Cxcr2* and (C) *Cxcr3* was performed using QPCR and normalised to TBP. Data are expressed as fold change in gene expression in the brain (■) and PBL (□) of LPS-injected mice relative to vehicle-injected controls. Data represent the mean \pm SEM. A statistical comparison was made, between the fold induction in the brains and PBL of LPS-injected mice and that of vehicle-injected controls, using two-way ANOVA: * $P \leq 0.05$, ** $P \leq 0.01$, *** $P \leq 0.001$. $n = 4$ /group.

5.2.2 Chemokines are differentially regulated in the brain and PBL

Despite the fact that all chemokine transcripts assayed using QPCR were upregulated in the brain on at least one of the three time points, none were differentially regulated in the PBL of LPS-treated mice (Figure 5.2A & Figure 5.3A). Thus, chronic exposure to LPS in the periphery triggers a brain-specific induction of genes encoding inflammatory chemokines.

5.2.3 Chemokine receptor transcripts are differentially induced in the brain and PBL

Having established that chemokine transcripts were induced specifically in the brain, QPCR was then performed to determine what impact this series of systemic LPS challenges had on the transcriptional modulation of genes encoding their cognate chemokine receptors. The relative induction of chemokine receptor transcripts was compared in the brain and PBL. In LPS-treated mice at day 2, the gene encoding CCR1, one of the two shared receptors for CCL3 and CCL5, was significantly upregulated in the brain and PBL by a similar fold change (Figure 5.2B). At days 5 and 7, whilst there was a trend towards an upregulation in the brain, *Ccr1* expression was comparable to baseline in the PBL of LPS-challenged mice. CCR5, the other shared receptor for CCL3 and CCL5, showed a different pattern of transcriptional regulation (Figure 5.2B). *Ccr5* was significantly upregulated by the PBL of LPS challenged mice on day 2. At days 5 and 7, whilst there was a trend towards an upregulation in the PBL of the LPS-treated group, *Ccr5* expression did not significantly differ from that of vehicle-treated controls in either the brain or the PBL. In addition to CCR1 and CCR5, CCL5 can bind to CCR3. Unlike *Ccr1* and *Ccr5*, transcript levels of CCR3 were not significantly regulated in either the brain or PBL following multiple systemic LPS injections (Figure 5.2B).

Neither of the CXC chemokine receptor transcripts assayed, *Cxcr2* or *Cxcr3* were differentially modulated by the PBL of LPS challenged mice (Figure 5.3B&C). In contrast, both genes were significantly upregulated in the brains of the LPS treatment group at day 2. In addition, both genes showed a trend towards an upregulation in the brain on day 5. By day 7, *Cxcr3* was again significantly upregulated in the brains of the LPS challenged group.

These different methods of gene expression analysis collectively demonstrate that a panel of inflammatory chemokine transcripts are elevated in the brain following several systemic LPS injections. Not only was the induction of these chemokine transcripts brain-specific, but it was coupled with an increase in mRNA encoding a number of their cognate receptors.

5.3 Leukocytes infiltrate the brain in response to chronic systemic LPS exposure

The induction of chemokine receptor transcripts within the brain may be due to brain-resident cell populations upregulating their chemokine receptor expression in response to peripheral or central TLR ligation. However, as the most characterised function of inflammatory chemokines is to recruit leukocytes to sites of inflammation, an alternative possibility is that an accumulation of leukocytes within the brain is responsible for the elevation in transcript levels. To explore this possibility further, mice were again challenged with a single dose of LPS (50 µg I.P.) or vehicle daily for 2, 5 or 7 consecutive days. Mice were culled and perfused 24 hours after their final injection. Brains were then harvested from the mice and analysed by flow cytometry. To control for the possibility of blood contamination, whole blood was also harvested from the mice and analysed by flow cytometry.

Prior to surface staining analysis, cells were first gated based on their forward scatter (FSC) and side scatter (SSC) (P1 gate). This was followed by the exclusion of Draq7⁺ dead cells (P2 gate). Doublets were then excluded so that only single cells (P3 gate) were considered for analysis (Figure 5.4).

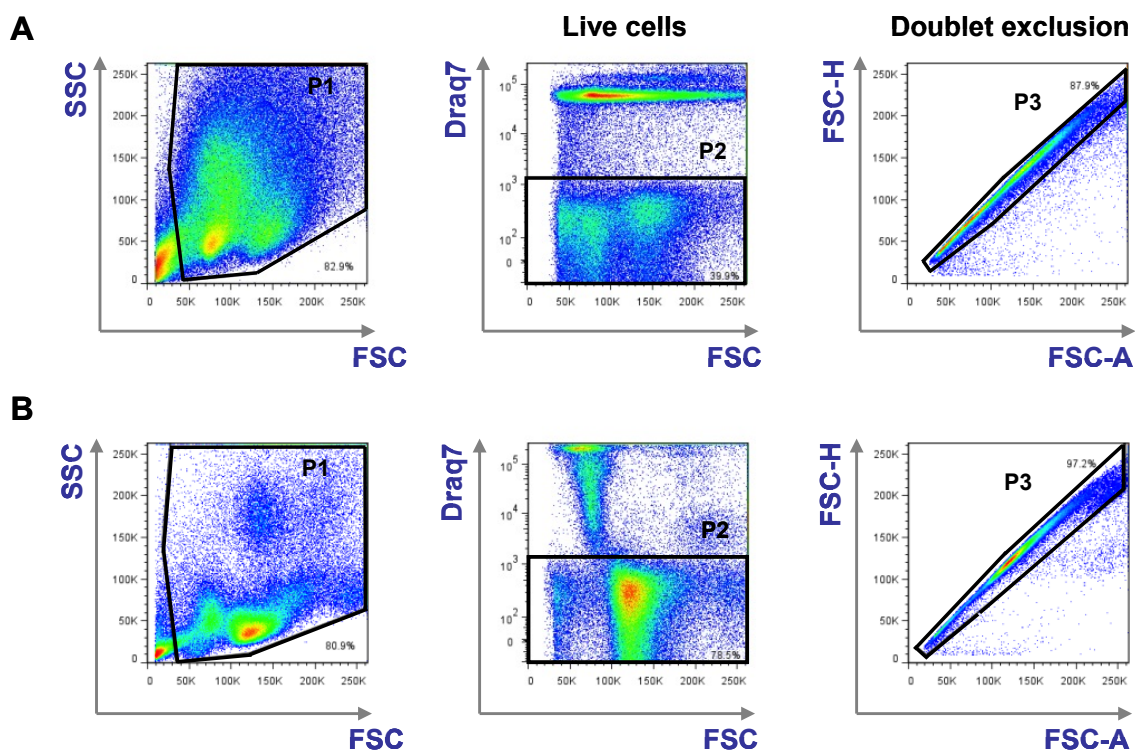


Figure 5.4 Gating on live, single cells in the brain and PBL

Representative dot plots showing the gating strategy used to define single live cells amongst total events recorded from (A) the brain and (B) whole blood. Cell populations were gated from total events based on their FSC and SSC (P1 gate). Dead cells and doublets were excluded (P2 and P3 gates respectively).

5.3.1 CD45^{hi} cells are increased in the brain following multiple systemic LPS challenges

To determine whether leukocytes infiltrated the brain following chronic systemic LPS exposure, the proportions of CD45-expressing cells in the treatment and the control groups was first compared using flow cytometry. As microglia characteristically express intermediate levels of CD45 on their surface (CD45^{int}), it was first necessary to distinguish between CD45^{int} microglia (P4 gate) and CD45^{hi} leukocytes (P5 gate) (Figure 5.5A). Having delineated these two populations of cells, the proportions of live, single CD45^{hi} leukocytes present in LPS-treated mouse brains was compared to that of the vehicle-treated control group. At day 2, after 2 doses of LPS, there was a highly significant increase in the proportion of CD45^{hi} cells in the brain (6.3-fold) (Figure 5.5B&C). Although on day 7 the proportion of CD45^{hi} cells was increased by approximately 2.7-fold, this was not statistically significant.

Using RNA from an independent experiment, QPCR was performed to determine whether there was a similar increase in CD45 transcript levels in the brains of LPS-challenged mice. At all time points assayed, there was a significant increase in *Cd45* mRNA (Figure 5.5D). The fold increase in *Cd45* expression in the brain was similar to the increase in proportions of CD45^{hi} leukocytes. Collectively, these observations suggest that CD45^{hi} cells may accumulate in the brain following 2 doses of systemic LPS.

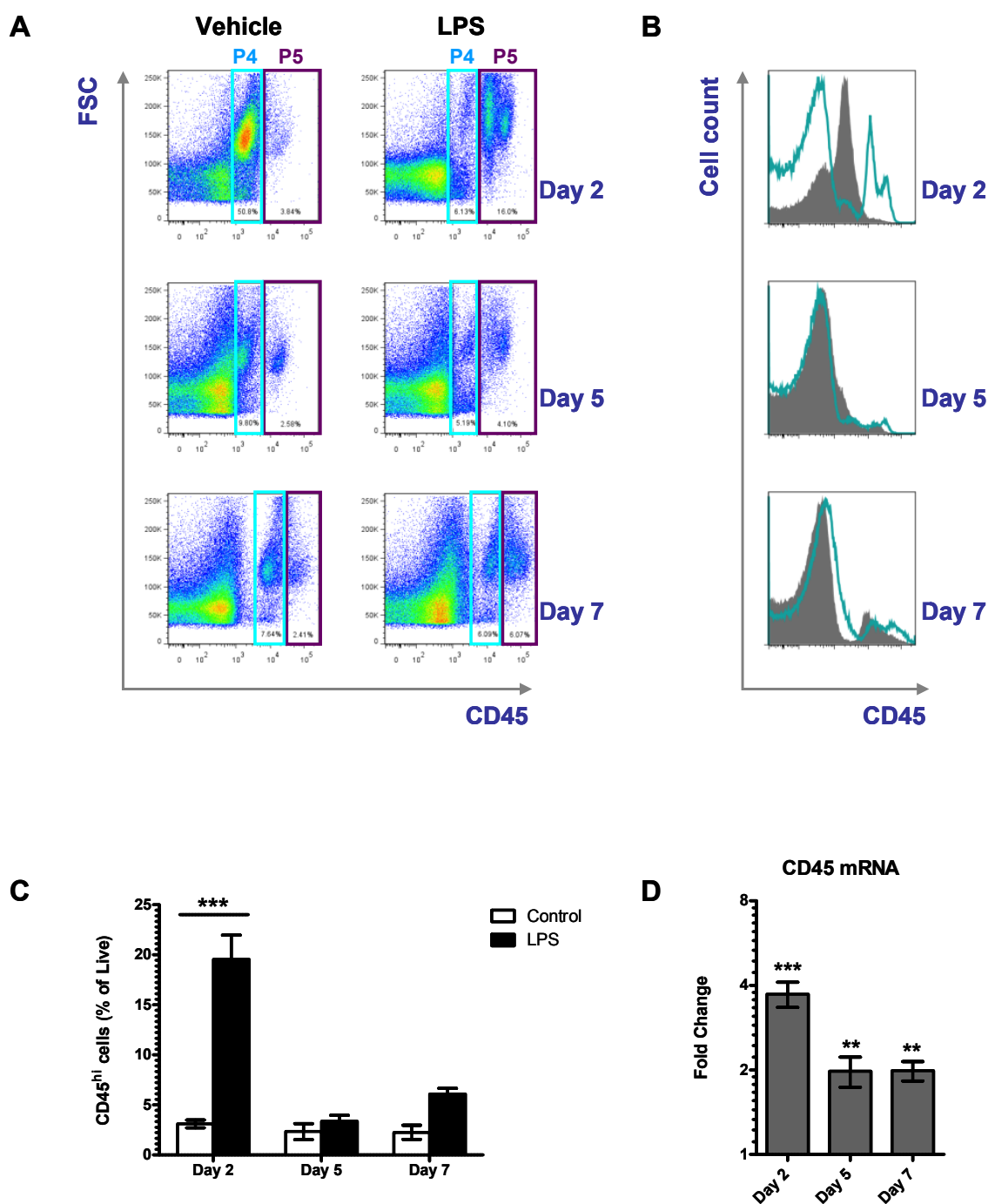


Figure 5.5 Proportions of CD45^{hi} cells in the brains of LPS and vehicle-challenged mice
Mice were injected daily with 50 μ g LPS or an equivalent volume of vehicle. Single cell suspensions were generated from whole brain tissue at days 2, 5 and 7 following initial LPS- or vehicle-injection. (A) Representative dots plots of single live cells (P3 gate, Figure 5.4) from each group. Cells were gated based on CD45-expression. P4 gate (■) represents CD45^{int} cells and will therefore contain microglial cells. P5 gate (■) represents CD45^{hi} leukocytes. (B) Histograms showing CD45-expression in LPS-injected (■) and vehicle-injected (shaded) groups over time. (C) Percentages of CD45^{hi} leukocytes (P5 gate) in the brain at each time point following injection. (D) Gene expression analysis of *Cd45* was performed using QPCR and normalised to TBP. mRNA was extracted from mouse brains from an independent experiment. Data are expressed as fold change in gene expression in the brain of LPS-injected mice relative to that of vehicle-injected controls. Data represent the mean \pm SEM. Significance of was calculated for using a two way ANOVA: *P \leq 0.05, **P \leq 0.01, ***P \leq 0.001. n = 3-4/group.

5.3.2 Proportions of microglial cells varied following two doses of LPS

Unexpectedly, at day 2 of the LPS model, there appeared to be a reduction in the percentage of live microglial cells following systemic LPS treatment (Figure 5.5 & Figure 5.6). However, not only were the percentages of microglial cells at days 5 and 7 statistically comparable in LPS- and vehicle-injected mice, but they were similar to the percentage of microglia observed in LPS-injected mouse brains on day 2 (Figure 5.6B). Microglia appeared as one uniform population based on their CD11b⁺ and F4/80-expression (Figure 5.6A) and were therefore readily identifiable from other cell populations in the brain. The variation in their percentages at this early time point could not be explained by an increase or decrease in CD45-expression as cells of a similar phenotype could not be detected in the CD45^{hi} fraction or the CD45^{lo} fraction (data not shown). This suggests that there was an increase in the numbers of viable microglial cells isolated from the brains of vehicle-injected control mice at day 2.

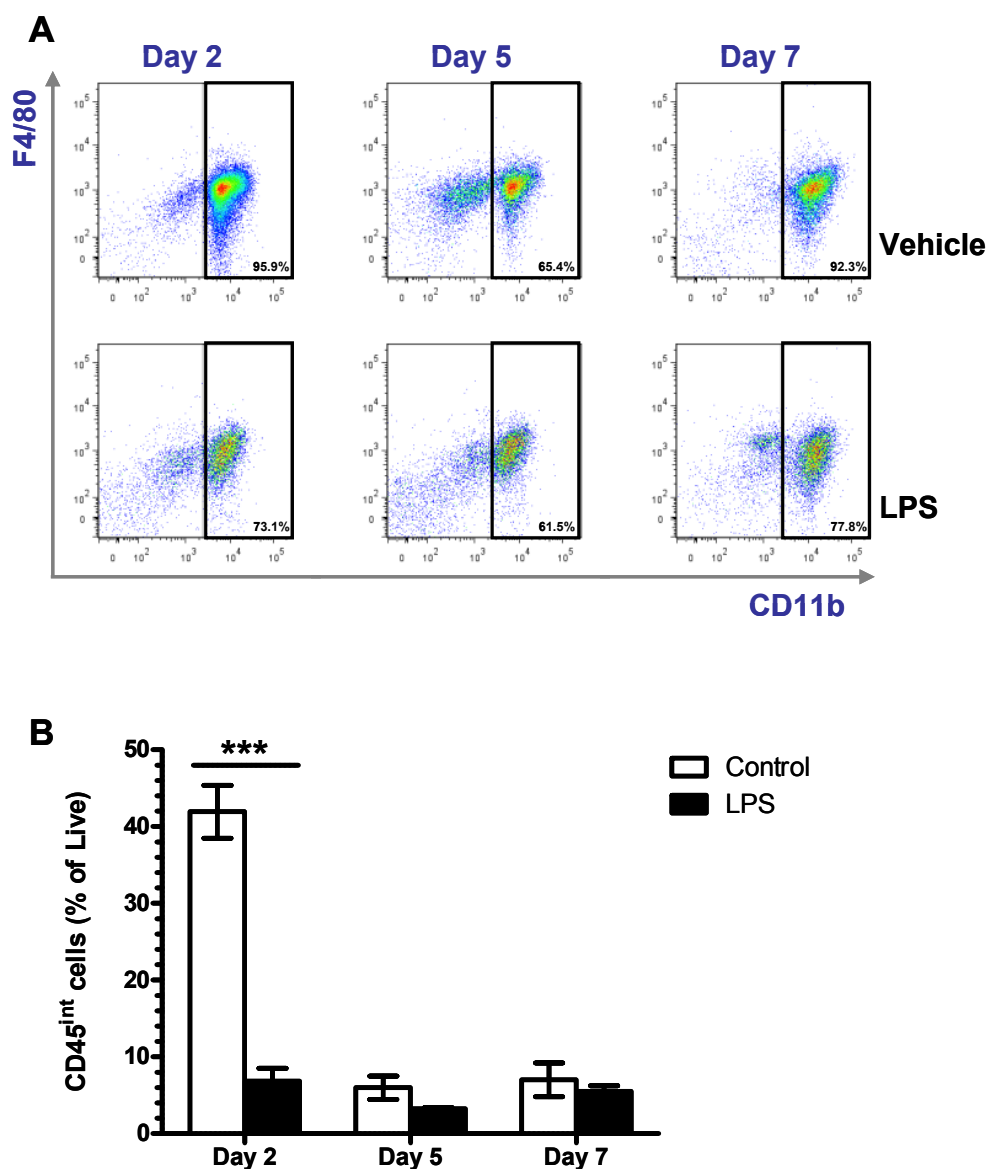


Figure 5.6 Variations in microglial cell numbers

Mice were injected daily with 50 μ g LPS or an equivalent volume of vehicle. Single cell suspensions were generated from whole brain tissue at days 2, 5 and 7 following initial LPS- or vehicle-injection. (A) Representative dots plots of single live CD45^{int} cells (P4 gate, Figure 5.5) from each group. Microglial cells were gated from other CD45^{int} cells based on CD11b- and F4/80-expression. (B) Percentages of microglial cells in the brain at each time point following injection. Data represent the mean \pm SEM. Significance of was calculated for using a two-way ANOVA: *P \leq 0.05, **P \leq 0.01, ***P \leq 0.001. n = 3/group.

5.3.3 CD11b⁺ leukocytes infiltrate the brain following multiple systemic LPS challenges

As described above, the proportion of infiltrating CD45^{hi} leukocytes was increased in the brains of LPS challenged mice at day 2 of the time course. With the aim of identifying which cell populations infiltrated the brain, flow cytometry was used to characterise the leukocyte populations present in the CD45^{hi} fraction. In the vehicle-treated mouse brains, there was a small population of CD45^{hi} leukocytes (Figure 5.5). Further characterisation of these cells revealed them to be CD11b^{hi}, F4/80⁺ cells (Figure 5.7A). As they expressed only marginally more of each surface antigen than microglia, these are likely to represent brain-resident macrophages, such as PVM. Interestingly, this population appeared to be reduced in the brain at day 2 of the LPS time course (Figure 5.7A) but had reappeared by day 5 (data not shown). On day 2, infiltrating leukocytes in the brains of LPS-challenged mice could be divided into two populations based on their level of CD45-expression (P6 and P7 gates, Figure 5.7A). Not only did these two populations differ in their level of CD11b-expression, but they also differed from each other, and from CD45^{int} microglial cells, in terms of their size and granularity. Both populations of cells were CD11b⁺, F4/80⁻. However, based on their size, granularity and level of CD11b, leukocytes within the P6 gate have been classed as CD11b^{hi} granulocyte-like cells whereas those within the P7 gate have been classed as CD11b⁺ monocyte-like cells.

At day 2 of the LPS model, the proportion of CD11b^{hi} granulocyte-like cells in the brains of LPS-challenged mice was significantly increased compared to the vehicle-treated control group (Figure 5.7B&D). Although this cell population could also be detected in the brains of the LPS-injected group on day 5, there was no significant difference at this time point. The percentage of CD11b⁺ monocyte-like cells was also elevated in the brains of LPS challenged mice at day 2 (Figure 5.7C&E). Unfortunately, this population was difficult to distinguish from other cell populations at day 5 and day 7 and thus could not be quantified (data not shown). Taken together, these data suggest that, on day 2, CD11b^{hi} granulocyte-like cells and CD11b⁺ monocyte-like cells may accumulate in the brains of LPS challenged mice.

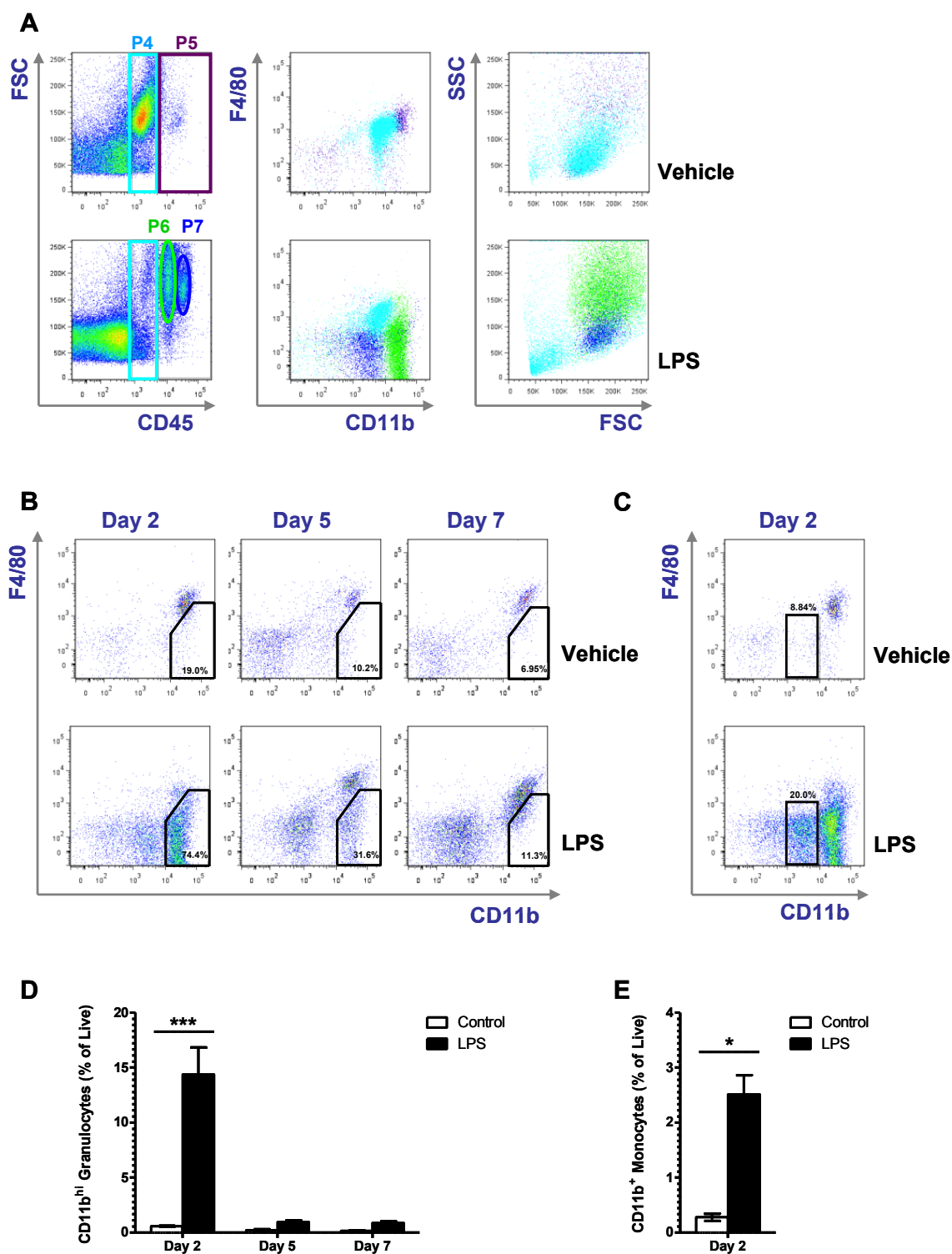


Figure 5.7 Characterisation and quantification of CD11b⁺ leukocyte populations in the brains of LPS-challenged mice

Mice were injected daily with 50µg LPS or an equivalent volume of vehicle. Single cell suspensions were generated from whole brain tissue at days 2, 5 and 7 following initial LPS- or vehicle-injection. (A) Representative dot plots from day 2 of the time course. Cells were gated based on level of CD45-expression. P4 gate (■) represents CD45^{int} cells. P5 gate (■) represents all CD45^{hi} leukocytes. In LPS-injected mice (bottom) there were two distinct populations of CD45^{hi} leukocytes: gates P6 (■) and P7 (■). The different populations of CD45-expressing cells from each group were overlaid to compare their CD11b- and F4/80-expression and their FSC and SSC. (B & C) Representative dots plots of CD45^{hi} leukocytes, P5 gate (■), from (B) each group and (C) day 2 of the model. Cells were gated based on CD11b- and F4/80-expression. (D) Percentages of CD11b⁺

granulocyte-like cells in the brain at each time point following injection. (E) Percentages of CD11b⁺ monocyte-like cells in the brain at day 2 of the model. Data represent the mean +/- SEM. Significance of was calculated for using a two-way ANOVA: *P ≤ 0.05, ***P ≤ 0.001. n = 3/group.

To establish whether the increased proportions of CD11b⁺ cell populations in the brain were reflected by a similar increase in the peripheral blood, the percentage of CD11b⁺ cells present in matched blood samples was also assessed by flow cytometry. The percentage of CD11b⁺ cells was significantly increased in the blood at all time points analysed (Figure 5.8A&B). This did not follow the pattern observed in the brain. Although in steady state conditions CD11b⁺ cells could be separated into two different cell populations based on their FSC and SSC, using the same parameters these two cell populations were indistinguishable from one another following LPS-treatment (Figure 5.8A). Furthermore, following LPS-treatment, CD11b⁺ cells could be separated into two different cell populations based on their level of CD45-expression. However, in steady-state conditions CD11b-expressing cell populations expressed similar levels of CD45. As a result, the specific proportions of granulocyte-like cells and monocyte-like cells present in the peripheral blood could not be established from this experiment.

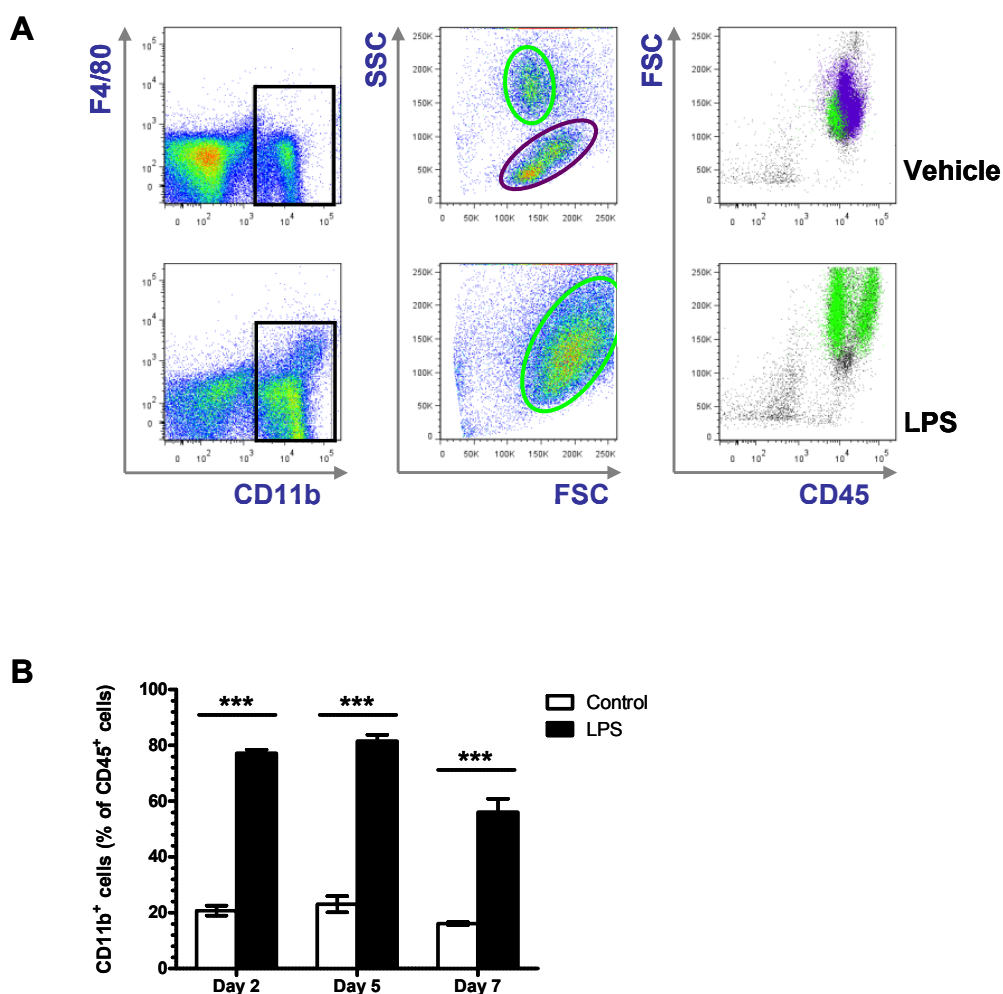


Figure 5.8 Characterisation and quantification of CD11b⁺ leukocyte populations in the peripheral blood of LPS-challenged mice

Mice were injected daily with 50 μ g LPS or an equivalent volume of vehicle. Single cell suspensions were generated from whole brain tissue at days 2, 5 and 7 following initial LPS- or vehicle-injection. (A) Representative dot plots from day 2 of the time course. Single live cells were gated based on level of CD11b-expression (left). CD11b⁺ leukocytes were then gated based on their FSC and SSC. Different populations of CD11b-expressing cells from each group were overlaid to compare their CD45-expression. (B) Percentages of CD11b⁺ leukocytes in the peripheral blood at each time point following injection. Data represent the mean \pm SEM. Significance of was calculated for using a two-way ANOVA: ***P \leq 0.001. n = 3/group.

5.3.4 CD3⁺ cell populations infiltrate the brain following multiple systemic LPS challenges

As *Ccl5* and *Cxcl10* were significantly upregulated in the brain, it is possible that T cells are recruited to the brain following multiple LPS challenges. This is supported by the observation that the chemokine receptor transcripts, *Ccr1* and *Cxcr3*, were also upregulated in the brain. To test this hypothesis, flow cytometry was used to compare the proportions of CD3⁺ cell populations in the brains of LPS- and vehicle-challenged mice. CD11b⁺ cells were first excluded from CD45^{hi} leukocytes (Figure 5.9A). Within the CD11b^{-/int} fraction were two distinct populations of CD3⁺ leukocytes, CD8⁺ T cells and CD8⁻ T cells. Quantification of these two populations revealed no differences in the percentage of either population in the brains of LPS-treated mice compared to vehicle-treated controls on day 2 or on day 5. However, by day 7, the proportions of both CD8⁺ and CD8⁻ T cell populations were significantly enriched in the brains of the LPS-treated animals (Figure 5.9B-D).

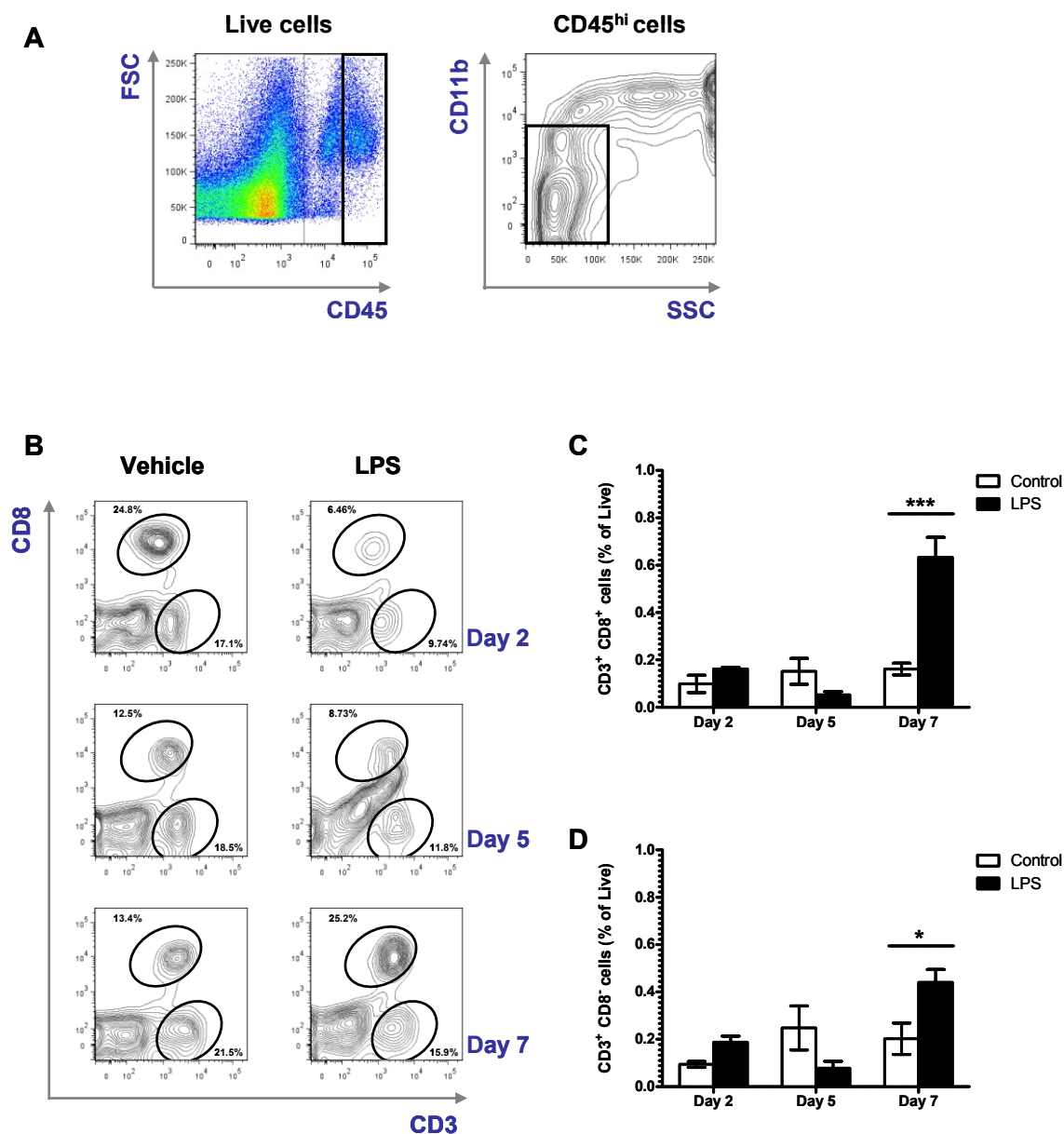


Figure 5.9 Characterisation and quantification of CD3⁺ leukocyte populations in the brains of LPS-challenged mice

Mice were injected daily with 50 μ g LPS or an equivalent volume of vehicle. Single cell suspensions were generated from whole brain tissue at days 2, 5 and 7 following initial LPS- or vehicle-injection. (A) Gating strategy. CD45^{hi} leukocytes were gated as described previously. CD11b⁺ cells were then excluded by gating on CD11b^{-/int} cells. (B) Representative contour plots of CD11b^{-/int} cells from each group. (C&D) Percentages of (C) CD3⁺ CD8⁺ leukocytes and (D) CD3⁺ CD8⁻ leukocytes in the brain at each time point following injection. Data represent the mean \pm SEM. Significance of was calculated for using a two way ANOVA. *P \leq 0.05, **P \leq 0.01, ***P \leq 0.001. n = 3/group.

The percentages of CD3⁺ T cell populations were also assessed in matched blood samples. CD11b⁺ cells were excluded from CD45⁺ leukocytes. Again there were two distinct populations of CD3⁺ T cells within the CD11b^{-/int} fraction. At all time points analysed, there was a highly significant reduction in the percentages of both CD8⁺ and CD8⁻ T cells present in the blood of LPS-treated mice (Figure 5.10).

Taken together, these data suggest that chronic exposure to LPS in the periphery triggers a substantial increase in the percentage of CD11b⁺ leukocytes in the peripheral blood and a concurrent decrease in the percentage of CD3⁺ T cells. At day 2, following 2 systemic LPS injections, this was coupled with an increase in the percentage of both CD11b^{hi} granulocyte-like cells and CD11b⁺ monocyte-like cells in the brain. Unlike the sustained increase in CD11b⁺ leukocytes that was observed in the blood, the elevated proportion of CD11b^{hi} granulocyte-like cells in the brain was transient, returning to baseline by day 5. The apparent infiltration of CD11b⁺ leukocytes to the brain was followed by an accumulation of both CD8⁺ and CD8⁻ T cells.

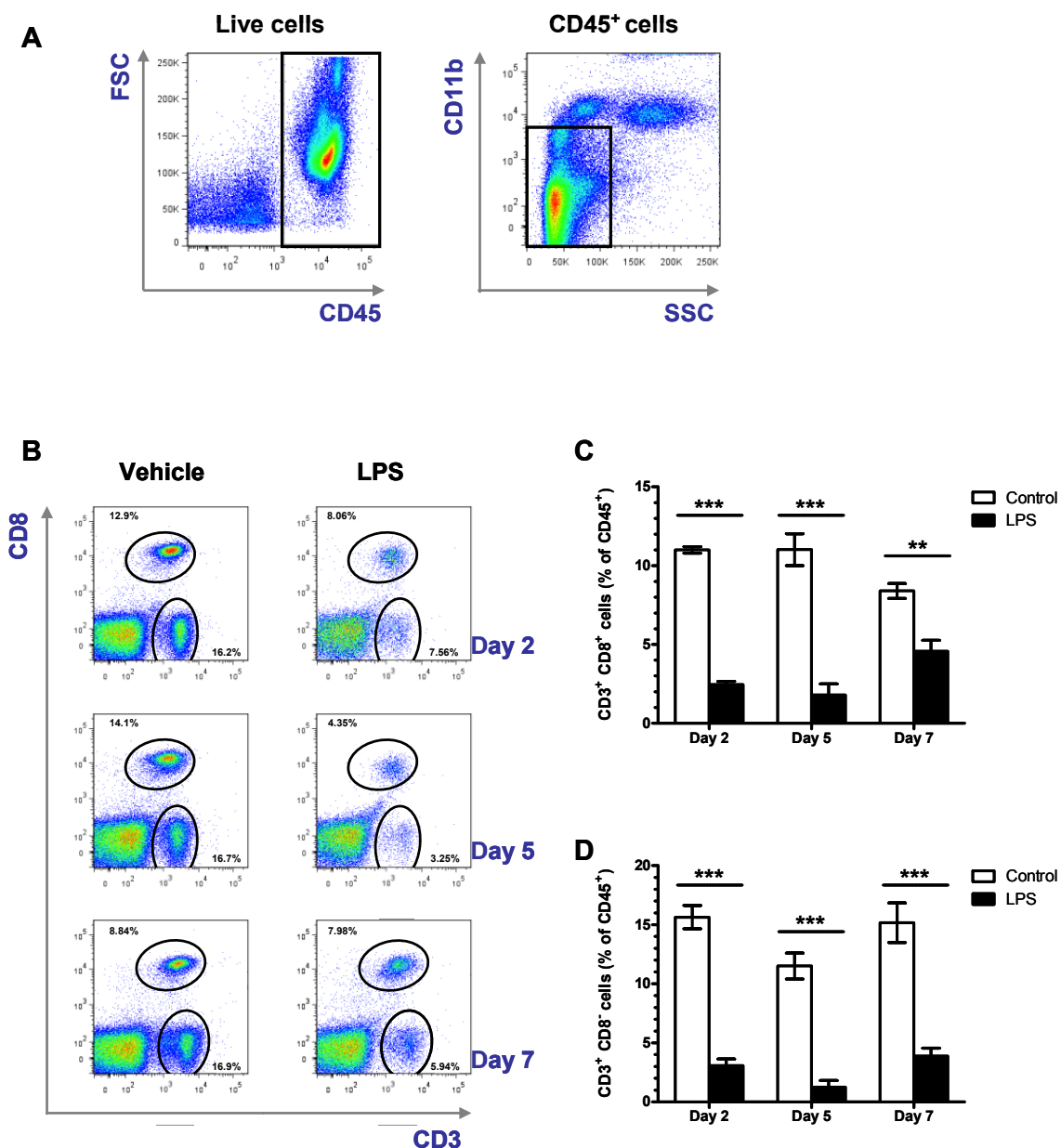


Figure 5.10 Characterisation and quantification of CD3⁺ leukocyte populations in the peripheral blood of LPS-challenged mice

Mice were injected daily with 50 μ g LPS or an equivalent volume of vehicle. Leukocytes were isolated from whole blood at days 2, 5 and 7 following initial LPS- or vehicle-injection. (A) Gating strategy. CD45^{hi} leukocytes were gated as described previously. CD11b⁺ cells were then excluded by gating on CD11b^{-int} cells. (B) Representative contour plots of CD11b^{-int} cells from each group. (C&D) Percentages of (C) CD3⁺ CD8⁺ leukocytes and (D) CD3⁺ CD8⁻ leukocytes in the blood at each time point following injection. Data represent the mean \pm SEM. Significance of was calculated using a two way ANOVA: *P \leq 0.05, **P \leq 0.01, ***P \leq 0.001. n = 3/group.

5.4 Identification of infiltrating leukocyte populations in the brain using histology

Although the flow cytometry dataset suggests that CD11b⁺ and CD3⁺ leukocyte populations may accumulate in the brain when mice are repeatedly challenged with LPS in the periphery, it does not indicate where in the brain these leukocytes are located. Furthermore, the experiment is limited as the absolute numbers of cells in the brain, and the blood, were not quantified due to technical constraints. Also, it is possible that the data may be skewed by peripheral blood contamination or by the marginalisation of leukocytes to the inflamed vasculature. To explore this further, mice were injected with a single dose of LPS daily for 2, 5 or 7 consecutive days. Brains were removed from the mice 24 hours after their final injection. With the aim of expanding on the data derived using flow cytometry, brain tissue was sectioned and stained for markers associated with relevant cell populations by immunohistochemistry. Stained tissue from the brains of LPS-challenged mice was compared to that of an untreated control group (day 0).

5.4.1 Neutrophil accumulation in the brain

Based on their size, granularity and high surface expression of CD11b, the CD11b^{hi} granulocyte-like cells that were detected in the brains of LPS-treated mice at day 2 of the time course are likely to be neutrophils. To confirm this hypothesis, brain tissue from LPS-challenged mice was stained for the presence of the neutrophil granular enzyme myeloperoxidase (MPO). In all LPS challenged mice, neutrophils were distributed throughout the brain parenchyma and were detectable in the meninges (Figure 5.11A&B). However, the dissemination of these cells throughout the brain was sparse by days 5 and 7. On days 2 and 5, neutrophils could occasionally be associated with blood vessels (Figure 5.11C). This was no longer observed by day 7.

The absolute cell counts present in whole sections from equivalent brain regions were used to quantify the infiltrating neutrophils. Consistent with the flow cytometry data, on day 2 there was a significant increase in neutrophil numbers within the brains of LPS-challenged mice (Figure 5.12). This was predominantly due to the increased numbers of neutrophils infiltrating the parenchyma.

Although neutrophils were detected in the brain at the other time points following LPS treatment, their increase in numbers was not significant.

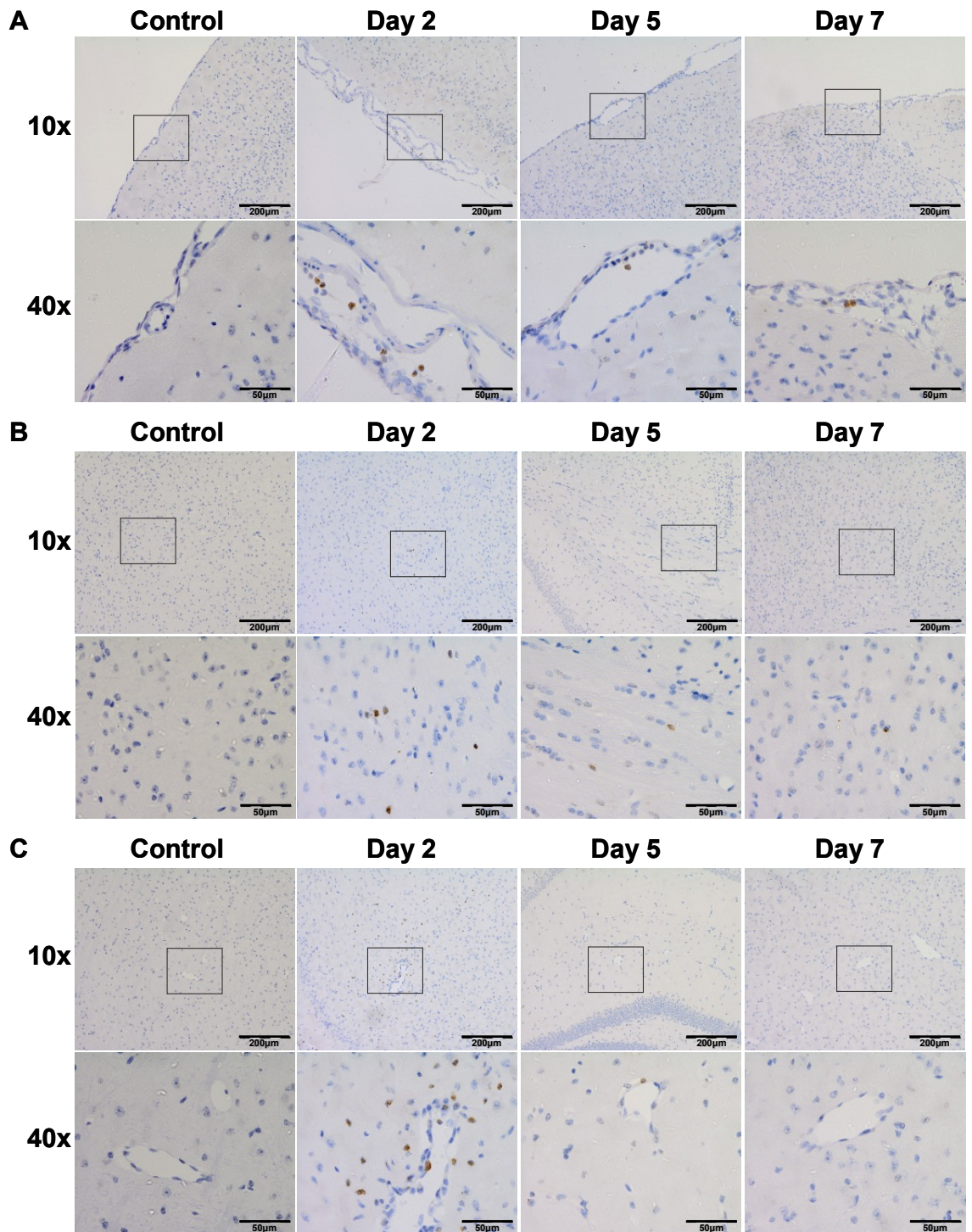


Figure 5.11 Accumulation of neutrophils in the brain over time

Mice were injected daily with 50µg LPS. Brain tissue was taken from mice at day 0 (naïve), 2, 5 or 7 following injection. Tissue was formalin-fixed, embedded in paraffin and cut into 5µm sections before being analysed by immunohistochemistry. (A-C) Examples of anti-myeloperoxidase staining within (A) the meninges, (B) the parenchyma and (C) blood vessels at each time point. n=3/group.

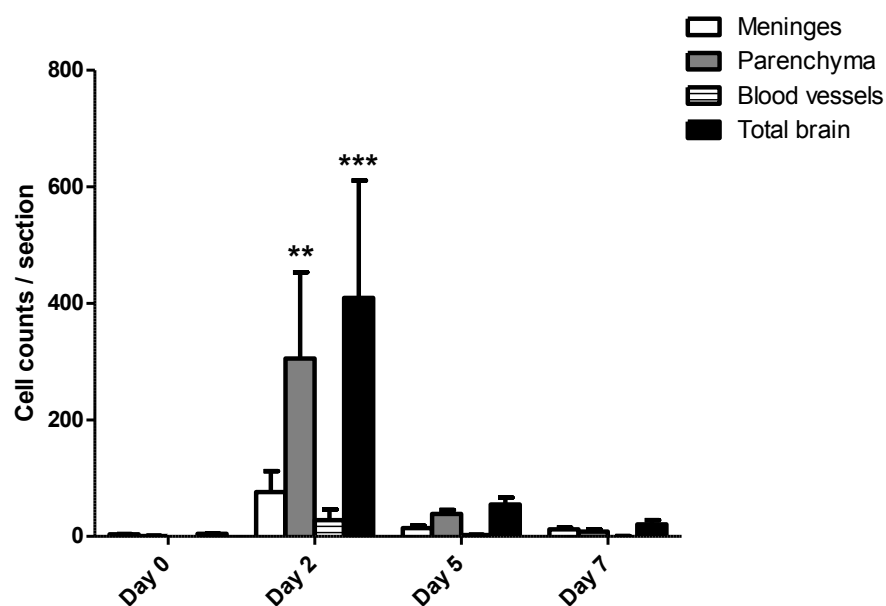


Figure 5.12 Relative neutrophil numbers in the brains of LPS-treated mice compared to naïve control mice

Mice were injected daily with 50µg LPS. Brain tissue, taken from mice at day 0, 2, 5 or 7 following injection, was formalin-fixed, embedded in paraffin and cut into 5µm sections before being analysed by immunohistochemistry. MPO⁺ cells (Figure 5.11) in the meninges, the parenchyma and adhered to blood vessels were quantified. Cells were quantified by counting every MPO⁺ neutrophil in 3 coronal sections from equivalent brain regions of each sample. Cell counts represent the mean number of cells per section in each sample. Data are displayed as the mean cell count +/- SEM. Significance of was calculated using a two way ANOVA: **P ≤ 0.01, ***P ≤ 0.001. n = 3/group.

5.4.2 CD3⁺ leukocyte accumulation in the brain

To confirm that T cells did indeed accumulate in the brain and to establish where these cells were localised, brain sections from LPS-treated and control mice were stained for T cell surface antigen, CD3. In all LPS-challenged and naïve mice, CD3⁺ cells could be detected in the meninges and in the parenchyma (Figure 5.13A&B and Figure 5.14). However, these cells were infrequent in naïve mice and in LPS-challenged mice at day 2. By days 5 and 7, there was a significant increase in the number of CD3⁺ cells in the parenchyma of LPS-challenged mice (Figure 5.13B and Figure 5.14). These cells were distributed throughout the parenchyma and were not specifically associated with distinct brain regions (data not shown). Despite their accumulation in the parenchyma, the numbers of CD3⁺ cells associated with either the blood vessels or the meninges remained statistically comparable to naïve mice throughout the model (Figure 5.13 and Figure 5.14).

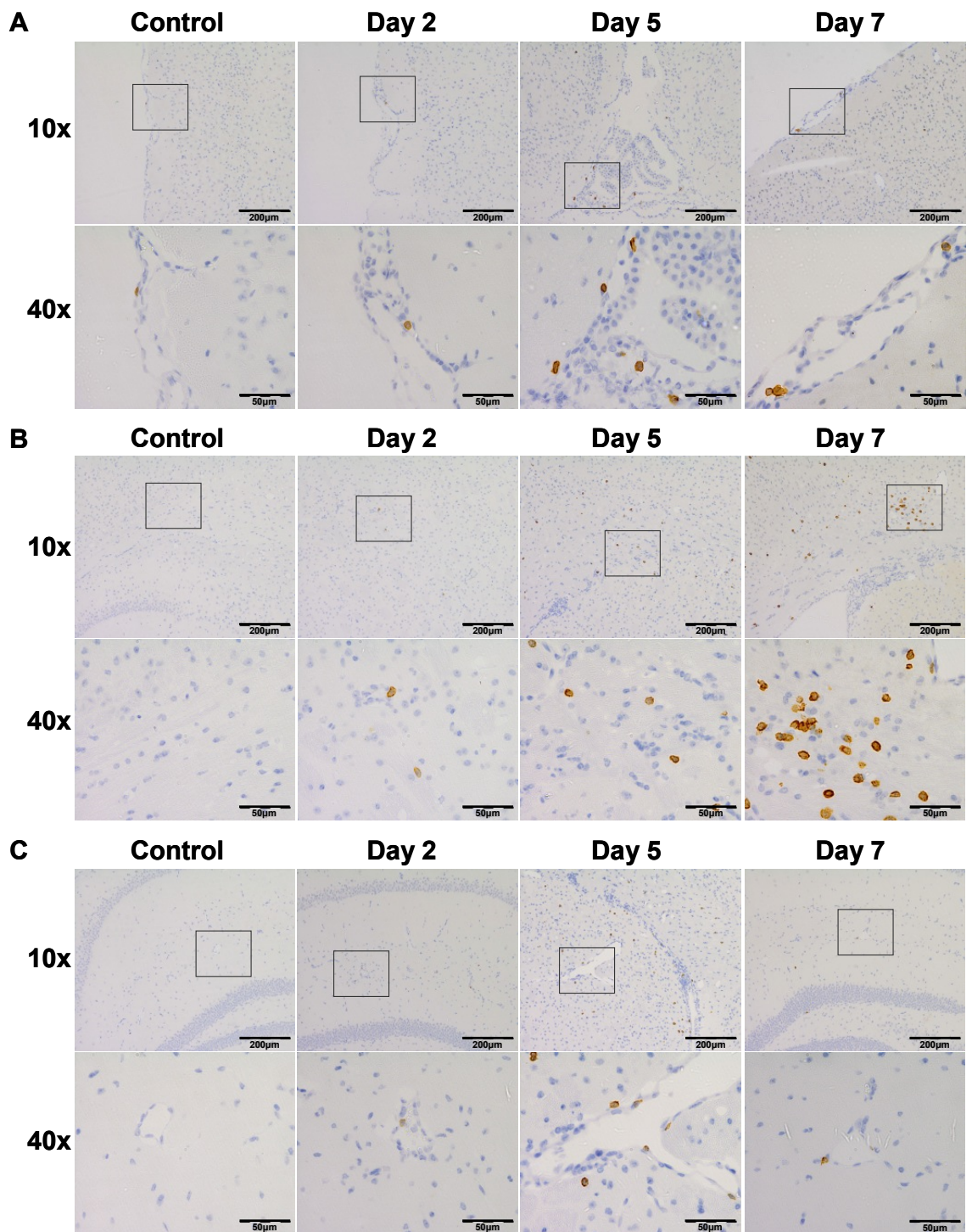


Figure 5.13 Accumulation of T cells in the brain over time

Mice were injected daily with 50µg LPS. Brain tissue, taken from mice at day 0, 2, 5 or 7 following injection, was formalin-fixed, embedded in paraffin and cut into 5µm sections before being analysed by immunohistochemistry. (A-C) Examples of anti-CD3 staining within (A) the meninges, (B) the parenchyma and (C) blood vessels at each time point. n=3/group.

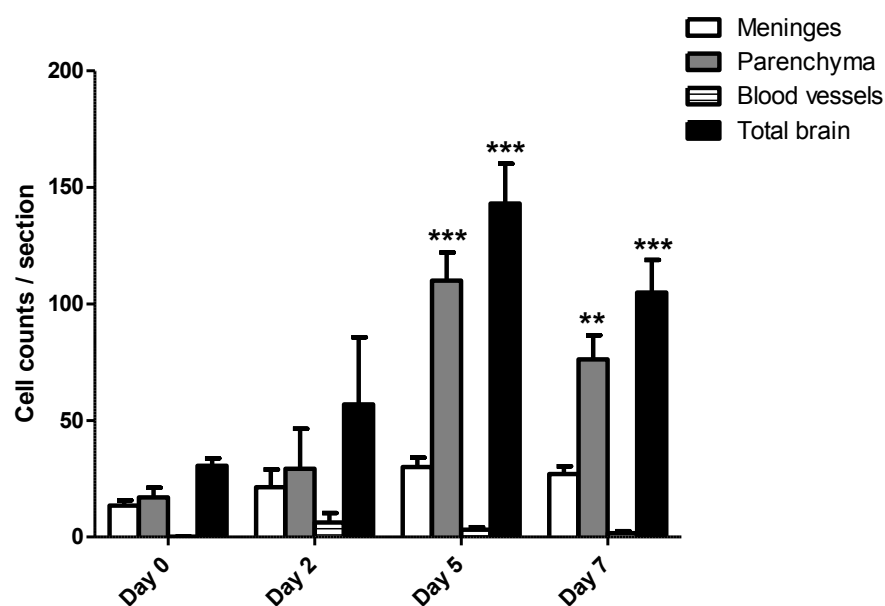


Figure 5.14 Relative T cell numbers in the brains of LPS-treated mice compared to naïve control mice

Mice were injected daily with 50µg LPS. Brain tissue, taken from mice at day 0, 2, 5 or 7 following injection, was formalin-fixed, embedded in paraffin and cut into 5µm sections before being analysed by immunohistochemistry. CD3⁺ cells (Figure 5.13) in the meninges, the parenchyma and adhered to blood vessels were quantified. Cells were quantified by counting every CD3⁺ cell in 3 coronal sections from equivalent brain regions of each sample. Cell counts represent the mean number of cells per section in each sample. Data are displayed as the mean cell count +/- SEM. Significance of was calculated using a two way ANOVA: **P ≤ 0.01, ***P ≤ 0.001. n = 3/group.

5.4.3 Monocyte accumulation in the brain

As there was a significant increase in the percentage of CD11b⁺ monocyte-like cells in the brains, brain sections were stained with a MAC387 antibody, specific to the macrophage marker calprotectin. No positive staining was detectable in the control mice or the LPS-treated mice at either day 2 or day 5. By day 7, MAC387⁺ monocytes were occasionally detected within the cerebral vasculature of LPS-treated mice (Figure 5.15A). However, the majority of the positive staining was located throughout the parenchyma, particularly in the piriform cortex and the thalamus (Figure 5.15C&D). With obvious cytoplasmic projections, the MAC387⁺ cells in the parenchyma morphologically resembled macrophages. However, MAC387 can also bind to microglial cells. Due to the lack of evidence of monocyte/macrophage infiltration, i.e. perivascular cuffs or

clusters of positive cells situated in close proximity to the meninges, it was impossible to determine whether monocytes had indeed infiltrated the brain and differentiated into macrophages or whether microglial cells had upregulated calprotectin in response to systemic LPS. As a result, the MAC387⁺ cells were not quantified.

In summary, histological characterisation of the leukocyte infiltrate in the brains of LPS-challenged mice revealed that by day 2, following two systemic LPS injections, neutrophils had accumulated within the brain. This infiltration was transient and had returned to a level statistically comparable to that of naïve mice by day 5. Consistent with the flow cytometry data, the accumulation of neutrophils was followed by the recruitment of CD3⁺ T cells. However, in this experiment T cells entered the brain between days 2 and 5 rather than between days 5 and 7. These cells invaded the parenchyma of LPS-challenged mice where they remained until at least day 7. Importantly, these data confirm that the increased proportions of T cells, and CD11b⁺ granulocyte-like cells, which were detected in the brains of LPS treated mice using flow cytometry, represent a genuine increase in absolute cell numbers in the brain. Although there was some evidence to suggest that monocytes may also infiltrate the brain and differentiate into MAC387⁺ macrophages between days 5 and 7, this could not fully be verified by histology.

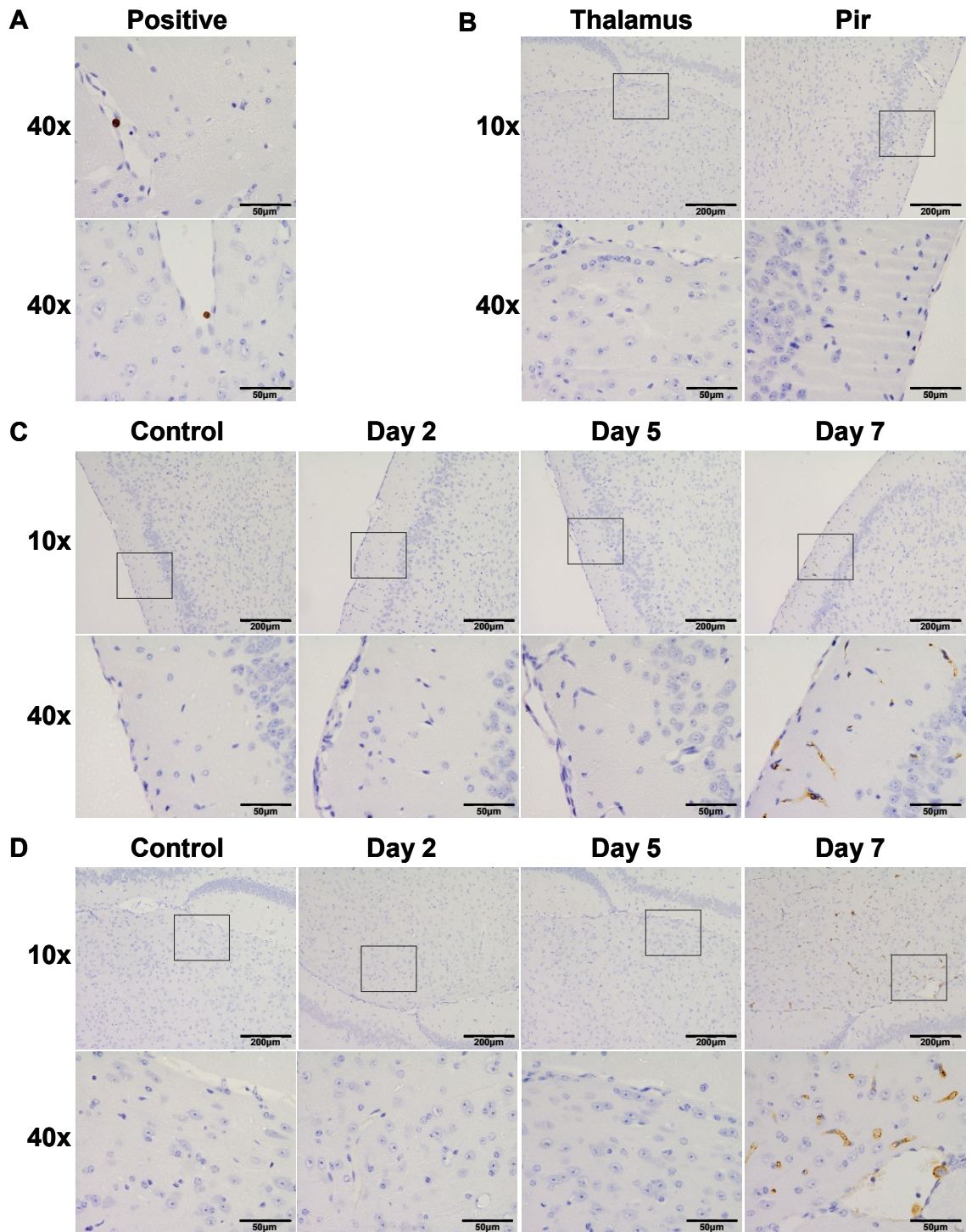


Figure 5.15 Detection of monocytes/macrophages in the brain over time

Mice were injected daily with 50µg LPS. Brain tissue was taken from mice at day 0, 2, 5 or 7 following injection. Tissue was formalin-fixed, embedded in paraffin and cut into 5µm sections before being analysed by immunohistochemistry. (A) Examples of anti-calprotectin (MAC387) staining on monocytes within blood vessels at day 7 of the LPS model. (B) Examples of isotype staining in the piriform cortex (Pir) and the thalamus at day 7 of the LPS model. (C&D) Examples of MAC387 staining within (C) the Pir and (D) the thalamus at each time point. n=3/group.

5.5 Discussion and conclusions

In this chapter, a combination of gene expression assays was used to determine whether chemokine and/or chemokine receptor transcripts were elevated in the brain following chronic exposure to LPS in the periphery. Mice received a single I.P. injection of a high dose of LPS, or an equivalent volume of vehicle, daily for 2, 5 or 7 consecutive days. Many of the chemokine transcripts assayed were significantly upregulated in the brains of the LPS challenged mice at day 2, following 2 doses of systemic LPS. Although a number remained upregulated until at least day 5 of the model, the majority of the chemokine transcripts had returned to baseline by this time point. It was previously demonstrated in Section 4.3.2 that, as a result of endotoxin tolerance, daily I.P. injections of LPS suppressed inflammatory cytokine production in the periphery but not in the brain. Interestingly, inflammatory chemokine induction was also brain-specific, i.e. was not mirrored by a similar increase by PBL. This is in keeping with a previous report by Erickson *et al.* which demonstrated that protein levels of CCL2, CCL3, CCL5 and CXCL1 were significantly increased in the brain, but not the serum, of mice following repeated I.P. injections of LPS²³⁸. However, the LPS model used by Erickson *et al.* differed somewhat from the model used to conduct these studies as, instead of daily LPS challenges, mice received several LPS injections within a 24 hour period.

Amongst the panel of chemokine genes that were highly upregulated in the brain following multiple LPS challenges were those encoding the neutrophil chemoattractants, CXCL1 and CXCL2. It has previously been demonstrated that, following a single I.P injection of LPS, the main source of these chemokines are activated endothelial cells⁴⁴³. However, as both chemokines can be expressed by reactive astrocytes in models of CNS injury or demyelination⁴⁴⁴⁻⁴⁴⁶, this cell population may also express CXCL1 and CXCL2 in response to the prolonged CNS inflammation that occurs following multiple injections of LPS. Interestingly, at day 2 of the LPS model, the gene encoding CXCR2, the sole receptor for these two chemokine ligands, also appeared to be upregulated in the brain. As the most characterised function of these chemokines is to recruit CXCR2-expressing leukocytes to sites of inflammation, it was hypothesised that the increase in *Cxcr2* mRNA may have occurred as a result of leukocyte accumulation in the brain.

In mice, CXCR2 is most prominently expressed by neutrophils. As a result it has previously been used as a surrogate marker to indicate their presence in the brain⁴⁴⁷. However, as it is also expressed in the CNS of both humans and rodents, an increase in *Cxcr2* mRNA is insufficient to fully determine whether neutrophils infiltrate the brains of LPS challenged mice. Flow cytometric analysis of brain tissue revealed that the percentage of CD11b^{hi} granulocyte-like cells was increased in the brains of LPS-challenged mice at day 2 of the model. Although this cell population phenotypically resembled neutrophils, due to the lack of surface markers stained, these cells were impossible to fully characterise from this experiment alone. However, it was subsequently demonstrated using histology that by day 2 of the LPS model, MPO⁺ neutrophils had invaded the brain parenchyma. Surprisingly, the neutrophils did not appear to be localised within perivascular cuffs, nor were they significantly enriched in the meninges. It is therefore unclear whether they had entered the brain via the BBB or the BCSFB. There was occasionally evidence of neutrophils both within and surrounding the same blood vessel. Therefore, it seems likely that at least some of the neutrophils crossed the BBB and the glia limitans. Histological analysis of brain sections at earlier time points would be required in order to establish the precise time point these cells entered the brain and their route of entry. Thus by day 2 of the LPS model, not only was the induction of *Cxcl1* and *Cxcl2* in the brain accompanied by a transient elevation in *Cxcr2* mRNA, but it coincided with a transient increase in neutrophil numbers within the brain.

Although it was difficult to distinguish between CD11⁺ granulocyte-like cells and CD11b⁺ macrophage-like cells in the blood, the proportion of CD11b⁺ leukocytes present in the circulation of LPS-treated mice was increased throughout the model. This is unsurprising as granulocytes and monocytes are rapidly deployed from the bone marrow in response to bacterial infection or endotoxin administration⁴⁴⁸⁻⁴⁵⁰. Despite an impaired inflammatory cytokine response in the periphery, there is one report to suggest that endotoxin-induced granulocyte mobilisation from the bone marrow occurs to a similar extent in naïve and endotoxin-tolerant mice⁴⁵¹. To my knowledge there are no published data regarding monocyte mobilisation under these circumstances. Interestingly, the transcriptional chemokine receptor transcript data would suggest that, in this model, neutrophil numbers are unlikely to be increased to a great extent in the

peripheral blood, as the levels of *Cxcr2* mRNA extracted from PBL remains comparable to baseline throughout the time course. It is possible that the increased proportion of CD11b⁺ cells in the blood is predominantly due to an elevation in circulating monocyte numbers. A more comprehensive flow cytometry staining panel would be required in order to confirm this. In addition, as CCR2 signalling is pivotal in triggering monocyte egress from the bone marrow, the levels of *Ccr2* mRNA could be compared in PBL from LPS- and vehicle-treated mice. Thus, the elevated proportions of CD11b⁺ leukocyte populations detectable in the circulation are likely to be due to an increase in monocyte and/or granulocyte recruitment from the bone marrow.

The chemokines CCL3 and CCL5 share the capacity to attract a number of different leukocyte populations to the brain. Both chemokines can activate the chemokine receptors CCR1 and CCR5. In addition, CCL5 can activate CCR3. The leukocyte populations that respond to these chemokines are diverse and include, monocytes/macrophages, T cells and NK cells^{93,95,452,453}. As the genes encoding a number of other monocyte-associated chemoattractants, namely *Ccl2*, *Ccl7* and *Ccl8*, were significantly upregulated in the brain on day 2 of the LPS model, it was hypothesised that this might result in monocyte infiltration. At the same time point, there was a significant increase in both *Ccr1* mRNA and CD11b⁺ monocyte-like cells in the brain. Although this could be indicative of an influx of monocytes, there was no MAC387 staining visible in the brain until day 7.

An alternative explanation that would also account for the increase in CD11b⁺ leukocytes and *Ccr1* mRNA in the brain is a potential infiltration of NK cells at day 2 of the LPS model. This would also explain why there was an increase in *Cxcr3* mRNA in the absence of T cell infiltration at this time point. Attempts were made to stain brain sections for NK cells using antibodies specific to NK cell marker CD49b (data not shown). Unfortunately, the antibodies reacted non-specifically to a population of non-haematopoietic cells in the brain and therefore could not be used to identify NK cells. Thus, although it is possible that NK cells enter the brains of mice following prolonged exposure to LPS in the periphery, more work would be required in order to investigate this hypothesis. This could be done using either flow cytometry or histology.

By day 5 of the LPS model, neutrophils were no longer detectable in the brain. However, there was a significant increase in the number of CD3⁺ T cells in the brain parenchyma that was detectable only by histology. As there was no evidence of T cells within perivascular cuffs or specifically surrounding the meninges, their route of entry could not be established. Like neutrophils, T cells could be observed within and surrounding the same blood vessels which suggests that the BBB was one likely route of entry. It is possible that the T cells entered the brain after day 2, giving them time to become fully dispersed throughout the parenchyma by day 5. Again, histological examination of brain sections taken at different time points between days 2 and 5 would be required to confirm this. By day 7, both flow cytometric and histological analysis of brain tissue collectively revealed a significant increase in the frequency and absolute numbers of T cells in the brain. The majority of infiltrating T cells at this time point expressed CD8. However, CD8⁻ T cells, most likely CD4⁺, were also significantly enriched in the brains of LPS-challenged mice on day 7.

Both CD8⁺ T cells and CD4⁺ Th1 cells characteristically express the chemokine receptors CCR5 and CXCR3. Therefore, their entry to the brain may be mediated by the ligands for one or both of these receptors. In keeping with this hypothesis, the genes encoding CXCL9 and CXCL10, the ligands for CXCR3, were significantly upregulated in the brain at day 2. Furthermore, transcripts for the CCR5 ligands, CCL3 and CCL5, were upregulated until day 5. However, on days 5 and 7, when T cells were detectable in the brain, there was only a small, but significant, increase in *Cxcr3* mRNA and slight trend towards an increase in *Ccr5* mRNA. Neither increase was as high as would be expected if the infiltrating T cells expressed mRNA for these chemokine receptors. Having said this, CCR5 and CXCR3 are both expressed by neurons and glial cells⁴⁵⁴⁻⁴⁵⁷. As the transcriptional data have been derived from whole brain homogenate, any differential gene expression of *Cxcr3* and/or *Ccr5* by brain-resident cell populations would bias these results. Therefore, although T cells accumulate in the brain following multiple systemic LPS injections, it is difficult to define what chemokine systems, if any, are responsible for their entry.

Unlike CD11b⁺ leukocyte populations, proportions of both CD8⁺ and CD8⁻ T cells were decreased in the blood throughout the LPS model. Rather than a genuine decrease in circulating T cell numbers, this is most likely to be a knock-on effect

of the increased proportion of CD11b⁺ leukocytes. Unfortunately the absolute cell numbers in the blood were not established. Therefore, if the increased proportion of T cells detected in the brain at day 7 was mirrored by a similar increase in the peripheral blood, this effect was masked by changes in the proportions of other populations of leukocytes.

At day 7, in addition to CD3⁺ T cells, MAC387⁺ cells were detectable in the brain parenchyma, particularly in the thalamus and the piriform cortex. As this marker can also bind microglia, it was not possible to fully establish whether the positive staining represented an influx of monocytes/macrophages to the brain, or the induced or upregulated expression of calprotectin by microglial cells in response to chronic LPS administration in the periphery. MAC387⁺ cells could be detected within blood vessels; therefore it is likely that at least some of the positive staining is attributable to monocyte/macrophage accumulation in the brain. Furthermore, although the upregulation of calprotectin by microglia has been reported previously in Schizophrenic patients⁴⁵⁸, to my knowledge it has never been reported in response to LPS. These observations indicate that monocytes may infiltrate the brain from the periphery in response to prolonged exposure to systemic LPS. However, a more detailed histological examination of the tissue, with additional macrophage markers, would be required to confirm this.

Taken together, the observations made from this chapter suggest that chronic exposure to LPS in the periphery results in the chemokine-mediated recruitment of leukocytes to the brain parenchyma. Infiltrating leukocytes include neutrophils, T cells and possibly monocytes/macrophages. As described in Section 1.3.1.3, neutrophil recruitment to the brain following systemic LPS challenge has been previously described^{236,237}. However, to my knowledge, this is the first time they have been shown to infiltrate the brain in the context of endotoxin tolerance. Furthermore, to my knowledge, this is the first time that an accumulation of T cells has been shown in the brains of mice challenged systemically with LPS.

Although intriguing, the data described in this chapter are limited and require follow-up studies or repetition. The transcriptional data could be strengthened by analysing chemokine and chemokine receptor protein levels.

Immunofluorescence staining could be used to determine where in the brain these chemokines were expressed and by what cell types. This method could also be used to establish whether the relevant chemokine receptors were predominantly expressed by infiltrating leukocytes or brain resident cell populations. However, as antibodies to chemokines and chemokine receptors are often poor, this can prove challenging. In addition, although there was increased transcription of numerous chemokine genes in the brain coupled with, or followed by, an influx of leukocyte populations, the involvement of chemokines in coordinating leukocyte recruitment to the brain under these circumstances remains unconfirmed. Follow up studies investigating leukocyte recruitment to the brain following treatment with specific chemokine receptor antagonists could be used to confirm this.

At day 5 of the time course, T cells could be detected in the brain by immunohistochemical CD3 staining but not by flow cytometry. The reason for this discrepancy is unclear. It is possible that T cells begin to infiltrate the brain on or around day 5. Although carried out in the same manner, the LPS models used for the flow cytometry experiment and the histology staining were independent experiments; set up at different times using different litters of C57BL6 mice. Therefore a slight variation in the exact time point that T cells entered the brain could explain the different results. The flow cytometry data described in this chapter have all been derived from a single experiment. To gain a better understanding of why T cells were not observed in the brain at day 5 using flow cytometry, this experiment would have to be repeated.

Another observation that will require further investigation was the increased frequency of microglial cells within the brains of vehicle-treated control mice on day 2 of the LPS time course. It is highly unlikely that this reflects a genuine decrease in microglial numbers in response to systemic LPS at this time point. Not only has nothing similar ever been reported in the literature, but at both of the later time points the percentages of microglial cells were similar in LPS- and vehicle-treated mice. This suggests that the numbers of microglial cells in the brain do not vary. Furthermore, microglial percentages at days 5 and 7, in both LPS-treated and control animals were comparable to that of LPS-injected mice on day 2. This implies that the increased frequency of microglial cells observed in the brains of vehicle-injected control mice at day 2 of the LPS model was

most likely to be an anomaly. It is possible that during the preparation of the brain tissue for flow cytometry there was reduction in microglial cell death in the control brains but there is no obvious reason why this would have happened. To fully establish whether the observed differences in microglial cell percentages reflected a true phenotype or just an anomaly, the flow cytometry experiment would again have to be repeated.

In summary, repeated injections of LPS in the periphery triggers a transient increase in chemokine transcription in the brain. Chemokine induction was brain-specific and not mirrored by a similar increase in the peripheral blood. In addition, the increased chemokine expression was accompanied with an infiltration of neutrophils, followed by the recruitment of T cells and possibly monocytes to the brain. Not only did these leukocytes cross either the BBB or the BSCB, but they surpassed the glia limitans to become fully dispersed throughout the brain parenchyma. Leukocyte infiltration was coupled with an increase in mRNA encoding the relative chemokine receptors. Although this cannot be fully verified from these data alone, the results outlined in this chapter strongly suggest that chronic exposure to LPS in the periphery triggers a chemokine-mediated recruitment of inflammatory leukocytes to the brain parenchyma.

6 Defining the chemokine receptor profile of CNS-derived pathogenic leukocytes

6.1 Introduction and aims

Having highlighted some of the potential chemokine systems involved in facilitating leukocyte entry into the brain following repeated LPS injections, I then sought to compare these data to a clinically relevant inflammatory disease. MS is a chronic, inflammatory autoimmune disease of the CNS. It is characterised by an accumulation of autoreactive and inflammatory leukocytes which form demyelinating lesions within the CNS parenchyma. The axonal degeneration that ensues can lead to neurological defects such as ataxia, paralysis, loss of vision and loss of cognitive function⁴⁵⁹. Although MS is not a peripheral inflammatory disorder, it is a chronic inflammatory disease in which the peripheral immune system and the CNS are both intrinsically involved. In addition, routine diagnosis of MS involves sampling a patient's CSF, enabling relatively easy access to a population of leukocytes that have crossed the BCSFB.

Chemokines play a pivotal role in MS. Not only are they associated with the trafficking of inflammatory leukocytes to and within the CNS, but they also play a role in the migration of regulatory lymphocytes to the CNS and in glial cell communication and activation^{210,228,460-462}. Due to their intimate involvement in MS pathogenesis, chemokines have been implicated as potential targets for therapeutic intervention. As a result, many studies have attempted to analyse and interpret the involvement of chemokine systems, i.e. specific chemokine/chemokine receptor interactions, in MS pathology. This research has been described in more detail in Section 1.3.1.2. Much of our current understanding regarding the potentially pathogenic role that specific chemokine systems play in MS is derived from studies using genetically manipulated animal models. However, knowledge gained from these models does not always translate across species. For that reason, more research is required to fully characterise the role of chemokine receptors and their respective ligands in driving MS pathology.

In order to establish the specific chemokine systems involved in facilitating leukocyte entry to human CNS, CSF and blood samples were to be collected from MS patients and a group of patients who were subjected to a lumbar puncture but ultimately deemed medically healthy. Patients with MS typically experience a massive leukocyte infiltrate across the BCSFB^{153,156,460}. As a result, 1ml of CSF

could contain tens of thousands of leukocytes. In contrast, CSF from apparently healthy patients, such as those to be used as a control group for this study, contains on average 1×10^3 leukocytes per ml. The aim of this study was 2-fold:

(1) Due to the limited number of cells that are present in control patient CSF, it was necessary to develop a protocol that would generate a sufficient quantity of RNA for the relevant downstream gene analyses.

(2) To use a combination of multiplex gene expression analysis and protein assays to systematically characterise the chemokine systems involved in governing leukocyte entry to the CNS during MS.

RNA was to be extracted from CSF-derived leukocytes. By amplifying this RNA using IVT, it would be possible to use multiplex gene expression assays such as TLDA plates to determine the differential chemokine receptor profile of CSF-derived leukocytes from MS patients, when compared to that of leukocytes from apparently healthy CSF. Additionally, this would allow the expression levels of chemokine receptors by CSF- and peripheral blood-derived leukocytes from matched patient samples to be examined comparatively. Chemokine levels in the residual sera and CSF could then be measured using Luminex® technology, identifying any aberrant expression of chemokines in the CSF that may trigger the infiltration of inflammatory leukocytes. Thus, providing that a protocol for amplifying RNA from low cell numbers could be established, multiplex gene expression analysis and protein assays could be employed to characterise the specific chemokine systems involved in allowing leukocytes to cross the BCSFB during MS.

6.2 Optimising RNA extraction and cDNA synthesis protocols

Prior to collection of precious samples, it was necessary to determine whether sufficient levels of RNA could be extracted from 1×10^3 leukocytes; the average number expected in control CSF samples. As RNA extraction from such small numbers of cells can prove challenging, different RNA extraction methods were compared to determine which would generate the greatest yield. In anticipation of a low yield of RNA from 10^3 leukocytes, even after amplification, the efficiency of two highly sensitive RT kits was also compared.

6.2.1 RNA extraction optimisation

To determine the most effective RNA extraction protocol, RNA was extracted from 1×10^3 , 1×10^4 , 1×10^5 and 5×10^5 peripheral blood mononuclear cells (PBMCs) using different methods. The efficiency of Qiagen columns and Trizol reagent were compared, both with, and without, carrier RNA (cRNA). cRNA, derived from *E. coli* transfer RNA was used in an attempt to improve yield by physically buffering extracted RNA. A disadvantage of this method is that the extracted RNA yield can not be accurately measured using either the nanodrop or the Agilent 2100 Bioanalyzer. Additionally, carrier RNA can sometimes interfere with downstream reactions. As it is compatible with both protocols, DNase I digestion was performed using a DNA-free™ kit. To test the efficiency of the two extraction methods, all of the extracted RNA was converted to cDNA and the relative transcript levels of housekeeping gene *Gapdh* were used as a method of comparison following either PCR (Figure 6.1A) or QPCR (Figure 6.1B). As all PBMCs originated from the same source, any differences in housekeeping gene expression would be due to differences in cDNA level; thus relatively quantifying RNA yield. Regardless of the extraction method, enough RNA was extracted from 10^3 PBMCs to generate a *Gapdh* signal when amplified by either PCR or QPCR. Both the PCR and QPCR results indicate that Qiagen RNeasy Micro kits are more effective than Trizol reagent at extracting RNA from low cell numbers. Therefore, subsequent RNA extractions directly from cells were all carried out using Qiagen RNeasy columns. cRNA significantly enhanced the yield of RNA extracted from 1×10^4 and 5×10^5 PBMCs (Figure 6.1B), however, the beneficial effect of cRNA seemed variable as it did not improve RNA yield when extracting

from either 1×10^3 or 1×10^5 PBMCs. In fact, although not deemed significant, its use appeared to have a detrimental effect when RNA was extracted from 1×10^3 PBMCs. As this was the expected average cell number of control CSF samples, the use of *E. coli* total RNA as a carrier was discontinued.

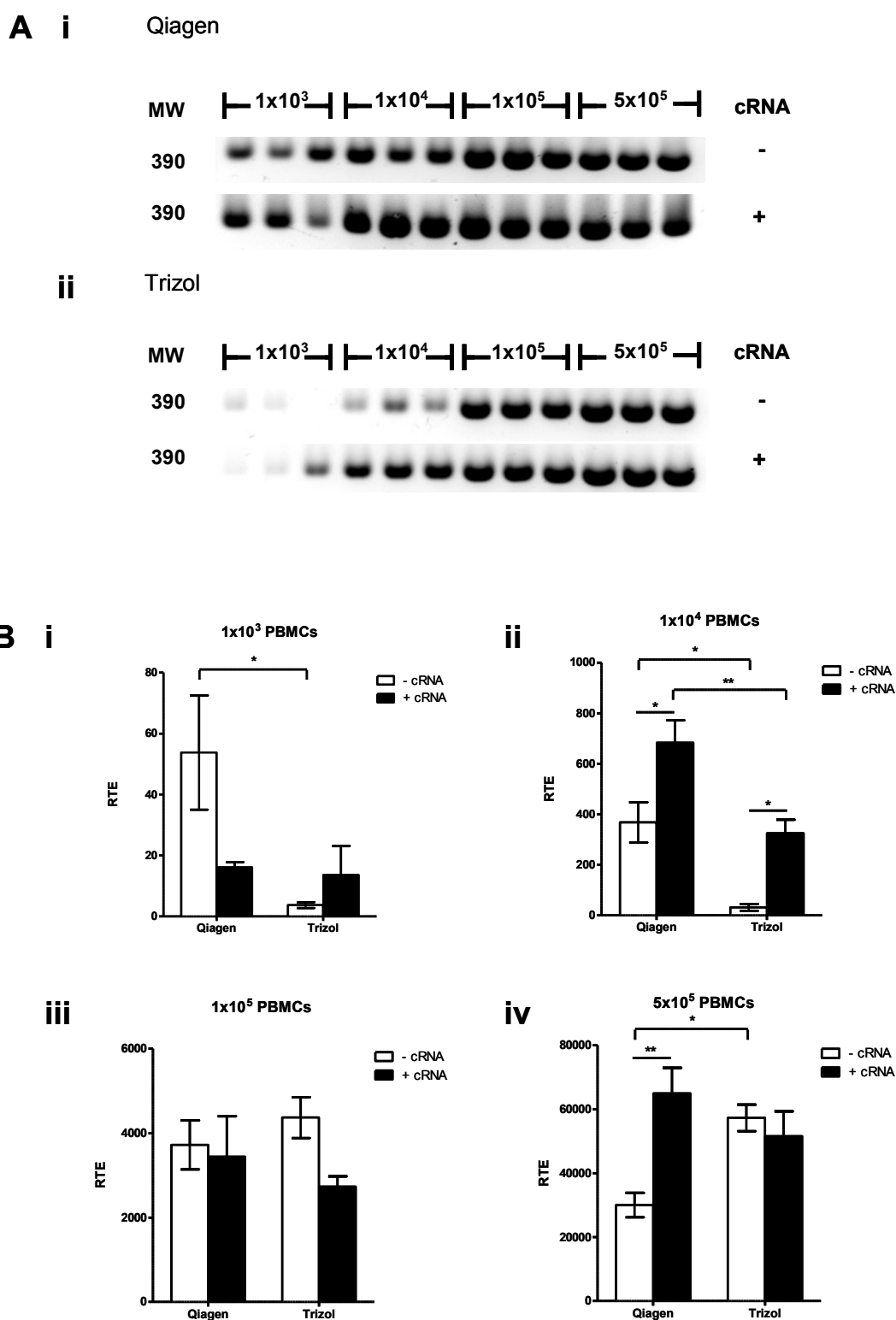


Figure 6.1 Comparison of different methods of RNA extraction

Relative *Gapdh* expression. (A) PCR of *Gapdh* visualized on a 2% agarose gel. cDNA was synthesized from RNA extracted from 1×10^3 , 1×10^4 , 1×10^5 and 5×10^5 PBMCs using (i) Qiagen kits or (ii) Trizol reagent in the presence (+) or absence (-) of *E. coli* cRNA. (B) Relative *Gapdh* expression was determined using QPCR. cDNA was synthesized from RNA extracted from (i) 1×10^3 , (ii) 1×10^4 , (iii) 1×10^5 and (iv) 5×10^5 PBMCs. Relative transcript expression (RTE) was calculated by the equations: $RTE = 2^X$, where $X = CT_{\text{baseline}} - CT_{\text{median}}$. Data represent data +/- SEM.

Significance was determined using two-way ANOVA: * $P \leq 0.05$, ** $P \leq 0.01$, *** $P \leq 0.001$. $n = 3/\text{group}$.

6.2.1.1 Determining the integrity of RNA extracted from low cell numbers

The Agilent 2100 Bioanalyzer was used to assess the quality of the RNA from 1×10^3 , 1×10^4 and 1×10^5 PBMCs that was extracted using the Qiagen columns in the absence of cRNA. Due to the low yield, RNA was assessed qualitatively using the RNA 6000 Pico chip. Each electropherogram below represents one of three biological replicates from each group. With 3 distinct peaks and low background, RNA extracted from 1×10^5 cells (Figure 6.2C) closely resembles the example of high quality RNA, previously shown in Figure 3.2A. RNA extracted from 1×10^4 PBMCs, however, is of inferior quality (Figure 6.2B). Although the 2 peaks corresponding to ribosomal subunits 18S and 28S are clearly visible, there is a high level of background, indicating a moderate level of degradation. RNA extracted from 1×10^3 cells was undetectable by the Pico chip (Figure 6.2A). As the RNA 6000 Pico chip has a range of 50-5000pg/ μl , it can be concluded that the level of RNA was present in the sample at a concentration of less than 50pg/ μl . These observations imply that, although RNA can be extracted from low cell numbers, a threshold may exist, below which RNA begins to lose its integrity. In this experiment, RNA began to lose integrity between 1×10^5 and 1×10^4 PBMCs and despite it being of sufficient yield to generate a *Gapdh* signal using PCR, RNA extracted from 1×10^3 PBMCs was too low to be detected by the Bioanalyzer.

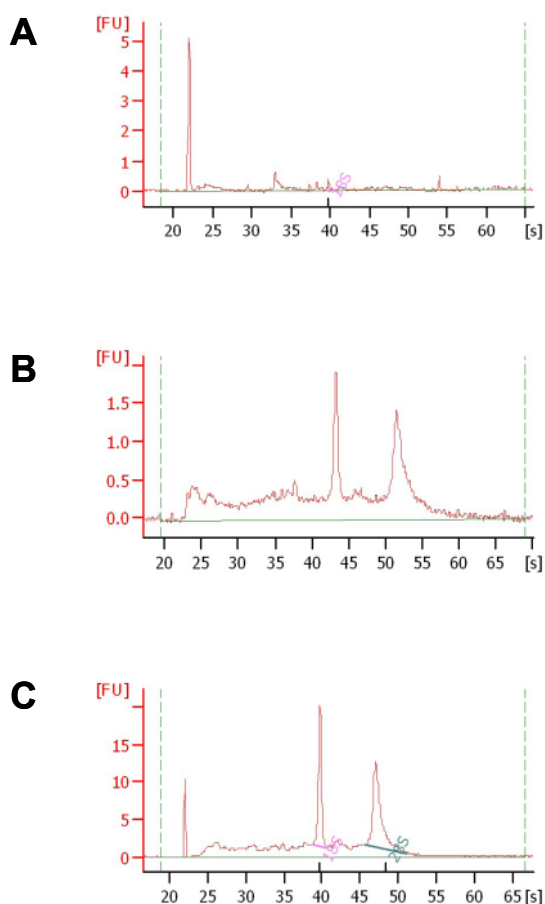


Figure 6.2 Integrity of RNA samples extracted from 1×10^3 , 1×10^4 and 1×10^5 PBMCs

RNA quality was determined using an Agilent 2100 Bioanalyzer on an RNA 6000 Pico chip. RNA was extracted from (A) 1×10^3 , (B) 1×10^4 and (C) 1×10^5 PBMCs using Qiagen columns without cRNA. Data represent fluorescence intensity (fluorescence units [FU]) measured over time in seconds [s]. One representative sample has been shown from each group. $n = 3/\text{group}$.

6.2.2 cDNA synthesis optimization

It has been shown above, that extracting RNA from as little as 1×10^3 leukocytes, generates a very low (immeasurable) yield of RNA; detectable only after RT followed by PCR amplification. Even after IVT, the level of amplified RNA in each sample has the potential to be low. In anticipation of amplifying sufficient RNA for multiplex gene expression analysis, a suitably sensitive cDNA synthesis kit had to be found that would maximise the cDNA yield. The efficiency of two different RT kits was compared. Although the High Capacity RNA-to-cDNA kit is recommended for downstream QPCR-based applications, the SuperscriptTM III reverse transcription kit is advertised as being more sensitive, and specific, than the other RT kits on the market. To test this claim, RNA was extracted from 1×10^3 , 5×10^3 and 1×10^4 PBMCs and converted to cDNA using the two different kits. As in Section 6.2.1, the relative transcript levels of *Gapdh* were used as a

method of comparison following QPCR (Figure 6.3). Again, all PBMCs originated from the same source. The only variable was the cDNA synthesis kit used and therefore, any differences in *Gapdh* signal could only be due to differences in cDNA yield. It is clear from Figure 6.3 that the High Capacity kit is significantly more effective than the SuperScript™ III kit ($p < 0.0001$). cDNA, synthesised using this kit, was of a significantly greater yield than that synthesised using the SuperScript™ III kit when using RNA extracted from 5×10^3 or 1×10^4 leukocytes as a template (Figure 6.3). In addition, there was a trend towards a higher yield when RNA from 1×10^3 leukocytes was converted to cDNA using the High Capacity kit. Conclusively, the High Capacity RNA-to-cDNA kit was more effective than the SuperScript™ III RT kit at synthesising cDNA from low levels of RNA.

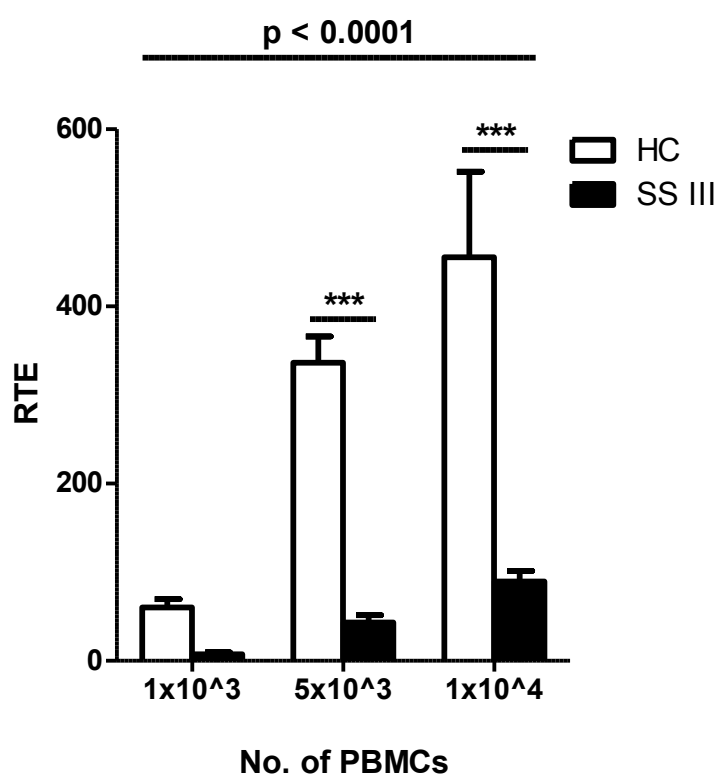


Figure 6.3 Comparison of High Capacity and SuperScript™ III reverse transcription kits
Relative *Gapdh* expression was determined using QPCR. RNA was extracted from 1×10^3 , 5×10^3 and 1×10^4 PBMCs and converted to cDNA using either the High Capacity RNA-to-cDNA kit (HC) or the SuperScript™ III RT kit (SS III). Relative transcript expression (RTE) was calculated by the equations: $RTE = 2^X$ where $X = CT_{baseline} - CT_{median}$. Significance was determined using two-way ANOVA: * $P \leq 0.05$, ** $P \leq 0.01$, *** $P \leq 0.001$. $n=3$ /group

6.3 Developing a protocol to amplify RNA from low cell numbers

As mentioned, CSF samples, particularly those from control subjects, may contain as few as 1×10^3 leukocytes. To guarantee sufficient levels of cDNA for TLDA gene expression analysis, RNA isolated from each sample would first have to be subjected to linear amplification using the SuperScript™ RNA amplification kit (Section 2.5.9) before being converted to cDNA. This method, which allows for a 1000-fold amplification of available RNA, is optimised to amplify RNA from a minimum starting quantity of 100ng. On the basis that each cell expresses approximately 50pg of RNA, even if the RNA extraction was 100% efficient, each control sample would only contain 50ng of RNA. As this is well below the minimum starting quantity defined by the manufacturers, the limitations of the RNA amplification kit were tested in order to determine whether RNA could successfully be amplified from as little as 1×10^3 leukocytes. In addition, the integrity of the amplified message RNA product (aRNA) was also determined. As an additional quality control, SYBR Green QPCR was then used to determine whether the transcriptional profile of aRNA accurately represented that of its template.

6.3.1 Testing the efficiency of the RNA amplification kit using control HeLa cell RNA

The SuperScript™ RNA amplification kit is designed to consistently amplify mRNA by at least 1000-fold. As a preliminary quality control mechanism, RNA from HeLa cells (provided with the kit) was amplified and the resulting yield quantified using a nanodrop. Control amplifications were performed in triplicate. The aRNA yield from these IVT reactions is listed in Table 6.1. As described by the manufacturers, amplification of 500ng HeLa total RNA should generate a minimum of 35µg aRNA. However, in these IVT reactions, a mean of only 4.66µg aRNA was transcribed from the control RNA. Therefore, although the control HeLa RNA was successfully amplified, the kit appeared to be functioning at only a fraction of its suggested capacity.

Total RNA	Expected Yield	Observed Yield (individual replicates)			Mean Yield	SEM
		Control 1	Control 2	Control 3		
500ng	≥35µg	3.03µg	4.61µg	6.34µg	4.66µg	0.96

Table 6.1 Yield of control amplifications from HeLa RNA

RNA was amplified from 500ng HeLa RNA as a control reaction in three independent experiments; control 1, control 2 and control 3. aRNA quantity was determined using a nanodrop.

6.3.2 Testing the limitations of the IVT kit using different starting quantities of template RNA

The SuperScript™ RNA amplification kit is designed to amplify RNA from a starting quantity of no less than 100 ng. As determined in Section 6.2.1.1, RNA extracted from 1×10^3 leukocytes may contain less than 50 pg/µl. Eluted in approximately 12µl, the total yield of RNA extracted from 1×10^3 leukocytes is considerably lower than the starting quantity recommended by the kit. As a consequence, before attempting to amplify RNA from precious CSF samples, it first had to be determined whether the amplification kit could cope with such low levels of starting RNA. To test the limitations of the kit, RNA was extracted from PBMCs and serially diluted 2-fold to acquire triplicates of 100 ng, 50 ng, 25 ng and 12.5 ng of total RNA. RNA amplification from these starting quantities yielded a mean of 4.22 µg, 2.34 µg, 1.22 µg and 0.48 µg aRNA respectively (Figure 6.4A). As TLDA plates require only 30 ng message RNA, 12.5 ng total RNA is an ample starting quantity to provide a sufficient aRNA yield post-amplification.

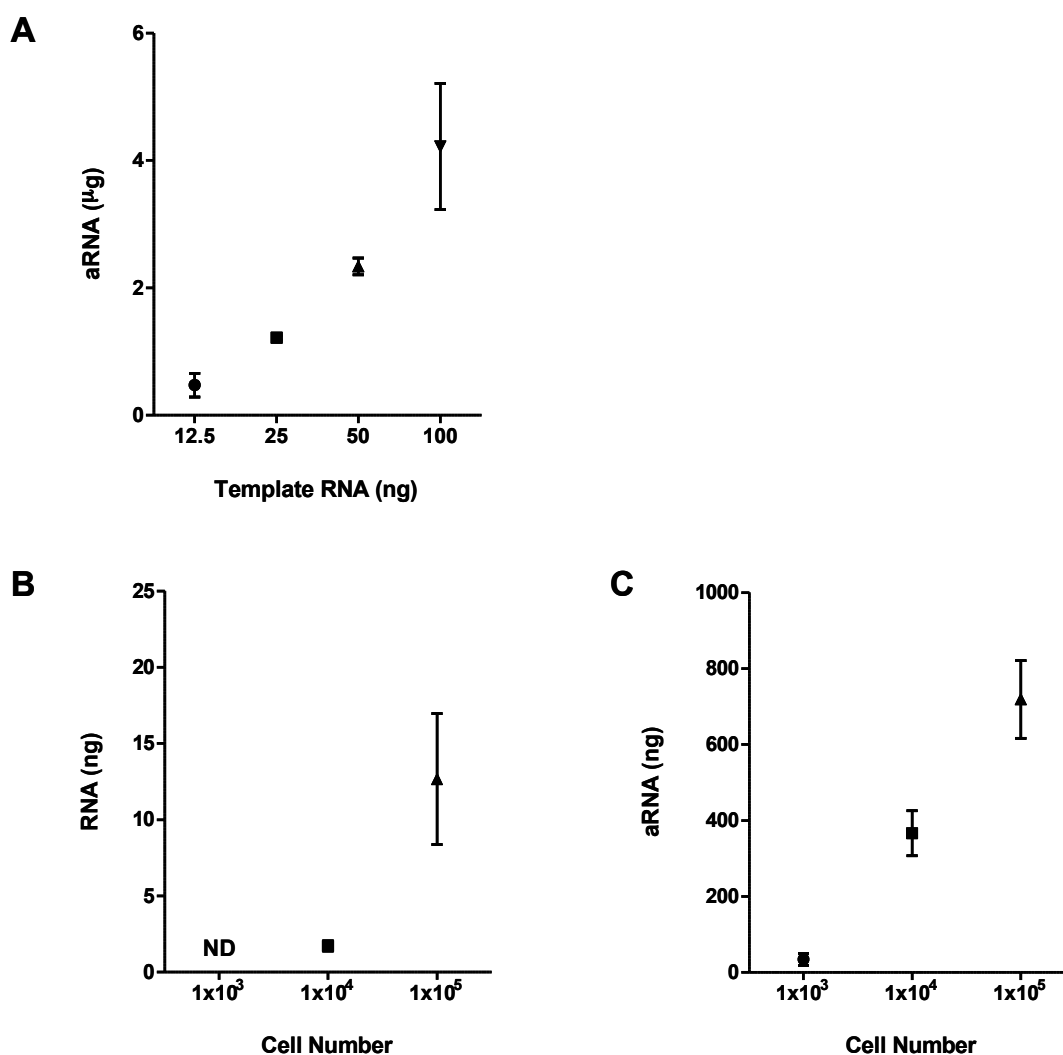


Figure 6.4 Yield of aRNA from different starting quantities

RNA was amplified from different starting quantities of template or from RNA extracted from different numbers of PBMCs. (A) Yield of aRNA generated from different starting quantities of template RNA. (B) The quantity of RNA extracted from 1×10^3 , 1×10^4 and 1×10^5 PBMCs prior to amplification. RNA extracted from 1×10^3 PBMCs was not detectable (ND). (C) Yield of aRNA generated from 1×10^3 , 1×10^4 and 1×10^5 PBMCs. aRNA yield was quantified using a nanodrop whereas unamplified template RNA was quantified using the 2100 Bioanalyzer. Data represent mean plus or minus SEM. $n = 3/\text{group}$.

6.3.3 Testing the limitations of the IVT kit using PBMCs

Having established that the SuperScript™ RNA amplification kit could successfully amplify RNA from almost one tenth of the minimum starting quantity defined by the manufacturers, the kit was then tested using RNA extracted from 1×10^3 , 1×10^4 and 1×10^5 PBMCs. Extracting RNA from 1×10^4 and 1×10^5 PBMCs yielded a mean of 1.7 ng and 21.7 ng of RNA respectively; as determined using an RNA Pico chip (Figure 6.4B). Again, RNA extracted from 1×10^3 cells was below the detection limit of the Bioanalyzer. The concentration

of the amplified product was measured using a nanodrop. Amplification of RNA extracted from 1×10^3 , 1×10^4 and 1×10^5 PBMCs generated a mean of 34 ng, 367 ng and 719 ng of aRNA respectively (Figure 6.4C). Therefore, although the template RNA derived from the cells was undetectable, it appears that sufficient RNA for TLDA analysis can be amplified from as few as 1×10^3 leukocytes.

6.3.4 Determining the transcriptional fidelity of aRNA

When using amplified RNA to study gene expression, it must accurately represent the RNA profile retrieved from the sample. If, for instance, the amplification process favours smaller transcripts, then the number of small transcripts, such as chemokines, may be disproportionately greater than that of larger transcripts, such as chemokine receptors. To determine whether there was any bias in the amplification process towards particular transcript lengths, aRNA was converted to cDNA using reverse transcriptase. Using cDNA from both amplified and unamplified RNA, QPCR was performed to amplify genes with a range of different transcript lengths. The C_T value, i.e. the number of PCR cycles required for the copy number of each transcript to reach an automatically set threshold, was used to compare the transcriptional ratios of three genes: *Ccl2* (732bp), *Gapdh* (1875bp) and *Tlr2* (3224bp). The C_T value of housekeeping gene TBP was used to normalise the results.

All gene transcripts amplified equally: the ratio between the C_T values remaining the same regardless of the starting quantity of RNA (Figure 6.5B) or the starting number of cells (Figure 6.5D). Only marginal discrepancies were observed when comparing aRNA to its template. *Tlr2* and *Gapdh* expression were increased slightly in comparison to TBP after amplification (Figure 6.5A&C). As these two transcripts are the longest of the target genes amplified, it can be assumed that the IVT kit does not favour the amplification of smaller transcripts. The order of expression of each transcript was unchanged after amplification indicating that amplified RNA exhibits an adequate representation of the gene profile expressed by a target cell population. Although amplification from 1×10^3 cells appeared to generate enough aRNA to perform TLDA gene expression analysis (Figure 6.4B), transcript levels of the target genes amplified by QPCR were weak to undetectable. For that reason the ratios between the target genes were not

included in Figure 6.5D. With the exception of RNA amplified from 1×10^3 cells, aRNA reasonably reflects the transcriptional profile of its template.

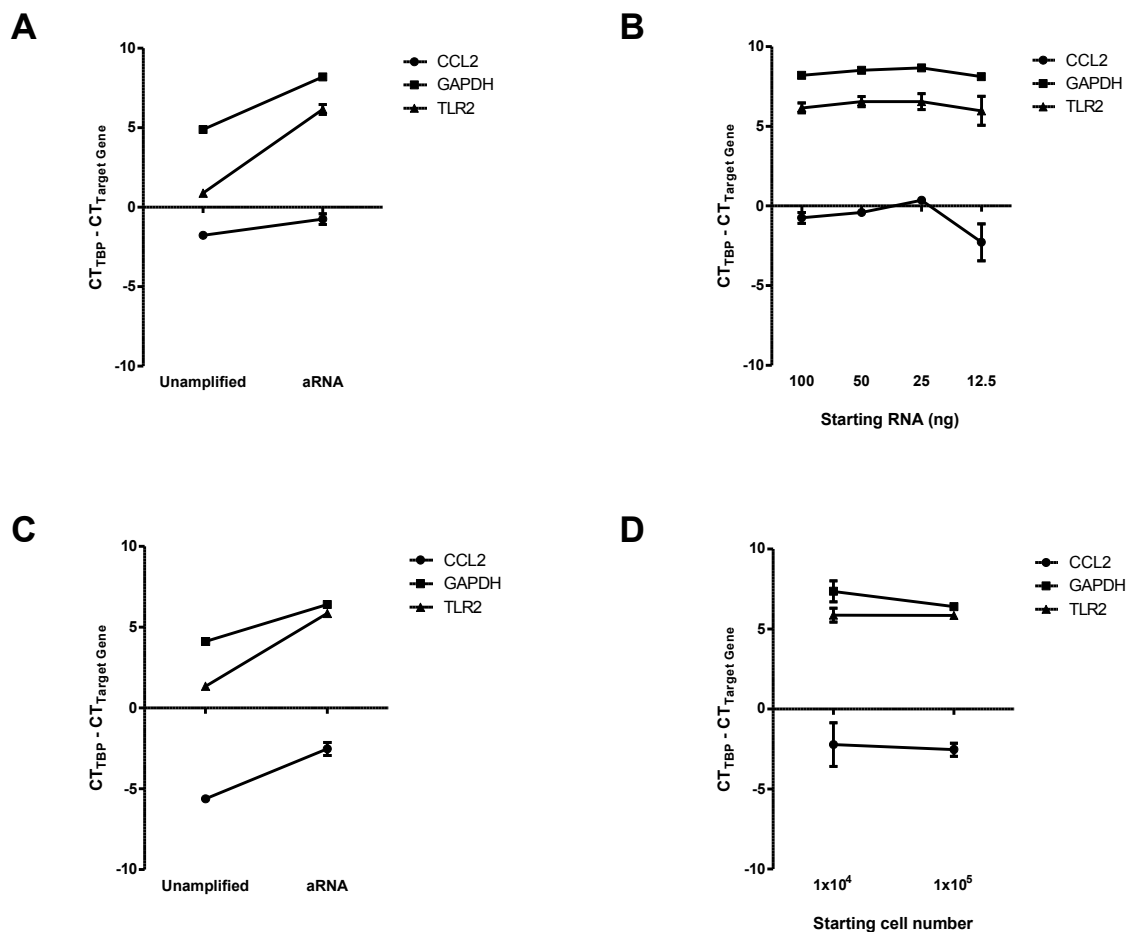


Figure 6.5 Comparison of the transcriptional profile of template RNA and aRNA

RNA was amplified from different starting quantities and from different numbers of PBMCs. QPCR was performed to determine the expression ratio of three genes of different transcript lengths: *Ccl2* (732bp) (●), *Gapdh* (1875bp) (■) and *Tlr2* (3224bp) (▲). The difference between the C_T value of the target genes and the C_T value of housekeeping gene, *Tbp*, was used as a method of comparison ($-\Delta C_T$). Comparisons were made between: (A) unamplified template RNA and the amplified product (aRNA) generated from 100 ng template, (B) aRNA amplified from 100 ng, 50 ng, 25 ng and 12.5 ng of template RNA, (C) aRNA from 1×10^5 PBMCs and unamplified RNA from the same PBMC sample, and (D) aRNA amplified from 1×10^4 and 1×10^5 PBMCs. Data represents mean plus or minus SEM. $n = 3$ samples/group.

6.3.5 Determining the integrity of aRNA generated from different starting quantities of template RNA

Having established that amplifying RNA, from as little as 12.5 ng starting RNA, produces enough aRNA output to be used for TLDA analysis; it had then to be determined whether the amplified product was of sufficient quality. RNA integrity was assessed, before and after amplification, using an Agilent 2100 Bioanalyzer. The quality of the total RNA that was used as template is shown in Figure 6.6A. Although two distinct peaks mark ribosomal subunits 18S and 28S, there is a considerable level of background noise indicating partially degraded RNA. In spite of this, as will be discussed below, mRNA was amplified successfully from different starting quantities of template RNA. Figure 6.6B shows an example of high quality aRNA. The electrophoretic trace exhibits a broad arch, indicative of a range of sizes of RNA fragments. As only mRNA is amplified by IVT, no ribosomal peaks are visible. The most commonly occurring fragment length in the sample was 1007 nucleotides long; as determined by comparing the speed at which these fragments moved through the microchannel (37.26 s) to the standard curve generated from the RNA ladder.

A representative electropherogram for each of the four groups of amplified RNA samples is shown in Figure 6.6. RNA amplified from 50 ng and 100 ng template RNA was of a sufficient concentration to be assessed using an RNA Nano chip. These were compared on the electropherograms to the RNA ladder (Figure 6.6). Considerably reduced in quantity than that of the high quality aRNA, the electrophoretic trace of these samples signifies a relatively lower quantity of aRNA; which is unsurprising given the low starting quantity. It is the lateral position of the peaks that signifies quality. Although the curves on the graphs are small, they are also broad, indicating a range of transcript lengths. This implies that the amplification was successful; generating aRNA of moderate quality. However, amplified RNA contained very few transcripts greater than 2000bp. Peaking between 200 and 500 nucleotides, the average fragment length in RNA, amplified from 100ng, is below half that of the high quality aRNA; implying partial degradation. Likewise, aRNA from 50ng of template peaks at approximately 500 nucleotides. However, as there is no sharp peak to the left of these graphs, a characteristic of high level degradation, the aRNA can be considered of satisfactory quality. Too low in concentration to be detected by

the Nano chip, RNA amplified from 12.5 ng and 25 ng of template RNA was assessed using the RNA Pico chip and evaluated over time. RNA amplified from 25 ng and 12.5 ng of starting template RNA, again generated a broad curve; similar in shape to that of the high quality aRNA (Figure 6.6C&D). However, the curves peaked at an earlier time point than the high quality aRNA (Figure 6.6B), again indicating a slight shift towards a smaller average transcript length. Whether assessed using the Nano chip or the Pico chip, aRNA samples contained noticeably less large transcripts than that of the high quality aRNA sample. This is a likely indication of partial RNA degradation. Imperfections in the quality of the amplified RNA may have arisen due to the poor quality of the starting RNA (Figure 6.6A). Taken together, these results show that RNA of a reasonable quality can be amplified from as little as 12.5 ng starting RNA, even when partially degraded RNA is used as template.

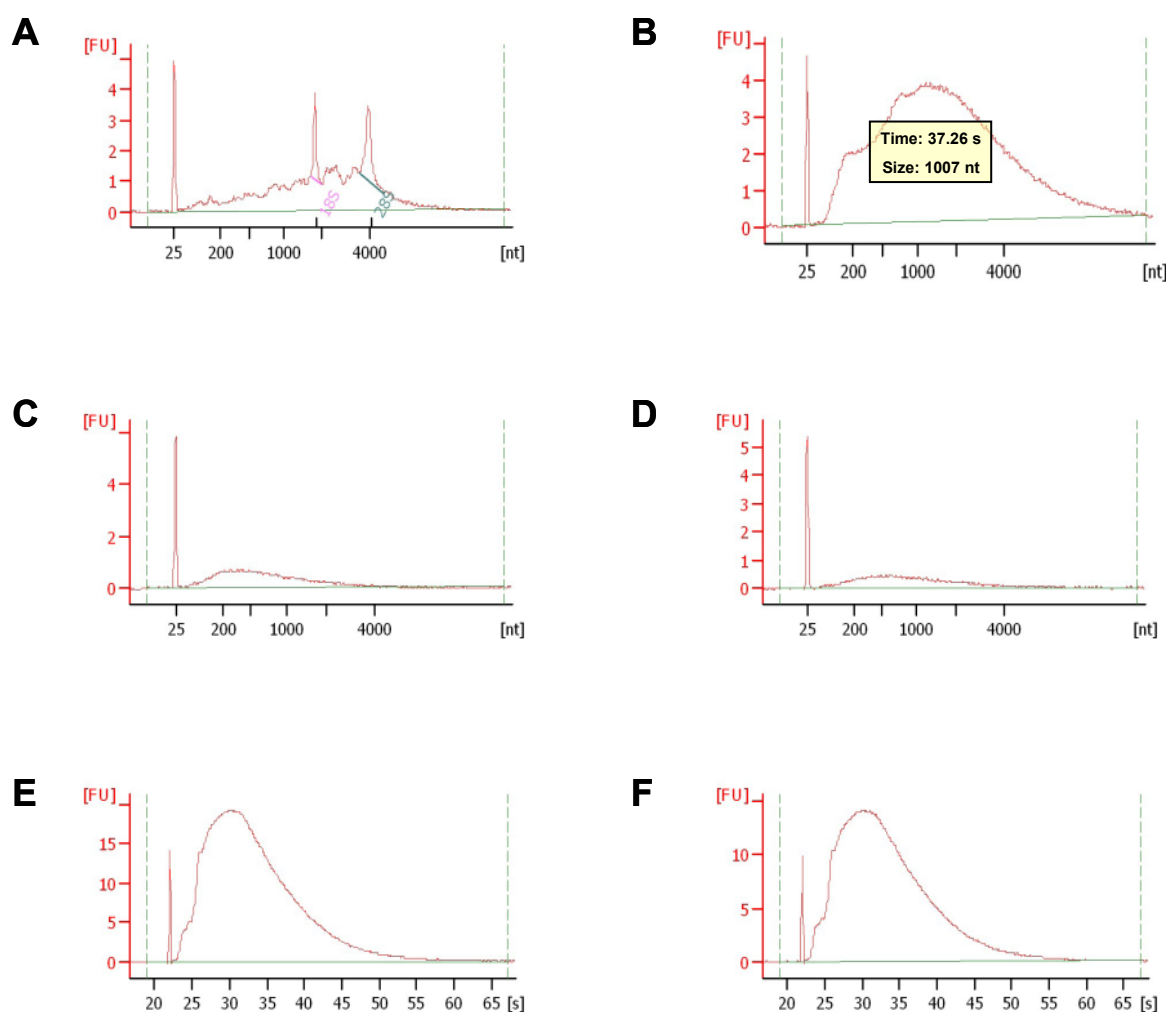


Figure 6.6 Integrity of RNA before and after amplification from different RNA starting quantities

Using a SuperScript™ RNA amplification kit, RNA was amplified from starting concentrations 100 ng, 50 ng, 25 ng and 12.5 ng of total RNA. The integrity of template RNA and the amplified message (aRNA) was determined using an Agilent 2100 Bioanalyzer. Electropherograms display: (A) Template RNA, (B) High quality aRNA, peaking at 37.26 seconds [s] and 1007 nucleotides [nt], and RNA amplified from (C) 12.5 ng, (D) 25 ng, (E) 50 ng and (F) 100 ng of template RNA. Data represent fluorescence intensity (fluorescence units [FU]) measured over time in seconds [s]. (A-D) have been compared over time to an RNA marker containing transcripts of known sizes [nt]. (C-F) Data shown are one representative sample from each group. $n = 3/\text{group}$.

6.3.6 Determining the integrity of aRNA generated from PBMCs

Amplifying RNA from 1×10^3 PBMCs had apparently yielded enough aRNA to perform TLDA analysis. To determine why the amplified product did not generate sufficient aRNA for QPCR, the integrity of amplified and unamplified RNA was assessed; again using the Bioanalyzer. Similar to previous results (Figure 6.2), RNA extracted from 1×10^3 leukocytes, was of too low a concentration to be detected using the RNA Pico chip (Figure 6.7A). RNA extracted from 1×10^4 and 1×10^5 PBMCs however, was of high quality (Figure 6.7B&C) suggesting that the extraction process itself was successful.

In contrast to aRNA quantification using the nanodrop, which showed that amplifying RNA from 10^3 PBMCs yielded an average of 34 ng (Figure 6.4), it is clear from Figure 6.7A that this amplified product is barely detectable by the RNA Pico chip. Only a minute peak is visible on the electropherogram. This discrepancy may have arisen because the RNA in these samples is present at too low a concentration to be accurately quantified by nanodrop. In addition, the little RNA that was detectable in the amplified sample was of poor quality. The location of the only peak on the graph, directly adjacent to the RNA marker, is a clear indication of sample degradation. As no RNA was detectable in the template, it was unclear whether the degradation had occurred prior to, or during the amplification process. RNA degradation, in addition to a low starting yield preceding IVT, would explain why amplification from 1×10^3 PBMCs did not generate sufficient RNA for QPCR.

Although clearly containing detectable levels, aRNA samples from 1×10^4 and 1×10^5 PBMCs also appeared to be degraded (Figure 6.7B&C). Electropherograms are dominated by a sharp spike at around 27 seconds; implying an enrichment of small fragments in the aRNA samples. As there is no indication of the IVT process favouring smaller transcripts (Figure 6.5), this is most probably degraded RNA. Thus, although it would appear from the nanodrop data that amplifying RNA generates a sufficient yield to use for multiplex gene arrays, this RNA is degraded.

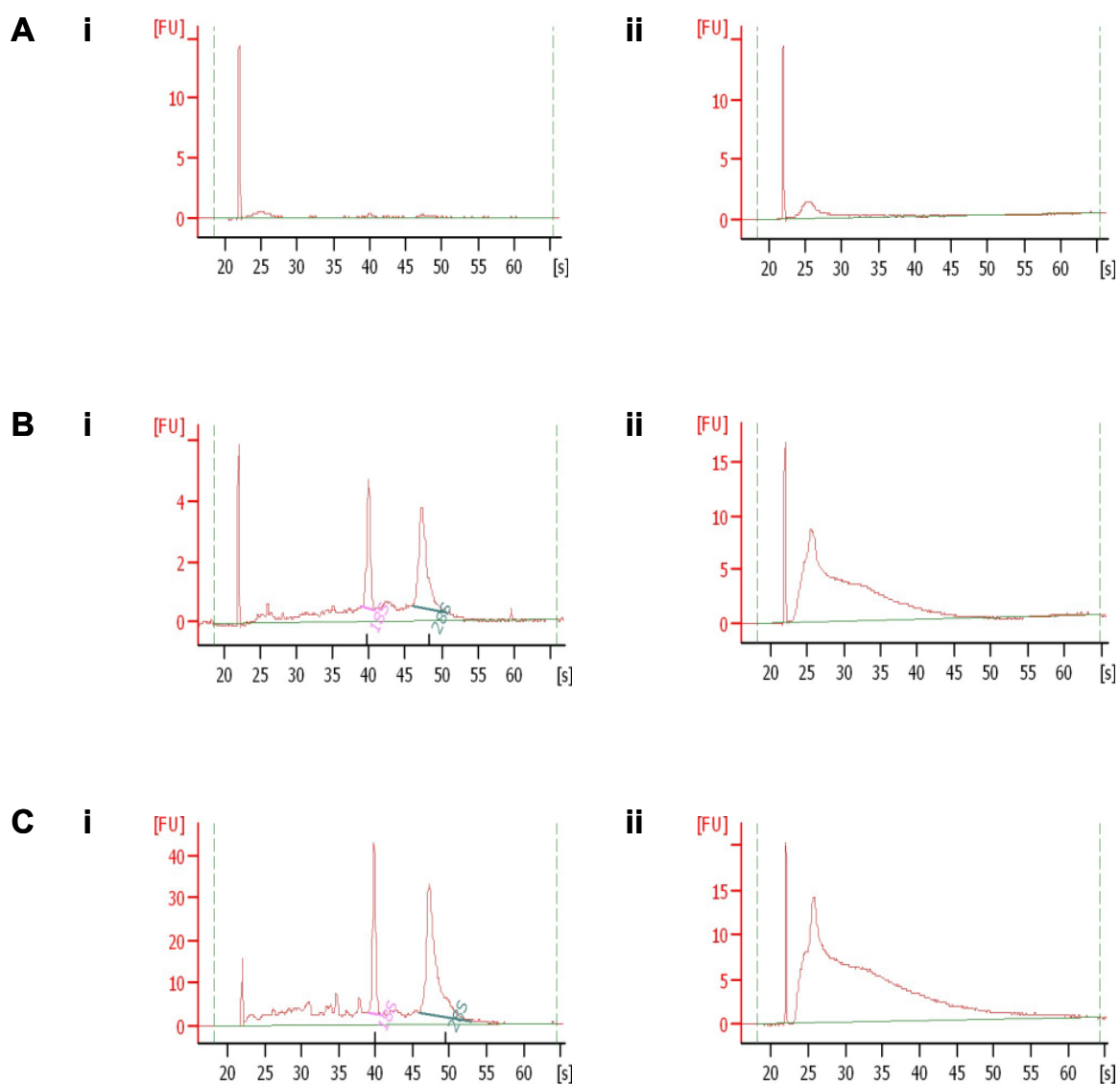


Figure 6.7 Integrity of RNA before and after amplification from different numbers of cells
 RNA was extracted from 1×10^3 , 1×10^4 and 1×10^5 PBMCs and amplified using a SuperScript™ RNA amplification kit. The integrity of RNA before and after amplification was determined using an Agilent 2100 Bioanalyzer. Electropherograms display: (A) RNA from 1×10^3 PBMCs (i) before and (ii) after amplification. (B) RNA from 1×10^4 PBMCs (i) before and (ii) after amplification. (C) RNA from 1×10^5 PBMCs (i) before and (ii) after amplification. Data represent fluorescence intensity (fluorescence units [FU]) measured over time in seconds [s]. Data shown are one representative sample from each group. $n = 3/\text{group}$.

6.4 Discussion and conclusions

The initial aim of this study was to develop the most effective protocol for extracting RNA from low numbers of cells, amplifying it using IVT and converting the amplified product to cDNA. Entirely dependent on the development of this protocol, the second aim was to systematically define the chemokine systems involved in governing leukocyte infiltration of the CNS during MS.

Preliminary experiments were set up to compare the efficiency of different methods of RNA extraction and different RT kits. Using relative *Gapdh* transcript level as a method of comparison, these experiments highlighted the optimum methods of extracting RNA from low cell numbers and of synthesizing cDNA from low amounts of template RNA. In addition, it was demonstrated that RNA could be extracted from as little as 1×10^3 leukocytes; the average number expected in control CSF samples. Although the yield of RNA was sufficient to generate a *Gapdh* signal using PCR, it was below the detection limit of the RNA Pico chip and thus unable to be quantified. As a result, it could not be determined whether RNA extraction from 1×10^3 leukocytes generated a great enough yield of template RNA for amplification by IVT.

To validate the efficiency of the SuperScript™ RNA Amplification System in the proposed study, experiments were set up to test the limitations of the kit. Prior to sample collection, the capacity of the kit to amplify RNA from 1×10^3 leukocytes had to be demonstrated. RNA was amplified from different starting quantities of template RNA and from different starting quantities of leukocytes. Encouragingly, the results demonstrate that an adequate amount of aRNA can be generated from as little as 12.5 ng of template RNA. Not only was the quantity sufficient, but the transcriptional profile of the amplified product, assessed using QPCR, was shown to reasonably reflect that of the unamplified template RNA from which it was derived. However, a paucity of long transcripts in the amplified product suggests that the RNA may have been partially degraded during amplification. Another possibility is that the RNA polymerase failed to extend the full length of the longer transcripts during amplification. This could prove problematic if any of the probe sets used on the TLDA plates are located at the 5' end of a long transcript. As there was no problem amplifying *Gapdh*, a housekeeping gene of comparable transcript length to a chemokine receptor,

using primers located in the 5' region, there is no reason to suggest that transcripts of this length might be inaccurately represented. The most likely explanation for the lack of long transcripts is the use of partially degraded starting RNA. Thus, in this instance it appears that RNA amplification starting from only 12.5ng total RNA generates a great enough yield of reasonable quality RNA for TLDA gene expression assays.

Although amplifying from different starting quantities of RNA generated aRNA of an adequate quality and quantity, RNA amplification from 1×10^3 leukocytes was not a success. Only a minute level of aRNA generated from 1×10^3 leukocytes was detectable using the Bioanalyzer. This RNA appeared to be degraded and no *Gapdh*, *Tlr2* or *Ccl2* signal was detectable following QPCR. In Section 6.2.1, it was shown that, without any requirement of IVT, QPCR could be successfully used to amplify *Gapdh* when RNA from 10^3 PBMCs was converted to cDNA. As a result, it would appear as if the amplification process deteriorates the quality of the RNA; rendering it useless when amplifying from such a low cell number. From these data, it is apparent that RNA extracted from 1×10^3 leukocytes, is below the threshold of what is required for amplification.

A previous report by Baugh *et al.* demonstrated that RNA could be successfully amplified from as little as 2 ng of total RNA⁴⁶³. These aRNA products, however, did not perform as well in downstream applications as aRNA generated from over 10ng of template. Similarly, it has been demonstrated above that RNA can successfully be amplified from as little as 1.7ng of template RNA; extracted from 1×10^4 PBMCs. Not only was the amplification successful, but it yielded sufficient levels of aRNA for subsequent gene expression analysis. In addition, the transcription profile of the aRNA product was comparable to the template RNA from which it was derived. However, much of the amplified product appeared to be degraded and the use of partially degraded RNA for multiplex gene expression analysis is ill-advised. Consequently, either new technology or further optimisation of the IVT protocol would be required in order to accurately determine aberrant chemokine receptor expression in CSF-derived pathogenic leukocytes.

As they have a profoundly higher leukocyte presence in their CSF, an alternative approach might be to derive as much information as possible using only MS

patient samples. The chemokine receptor profile of leukocytes from diseased CSF could simply be compared with that of peripheral blood leukocytes from matched patient samples. Although this would not precisely define the particular chemokine receptors that are involved in MS pathogenesis, it would highlight any receptors that are enriched in the CSF compared to the peripheral blood. As it would include the chemokine receptors that are associated with pathogenesis, this transcriptional comparison would be beneficial as it would provide a list of target receptors to which subsequent gene expression analyses could be tailored. However, it was decided that the degree of difficulty involved in acquiring the MS patient samples, combined with the expenditure of the proposed experiments, outweighed the potential benefits of obtaining this information. Thus this work was discontinued.

A superior method of determining chemokine receptor expression in CSF-derived leukocytes might be to use Fluidigm® BioMark™ dynamic array chips. This cutting edge technology uses a series of integrated microchannels to link up 48 samples with 48 TaqMan® assays. This would allow the relative quantification of the expression of 48 genes from each sample. Results are reproducible from <100 cells. In addition, the chips negate the need to both extract RNA and amplify it using an IVT kit: both processes that could result in RNA degradation. Consequently, the relative expression of chemokine receptors by CSF- and peripheral blood-derived leukocytes could be examined comparatively using BioMark™ dynamic array chips. Unfortunately, this technology was not available at the time of this study.

The initial aim of this work was to optimise and validate the protocols required to extract and amplify RNA: ultimately generating sufficient levels of high-quality cDNA for TLDA plates. Despite the limitations described by the manufacturers of the amplification kit, there have been some preliminary successes in amplifying RNA from low starting quantities. However, the amplified product often shows signs of degradation, particularly when RNA was amplified from low starting numbers of cells. This rendered the aRNA unfit for downstream TLDA assays and thus rendered the RNA amplification kit unsuitable for the proposed study. As a suitable protocol for amplifying RNA from 1×10^3 leukocytes was not established, the complete chemokine receptor profile of CSF- and peripheral blood-derived leukocytes could not be determined. Therefore, the

specific chemokine systems involved in governing leukocyte entry to the CSF remain to be defined.

7 General Discussion

7.1 Introduction

There is now a growing body of evidence to suggest that inflammatory mediators can modulate mood and behaviour. Furthermore, prolonged exposure to these mediators may be involved in the manifestation of neuropsychiatric symptoms, such as depression, anxiety and fatigue. Despite the recent advances in our understanding of neuroimmune communication pathways, the molecular mechanisms behind these co-morbidities remain unclear. *Thus the primary aim of this thesis was to establish a better understanding of the bidirectional relationship, and communication pathways, that exist between the immune system and the brain.*

In Chapter 3, the transmission of inflammatory signals from the periphery to the brain was initially investigated using a model of systemic LPS-induced inflammation, which is well known for its impact on behaviour. 48 hours after intraperitoneal injection, the transcriptional profile in the brains of LPS challenged mice was comprehensively interrogated using whole transcriptome microarrays. Expression of a number of genes was induced in the brain 48 hours following systemic LPS-challenge. A novel comparative approach was then taken to explore a potential molecular mechanism behind this induction. Specifically, in Chapter 4 of this thesis, the transcriptional modulation of the genes of interest was compared in the brain following different sterile, and TLR-dependent, models of peripheral inflammation. To establish whether target genes were induced in the brain in response to elevated circulating inflammatory cytokines, gene induction was assessed following systemic TNF α -induced inflammation. Supplementing the data derived from this study, a model of endotoxin tolerance was used to assess the ability of systemic LPS to modulate target gene expression in the brain, without the synergistic effects of circulating IL-1 β , IL-6 or TNF α . Finally, a model of LTA-induced peripheral inflammation was used to determine whether activation of the MyD88-dependent signalling pathway was sufficient to modulate target gene expression in the brain. Therefore, by characterising, and comparing, the gene expression profiles in the brains of mice following a number of well-characterised models of peripheral inflammation, I have started to investigate the molecular mechanisms by which inflammation originating in the periphery can induce neurological transcriptional modulation.

Chemokine induction, and leukocyte recruitment, to the brain was also assessed following systemic LPS challenge. As it may better reflect physiological conditions, such as bacterial infection or septicaemia, these studies were exclusively performed using a model of endotoxin tolerance, in which mice were systemically injected with LPS daily. In Chapter 5 of this thesis, I have systematically characterised, for the first time, the transcriptional inflammatory chemokine profile in the brain following prolonged exposure to LPS in the periphery. In addition, the work in this chapter demonstrates that, in this model of endotoxin tolerance, systemic LPS challenge may remotely modulate the recruitment of leukocytes to the brain.

7.2 Characterisation of the transcriptional profile in the brains of systemic LPS-challenged mice

Current literature suggests that systemic LPS itself, and LPS-induced inflammatory cytokines, can activate the cerebral vasculature and TLR4-expressing phagocytic cells resident in CVOs (Section 1.4.2.2). Beginning in the CVOs and regions surrounding the blood vessels, the choroid plexus and meninges, this triggers a wave of microglial activation that can spread throughout the parenchyma via the autocrine and paracrine effects of TNF α and IL-1 β ^{315,317,318}. Not only might these cytokines activate IDO in the brain, which can modulate behaviour (Section 1.4.2.2), but IL-1 β and inflammation-induced secondary messengers, such as PGE₂, can stimulate the control circuitry of the HPA axis to activate the neuroendocrine system and induce a febrile response (Section 1.4.3.1). These central responses to systemic LPS-induced inflammation have been well characterised. Activation of the HPA axis is rapid and transient, peaking within 1-3 hours of systemic LPS injection⁴⁶⁴⁻⁴⁶⁶. Microglial activation, characterised by a robust increase in *Cd14*, *Tlr2* and *Il1b* mRNA, is similarly rapid^{315,317,318} and evidence of activation in CVOs has been shown as early as 30 minutes following I.P. injection^{315,318}. Microglial activation in the parenchyma then peaks within 8-12 hours of injection and clusters of cells remain activated until 24 hours. In contrast, IDO activity in the brain occurs much later, with no significant differences in activity detected until 24 hours following systemic LPS challenge⁴⁶⁷. This delay may be due to the time it takes for cytokines to be transcribed and translated in the brain. To my knowledge there is currently no literature to suggest that any of these characterised central responses last

longer than 24 hours following injection. However it was demonstrated in Chapter 3 of this thesis, that 48 hours following an acute systemic LPS challenge, a number of immune/inflammatory genes were upregulated in the brain. The differential transcriptional profile in the brains of LPS-challenged mice was markedly enriched with ISGs. This induction appeared to be triggered rapidly following systemic LPS administration as a number of ISGs were upregulated in the brain by 6 hours post-injection. However, aside from the characterised effects described above, there is a paucity of literature describing the impact that systemic LPS-induced inflammation has on the brain. This makes it difficult to hypothesise what pathways may have been involved in triggering the induction of ISGs, and other target genes, in the brain following an acute systemic LPS challenge.

Interestingly, it was demonstrated in Chapter 4 that the majority of microarray target genes were not upregulated in the brain following systemic TNF α -induced inflammation. Furthermore a selection of target genes, predominantly ISGs, remained induced in the brain during endotoxin tolerance, in the absence of a detectable inflammatory cytokine response in the periphery. This suggests that, rather than being a downstream effect of heightened peripheral inflammation, target gene induction in the brain following LPS injection may be a direct consequence of LPS-triggered TLR4 signalling either in the periphery, in one of the brain's barriers, or in the brain itself. Importantly, there are few natural scenarios that would result in an acute systemic exposure to endotoxin. Therefore, prolonged ISG expression in the brain following repeated LPS challenge may more accurately reflect what occurs during chronic bacterial infection, or sepsis, than a single dose of LPS.

Despite the hypothesis that LPS-induced ISG modulation was a TLR-specific phenomenon, these effects of LPS on the brain were not reproduced by systemic administration of the TLR2 ligand, LTA. TLR2 has a signalling profile that is distinct from that of TLR4 in that it does not activate IRF3-mediated type I IFN induction. Therefore, my results from the LPS experiments could reflect a TLR4-induced type I IFN response via the non-canonical signalling pathway. This could be further investigated by repeating both the acute LPS model, and the endotoxin tolerance model, in TRIF-deficient mice or using small molecule inhibitors such as Resveratrol, which specifically targets the TRIF-dependent

signalling pathway⁴⁶⁸. As described in Chapter 4, the most characterised routes of immune-to-brain communication following systemic LPS challenge involves MyD88-dependent signalling pathway activation, or the intermediary actions of inflammatory cytokines. Therefore, if ISG induction is triggered in the brain in response to a TLR4-mediated IFN response, the data described in this thesis may help to broaden perceptions of how inflammatory signals are received by the brain.

Although a TLR-dependent IFN response has been suggested to play a role, it has yet to be established how inflammatory signals are transmitted from the periphery to the brain in these models to induce ISG expression. This is particularly unclear following repeated LPS injections, when the synergistic effects of circulating IL-1 β , IL-6 or TNF α were lost as a result of endotoxin tolerance. Several possible scenarios to account for the observed ISG induction in the brain have been described below:

(1) In addition to being expressed in the periphery, the IFNAR is widely expressed in the brain (Figure 7.1). It is possible that circulating type I IFNs themselves may have directly accessed the brain to stimulate one of the many IFNAR-expressing cell types. As described in Chapter 3, this mechanism of action has previously been proposed to account for ISG induction in the brains of mice following an I.P. injection of IFN α ⁴²³. However, it was demonstrated in Chapter 4 that ISGs remained induced in the brain during endotoxin tolerance, which has been shown to inhibit both the classical MyD88-dependent, and the non-canonical TRIF-dependent, signalling pathways downstream of TLR4⁴⁶⁹. As a consequence, endotoxin tolerance results in impaired type I IFN production. Therefore, in these studies, leukocytes in the periphery were unlikely to have been the source of the putative type I IFNs that stimulated the brain following daily LPS injections.



Figure 7.1 *Ifnar1* expression in the mouse brain.

A high-resolution map of *Ifnar1* expression in a coronal section of the mouse brain. Expression levels were established using *in situ* hybridisation. Image was downloaded from the Allen Brain Atlas (<http://www.brain-map.org/>).

(2) In the models described in this thesis, LPS may itself gain access to the brain. Although Banks *et al.* could not detect radio-labelled LPS crossing the BBB of mice⁴²¹, there are reports that LPS can increase BBB permeability³¹⁰. The capacity of LPS to alter BBB integrity may depend on the dose and strain of LPS administered and the species and strain of mouse used experimentally. Therefore, in the acute model of LPS-mediated systemic inflammation that I used in these studies, 100 µg of LPS may have been sufficient to disrupt the integrity of the BBB and allow LPS to enter the brain. Due to the potency of LPS, only a minute amount would have been required to cross the BBB to elicit a detectable response. Breakdown of the BBB is even more likely to have occurred during the endotoxin tolerance model, when mice were treated with a high dose of LPS daily. To explore this possibility, BBB permeability could be assessed after LPS treatment by injecting mice intravenously with visible tracers and screening for their presence in the brain. This is commonly done using fluorescently-labelled dextran amines⁴⁷⁰, although a more relevant method would be to inject mice systemically with fluorescently-labelled LPS and then use confocal imaging to establish whether it crossed the BBB. Breaching of the BBB by LPS is certainly

worth investigating as a potential mechanism that could account for the prolonged ISG induction following repeated LPS challenge. However, to my knowledge the occurrence of endotoxin tolerance in the brain has not been defined. Therefore, rather than type I IFN production and ISG regulation, chronic exposure to LPS in the brain might result in endotoxin tolerance.

(3) Phagocytic cells resident in the CVOs, and/or cerebral vascular endothelial cells, may have responded to circulating LPS by producing type I IFNs. This could either have led to the autocrine induction of ISGs, or the induction of ISG expression in adjacent cell populations in a paracrine manner. Due to their similarity to peripheral myeloid cells, it might be expected that macrophages and microglia in the CVOs would become tolerised in response to repeated LPS challenge. However, endotoxin tolerance in cerebral vasculature endothelial cells has not been described. Therefore, even if CVO-resident phagocytes do become tolerised, it remains possible that cerebral endothelial cells may have continued to produce IFN β during this model.

Thus, a number of possible mechanisms exist that could account for the induction of ISGs in response to systemic LPS, none of which are mutually exclusive. Further investigation is required in order to pinpoint the precise mode of action behind systemic LPS-induced ISG modulation in the brain.

Although I did not investigate what impact an LPS-induced IFN response might have on brain function and behaviour, there is considerable evidence that therapeutic use of type I IFNs in humans can lead to significant neuropsychiatric disorders, especially major depression⁴⁷¹⁻⁴⁷³. It has been shown that injecting rodents with LPS initiates a number of behavioural adaptations, including depression-like behaviours that persevere after other sickness behaviours have resolved²⁶⁶. My results suggest that the induction of type I ISGs in the brain in response to systemic LPS was likely to be mediated by the action of type I IFNs. This indicates that type I IFN production, either in the brain or the periphery, may represent a crucial mechanism linking systemic LPS-induced inflammation with behavioural changes.

7.3 Characterising the chemokine profile and leukocyte infiltrate in the brains of LPS-treated mice

Of the ISGs that were upregulated in the brain in response to acute LPS exposure, CXCL10 showed the biggest induction. Moreover, in this LPS model there was a significant enrichment of transcripts involved in leukocyte extravasation. This prompted me to investigate directly whether systemic LPS challenge resulted in leukocyte recruitment to the brain. To better represent physiological conditions, and to maximise the chance of detecting infiltrating leukocytes, this was investigated over a 7 day window following daily injections of LPS.

First, the inflammatory chemokine repertoire in the brains of LPS treated mice was systematically characterised. In addition to *Cxcl10*, the chemokine transcripts that were upregulated in the brains of LPS-challenged mice included a number of neutrophil, monocyte and T cell chemoattractants, including *Cxcl1*, *Cxcl2*, *Ccl3*, *Ccl5*, *Cxcl9* and *Cxcl10*. As IFNs are known to increase the expression of CXCL9 and CXCL10 in a number of cell types and tissues⁴⁷⁴⁻⁴⁷⁸, there is a strong likelihood that these chemokines were upregulated in the brain downstream of the systemic LPS-induced IFN response discussed above. The remainder of the upregulated chemokine transcripts could have been upregulated in the brain in response to TNF α or IL-1 β , or were possibly induced directly in response to TLR4 signalling pathway activation⁴⁷⁹⁻⁴⁸⁴.

On day 2 of the LPS model, the induction of *Cxcl1* and *Cxcl2* was associated with an early infiltration of neutrophils to the brain and a simultaneous increase in *Cxcr2* mRNA. Neutrophils are pivotal in mounting a successful response against a number of pathogens, but they are also associated with tissue damage⁴⁸⁵ and thus their recruitment to the uninfected brain is likely to be harmful. There are many ways in which neutrophils could be damaging to the CNS. Following an acute injection of LPS, neutrophil recruitment has been shown to amplify central inflammatory processes leading to elevated IL-1 β , TNF α and ICAM1 mRNA levels in the brain and increased transcription of the genes encoding CXCL1 and CXCL2²³⁶. This may account for the prolonged expression of IL-1 β and TNF α that I observed in the brain following daily LPS injections. Neutrophils are also known to release toxic agents, such as MPO-derived oxidants, which can have a

debilitating effect on BBB integrity⁴⁸⁶. Therefore, their accumulation in the brain may facilitate the entry of circulating LPS, cytokines and/or other leukocytes into the brain. Blocking neutrophil entry to the brain using a CXCR2 antagonist and performing a BBB permeability assay, would be required in order to confirm this. The model that I used to assess neutrophil entry to the brain in this thesis differed from those used previously, as mice received daily systemic LPS injections. As a result, the neutrophils that were recruited to the brain in this model may have been tolerised to LPS in the periphery. However, neutrophils may not be as susceptible to endotoxin tolerance as monocytes and macrophages⁴⁸⁷ and it is not known whether they are likely to retain their tolerant phenotype after being exposed to the inflamed CNS. Therefore, it is unclear to what extent they would contribute to local inflammatory responses in the brain following multiple systemic LPS challenges.

Neutrophil accumulation in the brain was followed by the recruitment of CD8⁺ and CD8⁻ T cells. This may have occurred in response to the enhanced production of T cell chemoattractants, such as CCL5, CXCL9 and CXCL10, in the brain. The current literature suggests that only activated T cells can enter the brain. As T cells do not recognise LPS, those infiltrating the brain were likely to be memory cells of various specificities. Although LPS is not presented to T cells, chronic inflammatory conditions can result in epitope spreading which could lead to T cell activation in the brain⁴⁸⁸. When stimulated, memory T cells have the potential to secrete large amounts of cytokines, such as IFN γ ⁴⁸⁹, which could amplify inflammatory responses in the brain and activate IDO, thus resulting in depressive behaviours. However, the influx of T cells to the brain could also be protective. Chronic exposure to LPS in the periphery may mimic a systemic bacterial infection, thus resulting in enhanced T cell immunosurveillance. Although not described previously following LPS challenge, increased surveillance of the brain by both CD4⁺ and CD8⁺ T cells has been reported following systemic *Listeria monocytogenes* infection^{490,491}. However, in these reports, the T cells were predominantly situated in the leptomeninges, the choroid plexus and in the CSF with few, or none, invading the parenchyma. It has been hypothesised that, following systemic *L. monocytogenes* infection, T cell recruitment to the brain is protective against cerebral listeriosis⁴⁹¹. T cell accumulation in the brain following systemic LPS challenge is a novel observation

and it is therefore unclear whether this response contributes to pathogenesis or whether T cells are recruited in order to protect the brain from a potential infection.

From the data presented in this thesis, it appeared as if monocytes might have infiltrated the brains of LPS-challenged mice and differentiated into macrophages or microglia. Further studies would be required in order to confirm this. T cell entry to the brain is known to contribute to monocyte recruitment during viral infections of the CNS^{190,442}. Furthermore, monocytes are known to infiltrate the brain during systemic *L. monocytogenes* infection⁴⁹² and during a model of hepatic inflammation²⁴¹. By increasing the production of inflammatory cytokines and the brain²⁴¹ and causing bystander tissue damage⁴⁹³, the recruitment of inflammatory monocytes to the brain has the potential to be detrimental. As described in Section 1.3.1.1, MHV infection is associated with monocyte-mediated inflammation and demyelination. Monocyte-mediated damage can also influence behaviour. Following picornavirus infection, monocyte recruitment to the hippocampus resulted in neuronal loss and impaired cognitive function⁴⁹³. However, in some settings, the recruitment of monocytes to the brain can be beneficial. Following bacterial meningitis, or during transgenic models of Alzheimer's disease, peripheral monocytes accumulate in the brain and differentiate into microglia⁴⁹⁴⁻⁴⁹⁶. This has been shown to play an important role in the resolution of tissue damage, and in the clearance of amyloid deposits, respectively. Thus, whilst it is unclear what role they might play in protection or pathology, monocyte recruitment to the brain following daily systemic LPS challenges is worth further investigation.

Although these studies have generated some interesting and novel observations, the physiological and pathological implications of leukocytes accumulation in the brains of LPS-treated mice have yet to be established. It is possible that leukocyte recruitment to the brain is a characteristic response to chronic bacterial infection and serves to provide protection against cerebral infection. However, by amplifying central inflammatory responses, these responses could also cause damage to the brain and perhaps have downstream effects on behaviour.

7.3.1 Potential brain-specific effects of chemokine induction in the inflamed brain

As well as recruiting inflammatory cells from the bloodstream into the brain, the central upregulation of chemokines could have a direct impact on the brain itself. As has been described in Section 1.3.2.1, chemokines have been postulated to play a neuromodulatory role in the CNS and indeed, all of the chemokine receptors that were upregulated in the brain in response to LPS treatment are also expressed by neurons and/or glia. Whilst very little is known about the role of these receptors or their respective ligands in the brain, a variety of theories have been postulated. As will be discussed below, there are reports that chemokines can act as neuronal survival factors and neuromodulators. Furthermore, they may act on glial cells to modulate the extracellular inflammatory milieu. As a result, the upregulation of chemokines and their cognate receptors in the brain may modulate brain function and so impact on behaviour.

Interestingly, a number of the chemokines that were induced in the brain in response to multiple systemic LPS challenges can directly stimulate a Ca^{2+} influx in cultured neurons via pertussis toxin-sensitive GPCRs⁴⁹⁷⁻⁵⁰². It has been suggested that this may allow chemokines to act pre-synaptically to modulate the post-synaptic release of neurotransmitters⁵⁰³. However, the evidence for this is sparse and at times contradictory (Section 1.3.2.1). There are reports to suggest that CCL5 may have the capacity to modulate glutamatergic transmission in cultured neurons^{455,504}. Musante *et al.* demonstrated that CCL5 treatment triggered the spontaneous release, but inhibited the potassium-evoked release, of glutamate from neurons in the human neocortex⁴⁵⁵. In contrast to these findings, Prisco *et al.* described a dose-dependent increase in potassium-evoked glutamate release when cultured spinal cord neurons were treated with CCL5, whilst basal release was unaffected⁵⁰⁴. This discrepancy may be due to the different populations of cultured neurons being used in the two studies and thus require further investigation.

Although CXCR2 expression has also been reported on neurons in the CNS of both humans and rodents^{497,498,505}, there has been little published regarding its role in neuromodulation. However one report suggests that CXCL1-induced Ca^{2+}

mobilisation resulted in increased neurotransmitter release from cerebellar Purkinje neurons⁴⁹⁸. Exposing cultured hippocampal neurons to CXCL10 has been shown to induce intracellular Ca^{2+} mobilisation and so increase both spontaneous, and evoked, synaptic transmission⁵⁰⁶. In addition, electrophysiological recordings taken from hippocampal slices have shown that acute exposure to exogenous CXCL10 alters synaptic plasticity in wild-type mice by inhibiting long term potentiation⁵⁰⁷. However, in transgenic mice which chronically produced CXCL10 under the astrocytic GFAP promotor, there was no effect on synaptic plasticity⁵⁰⁷. This study highlights the confounding data that can be derived from acutely exposing neurons to high concentrations of inflammatory chemokines and underlies the caution needed in making conclusions about the potential impact that LPS-mediated chemokine production may have on synaptic plasticity and behavioural responses.

It has been discussed at various points in this thesis that injecting mice systemically with LPS results in the central production of numerous inflammatory mediators. This can have a multitude of detrimental effects on the brain and may create an environment that is toxic to neurons. There have been reports that CXCL1 can inhibit the induced apoptosis of cultured cerebellar granule cells by promoting the phosphorylation of extracellular signal-regulated kinase (ERK)^{505,508}. Although no mechanism has been proposed, there are several studies demonstrating that CCL5 can also act as a survival factor in cultured neurons^{499,502,509}. However, in contrast to these reports, CXCL10 has been reported to contribute to the apoptosis of primary neurons via caspase 9 activation⁴⁵⁶. Consequently, following LPS treatment, the induction of chemokines in the brain may either positively, or negatively, influence neuronal survival.

Injecting LPS directly into the CNS results in oligodendrocyte death and the subsequent formation of demyelinating lesions^{510,511}. Therefore, in the event that LPS does have the capacity to breach the BBB following multiple systemic challenges, it could cause demyelination. CXCR2 ligands are thought to play a protective role in demyelinating CNS disorders, either by blocking oligodendrocyte apoptosis or by attracting oligodendrocyte precursor cells to damages sites in the brain to promote tissue repair^{446,512}. As a result, the

induction of CXCL1 and CXCL2 may serve to protect the brain from direct LPS-induced toxicity.

In addition to potentially modulating neuronal transmission and survival, chemokines are known to act as communication molecules between glial cells and therefore may influence how these cells respond to systemic LPS challenge. Indeed, it has been reported that treating microglia with CCL5 *in vitro* results in a CCR5-dependent dampening of LPS-induced inflammatory cytokine and iNOS production⁵¹³. This suggests that CCR5 signalling may protect the brain from microglial neurotoxicity. Conversely, stimulating cultured astrocytes with CCL5 leads to an increase in the induction of inflammatory cytokine and chemokine transcripts, including *Ccl3*, *Ccl5*, *Cxcl1* and *Cxcl2*⁵¹⁴. Although this effect was dependent on pertussis toxin-sensitive GPCRs, it was not attenuated by individually knocking out CCL1, CCL3 or CCL5, indicating redundancy of CCR usage in this setting. Little has been described regarding the role of CXCL1 or CXCL2 in glial cell communication and activation. However, it has been suggested that both chemokines can trigger the induction of inflammatory cytokines and chemokines, including CCL5 and CXCL10 from primary murine astrocytes⁵¹⁵. Thus, signalling through glial chemokine receptors may modulate the extracellular cytokine and chemokine milieu of the brain during inflammation.

These studies highlight a number of brain-specific responses that may arise following chemokine induction in the brain. The chemokines that are most upregulated in the brain in response to repeated LPS challenges potentially share the capacity to modulate neuronal transmission and survival. By mediating communication between, and activation of, glial cells in the brain, they may also modulate the extracellular inflammatory environment. There is therefore a number of ways in which the chemokines induced in this model might impact on behaviour. CCL5 has been shown to modulate glutamate release from nerve endings. As described in Chapter 1, aberrant glutamate production has been linked to the pathophysiology of depression. In support of a role for CCL5 in modulating behaviour, there are some preliminary data, from Kalkonde *et al.*, to suggest that CCR5 ligands may impair social recognition in mice⁵¹⁶. In addition, a report by Lee *et al.* demonstrated that long-term and spatial memory was impaired in CCR5-deficient mice⁴⁵⁴. However, this was not consistent with the

study by Kalkonde *et al.* who showed that spatial memory was comparable in wild-type and CCR5-deficient mice⁵¹⁶. In addition to glutamate modulation, chemokine induction in the brain may also contribute to behavioural deficits by stimulating the production of inflammatory cytokines by glial cells. The impact that cytokines can have on behaviour has been described in Chapter 1. In summary, based on the current literature regarding their brain-specific effects, a role for chemokines in mediating LPS-induced behavioural changes could be hypothesised. However, the data available on this subject sparse and often contradictory, making this hypothesis highly speculative.

7.4 Overview and hypotheses

In order to recognise, and respond to, a viral or bacterial infection, the innate immune system utilises a number of different PRRs which specifically recognise PAMPs from various sources. LPS is a carbohydrate-rich derivative of bacterial cell walls. By interacting with TLR4, LPS alerts the immune system to the presence of a bacterial infection, resulting in a potent inflammatory response in the periphery. In addition to mobilising the effector arms of the innate immune system, LPS-induced inflammation is transmitted to the brain to evoke an appropriate behavioural response. The experiments outlined in this thesis suggest that systemic LPS may trigger the production of type I IFNs in the brain, or that peripherally produced type I IFNs can directly access the brain (Figure 7.2). The impact that type I IFNs have on behaviour has been well characterised and I have therefore hypothesised that systemic LPS-mediated type I IFN production, either in the periphery or the brain, may contribute to LPS-induced behavioural changes.

Following an acute systemic LPS challenge, transcripts encoding the T cell chemoattractant CXCL10, and the cellular adhesion molecules ICAM-1 and VCAM-1, were elevated in the brain (Figure 7.2). Due to the adversity of a cerebral bacterial infection, this transcriptional response may represent a protective strategy whereby the brain is being primed for the infiltration of memory T cells. Following daily injections of systemic LPS, a number of inflammatory chemokine transcripts were induced in the brain. Due to their proposed effects on neuronal transmission and survival, these chemokines may directly modulate behaviour. However, in this model, chemokine induction was associated with the recruitment of neutrophils, and then T cells, to the brain from the periphery (Figure 7.3). Both of these cell types have the capacity to amplify local inflammatory responses in the brain, which could result in neuronal damage and/or have an impact on behaviour. Although this appears counterproductive, the effects of repeated LPS injection might mimic the effects of a chronic bacterial infection in the periphery, and these leukocytes may confer protection against the threat of cerebral infection. Therefore, following a single LPS challenge, the brain may become sensitised to LPS-induced inflammation and prime itself for leukocyte recruitment. If LPS exposure continues, neutrophils and T cells are recruited to the brain, possibly with a principle goal of providing protection.

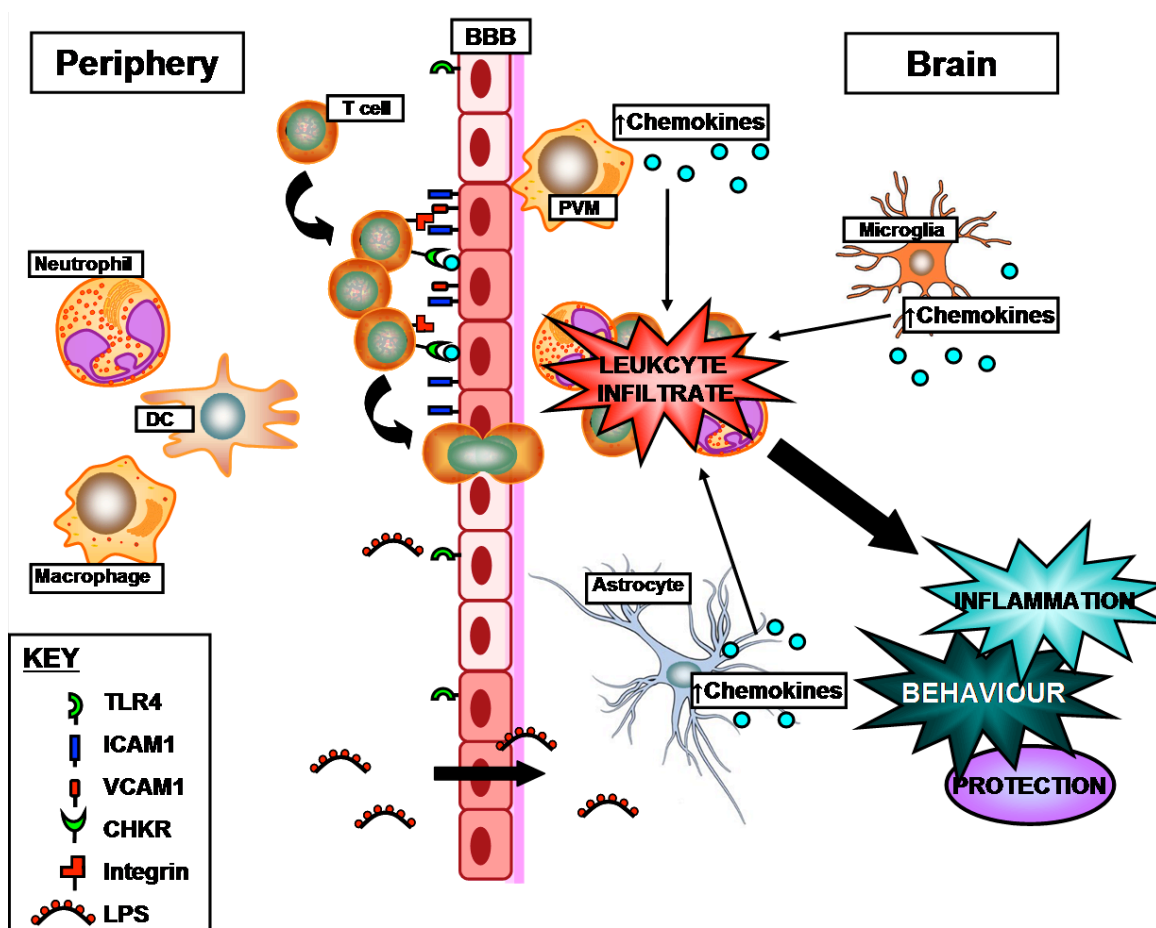


Figure 7.3 Response in the brain to daily systemic LPS injections: Observations and hypotheses

Chronic exposure to LPS in the periphery results in endotoxin tolerance, which is associated with a downregulation of TLR4 on leukocytes⁵¹⁷ and attenuated inflammatory cytokine production in the periphery. However, the brain continues to respond to circulating LPS by upregulating inflammatory chemokine transcripts. This could be due to the continued response of cerebral endothelial cells to circulating LPS, or chronic LPS exposure may increase the permeability of the blood brain barrier (BBB) and thus enable LPS to enter the brain. Chemokine induction in the brain was associated with the infiltration of leukocytes from the periphery to the brain parenchyma. Neutrophils were recruited first, presumably in response to increased CXCL1 and CXCL2. This was followed by an accumulation of T cells in the brain. As neutrophils can enhance inflammatory chemokine production, and release toxic agents which can disrupt BBB integrity, their recruitment to the brain may pave the way for these infiltrating T cells. Leukocyte recruitment may serve to protect the brain from the threat of a possible bacterial infection. However, both T cells and monocytes can produce inflammatory cytokines which would contribute to the inflammatory milieu of the brain. In addition, these cytokines, and LPS-induced inflammatory chemokines, may play a role in modulating brain function and behaviour.

7.5 Conclusions

The findings described in this thesis provide novel concepts that demonstrate a molecular link between peripheral inflammation and interferon responses in the brain. Systemic LPS has the capacity to remotely trigger an immune response in the brain. Following acute exposure to LPS in the periphery, the expression of ISGs, and other microarray target genes, in the brain was distally modulated in a manner that may be dependent on TLR-induced type I IFN production. Whether type I IFNs were produced in the brain, or whether peripherally induced IFNs directly access the brain to modulate ISG expression, remains open to further investigation; as does the downstream effects of central ISG induction. Due to the well established link between type I IFNs and depression, TLR-induced IFN production is worth investigating as a potential key mechanism linking peripheral inflammation with sickness behaviour.

Repeated injection of LPS in the periphery triggered a transient increase in chemokine transcription in the brain. As there are reports to suggest that chemokines can modulate neurotransmitter release and the extracellular cytokine environment, this chemokine induction could indirectly impact behaviour. However, the most characterised function of chemokines is to recruit leukocytes to sites of inflammation. Accordingly, chemokine induction in the brain during this model was associated with an influx of leukocytes from the periphery, and an increase in mRNA encoding the relevant chemokine receptors. Thus, whilst their role in modulating brain activity and behaviour cannot be excluded, it seems likely that chemokine induction in the brain following daily systemic LPS injections mediates the recruitment of leukocytes from the periphery. These data highlight a potential protective mechanism that could prevent a chronic bacterial infection from spreading from the periphery to the brain.

7.6 Future directions

Although the studies described in this thesis have generated some interesting and novel data, these data are largely descriptive and would benefit from more rigorous testing of the involved mechanisms. There are a number of possible experiments that could be done to further explore the potential mechanisms of ISG induction in the brain which have been described above.

As well as being mainly descriptive, the data described in this thesis are limited as, instead of focusing on specific brain regions and neuronal cell populations, they concentrate on global gene expression occurring throughout the entire brain. As described, gene expression was assessed in these studies 48 hours following systemic LPS injection. With nothing published, to my knowledge, regarding the response in the brain at this time point, taking an unbiased approach in terms of which brain regions to focus on was an obvious decision. However, it would now be interesting to narrow down on the specific brain regions or cell types that respond to peripheral inflammation by upregulating ISGs and chemokine transcripts.

Regional induction of ISGs and chemokine transcripts could be assessed by performing gene expression assays on micro-dissected regions of the mouse brain following LPS-challenge. However, a more in-depth approach to explore the region-specific effects of systemic LPS challenge would be to use fluorescent *in situ* hybridisation (FISH). FISH involves the use of fluorescently-labelled probes, specifically designed to bind to transcripts of interest on tissue sections. It can be combined with fluorescent immunohistochemistry so that the expression of a number of target genes and proteins can be visualised on one section simultaneously. Not only would this technique answer the question of which cell types respond to peripheral inflammation, but it would facilitate the temporal and spatial mapping of target gene expression in the brains of LPS-challenged mice. This method could also be used to establish whether IFN transcripts were induced in the brain and whether there was any colocalisation between IFN and chemokine transcripts that could highlight a potential mechanism of chemokine regulation. Moreover, by identifying the expression sites of IFNs, chemokines and their respective cognate receptors, hypotheses could be developed as to what

potential neurological effects these molecules might have that could impact behaviour.

Although a number of observations have been made from this work, the extent to which these are biologically linked remains unclear. Although FISH would help to gain a better understanding of the temporal and spatial pattern of events in the brain following systemic LPS challenge, it is not sufficient to directly link any of the observed responses. As described previously, the involvement of TLR4-induced non-canonical signalling in inducing ISG expression in the brain could be established using TRIF- or IRF3-deficient mice. Similarly, the effect of type I IFNs on the induction of chemokines in the brain could be easily investigated using IFNAR-deficient mice. In addition, as was described in Chapter 5, the role of specific chemokines in recruiting leukocytes to the brain could be verified using chemokine receptor antagonists. Therefore, genetically manipulated mice and chemokine receptor antagonists could be used to generate a better understanding of the pathways linking peripheral inflammation to IFN responses and chemokine induction in the brain.

Finally, whilst it was beyond the scope of this project, the data described in this thesis would greatly benefit from an in depth investigation into the possible impacts that LPS-induced IFN responses may have on the brain and on behaviour. Although behavioural deficits have been reported in mice following peripheral LPS or IFN α administration^{281,282,284,518}, there is nothing in the literature to suggest that type I IFNs play a role in LPS-induced sickness behaviour. An important experiment that could link type I IFNs to LPS-induced behavioural changes would be to compare sickness behaviours, and depression-like behaviours, in wild-type and IFNAR-deficient mice following systemic LPS injection. As LPS-induced ISG induction appears to be a TLR-driven response, this may underpin behavioural changes in infectious pathologies.

References

1. Broz, P. and D. M. Monack. 2013. Newly described pattern recognition receptors team up against intracellular pathogens. *Nature Reviews Immunology* 13:551-565.
 2. Schwartz, Y. S. and A. V. Svistelnik. 2012. Functional phenotypes of macrophages and the M1-M2 polarization concept. Part I. Proinflammatory phenotype. *Biochemistry (Moscow)* 77:246-260.
 3. Murphy, K. M. *Janeway's Immunobiology 8th Ed.* Garland Science.
 4. Borregaard, N., O. E. Sørensen, and K. Theilgaard-Mönch. 2007. Neutrophil granules: a library of innate immunity proteins. *Trends in Immunology* 28:340-345.
 5. Branzk, Nora and Papayannopoulos, Venizelos. Molecular mechanisms regulating NETosis in infection and disease. 1-18. 2013. Springer.
- Ref Type: Conference Proceeding
6. Galli, S. J., N. Borregaard, and T. A. Wynn. 2011. Phenotypic and functional plasticity of cells of innate immunity: macrophages, mast cells and neutrophils. *Nat Immunol* 12:1035-1044.
 7. Kolaczowska, E. and P. Kubes. 2013. Neutrophil recruitment and function in health and inflammation. *Nature Reviews Immunology* 13:159-175.
 8. Mosser, D. M. and J. P. Edwards. 2008. Exploring the full spectrum of macrophage activation. *Nature Reviews Immunology* 8:958-969.
 9. Silva, M. T. 2010. When two is better than one: macrophages and neutrophils work in concert in innate immunity as complementary and cooperative partners of a myeloid phagocyte system. *Journal of leukocyte biology* 87:93-106.
 10. Swindle, E. J., J. A. Hunt, and J. W. Coleman. 2002. A Comparison of Reactive Oxygen Species Generation by Rat Peritoneal Macrophages and Mast Cells Using the Highly Sensitive Real-Time Chemiluminescent Probe Pholasin: Inhibition of Antigen-Induced Mast Cell Degranulation by Macrophage-Derived Hydrogen Peroxide. *The Journal of Immunology* 169:5866-5873.
 11. Shi, F. D., H. G. Ljunggren, A. La Cava, and L. Van Kaer. 2011. Organ-specific features of natural killer cells. *Nature Reviews Immunology* 11:658-671.
 12. Gros, P., F. J. Milder, and B. J. Janssen. 2008. Complement driven by conformational changes. *Nature Reviews Immunology* 8:48-58.
 13. Ricciotti, E. and G. A. FitzGerald. 2011. Prostaglandins and Inflammation. *Arteriosclerosis, Thrombosis, and Vascular Biology* 31:986-1000.

14. Moncada, S. and S. F. J. Vane. 1973. Prostaglandins, aspirin-like drugs and the oedema of inflammation.
15. Ferreira, S. r. H., M. Nakamura, and M. S. de Abreu Castro. 1978. The hyperalgesic effects of prostacyclin and prostaglandin E₂. *Prostaglandins* 16:31-37.
16. Levy, B. D., C. B. Clish, B. Schmidt, K. Gronert, and C. N. Serhan. 2001. Lipid mediator class switching during acute inflammation: signals in resolution. *Nat Immunol* 2:612-619.
17. Tsou, C. L., W. Peters, Y. Si, S. Slaymaker, A. M. Aslanian, S. P. Weisberg, M. Mack, and I. F. Charo. 2007. Critical roles for CCR2 and MCP-3 in monocyte mobilization from bone marrow and recruitment to inflammatory sites. *Journal of Clinical Investigation* 117:902-909.
18. Serbina, N. V. and E. G. Pamer. 2006. Monocyte emigration from bone marrow during bacterial infection requires signals mediated by chemokine receptor CCR2. *Nat Immunol* 7:311-317.
19. LeGrand, E. K. and J. Alcock. 2012. Turning up the heat: immune brinkmanship in the acute-phase response. *The Quarterly Review of Biology* 87:3-18.
20. Sixt, M., N. Kanazawa, M. Selg, T. Samson, G. Roos, D. P. Reinhardt, R. Pabst, M. B. Lutz, and L. Sorokin. 2005. The conduit system transports soluble antigens from the afferent lymph to resident dendritic cells in the T cell area of the lymph node. *Immunity* 22:19-29.
21. Tal, O., H. Y. Lim, I. Gurevich, I. Milo, Z. Shipony, L. G. Ng, V. Angeli, and G. Shakhar. 2011. DC mobilization from the skin requires docking to immobilized CCL21 on lymphatic endothelium and intralymphatic crawling. *The Journal of Experimental Medicine* 208:2141-2153.
22. Kim, C. H., L. S. Rott, I. Clark-Lewis, D. J. Campbell, L. Wu, and E. C. Butcher. 2001. Subspecialization of Cxcr5+ T Cells B Helper Activity Is Focused in a Germinal Center-Localized Subset of Cxcr5+ T Cells. *The Journal of Experimental Medicine* 193:1373-1382.
23. Carrasco, Y. R. and F. D. Batista. 2007. B Cells Acquire Particulate Antigen in a Macrophage-Rich Area at the Boundary between the Follicle and the Subcapsular Sinus of the Lymph Node. *Immunity* 27:160-171.
24. Junt, T., E. A. Moseman, M. Iannacone, S. Massberg, P. A. Lang, M. Boes, K. Fink, S. E. Henrickson, D. M. Shayakhmetov, and N. C. Di Paolo. 2007. Subcapsular sinus macrophages in lymph nodes clear lymph-borne viruses and present them to antiviral B cells. *Nature* 450:110-114.
25. Okada, T., M. J. Miller, I. Parker, M. F. Krummel, M. Neighbors, S. B. Hartley, A. O'Garra, M. D. Cahalan, and J. G. Cyster. 2005. Antigen-engaged B cells undergo chemotaxis toward the T zone and form motile conjugates with helper T cells. *PLoS biology* 3:e150.

26. Kapsenberg, M. L. 2003. Dendritic-cell control of pathogen-driven T-cell polarization. *Nature Reviews Immunology* 3:984-993.
27. Jutel, M. and C. A. Akdis. 2011. T-cell subset regulation in atopy. *Current allergy and asthma reports* 11:139-145.
28. Andersen, M. H., D. Schrama, P. thor Straten, and J. C. Becker. 2006. Cytotoxic T cells. *Journal of investigative dermatology* 126:32-41.
29. Sallusto, F., J. Geginat, and A. Lanzavecchia. 2004. Central memory and effector memory T cell subsets: function, generation, and maintenance. *Annu.Rev.Immunol.* 22:745-763.
30. Moser, B. and P. Loetscher. 2001. Lymphocyte traffic control by chemokines. *Nat Immunol* 2:123-128.
31. Kaech, S. M., E. J. Wherry, and R. Ahmed. 2002. Effector and memory T-cell differentiation: implications for vaccine development. *Nature Reviews Immunology* 2:251-262.
32. Hasday, J. D., K. D. Fairchild, and C. Shanholtz. 2000. The role of fever in the infected host. *Microbes and Infection* 2:1891-1904.
33. Ostberg, J. R., B. E. Dayanc, M. Yuan, E. Oflazoglu, and E. A. Repasky. 2007. Enhancement of natural killer (NK) cell cytotoxicity by fever-range thermal stress is dependent on NKG2D function and is associated with plasma membrane NKG2D clustering and increased expression of MICA on target cells. *Journal of leukocyte biology* 82:1322-1331.
34. Chen, Q., D. T. Fisher, K. A. Clancy, J. M. Gauguet, W. C. Wang, E. Unger, S. Rose-John, U. H. von Andrian, H. Baumann, and S. S. Evans. 2006. Fever-range thermal stress promotes lymphocyte trafficking across high endothelial venules via an interleukin 6 trans-signaling mechanism. *Nat Immunol* 7:1299-1308.
35. Straub, R. H., M. Cutolo, F. Buttgereit, and G. Pongratz. 2010. Energy regulation and neuroendocrine-immune control in chronic inflammatory diseases. *Journal of Internal Medicine* 267:543-560.
36. Kotenko, S. V., G. Gallagher, V. V. Baurin, A. Lewis-Antes, M. Shen, N. K. Shah, J. A. Langer, F. Sheikh, H. Dickensheets, and R. P. Donnelly. 2002. IFN- λ s mediate antiviral protection through a distinct class II cytokine receptor complex. *Nat Immunol* 4:69-77.
37. Sheppard, P., W. Kindsvogel, W. Xu, K. Henderson, S. Schlutsmeyer, T. E. Whitmore, R. Kuestner, U. Garrigues, C. Birks, and J. Roraback. 2002. IL-28, IL-29 and their class II cytokine receptor IL-28R. *Nat Immunol* 4:63-68.
38. Sommereyns, C., S. Paul, P. Staeheli, and T. Michiels. 2008. IFN-lambda (IFN- λ) is expressed in a tissue-dependent fashion and primarily acts on epithelial cells in vivo. *PLoS pathogens* 4:e1000017.
39. Hertzog, P., S. Forster, and S. Samarajiwa. 2011. Systems biology of interferon responses. *Journal of Interferon & Cytokine Research* 31:5-11.

40. Hefti, H. P., M. Frese, H. Landis, C. Di Paolo, A. Aguzzi, O. Haller, and J. Pavlovic. 1999. Human MxA Protein Protects Mice Lacking a Functional Alpha/Beta Interferon System against La Crosse Virus and Other Lethal Viral Infections. *Journal of Virology* 73:6984-6991.
41. Leib, D. A., T. E. Harrison, K. M. Laslo, M. A. Machalek, N. J. Moorman, and H. W. Virgin. 1999. Interferons Regulate the Phenotype of Wild-type and Mutant Herpes Simplex Viruses In Vivo. *The Journal of Experimental Medicine* 189:663-672.
42. Hwang, S. Y., P. J. Hertzog, K. A. Holland, S. H. Sumarsono, M. J. Tymms, J. A. Hamilton, G. Whitty, I. Bertoncello, and I. Kola. 1995. A null mutation in the gene encoding a type I interferon receptor component eliminates antiproliferative and antiviral responses to interferons alpha and beta and alters macrophage responses. *Proceedings of the National Academy of Sciences* 92:11284-11288.
43. Muller, U., U. Steinhoff, L. F. Reis, S. Hemmi, J. Pavlovic, R. M. Zinkernagel, and M. Aguet. 1994. Functional role of type I and type II interferons in antiviral defense. *Science* 264:1918-1921.
44. Harty, J. T. and M. J. Bevant. 1995. Specific immunity to listeria monocytogenes in the absence of IFN γ . *Immunity* 3:109-117.
45. Heath, L., C. Crisp, G. Huffnagle, M. LeGendre, Y. Osawa, M. Hurley, C. Engleberg, J. Fantone, and J. Brieland. 1996. Effector mechanisms responsible for gamma interferon-mediated host resistance to Legionella pneumophila lung infection: the role of endogenous nitric oxide differs in susceptible and resistant murine hosts. *Infection and Immunity* 64:5151-5160.
46. Dalton, D. K., S. Pitts-Meek, S. Keshav, I. S. Figari, A. Bradley, and T. A. Stewart. 1993. Multiple defects of immune cell function in mice with disrupted interferon-gamma genes. *Science* 259:1739-1742.
47. Flynn, J. L., J. Chan, K. J. Triebold, D. K. Dalton, T. A. Stewart, and B. R. Bloom. 1993. An essential role for interferon gamma in resistance to Mycobacterium tuberculosis infection. *The Journal of Experimental Medicine* 178:2249-2254.
48. Cooper, A. M., D. K. Dalton, T. A. Stewart, J. P. Griffin, D. G. Russell, and I. M. Orme. 1993. Disseminated tuberculosis in interferon gamma gene-disrupted mice. *The Journal of Experimental Medicine* 178:2243-2247.
49. Ghosh, S. K., J. Kusari, S. K. Bandyopadhyay, H. Samanta, R. Kumar, and G. C. Sen. 1991. Cloning, sequencing, and expression of two murine 2'-5'-oligoadenylate synthetases. Structure-function relationships. *Journal of Biological Chemistry* 266:15293-15299.
50. Haller, O. and G. Kochs. 2002. Interferon-Induced Mx Proteins: Dynamin-Like GTPases with Antiviral Activity. *Traffic* 3:710-717.

51. Prasanna, S. J., B. Saha, and D. Nandi. 2007. Involvement of oxidative and nitrosative stress in modulation of gene expression and functional responses by IFN γ . *International Immunology* 19:867-879.
52. Ank, N., H. West, C. Bartholdy, K. Eriksson, A. R. Thomsen, and S. R. Paludan. 2006. Lambda Interferon (IFN- λ), a Type III IFN, Is Induced by Viruses and IFNs and Displays Potent Antiviral Activity against Select Virus Infections In Vivo. *Journal of Virology* 80:4501-4509.
53. Zhou, Z., O. J. Hamming, N. Ank, S. r. R. Paludan, A. L. Nielsen, and R. Hartmann. 2007. Type III Interferon (IFN) Induces a Type I IFN-Like Response in a Restricted Subset of Cells through Signaling Pathways Involving both the Jak-STAT Pathway and the Mitogen-Activated Protein Kinases. *Journal of Virology* 81:7749-7758.
54. Mordstein, M., G. Kochs, L. Dumoutier, J. C. Renauld, S. r. R. Paludan, K. Klucher, and P. Staeheli. 2008. Interferon- λ contributes to innate immunity of mice against influenza A virus but not against hepatotropic viruses. *PLoS pathogens* 4:e1000151.
55. Decker, T., M. Muller, and S. Stockinger. 2005. The Yin and Yang of type I interferon activity in bacterial infection. *Nat Rev Immunol* 5:675-687.
56. Pomeroy, C., D. DeLong, C. Clabots, P. Riciputi, and G. A. Filice. 1998. Role of interferon- γ in murine cytomegalovirus infection. *Journal of Laboratory and Clinical Medicine* 132:124-133.
57. Yu, Z., E. Manickan, and B. T. Rouse. 1996. Role of interferon-gamma in immunity to herpes simplex virus. *Journal of leukocyte biology* 60:528-532.
58. Patterson, C. E., D. M. P. Lawrence, L. A. Echols, and G. F. Rall. 2002. Immune-Mediated Protection from Measles Virus-Induced Central Nervous System Disease Is Noncytolytic and Gamma Interferon Dependent. *Journal of Virology* 76:4497-4506.
59. Bierne, H., L. Travier, T. Mahlaköiv, L. Tailleux, A. Subtil, A. Lebreton, A. Paliwal, B. Gicquel, P. Staeheli, and M. Lecuit. 2012. Activation of type III interferon genes by pathogenic bacteria in infected epithelial cells and mouse placenta. *PLoS one* 7:e39080.
60. Buß, C., B. Opitz, A. C. Hocke, J. Lippmann, V. van Laak, S. Hippenstiel, M. Krüll, N. Suttorp, and J. Eitel. 2010. Essential Role of Mitochondrial Antiviral Signaling, IFN Regulatory Factor (IRF)3, and IRF7 in Chlamydomonas pneumoniae-Mediated IFN- β Response and Control of Bacterial Replication in Human Endothelial Cells. *The Journal of Immunology* 184:3072-3078.
61. Lebreton, A., G. Lakisic, V. Job, L. Fritsch, T. N. Tham, A. Camejo, P. J. Matteï, B. Regnault, M. A. Nahori, and D. Cabanes. 2011. A bacterial protein targets the BAHD1 chromatin complex to stimulate type III interferon response. *Science* 331:1319-1321.

62. Mancuso, G., A. Midiri, C. Biondo, C. Beninati, S. Zummo, R. Galbo, F. Tomasello, M. Gambuzza, G. Macrì, A. Ruggeri, T. Leanderson, and G. Teti. 2007. Type I IFN Signaling Is Crucial for Host Resistance against Different Species of Pathogenic Bacteria. *The Journal of Immunology* 178:3126-3133.
63. Plumlee, C., C. Lee, A. A. Beg, T. Decker, H. A. Shuman, and C. Schindler. 2009. Interferons Direct an Effective Innate Response to *Legionella pneumophila* Infection. *Journal of Biological Chemistry* 284:30058-30066.
64. Ishihara, T., M. Aga, K. Hino, C. Ushio, M. Taniguchi, K. Iwaki, M. Ikeda, and M. Kurimoto. 2005. Inhibition of chlamydia trachomatis growth by human interferon-alpha: mechanisms and synergistic effect with interferon-gamma and tumor necrosis factor-alpha. *Biomedical research (Tokyo, Japan)* 26:179-185.
65. de la Maza, L. M., E. M. Peterson, J. M. Goebel, C. W. Fennie, and C. W. Czarniecki. 1985. Interferon-induced inhibition of *Chlamydia trachomatis*: dissociation from antiviral and antiproliferative effects. *Infection and Immunity* 47:719-722.
66. Henry, T., G. S. Kirimanjswara, T. Ruby, J. W. Jones, K. Peng, M. Perret, L. Ho, J. D. Sauer, Y. Iwakura, D. W. Metzger, and D. M. Monack. 2010. Type I IFN Signaling Constrains IL-17A/F Secretion by $\gamma\delta$ T Cells during Bacterial Infections. *The Journal of Immunology* 184:3755-3767.
67. Carrero, J. A., B. Calderon, and E. R. Unanue. 2004. Type I Interferon Sensitizes Lymphocytes to Apoptosis and Reduces Resistance to *Listeria* Infection. *The Journal of Experimental Medicine* 200:535-540.
68. Auerbuch, V., D. G. Brockstedt, N. Meyer-Morse, M. O'Riordan, and D. A. Portnoy. 2004. Mice Lacking the Type I Interferon Receptor Are Resistant to *Listeria monocytogenes*. *The Journal of Experimental Medicine* 200:527-533.
69. Fehr, T., G. Schoedon, B. Odermatt, T. Holtschke, M. Schneemann, M. F. Bachmann, T. W. Mak, I. Horak, and R. M. Zinkernagel. 1997. Crucial Role of Interferon Consensus Sequence Binding Protein, but neither of Interferon Regulatory Factor 1 nor of Nitric Oxide Synthesis for Protection Against Murine Listeriosis. *The Journal of Experimental Medicine* 185:921-932.
70. Murphy, P. M., M. Baggiolini, I. F. Charo, C. A. Hébert, R. Horuk, K. Matsushima, L. H. Miller, J. J. Oppenheim, and C. A. Power. 2000. International Union of Pharmacology. XXII. Nomenclature for Chemokine Receptors. *Pharmacological reviews* 52:145-176.
71. Allen, S. J., S. E. Crown, and T. M. Handel. 2007. Chemokine: receptor structure, interactions, and antagonism. *Annu.Rev.Immunol.* 25:787-820.
72. Nomiya, H., N. Osada, and O. Yoshie. 2011. A family tree of vertebrate chemokine receptors for a unified nomenclature. *Developmental & Comparative Immunology* 35:705-715.

73. Patel, L., S. J. Charlton, J. K. Chambers, and C. H. Macphee. 2001. Expression and functional analysis of chemokine receptors in human peripheral blood leukocyte populations. *Cytokine* 14:27-36.
74. Mantovani, A. 1999. The chemokine system: redundancy for robust outputs. *Immunology today* 20:254-257.
75. Viola, A. and N. Gupta. 2007. Tether and trap: regulation of membrane-raft dynamics by actin-binding proteins. *Nature Reviews Immunology* 7:889-896.
76. Johnson, Z., A. E. Proudfoot, and T. M. Handel. 2005. Interaction of chemokines and glycosaminoglycans: A new twist in the regulation of chemokine function with opportunities for therapeutic intervention. *Cytokine & Growth Factor Reviews* 16:625-636.
77. Ley, K., C. Laudanna, M. I. Cybulsky, and S. Nourshargh. 2007. Getting to the site of inflammation: the leukocyte adhesion cascade updated. *Nature Reviews Immunology* 7:678-689.
78. Weber, M., R. Hauschild, J. Schwarz, C. Moussion, I. de Vries, D. F. Legler, S. A. Luther, T. Bollenbach, and M. Sixt. 2013. Interstitial dendritic cell guidance by haptotactic chemokine gradients. *Science* 339:328-332.
79. Yoshida, R., T. Imai, K. Hieshima, J. Kusuda, M. Baba, M. Kitaura, M. Nishimura, M. Kakizaki, H. Nomiyama, and O. Yoshie. 1997. Molecular Cloning of a Novel Human CC Chemokine EBI1-ligand Chemokine That Is a Specific Functional Ligand for EBI1, CCR7. *Journal of Biological Chemistry* 272:13803-13809.
80. Yoshida, R., M. Nagira, M. Kitaura, N. Imagawa, T. Imai, and O. Yoshie. 1998. Secondary Lymphoid-tissue Chemokine Is a Functional Ligand for the CC Chemokine Receptor CCR7. *Journal of Biological Chemistry* 273:7118-7122.
81. Förster, R., A. Schubel, D. Breitfeld, E. Kremmer, I. Renner-Müller, E. Wolf, and M. Lipp. 1999. CCR7 Coordinates the Primary Immune Response by Establishing Functional Microenvironments in Secondary Lymphoid Organs. *Cell* 99:23-33.
82. Gunn, M. D., V. N. Ngo, K. M. Ansel, E. H. Eklund, J. G. Cyster, and L. T. Williams. 1998. A B-cell-homing chemokine made in lymphoid follicles activates Burkitt's lymphoma receptor-1. *Nature* 391:799-803.
83. Shirozu, M., T. Nakano, J. Inazawa, K. Tashiro, H. Tada, T. Shinohara, and T. Honjo. 1995. Structure and chromosomal localization of the human stromal cell-derived factor 1 (SDF1) gene. *Genomics* 28:495-500.
84. David, N. B., D. Sapède, L. Saint-Etienne, C. Thisse, B. Thisse, C. Dambly-Chaudière, F. d. r. M. Rosa, and A. Ghysen. 2002. Molecular basis of cell migration in the fish lateral line: Role of the chemokine receptor CXCR4 and of its ligand, SDF1. *Proceedings of the National Academy of Sciences* 99:16297-16302.

85. Zou, Y. R., A. H. Kottmann, M. Kuroda, I. Taniuchi, and D. R. Littman. 1998. Function of the chemokine receptor CXCR4 in haematopoiesis and in cerebellar development. *Nature* 393:595-599.
86. Nagasawa, T., S. Hirota, K. Tachibana, N. Takakura, S. i. Nishikawa, Y. Kitamura, N. Yoshida, H. Kikutani, and T. Kishimoto. 1996. Defects of B-cell lymphopoiesis and bone-marrow myelopoiesis in mice lacking the CXC chemokine PBSF/SDF-1. *Nature* 382:635-638.
87. Ma, Q., D. Jones, P. R. Borghesani, R. A. Segal, T. Nagasawa, T. Kishimoto, R. T. Bronson, and T. A. Springer. 1998. Impaired B-lymphopoiesis, myelopoiesis, and derailed cerebellar neuron migration in CXCR4- and SDF-1-deficient mice. *Proceedings of the National Academy of Sciences* 95:9448-9453.
88. Sugiyama, T., H. Kohara, M. Noda, and T. Nagasawa. 2006. Maintenance of the Hematopoietic Stem Cell Pool by CXCL12-CXCR4 Chemokine Signaling in Bone Marrow Stromal Cell Niches. *Immunity* 25:977-988.
89. Del Rio, L., S. Bennouna, J. Salinas, and E. Y. Denkers. 2001. CXCR2 Deficiency Confers Impaired Neutrophil Recruitment and Increased Susceptibility During *Toxoplasma gondii* Infection. *The Journal of Immunology* 167:6503-6509.
90. Soehnlein, O., L. Lindbom, and C. Weber. 2009. Mechanisms underlying neutrophil-mediated monocyte recruitment. *Blood* 114:4613-4623.
91. Coelho, F. M., V. Pinho, F. A. Amaral, D. Sachs, V. v. V. Costa, D. H. Rodrigues, A. l. T. Vieira, T. l. A. Silva, D. G. Souza, R. Bertini, A. n. L. Teixeira, and M. M. Teixeira. 2008. The chemokine receptors CXCR1/CXCR2 modulate antigen-induced arthritis by regulating adhesion of neutrophils to the synovial microvasculature. *Arthritis & Rheumatism* 58:2329-2337.
92. Casilli, F., A. Bianchini, I. Gloaguen, L. Biordi, E. Alesse, C. Festuccia, B. Cavalieri, R. Strippoli, M. N. Cervellera, R. D. Bitondo, E. Ferretti, F. Mainiero, C. Bizzarri, F. Colotta, and R. Bertini. 2005. Inhibition of interleukin-8 (CXCL8/IL-8) responses by repertaxin, a new inhibitor of the chemokine receptors CXCR1 and CXCR2. *Biochemical Pharmacology* 69:385-394.
93. Geissmann, F., S. Jung, and D. R. Littman. 2003. Blood Monocytes Consist of Two Principal Subsets with Distinct Migratory Properties. *Immunity* 19:71-82.
94. Weber, C., K. U. Belge, P. von Hundelshausen, G. Draude, B. Steppich, M. Mack, M. Frankenberger, K. S. Weber, and H. W. Ziegler-Heitbrock. 2000. Differential chemokine receptor expression and function in human monocyte subpopulations. *Journal of leukocyte biology* 67:699-704.
95. Kaufmann, A., R. Salentin, D. Gemsa, and H. Sprenger. 2001. Increase of CCR1 and CCR5 expression and enhanced functional response to MIP-1 α during differentiation of human monocytes to macrophages. *Journal of leukocyte biology* 69:248-252.

96. Tuttle, D. L., J. K. Harrison, C. Anders, J. W. Sleasman, and M. M. Goodenow. 1998. Expression of CCR5 Increases during Monocyte Differentiation and Directly Mediates Macrophage Susceptibility to Infection by Human Immunodeficiency Virus Type 1. *Journal of Virology* 72:4962-4969.
97. Farber, J. M. 1990. A macrophage mRNA selectively induced by gamma-interferon encodes a member of the platelet factor 4 family of cytokines. *Proceedings of the National Academy of Sciences* 87:5238-5242.
98. Luster, A. D. and J. V. Ravetch. 1987. Biochemical characterization of a gamma interferon-inducible cytokine (IP-10). *The Journal of Experimental Medicine* 166:1084-1097.
99. Cole, K. E., C. A. Strick, T. J. Paradis, K. T. Ogborne, M. Loetscher, R. P. Gladue, W. Lin, J. G. Boyd, B. Moser, D. E. Wood, B. G. Sahagan, and K. Neote. 1998. Interferon-inducible T Cell Alpha Chemoattractant (I-TAC): A Novel Non-ELR CXC Chemokine with Potent Activity on Activated T Cells through Selective High Affinity Binding to CXCR3. *The Journal of Experimental Medicine* 187:2009-2021.
100. Martín-Fontecha, A., L. L. Thomsen, S. Brett, C. Gerard, M. Lipp, A. Lanzavecchia, and F. Sallusto. 2004. Induced recruitment of NK cells to lymph nodes provides IFN- γ for TH1 priming. *Nat Immunol* 5:1260-1265.
101. Loetscher, M., B. Gerber, P. Loetscher, S. A. Jones, L. Piali, I. Clark-Lewis, M. Baggiolini, and B. Moser. 1996. Chemokine receptor specific for IP10 and mig: structure, function, and expression in activated T-lymphocytes. *The Journal of Experimental Medicine* 184:963-969.
102. Weller, R. O., I. Galea, R. O. Carare, and A. Minagar. 2010. Pathophysiology of the lymphatic drainage of the central nervous system: Implications for pathogenesis and therapy of multiple sclerosis. *Pathophysiology* 17:295-306.
103. Matyszak, M. K. and V. H. Perry. 1996. The potential role of dendritic cells in immune-mediated inflammatory diseases in the central nervous system. *Neuroscience* 74:599-608.
104. Ghersi-Egea, J. F., B. Leininger-muller, R. o. Cecchelli, and J. D. Fenstermacher. 1995. Blood-brain interfaces: relevance to cerebral drug metabolism. *Toxicology Letters* 82:645-653.
105. Herrup, K. and Y. Yang. 2007. Cell cycle regulation in the postmitotic neuron: oxymoron or new biology? *Nature Reviews Neuroscience* 8:368-378.
106. Bsibsi, M., R. Ravid, D. Gveric, and J. M. van Noort. 2002. Broad expression of Toll-like receptors in the human central nervous system. *J Neuropathol Exp Neurol* 61:1013-1021.
107. Butchi, N. B., S. Pourciau, M. Du, T. W. Morgan, and K. E. Peterson. 2008. Analysis of the Neuroinflammatory Response to TLR7 Stimulation in the

Brain: Comparison of Multiple TLR7 and/or TLR8 Agonists. *The Journal of Immunology* 180:7604-7612.

108. Jack, C. S., N. Arbour, J. Manusow, V. Montgrain, M. Blain, E. McCrea, A. Shapiro, and J. P. Antel. 2005. TLR Signaling Tailors Innate Immune Responses in Human Microglia and Astrocytes. *The Journal of Immunology* 175:4320-4330.
109. Olson, J. K. and S. D. Miller. 2004. Microglia Initiate Central Nervous System Innate and Adaptive Immune Responses through Multiple TLRs. *The Journal of Immunology* 173:3916-3924.
110. Farina, C., M. Krumbholz, T. Giese, G. Hartmann, F. Aloisi, and E. Meinl. 2005. Preferential expression and function of Toll-like receptor 3 in human astrocytes. *Journal of Neuroimmunology* 159:12-19.
111. McKimmie, C. S. and J. K. Fazakerley. 2005. In response to pathogens, glial cells dynamically and differentially regulate Toll-like receptor gene expression. *Journal of Neuroimmunology* 169:116-125.
112. McKimmie, C. S. and G. J. Graham. 2010. Astrocytes modulate the chemokine network in a pathogen-specific manner. *Biochemical and Biophysical Research Communications* 394:1006-1011.
113. Carpentier, P. A., W. S. Begolka, J. K. Olson, A. Elhofy, W. J. Karpus, and S. D. Miller. 2005. Differential activation of astrocytes by innate and adaptive immune stimuli. *Glia* 49:360-374.
114. Takeshita, S., F. Takeshita, D. E. Haddad, N. Janabi, and D. M. Klinman. 2001. Activation of microglia and astrocytes by CpG oligodeoxynucleotides. *Neuroreport* 12.
115. Lee, S., J. Hong, S. Y. Choi, S. B. Oh, K. Park, J. S. Kim, M. Karin, and S. J. Lee. 2004. CpG oligodeoxynucleotides induce expression of proinflammatory cytokines and chemokines in astrocytes: the role of c-Jun N-terminal kinase in CpG ODN-mediated NF- κ B activation. *Journal of Neuroimmunology* 153:50-63.
116. Ginhoux, F., M. Greter, M. Leboeuf, S. Nandi, P. See, S. Gokhan, M. F. Mehler, S. J. Conway, L. G. Ng, E. R. Stanley, I. M. Samokhvalov, and M. Merad. 2010. Fate Mapping Analysis Reveals That Adult Microglia Derive from Primitive Macrophages. *Science* 330:841-845.
117. Tambuyzer, B. R., P. Ponsaerts, and E. J. Nouwen. 2009. Microglia: gatekeepers of central nervous system immunology. *Journal of leukocyte biology* 85:352-370.
118. Nimmerjahn, A., F. Kirchhoff, and F. Helmchen. 2005. Resting Microglial Cells Are Highly Dynamic Surveillants of Brain Parenchyma in Vivo. *Science* 308:1314-1318.
119. Wake, H., A. J. Moorhouse, S. Jinno, S. Kohsaka, and J. Nabekura. 2009. Resting Microglia Directly Monitor the Functional State of Synapses In Vivo

- and Determine the Fate of Ischemic Terminals. *The Journal of Neuroscience* 29:3974-3980.
120. Carson, M. J., C. R. Reilly, J. G. Sutcliffe, and D. Lo. 1998. Mature microglia resemble immature antigen-presenting cells. *Glia* 22:72-85.
 121. Zimmer, H., S. Riese, and A. Régnier-Vigouroux. 2003. Functional characterization of mannose receptor expressed by immunocompetent mouse microglia. *Glia* 42:89-100.
 122. Marzolo, M. P., R. von Bernhardi, and N. C. Inestrosa. 1999. Mannose receptor is present in a functional state in rat microglial cells. *J.Neurosci.Res.* 58:387-395.
 123. Sterka, J. and I. Marriott. 2006. Characterization of nucleotide-binding oligomerization domain (NOD) protein expression in primary murine microglia. *Journal of Neuroimmunology* 179:65-75.
 124. Ribes, S., S. Ebert, T. Regen, A. Agarwal, S. C. Tauber, D. Czesnik, A. Spreer, S. Bunkowski, H. Eiffert, U. K. Hanisch, S. Hammerschmidt, and R. Nau. 2010. Toll-Like Receptor Stimulation Enhances Phagocytosis and Intracellular Killing of Nonencapsulated and Encapsulated *Streptococcus pneumoniae* by Murine Microglia. *Infection and Immunity* 78:865-871.
 125. Smith, M. E., K. van der Maesen, and F. P. Somera. 1998. Macrophage and microglial responses to cytokines in vitro: Phagocytic activity, proteolytic enzyme release, and free radical production. *J.Neurosci.Res.* 54:68-78.
 126. Ebert, S., J. Gerber, S. Bader, F. Mühlhauser, K. Brechtel, T. J. Mitchell, and R. Nau. 2005. Dose-dependent activation of microglial cells by Toll-like receptor agonists alone and in combination. *Journal of Neuroimmunology* 159:87-96.
 127. Kielian, T., P. Mayes, and M. Kielian. 2002. Characterization of microglial responses to *Staphylococcus aureus*: effects on cytokine, costimulatory molecule, and Toll-like receptor expression. *Journal of Neuroimmunology* 130:86-99.
 128. Cardona, A. E., E. P. Piro, M. E. Sasse, V. Kostenko, S. M. Cardona, I. M. Dijkstra, D. Huang, G. Kidd, S. Dombrowski, R. Dutta, J. C. Lee, D. N. Cook, S. Jung, S. A. Lira, D. R. Littman, and R. M. Ransohoff. 2006. Control of microglial neurotoxicity by the fractalkine receptor. *Nature neuroscience* 9:917-924.
 129. Hoek, R. M., S. R. Ruuls, C. A. Murphy, G. J. Wright, R. Goddard, S. M. Zurawski, B. Blom, M. E. Homola, W. J. Streit, M. H. Brown, A. N. Barclay, and J. D. Sedgwick. 2000. Down-Regulation of the Macrophage Lineage Through Interaction with OX2 (CD200). *Science* 290:1768-1771.
 130. Rogers, J. T., J. M. Morganti, A. D. Bachstetter, C. E. Hudson, M. M. Peters, B. A. Grimmig, E. J. Weeber, P. C. Bickford, and C. Gemma. 2011. CX3CR1 Deficiency Leads to Impairment of Hippocampal Cognitive Function and Synaptic Plasticity. *The Journal of Neuroscience* 31:16241-16250.

131. Laflamme, N., H. Echchannaoui, R. Landmann, and S. Rivest. 2003. Cooperation between toll-like receptor 2 and 4 in the brain of mice challenged with cell wall components derived from gram-negative and gram-positive bacteria. *Eur.J.Immunol.* 33:1127-1138.
132. Zhou, H., B. t. M. Lapointe, S. R. Clark, L. Zbytnuik, and P. Kubes. 2006. A Requirement for Microglial TLR4 in Leukocyte Recruitment into Brain in Response to Lipopolysaccharide. *The Journal of Immunology* 177:8103-8110.
133. Town, T., D. Jeng, L. Alexopoulou, J. Tan, and R. A. Flavell. 2006. Microglia Recognize Double-Stranded RNA via TLR3. *The Journal of Immunology* 176:3804-3812.
134. Liu, S., Y. Liu, W. Hao, L. Wolf, A. J. Kiliaan, B. Penke, C. E. Rübke, J. Walter, M. T. Heneka, T. Hartmann, M. D. Menger, and K. Fassbender. 2012. TLR2 Is a Primary Receptor for Alzheimer's Amyloid β Peptide To Trigger Neuroinflammatory Activation. *The Journal of Immunology* 188:1098-1107.
135. Kim, C., D. H. Ho, J. E. Suk, S. You, S. Michael, J. Kang, S. Joong Lee, E. Masliah, D. Hwang, H. J. Lee, and S. J. Lee. 2013. Neuron-released oligomeric α -synuclein is an endogenous agonist of TLR2 for paracrine activation of microglia. *Nat Commun* 4:1562.
136. Wang, D. D. and A. I. Bordey. 2008. The astrocyte odyssey. *Progress in Neurobiology* 86:342-367.
137. McKimmie, C. S., N. Johnson, A. R. Fooks, and J. K. Fazakerley. 2005. Viruses selectively upregulate Toll-like receptors in the central nervous system. *Biochemical and Biophysical Research Communications* 336:925-933.
138. Lehnardt, S., C. Lachance, S. Patrizi, S. Lefebvre, P. L. Follett, F. E. Jensen, P. A. Rosenberg, J. J. Volpe, and T. Vartanian. 2002. The Toll-Like Receptor TLR4 Is Necessary for Lipopolysaccharide-Induced Oligodendrocyte Injury in the CNS. *The Journal of Neuroscience* 22:2478-2486.
139. Bowman, C. C., A. Rasley, S. L. Tranguch, and I. Marriott. 2003. Cultured astrocytes express toll-like receptors for bacterial products. *Glia* 43:281-291.
140. Gorina, R., M. Font-Nieves, L. Márquez-Kisinousky, T. Santalucia, and A. M. Planas. 2011. Astrocyte TLR4 activation induces a proinflammatory environment through the interplay between MyD88-dependent NF κ B signaling, MAPK, and Jak1/Stat1 pathways. *Glia* 59:242-255.
141. Van Neerven, S., T. Regen, D. Wolf, A. Nemes, S. Johann, C. Beyer, U. K. Hanisch, and J. Mey. 2010. Inflammatory chemokine release of astrocytes in vitro is reduced by all-trans retinoic acid. *Journal of Neurochemistry* 114:1511-1526.

142. Esen, N., F. Y. Tanga, J. A. DeLeo, and T. Kielian. 2004. Toll-like receptor 2 (TLR2) mediates astrocyte activation in response to the Gram-positive bacterium *Staphylococcus aureus*. *Journal of Neurochemistry* 88:746-758.
143. Nathan, C. and M. U. Shiloh. 2000. Reactive oxygen and nitrogen intermediates in the relationship between mammalian hosts and microbial pathogens. *Proceedings of the National Academy of Sciences* 97:8841-8848.
144. Chauhan, V. S., D. G. Sterka, S. R. Furr, A. B. Young, and I. Marriott. 2009. NOD2 plays an important role in the inflammatory responses of microglia and astrocytes to bacterial CNS pathogens. *Glia* 57:414-423.
145. Owens, T., I. Bechmann, and B. Engelhardt. 2008. Perivascular spaces and the two steps to neuroinflammation. *Journal of Neuropathology & Experimental Neurology* 67:1113-1121.
146. Karman, J., C. Ling, M. Sandor, and Z. Fabry. 2004. Initiation of Immune Responses in Brain Is Promoted by Local Dendritic Cells. *The Journal of Immunology* 173:2353-2361.
147. Harling-Berg, C., P. M. Knopf, J. Merriam, and H. F. Cserr. 1989. Role of cervical lymph nodes in the systemic humoral immune response to human serum albumin microinfused into rat cerebrospinal fluid. *Journal of Neuroimmunology* 25:185-193.
148. Stromnes, I. M. and J. M. Goverman. 2006. Active induction of experimental allergic encephalomyelitis. *Nature protocols* 1:1810-1819.
149. Phillips, M. J., R. O. Weller, S. Kida, and F. Iannotti. 1995. Focal brain damage enhances experimental allergic encephalomyelitis in brain and spinal cord. *Neuropathology and Applied Neurobiology* 21:189-200.
150. Phillips, M. J., M. Needham, and R. O. Weller. 1997. Role of cervical lymph nodes in autoimmune encephalomyelitis in the Lewis rat. *J.Pathol.* 182:457-464.
151. Engelhardt, B., K. Wolburg-Buchholz, and H. Wolburg. 2001. Involvement of the choroid plexus in central nervous system inflammation. *Microscopy research and technique* 52:112-129.
152. Engelhardt, B. and R. M. Ransohoff. 2005. The ins and outs of T-lymphocyte trafficking to the CNS: anatomical sites and molecular mechanisms. *Trends in Immunology* 26:485-495.
153. Kivisäkk, P., D. J. Mahad, M. K. Callahan, C. Trebst, B. Tucky, T. Wei, L. Wu, E. S. Baekkevold, H. Lassmann, S. M. Staugaitis, J. J. Campbell, and R. M. Ransohoff. 2003. Human cerebrospinal fluid central memory CD4+ T cells: Evidence for trafficking through choroid plexus and meninges via P-selectin. *Proceedings of the National Academy of Sciences* 100:8389-8394.
154. Steffen, B. J., G. Breier, E. C. Butcher, M. Schulz, and B. Engelhardt. 1996. ICAM-1, VCAM-1, and MAdCAM-1 are expressed on choroid plexus

epithelium but not endothelium and mediate binding of lymphocytes in vitro. *The American journal of pathology* 148:1819.

155. Carrithers, M. D., I. Visintin, C. Viret, and J. Janeway. 2002. Role of genetic background in P selectin-dependent immune surveillance of the central nervous system. *Journal of Neuroimmunology* 129:51-57.
156. Kivisäkk, P., C. Trebst, Z. Liu, B. H. Tucky, T. L. Sorensen, R. A. Rudick, M. Mack, and R. M. Ransohoff. 2002. T-cells in the cerebrospinal fluid express a similar repertoire of inflammatory chemokine receptors in the absence or presence of CNS inflammation: implications for CNS trafficking. *Clinical & Experimental Immunology* 129:510-518.
157. Navratil, E., A. Couvelard, A. Rey, D. Hénin, and J. Y. Scoazec. 1997. Expression of cell adhesion molecules by microvascular endothelial cells in the cortical and subcortical regions of the normal human brain: an immunohistochemical analysis. *Neuropathology and Applied Neurobiology* 23:68-80.
158. Anandasabapathy, N., G. D. Victora, M. Meredith, R. Feder, B. Dong, C. Kluger, K. Yao, M. L. Dustin, M. C. Nussenzweig, R. M. Steinman, and K. Liu. 2011. Flt3L controls the development of radiosensitive dendritic cells in the meninges and choroid plexus of the steady-state mouse brain. *The Journal of Experimental Medicine* 208:1695-1705.
159. Greter, M., F. L. Heppner, M. P. Lemos, B. M. Odermatt, N. Goebels, T. Laufer, R. J. Noelle, and B. Becher. 2005. Dendritic cells permit immune invasion of the CNS in an animal model of multiple sclerosis. *Nat Med* 11:328-334.
160. Wekerle, H., C. Linington, H. Lassmann, and R. Meyermann. 1986. Cellular immune reactivity within the CNS. *Trends in Neurosciences* 9:271-277.
161. Bailey, S. L., B. Schreiner, E. J. McMahon, and S. D. Miller. 2007. CNS myeloid DCs presenting endogenous myelin peptides 'preferentially' polarize CD4+ T(H)-17 cells in relapsing EAE. *Nat Immunol* 8:172-180.
162. de Vos, A. F., M. van Meurs, H. P. Brok, L. A. Boven, R. Q. Hintzen, P. van der Valk, R. Ravid, S. Rensing, L. Boon, B. A. Hart, and J. D. Laman. 2002. Transfer of Central Nervous System Autoantigens and Presentation in Secondary Lymphoid Organs. *The Journal of Immunology* 169:5415-5423.
163. Fabriek, B. O., E. S. Van Haastert, I. Galea, M. M. J. Polfliet, E. D. Döpp, M. M. Van Den Heuvel, T. K. Van Den Berg, C. J. A. De Groot, P. van der Valk, and C. D. Dijkstra. 2005. CD163-positive perivascular macrophages in the human CNS express molecules for antigen recognition and presentation. *Glia* 51:297-305.
164. Polfliet, M. M. J., F. van de Veerdonk, E. A. Döpp, E. M. L. Kesteren-Hendriks, N. van Rooijen, C. D. Dijkstra, and T. K. Van Den Berg. 2002. The role of perivascular and meningeal macrophages in experimental allergic encephalomyelitis. *Journal of Neuroimmunology* 122:1-8.

165. Aloisi, F., F. Ria, G. Penna, and L. Adorini. 1998. Microglia Are More Efficient Than Astrocytes in Antigen Processing and in Th1 But Not Th2 Cell Activation. *The Journal of Immunology* 160:4671-4680.
166. Havenith, C. E. G., D. Askew, and W. S. Walker. 1998. Mouse resident microglia: Isolation and characterization of immunoregulatory properties with naïve CD4+ and CD8+ T-cells. *Glia* 22:348-359.
167. Jarry, U., P. Jeannin, L. Pineau, S. Donnou, Y. Delneste, and D. Couez. 2013. Efficiently stimulated adult microglia cross-prime naïve CD8+T cells injected in the brain. *Eur.J.Immunol.* 43:1173-1184.
168. Beauvillain, C., S. Donnou, U. Jarry, M. Scotet, H. Gascan, Y. Delneste, P. Guermonprez, P. Jeannin, and D. Couez. 2008. Neonatal and adult microglia cross-present exogenous antigens. *Glia* 56:69-77.
169. Ford, A. L., E. Foulcher, F. A. Lemckert, and J. D. Sedgwick. 1996. Microglia induce CD4 T lymphocyte final effector function and death. *The Journal of Experimental Medicine* 184:1737-1745.
170. Carson, M. J., J. G. Sutcliffe, and I. L. Campbell. 1999. Microglia stimulate naïve T-cell differentiation without stimulating T-cell proliferation. *J.Neurosci.Res.* 55:127-134.
171. Konno, H., T. Yamamoto, Y. Iwasaki, T. Saitoh, H. Suzuki, and H. Terunuma. 1989. Ia-expressing microglial cells in experimental allergic encephalomyelitis in rats. *Acta neuropathologica* 77:472-479.
172. Boyle, E. A. and P. L. McGeer. 1990. Cellular immune response in multiple sclerosis plaques. *The American journal of pathology* 137:575.
173. Bö, L., S. Mörk, P. A. Kong, H. Nyland, C. A. Pardo, and B. D. Trapp. 1994. Detection of MHC class II-antigens on macrophages and microglia, but not on astrocytes and endothelia in active multiple sclerosis lesions. *Journal of Neuroimmunology* 51:135-146.
174. Wong, G. H., P. F. Bartlett, I. A. N. Clark-Lewis, F. Battye, and J. W. Schrader. 1984. Inducible expression of H-2 and Ia antigens on brain cells. *Nature*.
175. Tan, L., K. B. Gordon, J. P. Mueller, L. A. Matis, and S. D. Miller. 1998. Presentation of Proteolipid Protein Epitopes and B7-1-Dependent Activation of Encephalitogenic T Cells by IFN- γ -Activated SJL/J Astrocytes. *The Journal of Immunology* 160:4271-4279.
176. Cornet, A., E. Bettelli, M. Oukka, C. Cambouris, V. Avellana-Adalid, K. Kosmatopoulos, and R. S. Liblau. 2000. Role of astrocytes in antigen presentation and naïve T-cell activation. *Journal of Neuroimmunology* 106:69-77.
177. Soos, J. M., T. A. Ashley, J. Morrow, J. C. Patarroyo, B. E. Sente, and S. S. Zamvil. 1999. Differential expression of B7 co-stimulatory molecules by astrocytes correlates with T cell activation and cytokine production. *International Immunology* 11:1169-1179.

178. Horwitz, M. S., C. F. Evans, F. G. Klier, and M. B. Oldstone. 1999. Detailed in vivo analysis of interferon-gamma induced major histocompatibility complex expression in the the central nervous system: astrocytes fail to express major histocompatibility complex class I and II molecules. *Lab Invest* 79:235-242.
179. Gresser, O., A. Hein, S. Riese, and A. Regnier-Vigouroux. 2000. Tumor necrosis factor alpha and interleukin-1 alpha inhibit through different pathways interferon-gamma-induced antigen presentation, processing and MHC class II surface expression on astrocytes, but not on microglia. *Cell and Tissue Research* 300:373-382.
180. Girvin, A. M., K. B. Gordon, C. J. Welsh, N. A. Clipstone, and S. D. Miller. 2002. Differential abilities of central nervous system resident endothelial cells and astrocytes to serve as inducible antigen-presenting cells. *Blood* 99:3692-3701.
181. Constantinescu, C. S., M. Tani, R. M. Ransohoff, M. Wysocka, B. Hilliard, T. Fujioka, S. Murphy, P. J. Tighe, J. D. Sarma, G. Trinchieri, and A. Rostami. 2005. Astrocytes as antigen-presenting cells: expression of IL-12/IL-23. *Journal of Neurochemistry* 95:331-340.
182. Klein, R. S. and M. S. Diamond. 2008. Immunological headgear: antiviral immune responses protect against neuroinvasive West Nile virus. *Trends in Molecular Medicine* 14:286-294.
183. Glass, W. G., J. K. Lim, R. Cholera, A. G. Pletnev, J. L. Gao, and P. M. Murphy. 2005. Chemokine receptor CCR5 promotes leukocyte trafficking to the brain and survival in West Nile virus infection. *The Journal of Experimental Medicine* 202:1087-1098.
184. Shrestha, B., M. A. Samuel, and M. S. Diamond. 2006. CD8+ T cells require perforin to clear West Nile virus from infected neurons. *Journal of Virology* 80:119-129.
185. Sitati, E. M. and M. S. Diamond. 2006. CD4+ T-cell responses are required for clearance of West Nile virus from the central nervous system. *Journal of Virology* 80:12060-12069.
186. Lim, J. K., C. J. Obara, A. Rivollier, A. G. Pletnev, B. L. Kelsall, and P. M. Murphy. 2011. Chemokine receptor Ccr2 is critical for monocyte accumulation and survival in West Nile virus encephalitis. *The Journal of Immunology* 186:471-478.
187. Zhang, B., Y. K. Chan, B. Lu, M. S. Diamond, and R. S. Klein. 2008. CXCR3 mediates region-specific antiviral T cell trafficking within the central nervous system during West Nile virus encephalitis. *The Journal of Immunology* 180:2641-2649.
188. Klein, R. S., E. Lin, B. Zhang, A. D. Luster, J. Tollett, M. A. Samuel, M. Engle, and M. S. Diamond. 2005. Neuronal CXCL10 directs CD8+ T-cell recruitment and control of West Nile virus encephalitis. *Journal of Virology* 79:11457-11466.

189. Glass, W. G., D. H. McDermott, J. K. Lim, S. Lekhong, S. F. Yu, W. A. Frank, J. Pape, R. C. Cheshier, and P. M. Murphy. 2006. CCR5 deficiency increases risk of symptomatic West Nile virus infection. *The Journal of Experimental Medicine* 203:35-40.
190. Liu, M. T., H. S. Keirstead, and T. E. Lane. 2001. Neutralization of the chemokine CXCL10 reduces inflammatory cell invasion and demyelination and improves neurological function in a viral model of multiple sclerosis. *The Journal of Immunology* 167:4091-4097.
191. Chen, B. P., W. A. Kuziel, and T. E. Lane. 2001. Lack of CCR2 results in increased mortality and impaired leukocyte activation and trafficking following infection of the central nervous system with a neurotropic coronavirus. *The Journal of Immunology* 167:4585-4592.
192. Lane, T. E., V. r. C. Asensio, N. Yu, A. D. Paoletti, I. L. Campbell, and M. J. Buchmeier. 1998. Dynamic regulation of α - and β -chemokine expression in the central nervous system during mouse hepatitis virus-induced demyelinating disease. *The Journal of Immunology* 160:970-978.
193. Dufour, J. H., M. Dziejman, M. T. Liu, J. H. Leung, T. E. Lane, and A. D. Luster. 2002. IFN- γ -inducible protein 10 (IP-10; CXCL10)-deficient mice reveal a role for IP-10 in effector T cell generation and trafficking. *The Journal of Immunology* 168:3195-3204.
194. Liu, M. T., B. P. Chen, P. Oertel, M. J. Buchmeier, D. Armstrong, T. A. Hamilton, and T. E. Lane. 2000. Cutting edge: the T cell chemoattractant IFN-inducible protein 10 is essential in host defense against viral-induced neurologic disease. *The Journal of Immunology* 165:2327-2330.
195. Liu, M. T., D. Armstrong, T. A. Hamilton, and T. E. Lane. 2001. Expression of Mig (monokine induced by interferon- γ) is important in T lymphocyte recruitment and host defense following viral infection of the central nervous system. *The Journal of Immunology* 166:1790-1795.
196. Glass, W. G., M. T. Liu, W. A. Kuziel, and T. E. Lane. 2001. Reduced macrophage infiltration and demyelination in mice lacking the chemokine receptor CCR5 following infection with a neurotropic coronavirus. *Virology* 288:8-17.
197. Glass, W. G. and T. E. Lane. 2003. Functional expression of chemokine receptor CCR5 on CD4⁺ T cells during virus-induced central nervous system disease. *Journal of Virology* 77:191-198.
198. Lane, T. E., M. T. Liu, B. P. Chen, V. r. C. Asensio, R. M. Samawi, A. D. Paoletti, I. L. Campbell, S. L. Kunkel, H. S. Fox, and M. J. Buchmeier. 2000. A central role for CD4⁺ T cells and RANTES in virus-induced central nervous system inflammation and demyelination. *Journal of Virology* 74:1415-1424.
199. Sato, W., A. Tomita, D. Ichikawa, Y. Lin, H. Kishida, S. Miyake, M. Ogawa, T. Okamoto, M. Murata, Y. Kuroiwa, T. Aranami, and T. Yamamura. 2012. CCR2⁺CCR5⁺ T Cells Produce Matrix Metalloproteinase-9 and Osteopontin

- in the Pathogenesis of Multiple Sclerosis. *The Journal of Immunology* 189:5057-5065.
200. Sørensen, T. L., M. Tani, J. Jensen, V. Pierce, C. Lucchinetti, V. A. Folcik, S. Qin, J. Rottman, F. Sellebjerg, R. M. Strieter, J. L. Frederiksen, and R. M. Ransohoff. 1999. Expression of specific chemokines and chemokine receptors in the central nervous system of multiple sclerosis patients. *J Clin Invest* 103:807-815.
 201. Trebst, C., T. Lykke Sørensen, P. Kivisäkk, M. K. Cathcart, J. Hesselgesser, R. Horuk, F. Sellebjerg, H. Lassmann, and R. M. Ransohoff. 2001. CCR1+/CCR5+ Mononuclear Phagocytes Accumulate in the Central Nervous System of Patients with Multiple Sclerosis. *The American journal of pathology* 159:1701-1710.
 202. Nakajima, H., K. Fukuda, M. Sugino, F. Kimura, T. Hanafusa, T. Ikemoto, and A. Shimizu. 2004. Expression of TH1/TH2-related chemokine receptors on peripheral T cells and correlation with clinical disease activity in patients with multiple sclerosis. *European neurology* 52:162-168.
 203. Bartosik-Psujek, H. and Z. Stelmasiak. 2005. The levels of chemokines CXCL8, CCL2 and CCL5 in multiple sclerosis patients are linked to the activity of the disease. *European journal of neurology* 12:49-54.
 204. Simpson, J. E., J. Newcombe, M. L. Cuzner, and M. N. Woodroffe. 1998. Expression of monocyte chemoattractant protein-1 and other β -chemokines by resident glia and inflammatory cells in multiple sclerosis lesions. *Journal of Neuroimmunology* 84:238-249.
 205. Karpus, W. J., N. W. Lukacs, B. L. McRae, R. M. Strieter, S. L. Kunkel, and S. D. Miller. 1995. An important role for the chemokine macrophage inflammatory protein-1 alpha in the pathogenesis of the T cell-mediated autoimmune disease, experimental autoimmune encephalomyelitis. *The Journal of Immunology* 155:5003-5010.
 206. dos Santos, A. C., M. M. Barsante, R. M. Esteves Arantes, C. C. A. Bernard, M. M. Teixeira, and J. Carvalho-Tavares. 2005. CCL2 and CCL5 mediate leukocyte adhesion in experimental autoimmune encephalomyelitis—an intravital microscopy study. *Journal of Neuroimmunology* 162:122-129.
 207. Glabinski, A. R., V. K. Tuohy, and R. M. Ransohoff. 1998. Expression of chemokines RANTES, MIP-1alpha and GRO-alpha correlates with inflammation in acute experimental autoimmune encephalomyelitis. *Neuroimmunomodulation* 5:166-171.
 208. Tran, E. H., W. A. Kuziel, and T. Owens. 2000. Induction of experimental autoimmune encephalomyelitis in C57BL/6 mice deficient in either the chemokine macrophage inflammatory protein-1 α or its CCR5 receptor. *Eur.J.Immunol.* 30:1410-1415.
 209. Bennetts, B. H., S. M. Teutsch, M. M. Buhler, R. N. Heard, and G. J. Stewart. 1997. The CCR5 deletion mutation fails to protect against multiple sclerosis. *Human immunology* 58:52-59.

210. Rottman, J., A. J. Slavin, R. Silva, H. Weiner, C. Gerard, and W. Hancock. 2000. Leukocyte recruitment during onset of experimental allergic encephalomyelitis is CCR1 dependent. *Eur.J.Immunol.* 30:2372-2377.
211. Liang, M., C. Mallari, M. Rosser, H. P. Ng, K. May, S. Monahan, J. G. Bauman, I. Islam, A. Ghannam, and B. Buckman. 2000. Identification and characterization of a potent, selective, and orally active antagonist of the CC chemokine receptor-1. *Journal of Biological Chemistry* 275:19000-19008.
212. Zipp, F., H. P. Hartung, J. Hillert, S. Schimrigk, C. Trebst, M. Stangel, C. Infante-Duarte, P. Jakobs, C. Wolf, and R. Sandbrink. 2006. Blockade of chemokine signaling in patients with multiple sclerosis. *Neurology* 67:1880-1883.
213. Sindern, E., T. Patzold, L. M. Ossege, A. Gisevius, and J. P. Malin. 2002. Expression of chemokine receptor CXCR3 on cerebrospinal fluid T-cells is related to active MRI lesion appearance in patients with relapsing-remitting multiple sclerosis. *Journal of Neuroimmunology* 131:186-190.
214. Sørensen, T. L., C. Trebst, P. Kivisäkk, K. L. Klaege, A. Majmudar, R. Ravid, H. Lassmann, D. B. Olsen, R. M. Strieter, R. M. Ransohoff, and F. Sellebjerg. 2002. Multiple sclerosis: a study of CXCL10 and CXCR3 colocalization in the inflamed central nervous system. *Journal of Neuroimmunology* 127:59-68.
215. Fife, B. T., K. J. Kennedy, M. C. Paniagua, N. W. Lukacs, S. L. Kunkel, A. D. Luster, and W. J. Karpus. 2001. CXCL10 (IFN- γ -inducible protein-10) control of encephalitogenic CD4⁺ T cell accumulation in the central nervous system during experimental autoimmune encephalomyelitis. *The Journal of Immunology* 166:7617-7624.
216. Klein, R. S., L. Izikson, T. Means, H. D. Gibson, E. Lin, R. A. Sobel, H. L. Weiner, and A. D. Luster. 2004. IFN-inducible protein 10/CXC chemokine ligand 10-independent induction of experimental autoimmune encephalomyelitis. *The Journal of Immunology* 172:550-559.
217. Kohler, R. E., I. Comerford, S. Townley, S. Haylock-Jacobs, I. Clark-Lewis, and S. R. McColl. 2008. Antagonism of the chemokine receptors CXCR3 and CXCR4 reduces the pathology of experimental autoimmune encephalomyelitis. *Brain Pathology* 18:504-516.
218. Liu, L., D. Huang, M. Matsui, T. T. He, T. Hu, J. DeMartino, B. Lu, C. Gerard, and R. M. Ransohoff. 2006. Severe disease, unaltered leukocyte migration, and reduced IFN- γ production in CXCR3^{-/-} mice with experimental autoimmune encephalomyelitis. *The Journal of Immunology* 176:4399-4409.
219. Lalor, S. J. and B. M. Segal. 2013. Th1-mediated experimental autoimmune encephalomyelitis is CXCR3 independent. *Eur.J.Immunol.* 43:2866-2874.
220. Müller, M., S. L. Carter, M. J. Hofer, P. Manders, D. R. Getts, M. T. Getts, A. Dreykluft, B. Lu, C. Gerard, and N. J. King. 2007. CXCR3 signaling

- reduces the severity of experimental autoimmune encephalomyelitis by controlling the parenchymal distribution of effector and regulatory T cells in the central nervous system. *The Journal of Immunology* 179:2774-2786.
221. Carter, S. L., M. Müller, P. M. Manders, and I. L. Campbell. 2007. Induction of the genes for Cxcl9 and Cxcl10 is dependent on IFN- γ but shows differential cellular expression in experimental autoimmune encephalomyelitis and by astrocytes and microglia in vitro. *Glia* 55:1728-1739.
 222. McManus, C., J. W. Berman, F. M. Brett, H. Staunton, M. Farrell, and C. F. Brosnan. 1998. MCP-1, MCP-2 and MCP-3 expression in multiple sclerosis lesions: an immunohistochemical and in situ hybridization study. *Journal of Neuroimmunology* 86:20-29.
 223. Mahad, D. J., S. J. L. Howell, and M. N. Woodroffe. 2002. Expression of chemokines in the CSF and correlation with clinical disease activity in patients with multiple sclerosis. *Journal of Neurology, Neurosurgery & Psychiatry* 72:498-502.
 224. Mahad, D., M. K. Callahan, K. A. Williams, E. E. Ubogu, P. Kivisäkk, B. Tucky, G. Kidd, G. A. Kingsbury, A. Chang, and R. J. Fox. 2006. Modulating CCR2 and CCL2 at the blood-brain barrier: relevance for multiple sclerosis pathogenesis. *Brain* 129:212-223.
 225. Ransohoff, R. M., T. A. Hamilton, M. Tani, M. H. Stoler, H. E. Shick, J. A. Major, M. L. Estes, D. M. Thomas, and V. K. Tuohy. 1993. Astrocyte expression of mRNA encoding cytokines IP-10 and JE/MCP-1 in experimental autoimmune encephalomyelitis. *The FASEB Journal* 7:592-600.
 226. Glabinski, A. R., M. Tani, R. M. Strieter, V. K. Tuohy, and R. M. Ransohoff. 1997. Synchronous synthesis of alpha-and beta-chemokines by cells of diverse lineage in the central nervous system of mice with relapses of chronic experimental autoimmune encephalomyelitis. *The American journal of pathology* 150:617.
 227. Fife, B. T., G. B. Huffnagle, W. A. Kuziel, and W. J. Karpus. 2000. Cc Chemokine Receptor 2 Is Critical for Induction of Experimental Autoimmune Encephalomyelitis. *The Journal of Experimental Medicine* 192:899-906.
 228. Izikson, L., R. S. Klein, I. F. Charo, H. L. Weiner, and A. D. Luster. 2000. Resistance to experimental autoimmune encephalomyelitis in mice lacking the CC chemokine receptor (CCR2). *The Journal of Experimental Medicine* 192:1075-1080.
 229. Huang, D., J. Wang, P. Kivisäkk, B. J. Rollins, and R. M. Ransohoff. 2001. Absence of Monocyte Chemoattractant Protein 1 in Mice Leads to Decreased Local Macrophage Recruitment and Antigen-Specific T Helper Cell Type 1 Immune Response in Experimental Autoimmune Encephalomyelitis. *The Journal of Experimental Medicine* 193:713-726.

230. Bachelierie, F., A. Ben Baruch, A. M. Burkhardt, C. Combadiere, J. M. Farber, G. J. Graham, R. Horuk, A. H. Sparre-Ulrich, M. Locati, and A. D. Luster. 2014. International Union of Pharmacology. LXXXIX. Update on the Extended Family of Chemokine Receptors and Introducing a New Nomenclature for Atypical Chemokine Receptors. *Pharmacological reviews* 66:1-79.
231. Alt, C., M. Laschinger, and B. Engelhardt. 2002. Functional expression of the lymphoid chemokines CCL19 (ELC) and CCL 21 (SLC) at the blood-brain barrier suggests their involvement in G-protein-dependent lymphocyte recruitment into the central nervous system during experimental autoimmune encephalomyelitis. *Eur.J.Immunol.* 32:2133-2144.
232. Kivisäkk, P., D. J. Mahad, M. K. Callahan, K. Sikora, C. Trebst, B. Tucky, J. Wujek, R. Ravid, S. M. Staugaitis, and H. Lassmann. 2004. Expression of CCR7 in multiple sclerosis: implications for CNS immunity. *Annals of neurology* 55:627-638.
233. Reboldi, A., C. Coisne, D. Baumjohann, F. Benvenuto, D. Bottinelli, S. Lira, A. Uccelli, A. Lanzavecchia, B. Engelhardt, and F. Sallusto. 2009. CC chemokine receptor 6-regulated entry of TH-17 cells into the CNS through the choroid plexus is required for the initiation of EAE. *Nat Immunol* 10:514-523.
234. Hamann, I., F. Zipp, and C. Infante-Duarte. 2008. Therapeutic targeting of chemokine signaling in Multiple Sclerosis. *Journal of the neurological sciences* 274:31-38.
235. Wolff, S., S. Klatt, J. C. Wolff, J. Wilhelm, L. Fink, M. Kaps, and B. Rosengarten. 2009. Endotoxin-induced gene expression differences in the brain and effects of iNOS inhibition and norepinephrine. *Intensive care medicine* 35:730-739.
236. Rummel, C., W. Inoue, S. Poole, and G. N. Luheshi. 2009. Leptin regulates leukocyte recruitment into the brain following systemic LPS-induced inflammation. *Mol Psychiatry* 15:523-534.
237. Zhou, H., G. Andonegui, C. H. Wong, and P. Kubes. 2009. Role of endothelial TLR4 for neutrophil recruitment into central nervous system microvessels in systemic inflammation. *The Journal of Immunology* 183:5244-5250.
238. Erickson, M. A. and W. A. Banks. 2011. Cytokine and chemokine responses in serum and brain after single and repeated injections of lipopolysaccharide: multiplex quantification with path analysis. *Brain, Behavior, and Immunity* 25:1637-1648.
239. Konat, G. W., E. Borysiewicz, D. Fil, and I. James. 2009. Peripheral challenge with double-stranded RNA elicits global up-regulation of cytokine gene expression in the brain. *J.Neurosci.Res.* 87:1381-1388.
240. Fil, D., E. Borysiewicz, and G. W. Konat. 2011. A broad upregulation of cerebral chemokine genes by peripherally-generated inflammatory mediators. *Metabolic brain disease* 26:49-59.

241. D'Mello, C., T. Le, and M. G. Swain. 2009. Cerebral Microglia Recruit Monocytes into the Brain in Response to Tumor Necrosis Factor- α Signaling during Peripheral Organ Inflammation. *The Journal of Neuroscience* 29:2089-2102.
242. Tavares, E. and F. J. Miñano. 2004. Differential sensitivities of pyrogenic chemokine fevers to CC chemokine receptor 5 antibodies. *Fundamental & clinical pharmacology* 18:163-169.
243. Machado, R. R., D. M. Soares, A. E. Proudfoot, and G. r. E. Souza. 2007. CCR1 and CCR5 chemokine receptors are involved in fever induced by LPS (*E. coli*) and RANTES in rats. *Brain Research* 1161:21-31.
244. Wynne, A. M., C. J. Henry, Y. Huang, A. Cleland, and J. P. Godbout. 2010. Protracted downregulation of CX3CR1 on microglia of aged mice after lipopolysaccharide challenge. *Brain, Behavior, and Immunity* 24:1190-1201.
245. Corona, A., Y. Huang, J. O'Connor, R. Dantzer, K. Kelley, P. Popovich, and J. Godbout. 2010. Fractalkine receptor (CX3CR1) deficiency sensitizes mice to the behavioral changes induced by lipopolysaccharide. *Journal of Neuroinflammation* 7:93.
246. Banisadr, G., P. Fontanges, F. Haour, P. Kitabgi, W. Rostène, and S. Mélik Parsadaniantz. 2002. Neuroanatomical distribution of CXCR4 in adult rat brain and its localization in cholinergic and dopaminergic neurons. *European Journal of Neuroscience* 16:1661-1671.
247. Banisadr, G., D. Skrzydelski, P. Kitabgi, W. Rostène, and S. M. Parsadaniantz. 2003. Highly regionalized distribution of stromal cell-derived factor-1/CXCL12 in adult rat brain: constitutive expression in cholinergic, dopaminergic and vasopressinergic neurons. *European Journal of Neuroscience* 18:1593-1606.
248. Heinisch, S. and L. G. Kirby. 2010. SDF-1 α /CXCL12 enhances GABA and glutamate synaptic activity at serotonin neurons in the rat dorsal raphe nucleus. *Neuropharmacology* 58:501-514.
249. Callewaere, C., G. Banisadr, M. G. Desarménien, P. Mechighel, P. Kitabgi, W. H. Rostène, and S. Mélik Parsadaniantz. 2006. The chemokine SDF-1/CXCL12 modulates the firing pattern of vasopressin neurons and counteracts induced vasopressin release through CXCR4. *Proceedings of the National Academy of Sciences* 103:8221-8226.
250. Banisadr, G., R. D. Gosselin, P. Mechighel, W. Rostène, P. Kitabgi, and S. Mélik Parsadaniantz. 2005. Constitutive neuronal expression of CCR2 chemokine receptor and its colocalization with neurotransmitters in normal rat brain: Functional effect of MCP-1/CCL2 on calcium mobilization in primary cultured neurons. *J.Comp.Neurol.* 492:178-192.
251. Gosselin, R. D., C. Varela, G. Banisadr, P. Mechighel, W. Rostène, P. Kitabgi, and S. Mélik-Parsadaniantz. 2005. Constitutive expression of CCR2 chemokine receptor and inhibition by MCP-1/CCL2 of GABA-induced

- currents in spinal cord neurones. *Journal of Neurochemistry* 95:1023-1034.
252. Banisadr, G., R. D. Gosselin, P. Mechighel, P. Kitabgi, W. Rostène, and S. M. Parsadaniantz. 2005. Highly regionalized neuronal expression of monocyte chemoattractant protein-1 (MCP-1/CCL2) in rat brain: Evidence for its colocalization with neurotransmitters and neuropeptides. *J.Comp.Neurol.* 489:275-292.
 253. Guyon, A., D. Skrzydelski, C. Rovère, W. Rostène, S. Mélik Parsadaniantz, and J. L. Nahon. 2006. Stromal cell-derived factor-1 α modulation of the excitability of rat substantia nigra dopaminergic neurones: presynaptic mechanisms. *Journal of Neurochemistry* 96:1540-1550.
 254. Zhou, Y., H. Tang, J. Liu, J. Dong, and H. Xiong. 2011. Chemokine CCL2 modulation of neuronal excitability and synaptic transmission in rat hippocampal slices. *Journal of Neurochemistry* 116:406-414.
 255. Guyon, A., D. Skrzydelski, I. De Giry, C. Rovère, G. Conductier, J. M. Trocello, V. Daugé, P. Kitabgi, W. Rostène, J. L. Nahon, and S. Mélik Parsadaniantz. 2009. Long term exposure to the chemokine CCL2 activates the nigrostriatal dopamine system: a novel mechanism for the control of dopamine release. *Neuroscience* 162:1072-1080.
 256. Skrzydelski, D., A. Guyon, V. Daugé, C. Rovère, E. Apartis, P. Kitabgi, J. L. Nahon, W. Rostène, and S. M. l. Parsadaniantz. 2007. The chemokine stromal cell-derived factor-1/CXCL12 activates the nigrostriatal dopamine system. *Journal of Neurochemistry* 102:1175-1183.
 257. Hughes, P. M., M. S. Botham, S. Frenzel, A. Mir, and V. H. Perry. 2002. Expression of fractalkine (CX3CL1) and its receptor, CX3CR1, during acute and chronic inflammation in the rodent CNS. *Glia* 37:314-327.
 258. Nishiyori, A., M. Minami, Y. Ohtani, S. Takami, J. Yamamoto, N. Kawaguchi, T. Kume, A. Akaike, and M. Satoh. 1998. Localization of fractalkine and CX3CR1 mRNAs in rat brain: does fractalkine play a role in signaling from neuron to microglia? *FEBS Letters* 429:167-172.
 259. Jung, S., J. Aliberti, P. Graemmel, M. J. Sunshine, G. W. Kreutzberg, A. Sher, and D. R. Littman. 2000. Analysis of fractalkine receptor CX3CR1 function by targeted deletion and green fluorescent protein reporter gene insertion. *Molecular and Cellular Biology* 20:4106-4114.
 260. Bhaskar, K., M. Konerth, O. N. Kokiko-Cochran, A. Cardona, R. M. Ransohoff, and B. T. Lamb. 2010. Regulation of tau pathology by the microglial fractalkine receptor. *Neuron* 68:19-31.
 261. Chen, M., C. Luo, R. Penalva, and H. Xu. 2013. Paraquat-Induced Retinal Degeneration Is Exaggerated in CX3CR1-Deficient Mice and Is Associated with Increased Retinal Inflammation. *Investigative Ophthalmology & Visual Science* 54:682-690.
 262. Cho, S. H., B. Sun, Y. Zhou, T. M. Kauppinen, B. Halabisky, P. Wes, R. M. Ransohoff, and L. Gan. 2011. CX3CR1 Protein Signaling Modulates

Microglial Activation and Protects against Plaque-independent Cognitive Deficits in a Mouse Model of Alzheimer Disease. *Journal of Biological Chemistry* 286:32713-32722.

263. Bachstetter, A. D., J. M. Morganti, J. Jernberg, A. Schlunk, S. Mitchell, K. W. Brewster, C. E. Hudson, M. J. Cole, J. K. Harrison, P. C. Bickford, and C. Gemma. 2011. Fractalkine and CX3CR1 regulate hippocampal neurogenesis in adult and aged rats. *Neurobiol Aging* 32:2030-2044.
264. Sierra, A., J. M. Encinas, J. J. P. Deudero, J. H. Chancey, G. Enikolopov, L. S. Overstreet-Wadiche, S. E. Tsirka, and M. Maletic-Savatic. 2010. Microglia Shape Adult Hippocampal Neurogenesis through Apoptosis-Coupled Phagocytosis. *Cell Stem Cell* 7:483-495.
265. Ziemssen, T. and S. Kern. 2007. Psychoneuroimmunology-cross-talk between the immune and nervous systems. *Journal of neurology* 254:118-1111.
266. Dantzer, R., J. C. O'Connor, G. G. Freund, R. W. Johnson, and K. W. Kelley. 2008. From inflammation to sickness and depression: when the immune system subjugates the brain. *Nat Rev Neurosci* 9:46-56.
267. Viljoen, M. and A. Panzer. 2003. Sickness behaviour: causes and effects. *South African Family Practice* 45:9-12.
268. Dantzer, R. and K. W. Kelley. 2007. Twenty years of research on cytokine-induced sickness behavior. *Brain, Behavior, and Immunity* 21:153-160.
269. Reichenberg, A., R. Yirmiya, and A. Schuld. 2001. CYtokine-associated emotional and cognitive disturbances in humans. *Archives of General Psychiatry* 58:445-452.
270. Brydon, L., N. A. Harrison, C. Walker, A. Steptoe, and H. D. Critchley. 2008. Peripheral Inflammation is Associated with Altered Substantia Nigra Activity and Psychomotor Slowing in Humans. *Biol Psychiatry* 63:1022-1029.
271. Wright, C. E., P. C. Strike, L. Brydon, and A. Steptoe. 2005. Acute inflammation and negative mood: Mediation by cytokine activation. *Brain, Behavior, and Immunity* 19:345-350.
272. Krabbe, K. S., A. Reichenberg, R. Yirmiya, A. Smed, B. K. Pedersen, and H. Bruunsgaard. 2005. Low-dose endotoxemia and human neuropsychological functions. *Brain, Behavior, and Immunity* 19:453-460.
273. Fermo, S. L., R. Barone, F. Patti, P. Laisa, T. L. Cavallaro, A. Nicoletti, and M. Zappia. 2010. Outcome of psychiatric symptoms presenting at onset of multiple sclerosis: a retrospective study. *Multiple Sclerosis* 16:742-748.
274. Dickens, C., L. McGowan, D. Clark-Carter, and F. Creed. 2002. Depression in Rheumatoid Arthritis: A Systematic Review of the Literature With Meta-Analysis. *Psychosomatic Medicine* 64:52-60.

275. Addolorato, G., E. Capristo, G. F. Stefanini, and G. Gasbarrini. 1997. Inflammatory Bowel Disease: A Study of the Association between Anxiety and Depression, Physical Morbidity, and Nutritional Status. *Scand J Gastroenterol* 32:1013-1021.
276. Tying, S., A. Gottlieb, K. Papp, K. Gordon, C. Leonardi, A. Wang, D. Lalla, M. Woolley, A. Jahreis, and R. Zitnik. 2006. Etanercept and clinical outcomes, fatigue, and depression in psoriasis: double-blind placebo-controlled randomised phase III trial. *The Lancet* 367:29-35.
277. Capuron, L., J. F. Gumnick, D. L. Musselman, D. H. Lawson, A. Reemsnyder, C. B. Nemeroff, and A. H. Miller. 2002. Neurobehavioral effects of interferon-alpha in cancer patients: phenomenology and paroxetine responsiveness of symptom dimensions. *Neuropsychopharmacology* 26:643-652.
278. Schaefer, M., M. Schwaiger, A. S. Garkisch, M. Pich, A. Hinzpeter, R. Uebelhack, A. Heinz, F. van Boemmel, and T. Berg. 2005. Prevention of interferon-alpha associated depression in psychiatric risk patients with chronic hepatitis C. *Journal of Hepatology* 42:793-798.
279. Sockalingam, S., P. S. Links, and S. E. Abbey. 2011. Suicide risk in hepatitis C and during interferon-alpha therapy: a review and clinical update. *Journal of Viral Hepatitis* 18:153-160.
280. Kammula, U. S., D. E. White, and S. A. Rosenberg. 1998. Trends in the safety of high dose bolus interleukin-2 administration in patients with metastatic cancer. *Cancer* 83:797-805.
281. Chai, Z., S. Gatti, C. Toniatti, V. Poli, and T. Bartfai. 1996. Interleukin (IL)-6 gene expression in the central nervous system is necessary for fever response to lipopolysaccharide or IL-1 beta: a study on IL-6-deficient mice. *The Journal of Experimental Medicine* 183:311-316.
282. Kozak, W., M. J. Kluger, D. Soszynski, C. A. Conn, K. Rudolph, L. R. Leon, and H. Zheng. 1998. IL-6 and IL-1 beta in fever. Studies using cytokine-deficient (knockout) mice. *Ann N Y Acad Sci* 856:33-47.
283. Layé, S., G. Gheusi, S. Cremona, C. Combe, K. Kelley, R. Dantzer, and P. Parnet. 2000. Endogenous brain IL-1 mediates LPS-induced anorexia and hypothalamic cytokine expression. *American Journal of Physiology - Regulatory, Integrative and Comparative Physiology* 279:R93-R98.
284. Rivier, C., R. Chizzonite, and W. Vale. 1989. In the mouse, the activation of the hypothalamic-pituitary-adrenal axis by a lipopolysaccharide (endotoxin) is mediated through interleukin-1. *Endocrinology* 125:2800-2805.
285. Takemura, T., S. Makino, T. Takao, K. Asaba, S. Suemaru, and K. Hashimoto. 1997. Hypothalamic-pituitary-adrenocortical responses to single vs. repeated endotoxin lipopolysaccharide administration in the rat. *Brain Research* 767:181-191.

286. Bluthé, R. M., M. Pawlowski, S. Suarez, P. Parnet, Q. Pittman, K. W. Kelley, and R. Dantzer. 1994. Synergy between tumor necrosis factor α and interleukin-1 in the induction of sickness behavior in mice. *Psychoneuroendocrinology* 19:197-207.
287. Fleshner, M., L. E. Goehler, B. A. Schwartz, M. McGorry, D. Martin, S. F. Maier, and L. R. Watkins. 1998. Thermogenic and corticosterone responses to intravenous cytokines (IL-1 β and TNF α) are attenuated by subdiaphragmatic vagotomy. *Journal of Neuroimmunology* 86:134-141.
288. Kent, S., J. L. Bret-Dibat, K. W. Kelley, and R. Dantzer. 1996. Mechanisms of sickness-induced decreases in food-motivated behavior. *Neuroscience & Biobehavioral Reviews* 20:171-175.
289. Luheshi, G. N., R. M. Bluthé, D. Rushforth, N. Mulcahy, J. P. Konsman, M. Goldbach, and R. Dantzer. 2000. Vagotomy attenuates the behavioural but not the pyrogenic effects of interleukin-1 in rats. *Autonomic Neuroscience* 85:127-132.
290. Plata-Salamán, R. 1999. Brain mechanisms in cytokine-induced anorexia. *Psychoneuroendocrinology* 24:25-41.
291. Wieczorek, M., A. H. Swiergiel, H. Pournajafi-Nazarloo, and A. J. Dunn. 2005. Physiological and behavioral responses to interleukin-1 β and LPS in vagotomized mice. *Physiology & Behavior* 85:500-511.
292. Bluthé, R. M., R. Dantzer, and K. W. Kelley. 1992. Effects of interleukin-1 receptor antagonist on the behavioral effects of lipopolysaccharide in rat. *Brain Research* 573:318-320.
293. Frank, M. G., R. M. Barrientos, B. M. Thompson, M. D. Weber, L. R. Watkins, and S. F. Maier. 2012. IL-1RA injected intra-cisterna magna confers extended prophylaxis against lipopolysaccharide-induced neuroinflammatory and sickness responses. *Journal of Neuroimmunology* 252:33-39.
294. Kozak, W., H. Zheng, C. A. Conn, D. Soszynski, L. H. van der Ploeg, and M. J. Kluger. 1995. Thermal and behavioral effects of lipopolysaccharide and influenza in interleukin-1 beta-deficient mice. *American Journal of Physiology - Regulatory, Integrative and Comparative Physiology* 269:R969-R977.
295. Maier, S. F., E. P. Wiertelak, D. Martin, and L. R. Watkins. 1993. Interleukin-1 mediates the behavioral hyperalgesia produced by lithium chloride and endotoxin. *Brain Research* 623:321-324.
296. Yirmiya, R., Y. Pollak, O. Barak, R. Avitsur, H. Ovadia, M. Bette, E. Weihe, and J. Weidenfeld. 2001. Effects of Antidepressant Drugs on the Behavioral and Physiological Responses to Lipopolysaccharide (LPS) in Rodents. *Neuropsychopharmacology* 24:531-544.
297. Yirmiya, R., J. Weidenfeld, Y. Pollak, M. Morag, A. Morag, R. Avitsur, O. Barak, I. A. Reichenberg, E. Cohen, Y. Shavit, and H. Ovadia. 1999. Cytokines, "Depression Due to A General Medical Condition," and

- Antidepressant Drugs. In *Cytokines, Stress, and Depression*. R. Dantzer, E. Wollman, and R. Yirmiya, eds. Springer US, pp. 283-316.
298. Shen, Y., T. J. Connor, Y. Nolan, J. P. Kelly, and B. E. Leonard. 1999. Differential effect of chronic antidepressant treatments on lipopolysaccharide-induced depressive-like behavioural symptoms in the rat. *Life Sciences* 65:1773-1786.
 299. Frenois, F., M. t. Moreau, J. O'Connor, M. Lawson, C. Micon, J. Lestage, K. W. Kelley, R. Dantzer, and N. Castanon. 2007. Lipopolysaccharide induces delayed FosB/DeltaFosB immunostaining within the mouse extended amygdala, hippocampus and hypothalamus, that parallel the expression of depressive-like behavior. *Psychoneuroendocrinology* 32:516-531.
 300. Dowlati, Y., N. Herrmann, W. Swardfager, H. Liu, L. Sham, E. K. Reim, and K. L. Lanctôt. 2010. A Meta-Analysis of Cytokines in Major Depression. *Biol Psychiatry* 67:446-457.
 301. Akhondzadeh, S., S. Jafari, F. Raisi, A. A. Nasehi, A. Ghoreishi, B. Salehi, S. Mohebbi-Rasa, M. Raznahan, and A. Kamalipour. 2009. Clinical trial of adjunctive celecoxib treatment in patients with major depression: a double blind and placebo controlled trial. *Depress.Anxiety* 26:607-611.
 302. Müller, N., M. J. Schwarz, S. Dehning, A. Douhe, A. Cerovecki, B. Goldstein-Müller, I. Spellmann, G. Hetzel, K. Maino, N. Kleindienst, H. J. Möller, V. Arolt, and M. Riedel. 2006. The cyclooxygenase-2 inhibitor celecoxib has therapeutic effects in major depression: results of a double-blind, randomized, placebo controlled, add-on pilot study to reboxetine. *Mol Psychiatry* 11:680-684.
 303. Mendlewicz, J., P. Kriwin, P. Oswald, D. Souery, S. Alboni, and N. Brunello. 2006. Shortened onset of action of antidepressants in major depression using acetylsalicylic acid augmentation: a pilot open-label study. *International Clinical Psychopharmacology* 21.
 304. Banks, W. A., A. J. Kastin, and E. G. Gutierrez. 1994. Penetration of interleukin-6 across the murine blood-brain barrier. *Neuroscience Letters* 179:53-56.
 305. Banks, W. A., L. Ortiz, S. R. Plotkin, and A. J. Kastin. 1991. Human interleukin (IL) 1 alpha, murine IL-1 alpha and murine IL-1 beta are transported from blood to brain in the mouse by a shared saturable mechanism. *Journal of Pharmacology and Experimental Therapeutics* 259:988-996.
 306. Gutierrez, E. G., W. A. Banks, and A. J. Kastin. 1993. Murine tumor necrosis factor alpha is transported from blood to brain in the mouse. *Journal of Neuroimmunology* 47:169-176.
 307. Pan, W., W. A. Banks, and A. J. Kastin. 1997. Permeability of the blood-brain and blood-spinal cord barriers to interferons. *Journal of Neuroimmunology* 76:105-111.

308. Pan, W., Y. Ding, Y. Yu, H. Ohtaki, T. Nakamachi, and A. J. Kastin. 2006. Stroke upregulates TNF α transport across the blood-brain barrier. *Experimental Neurology* 198:222-233.
309. Jaeger, L. B., S. Dohgu, R. Sultana, J. L. Lynch, J. B. Owen, M. A. Erickson, G. N. Shah, T. O. Price, M. A. Fleegal-Demotta, D. A. Butterfield, and W. A. Banks. 2009. Lipopolysaccharide alters the blood-brain barrier transport of amyloid β protein: A mechanism for inflammation in the progression of Alzheimer's disease. *Brain, Behavior, and Immunity* 23:507-517.
310. Xiaio, H., W. A. Banks, M. L. Niehoff, and J. E. Morley. 2001. Effect of LPS on the permeability of the blood-brain barrier to insulin. *Brain Research* 896:36-42.
311. Banks, W. A., S. A. Farr, M. E. La Scola, and J. E. Morley. 2001. Intravenous Human Interleukin-1 β Impairs Memory Processing in Mice: Dependence on Blood-Brain Barrier Transport into Posterior Division of the Septum. *Journal of Pharmacology and Experimental Therapeutics* 299:536-541.
312. Nadeau, S. and S. Rivest. 1999. Effects of circulating tumor necrosis factor on the neuronal activity and expression of the genes encoding the tumor necrosis factor receptors (p55 and p75) in the rat brain: a view from the blood-brain-barrier. *Neuroscience* 93:1449-1464.
313. Vallières, L. and S. Rivest. 1997. Regulation of the Genes Encoding Interleukin-6, Its Receptor, and gp130 in the Rat Brain in Response to the Immune Activator Lipopolysaccharide and the Proinflammatory Cytokine Interleukin-1 β . *Journal of Neurochemistry* 69:1668-1683.
314. Vallières, L., S. Lacroix, and S. Rivest. 1997. Influence of Interleukin-6 on Neural Activity and Transcription of the Gene Encoding Corticotrophin-releasing Factor in the Rat Brain: An Effect Depending Upon the Route of Administration. *European Journal of Neuroscience* 9:1461-1472.
315. Quan, N., M. Whiteside, and M. Herkenham. 1998. Time course and localization patterns of interleukin-1 β messenger rna expression in brain and pituitary after peripheral administration of lipopolysaccharide. *Neuroscience* 83:281-293.
316. Chakravarty, S. and M. Herkenham. 2005. Toll-Like Receptor 4 on Nonhematopoietic Cells Sustains CNS Inflammation during Endotoxemia, Independent of Systemic Cytokines. *The Journal of Neuroscience* 25:1788-1796.
317. Nadeau, S. and S. Rivest. 2000. Role of microglial-derived tumor necrosis factor in mediating CD14 transcription and nuclear factor kappa B activity in the brain during endotoxemia. *J Neurosci* 20:3456-3468.
318. Laflamme, N., G. v. Soucy, and S. Rivest. 2001. Circulating cell wall components derived from gram-negative, not gram-positive, bacteria cause a profound induction of the gene-encoding Toll-like receptor 2 in the CNS. *Journal of Neurochemistry* 79:648-657.

319. Lacroix, S., D. Feinstein, and S. Rivest. 1998. The Bacterial Endotoxin Lipopolysaccharide has the Ability to Target the Brain in Upregulating Its Membrane CD14 Receptor Within Specific Cellular Populations. *Brain Pathology* 8:625-640.
320. Laflamme, N. and S. Rivest. 1999. Effects of Systemic Immunogenic Insults and Circulating Proinflammatory Cytokines on the Transcription of the Inhibitory Factor I κ B- α Within Specific Cellular Populations of the Rat Brain. *Journal of Neurochemistry* 73:309-321.
321. Zhang, Y. H., J. Lu, J. K. Elmquist, and C. B. Saper. 2003. Specific roles of cyclooxygenase-1 and cyclooxygenase-2 in lipopolysaccharide-induced fever and fos expression in rat brain. *J.Comp.Neurol.* 463:3-12.
322. Chun, K. S. and Y. J. Surh. 2004. Signal transduction pathways regulating cyclooxygenase-2 expression: potential molecular targets for chemoprevention. *Biochemical Pharmacology* 68:1089-1100.
323. Lacroix, S. and S. Rivest. 1998. Effect of Acute Systemic Inflammatory Response and Cytokines on the Transcription of the Genes Encoding Cyclooxygenase Enzymes (COX-1 and COX-2) in the Rat Brain. *Journal of Neurochemistry* 70:452-466.
324. Serrats, J., J. C. Schiltz, B. Garcia-Bueno, N. van Rooijen, T. M. Reyes, and P. E. Sawchenko. 2010. Dual Roles for Perivascular Macrophages in Immune-to-Brain Signaling. *Neuron* 65:94-106.
325. Ek, M., D. Engblom, S. Saha, A. Blomqvist, P. J. Jakobsson, and A. Ericsson-Dahlstrand. 2001. Inflammatory response: pathway across the blood-brain barrier. *Nature* 410:430-431.
326. Thorén, S. and P. J. Jakobsson. 2000. Coordinate up- and down-regulation of glutathione-dependent prostaglandin- α E synthase and cyclooxygenase-2 in A549 cells. *European Journal of Biochemistry* 267:6428-6434.
327. Laflamme, N., S. Lacroix, and S. Rivest. 1999. An Essential Role of Interleukin-1 β in Mediating NF- κ B Activity and COX-2 Transcription in Cells of the Blood-Brain Barrier in Response to a Systemic and Localized Inflammation But Not During Endotoxemia. *The Journal of Neuroscience* 19:10923-10930.
328. Yamagata, K., K. Matsumura, W. Inoue, T. Shiraki, K. Suzuki, S. Yasuda, H. Sugiura, C. Cao, Y. Watanabe, and S. Kobayashi. 2001. Coexpression of Microsomal-Type Prostaglandin E Synthase with Cyclooxygenase-2 in Brain Endothelial Cells of Rats during Endotoxin-Induced Fever. *The Journal of Neuroscience* 21:2669-2677.
329. Moore, S. A., A. A. Spector, and M. N. Hart. 1988. Eicosanoid metabolism in cerebromicrovascular endothelium. *American Journal of Physiology - Cell Physiolog* 254:C37-C44.
330. Lacroix, S., L. Vallières, and S. Rivest. 1996. C-fos mRNA pattern and corticotropin-releasing factor neuronal activity throughout the brain of

- rats injected centrally with a prostaglandin of E2 type. *Journal of Neuroimmunology* 70:163-179.
331. Verma, S., R. Nakaoke, S. Dohgu, and W. A. Banks. 2006. Release of cytokines by brain endothelial cells: A polarized response to lipopolysaccharide. *Brain, Behavior, and Immunity* 20:449-455.
 332. Rossi, B., S. Angiari, E. Zenaro, S. L. Budui, and G. Constantin. 2011. Vascular inflammation in central nervous system diseases: adhesion receptors controlling leukocyte-endothelial interactions. *Journal of leukocyte biology* 89:539-556.
 333. Yang, G. Y., Y. Mao, L. F. Zhou, C. Gong, H. L. Ge, and A. L. Betz. 1999. Expression of intercellular adhesion molecule 1 (ICAM-1) is reduced in permanent focal cerebral ischemic mouse brain using an adenoviral vector to induce overexpression of interleukin-1 receptor antagonist. *Molecular Brain Research* 65:143-150.
 334. Hirata, T., G. Merrill-Skoloff, M. Aab, J. Yang, B. C. Furie, and B. Furie. 2000. P-Selectin glycoprotein ligand 1 (PSGL-1) is a physiological ligand for E-selectin in mediating T helper 1 lymphocyte migration. *The Journal of Experimental Medicine* 192:1669-1676.
 335. Lee, S. J. and E. N. Benveniste. 1999. Adhesion molecule expression and regulation on cells of the central nervous system. *Journal of Neuroimmunology* 98:77-88.
 336. Gotsch, U., U. Jäger, M. Dominis, and D. Vestweber. 1994. Expression of P-selectin on endothelial cells is upregulated by LPS and TNF-alpha in vivo. *Cell Adhes Commun* 2:7-14.
 337. Henninger, D. D., J. Panés, M. Eppihimer, J. Russell, M. Gerritsen, D. C. Anderson, and D. N. Granger. 1997. Cytokine-induced VCAM-1 and ICAM-1 expression in different organs of the mouse. *J Immunol* 158:1825-1832.
 338. Henseleit, U., K. Steinbrink, M. Goebeler, J. Roth, D. Vestweber, C. Sorg, and C. Sunderkötter. 1996. E-selectin expression in experimental models of inflammation in mice. *J. Pathol.* 180:317-325.
 339. Piccio, L., B. Rossi, E. Scarpini, C. Laudanna, C. Giagulli, A. C. Issekutz, D. Vestweber, E. C. Butcher, and G. Constantin. 2002. Molecular mechanisms involved in lymphocyte recruitment in inflamed brain microvessels: critical roles for P-selectin glycoprotein ligand-1 and heterotrimeric Gi-linked receptors. *The Journal of Immunology* 168:1940-1949.
 340. Zhou, J., M. Schmidt, B. Johnston, F. Wilfart, S. Whynot, O. Hung, M. Murphy, V. Cerny, D. Pavlovic, and C. Lehmann. 2011. Experimental endotoxemia induces leukocyte adherence and plasma extravasation within the rat pial microcirculation. *Physiol Res* 60:853-859.
 341. Proescholdt, M. G., S. Chakravarty, J. A. Foster, S. B. Foti, E. M. Briley, and M. Herkenham. 2002. Intracerebroventricular but not intravenous interleukin-1 β induces widespread vascular-mediated leukocyte

- infiltration and immune signal mRNA expression followed by brain-wide glial activation. *Neuroscience* 112:731-749.
342. Pollak, Y., H. Ovadia, E. Orion, J. Weidenfeld, and R. Yirmiya. 2003. The EAE-associated behavioral syndrome: I. Temporal correlation with inflammatory mediators. *Journal of Neuroimmunology* 137:94-99.
 343. Kilbourn, R. G. and P. Belloni. 1990. Endothelial Cell Production of Nitrogen Oxides in Response to Interferon γ in Combination With Tumor Necrosis Factor, Interleukin-1, or Endotoxin. *Journal of the National Cancer Institute* 82:772-776.
 344. Werner, M. F. P., D. Fraga, M. C. C. Melo, G. E. P. Souza, and A. R. Zampronio. 2003. Importance of the vagus nerve for fever and neutrophil migration induced by intraperitoneal LPS injection. *Inflammation Research* 52:291-296.
 345. Hansen, M. K. and J. M. Krueger. 1997. Subdiaphragmatic vagotomy blocks the sleep and fever-promoting effects of interleukin-1 β . *American Journal of Physiology - Regulatory, Integrative and Comparative Physiology* 273:R1246-R1253.
 346. Romanovsky, A. A., C. T. Simons, M. Szekely, and V. A. Kulchitsky. 1997. The vagus nerve in the thermoregulatory response to systemic inflammation. *American Journal of Physiology - Regulatory, Integrative and Comparative Physiology* 273:R407-R413.
 347. Hansen, M. K., S. Daniels, L. E. Goehler, R. P. A. Gaykema, S. F. Maier, and L. R. Watkins. 2000. Subdiaphragmatic vagotomy does not block intraperitoneal lipopolysaccharide-induced fever. *Auton Neurosci* 85:83-87.
 348. Watkins, L. R., E. P. Wiertelak, L. E. Goehler, K. P. Smith, D. Martin, and S. F. Maier. 1994. Characterization of cytokine-induced hyperalgesia. *Brain Research* 654:15-26.
 349. Gaykema, R. P., I. Dijkstra, and F. J. Tilders. 1995. Subdiaphragmatic vagotomy suppresses endotoxin-induced activation of hypothalamic corticotropin-releasing hormone neurons and ACTH secretion. *Endocrinology* 136:4717-4720.
 350. Hansen, M. K., K. T. Nguyen, L. E. Goehler, R. P. A. Gaykema, M. Fleshner, S. F. Maier, and L. R. Watkins. 2000. Effects of vagotomy on lipopolysaccharide-induced brain interleukin-1 β protein in rats. *Autonomic Neuroscience* 85:119-126.
 351. Lanfumey, L., R. Mongeau, C. Cohen-Salmon, and M. Hamon. 2008. Corticosteroid-serotonin interactions in the neurobiological mechanisms of stress-related disorders. *Neuroscience & Biobehavioral Reviews* 32:1174-1184.
 352. Pariante, C. M. and S. L. Lightman. 2008. The HPA axis in major depression: classical theories and new developments. *Trends in Neurosciences* 31:464-468.

353. Pariante, C. M. 2006. The glucocorticoid receptor: part of the solution or part of the problem? *Journal of Psychopharmacology* 20:79-84.
354. Pariante, C. M. and A. H. Miller. 2001. Glucocorticoid receptors in major depression: relevance to pathophysiology and treatment. *Biol Psychiatry* 49:391-404.
355. Ridder, S., S. Chourbaji, R. Hellweg, A. Urani, C. Zacher, W. Schmid, M. Zink, H. Hörtnagl, H. Flor, F. A. Henn, G. Schütz, and P. Gass. 2005. Mice with Genetically Altered Glucocorticoid Receptor Expression Show Altered Sensitivity for Stress-Induced Depressive Reactions. *The Journal of Neuroscience* 25:6243-6250.
356. Turnbull, A. V. and C. L. Rivier. 1999. Regulation of the hypothalamic-pituitary-adrenal axis by cytokines: actions and mechanisms of action. *Physiol Rev* 79:1-71.
357. Goshen, I. and R. Yirmiya. 2009. Interleukin-1 (IL-1): A central regulator of stress responses. *Frontiers in Neuroendocrinology* 30:30-45.
358. Schotanus, K., F. J. Tilders, and F. Berkenbosch. 1993. Human recombinant interleukin-1 receptor antagonist prevents adrenocorticotropin, but not interleukin-6 responses to bacterial endotoxin in rats. *Endocrinology* 133:2461-2468.
359. Ebisui, O., J. Fukata, N. Murakami, H. Kobayashi, H. Segawa, S. Muro, I. Hanaoka, Y. Naito, Y. Masui, Y. Ohmoto, and al.et. 1994. Effect of IL-1 receptor antagonist and antiserum to TNF-alpha on LPS-induced plasma ACTH and corticosterone rise in rats. *American Journal of Physiology - Endocrinology and Metabolism* 266:E986-E992.
360. Dunn, A. J. 2000. Effects of the IL-1 receptor antagonist on the IL-1-and endotoxin-induced activation of the HPA axis and cerebral biogenic amines in mice. *Neuroimmunomodulation* 7:36.
361. Perlstein, R. S., M. H. Whitnall, J. S. Abrams, E. H. Mougey, and R. Neta. 1993. Synergistic roles of interleukin-6, interleukin-1, and tumor necrosis factor in the adrenocorticotropin response to bacterial lipopolysaccharide in vivo. *Endocrinology* 132:946-952.
362. Nguyen, K. T., T. Deak, M. J. Will, M. K. Hansen, B. N. Hunsaker, M. Fleshner, L. R. Watkins, and S. F. Maier. 2000. Timecourse and corticosterone sensitivity of the brain, pituitary, and serum interleukin-1 β protein response to acute stress. *Brain Research* 859:193-201.
363. Shintani, F., T. Nakaki, S. Kanba, K. Sato, G. Yagi, M. Shiozawa, S. Aiso, R. Kato, and M. Asai. 1995. Involvement of interleukin-1 in immobilization stress-induced increase in plasma adrenocorticotrophic hormone and in release of hypothalamic monoamines in the rat. *J Neurosci* 15:1961-1970.
364. Goshen, I., R. Yirmiya, K. Iverfeldt, and J. Weidenfeld. 2003. The Role of Endogenous Interleukin-1 in Stress-Induced Adrenal Activation and Adrenalectomy-Induced Adrenocorticotrophic Hormone Hypersecretion. *Endocrinology* 144:4453-4458.

365. Sapolsky, R., C. Rivier, G. Yamamoto, P. Plotsky, and W. Vale. 1987. Interleukin-1 stimulates the secretion of hypothalamic corticotropin-releasing factor. *Science (New York, N.Y.)* 238:522-524.
366. Berkenbosch, F., J. van Oers, A. del Rey, F. Tilders, and H. Besedovsky. 1987. Corticotropin-releasing factor-producing neurons in the rat activated by interleukin-1. *Science (New York, N.Y.)* 238:524-526.
367. Bernton, E. W., J. E. Beach, J. W. Holaday, R. C. Smallridge, and H. G. Fein. 1987. Release of multiple hormones by a direct action of interleukin-1 on pituitary cells. *Science* 238:519.
368. Kariagina, A., D. Romanenko, S. G. Ren, and V. Chesnokova. 2004. Hypothalamic-Pituitary Cytokine Network. *Endocrinology* 145:104-112.
369. Pace, T. W., F. Hu, and A. H. Miller. 2007. Cytokine-effects on glucocorticoid receptor function: relevance to glucocorticoid resistance and the pathophysiology and treatment of major depression. *Brain, Behavior, and Immunity* 21:9-19.
370. Naughton, M., J. B. Mulrooney, and B. E. Leonard. 2000. A review of the role of serotonin receptors in psychiatric disorders. *Hum.Psychopharmacol.Clin.Exp.* 15:397-415.
371. LaHoste, G. J., J. M. Swanson, S. B. Wigal, C. Glabe, T. Wigal, N. King, and J. L. Kennedy. 1996. Dopamine D4 receptor gene polymorphism is associated with attention deficit hyperactivity disorder. *Mol Psychiatry* 1:121-124.
372. Kapur, S. and D. Mamo. 2003. Half a century of antipsychotics and still a central role for dopamine D2 receptors. *Progress in Neuro-Psychopharmacology and Biological Psychiatry* 27:1081-1090.
373. Laasonen-Balk, T. J. H.-S. M. J. J. 1999. Striatal dopamine transporter density in major depression. *Psychopharmacology* 144:282.
374. Zhu, C. B., R. D. Blakely, and W. A. Hewlett. 2006. The proinflammatory cytokines interleukin-1beta and tumor necrosis factor-alpha activate serotonin transporters. *Neuropsychopharmacology* 31:2121-2131.
375. Malynn, S., A. Campos-Torres, P. Moynagh, and J. Haase. 2013. The Pro-inflammatory Cytokine TNF- α Regulates the Activity and Expression of the Serotonin Transporter (SERT) in Astrocytes. *Neurochem Res* 38:694-704.
376. Cavanagh, J., C. Paterson, J. McLean, S. Pimlott, M. McDonald, J. Patterson, D. Wyper, and I. McInnes. 2010. Tumour necrosis factor blockade mediates altered serotonin transporter availability in rheumatoid arthritis: a clinical, proof-of-concept study. *Annals of the Rheumatic Diseases* 69:1251-1252.
377. Lai, Y. T., Y. P. Tsai, C. G. Cherg, J. J. Ke, M. C. Ho, C. W. Tsai, and L. Yu. 2009. Lipopolysaccharide mitigates methamphetamine-induced striatal dopamine depletion via modulating local TNF-alpha and dopamine transporter expression. *J Neural Transm* 116:405-415.

378. Zhu, C. B., K. M. Lindler, A. W. Owens, L. C. Daws, R. D. Blakely, and W. A. Hewlett. 2010. Interleukin-1 receptor activation by systemic lipopolysaccharide induces behavioral despair linked to MAPK regulation of CNS serotonin transporters. *Neuropsychopharmacology* 35:2510-2520.
379. Kitagami, T., K. Yamada, H. Miura, R. Hashimoto, T. Nabeshima, and T. Ohta. 2003. Mechanism of systemically injected interferon-alpha impeding monoamine biosynthesis in rats: role of nitric oxide as a signal crossing the blood-brain barrier. *Brain Research* 978:104-114.
380. Fujigaki, H., K. Saito, S. Fujigaki, M. Takemura, K. Sudo, H. Ishiguro, and M. Seishima. 2006. The Signal Transducer and Activator of Transcription 1 α and Interferon Regulatory Factor 1 Are Not Essential for the Induction of Indoleamine 2,3-Dioxygenase by Lipopolysaccharide: Involvement of p38 Mitogen-Activated Protein Kinase and Nuclear Factor- κ B Pathways, and Synergistic Effect of Several Proinflammatory Cytokines. *Journal of Biochemistry* 139:655-662.
381. O'Connor, J. C., M. A. Lawson, C. André, M. Moreau, J. Lestage, N. Castanon, K. W. Kelley, and R. Dantzer. 2009. Lipopolysaccharide-induced depressive-like behavior is mediated by indoleamine 2,3-dioxygenase activation in mice. *Mol Psychiatry* 14:511-522.
382. Jhamandas, K. H., R. J. Boegman, R. J. Beninger, A. F. Miranda, and K. A. Lipic. 2000. Excitotoxicity of quinolinic acid: modulation by endogenous antagonists. *Neurotoxicity research* 2:139-155.
383. Borland, L. M. and A. C. Michael. 2004. Voltammetric study of the control of striatal dopamine release by glutamate. *Journal of Neurochemistry* 91:220-229.
384. Kendell, S. F., J. H. Krystal, and G. Sanacora. 2005. GABA and glutamate systems as therapeutic targets in depression and mood disorders. *Expert opinion on therapeutic targets* 9:153-168.
385. Sanacora, G., R. Gueorguieva, C. N. Epperson, Y. T. Wu, M. Appel, D. L. Rothman, J. H. Krystal, and G. F. Mason. 2004. Subtype-Specific Alterations of γ -Aminobutyric Acid and Glutamate in Patients With Major Depression. *Archives of General Psychiatry* 61:705-713.
386. Moghaddam, B. 1993. Stress preferentially increases extraneuronal levels of excitatory amino acids in the prefrontal cortex: comparison to hippocampus and basal ganglia. *Journal of Neurochemistry* 60:1650-1657.
387. Walter, M., A. Henning, S. Grimm, R. F. Schulte, J. Beck, U. Dydak, B. Schnepf, H. Boeker, P. Boesiger, and G. Northoff. 2009. The relationship between aberrant neuronal activation in the pregenual anterior cingulate, altered glutamatergic metabolism, and anhedonia in major depression. *Archives of General Psychiatry* 66:478-486.
388. Choudary, P. V., M. Molnar, S. J. Evans, H. Tomita, J. Z. Li, M. P. Vawter, R. M. Myers, W. E. Bunney, H. Akil, S. J. Watson, and E. G. Jones. 2005. Altered cortical glutamatergic and GABAergic signal transmission with

- glial involvement in depression. *Proc Natl Acad Sci U S A* 102:15653-15658.
389. Zarate, C. A., J. B. Singh, P. J. Carlson, N. E. Brutsche, R. Ameli, D. A. Luckenbaugh, D. S. Charney, and H. K. Manji. 2006. A randomized trial of an N-methyl-D-aspartate antagonist in treatment-resistant major depression. *Archives of General Psychiatry* 63:856-864.
 390. Maeng, S., C. A. Zarate Jr, J. Du, R. J. Schloesser, J. McCammon, G. Chen, and H. K. Manji. 2008. Cellular Mechanisms Underlying the Antidepressant Effects of Ketamine: Role of α -Amino-3-Hydroxy-5-Methylisoxazole-4-Propionic Acid Receptors. *Biol Psychiatry* 63:349-352.
 391. Zarate, C. A., J. L. Payne, J. Quiroz, J. Sporn, K. K. Denicoff, D. Luckenbaugh, D. S. Charney, and H. K. Manji. 2004. An open-label trial of riluzole in patients with treatment-resistant major depression. *American Journal of Psychiatry* 161:171-174.
 392. Vianna, M. R. M., M. Alonso, H. Viola, J. Quevedo, F. de Paris, M. Furman, M. L. de Stein, J. H. Medina, and I. Izquierdo. 2000. Role of Hippocampal Signaling Pathways in Long-Term Memory Formation of a Nonassociative Learning Task in the Rat. *Learning & Memory* 7:333-340.
 393. Sheline, Y. I., P. W. Wang, M. H. Gado, J. G. Csernansky, and M. W. Vannier. 1996. Hippocampal atrophy in recurrent major depression. *Proc Natl Acad Sci U S A* 93:3908-3913.
 394. Anacker, C., P. A. Zunszain, A. Cattaneo, L. A. Carvalho, M. J. Garabedian, S. Thuret, J. Price, and C. M. Pariante. 2011. Antidepressants increase human hippocampal neurogenesis by activating the glucocorticoid receptor. *Mol Psychiatry* 16:738-750.
 395. Duman, R. S., S. Nakagawa, and J. Malberg. 2001. Regulation of adult neurogenesis by antidepressant treatment. *Neuropsychopharmacology* 25:836-844.
 396. Malberg, J. E., A. J. Eisch, E. J. Nestler, and R. S. Duman. 2000. Chronic Antidepressant Treatment Increases Neurogenesis in Adult Rat Hippocampus. *The Journal of Neuroscience* 20:9104-9110.
 397. Santarelli, L., M. Saxe, C. Gross, A. Surget, F. Battaglia, S. Dulawa, N. Weisstaub, J. Lee, R. Duman, O. Arancio, C. Belzung, and R. Hen. 2003. Requirement of hippocampal neurogenesis for the behavioral effects of antidepressants. *Science (New York, N.Y.)* 301:805-809.
 398. Koo, J. W. and R. S. Duman. 2008. IL-1 β is an essential mediator of the antineurogenic and anhedonic effects of stress. *Proceedings of the National Academy of Sciences* 105:751-756.
 399. Monje, M. L., H. Toda, and T. D. Palmer. 2003. Inflammatory Blockade Restores Adult Hippocampal Neurogenesis. *Science* 302:1760-1765.
 400. Kaneko, N., K. Kudo, T. Mabuchi, K. Takemoto, K. Fujimaki, H. Wati, H. Iguchi, H. Tezuka, and S. Kanba. 2006. Suppression of cell proliferation by

interferon-alpha through interleukin-1 production in adult rat dentate gyrus. *Neuropsychopharmacology* 31:2619-2626.

401. Goshen, I., T. Kreisel, O. Menachem-Zidon, T. Licht, J. Weidenfeld, T. Ben Hur, and R. Yirmiya. 2008. Brain interleukin-1 mediates chronic stress-induced depression in mice via adrenocortical activation and hippocampal neurogenesis suppression. *Mol Psychiatry* 13:717-728.
402. Schloesser, R. J., H. K. Manji, and K. Martinowich. 2009. Suppression of adult neurogenesis leads to an increased hypothalamo-pituitary-adrenal axis response. *Neuroreport* 20:553-557.
403. Lapchak, P. A., D. M. Araujo, and F. Hefti. 1993. Systemic interleukin-1 β decreases brain-derived neurotrophic factor messenger RNA expression in the rat hippocampal formation. *Neuroscience* 53:297-301.
404. Lotrich, F. E., S. Albusaysi, and R. E. Ferrell. 2013. Brain-derived neurotrophic factor serum levels and genotype: association with depression during interferon- α treatment. *Neuropsychopharmacology* 38:985-995.
405. Lee, J., W. Duan, and M. P. Mattson. 2002. Evidence that brain-derived neurotrophic factor is required for basal neurogenesis and mediates, in part, the enhancement of neurogenesis by dietary restriction in the hippocampus of adult mice. *Journal of Neurochemistry* 82:1367-1375.
406. Wu, S. Y., T. F. Wang, L. Yu, C. J. Jen, J. I. Chuang, F. S. Wu, C. W. Wu, and Y. M. Kuo. 2011. Running exercise protects the substantia nigra dopaminergic neurons against inflammation-induced degeneration via the activation of BDNF signaling pathway. *Brain, Behavior, and Immunity* 25:135-146.
407. Stellwagen, D., E. C. Beattie, J. Y. Seo, and R. C. Malenka. 2005. Differential regulation of AMPA receptor and GABA receptor trafficking by tumor necrosis factor-alpha. *J Neurosci* 25:3219-3228.
408. Ida, T., M. Hara, Y. Nakamura, S. Kozaki, S. Tsunoda, and H. Ihara. 2008. Cytokine-induced enhancement of calcium-dependent glutamate release from astrocytes mediated by nitric oxide. *Neuroscience Letters* 432:232-236.
409. Pitt, D., I. E. Nagelmeier, H. C. Wilson, and C. S. Raine. 2003. Glutamate uptake by oligodendrocytes: Implications for excitotoxicity in multiple sclerosis. *Neurology* 61:1113-1120.
410. Zou, J. Y. and F. T. Crews. 2005. TNF α potentiates glutamate neurotoxicity by inhibiting glutamate uptake in organotypic brain slice cultures: neuroprotection by NF κ B inhibition. *Brain Research* 1034:11-24.
411. Huang, D. W., B. T. Sherman, and R. A. Lempicki. 2009. Bioinformatics enrichment tools: paths toward the comprehensive functional analysis of large gene lists. *Nucleic Acids Research* 37:1-13.

412. Huang, D. W., B. T. Sherman, and R. A. Lempicki. 2008. Systematic and integrative analysis of large gene lists using DAVID bioinformatics resources. *Nat.Protocols* 4:44-57.
413. Samarajiwa, S. A., S. Forster, K. Auchetl, and P. J. Hertzog. 2009. INTERFEROME: the database of interferon regulated genes. *Nucleic Acids Research* 37:D852-D857.
414. Jones, K. L., A. Mansell, S. Patella, B. J. Scott, M. P. Hedger, D. M. de Kretser, and D. J. Phillips. 2007. Activin A is a critical component of the inflammatory response, and its binding protein, follistatin, reduces mortality in endotoxemia. *Proceedings of the National Academy of Sciences* 104:16239-16244.
415. Kessler, D. S., D. E. Levy, and J. E. Darnell. 1988. Two interferon-induced nuclear factors bind a single promoter element in interferon-stimulated genes. *Proceedings of the National Academy of Sciences* 85:8521-8525.
416. Spiller, S., G. Elson, R. Ferstl, S. Dreher, T. Mueller, M. Freudenberg, B. Daubeuf, H. Wagner, and C. J. Kirschning. 2008. TLR4-induced IFN- γ production increases TLR2 sensitivity and drives Gram-negative sepsis in mice. *The Journal of Experimental Medicine* 205:1747-1754.
417. Buttini, M. and H. Boddeke. 1995. Peripheral lipopolysaccharide stimulation induces interleukin-1 β messenger RNA in rat brain microglial cells. *Neuroscience* 65:523-530.
418. Quan, N., M. Whiteside, and M. Herkenham. 1998. Cyclooxygenase 2 mRNA expression in rat brain after peripheral injection of lipopolysaccharide. *Brain Research* 802:189-197.
419. Saijo, K. and C. K. Glass. 2011. Microglial cell origin and phenotypes in health and disease. *Nat Rev Immunol* 11:775-787.
420. Marques, F., J. C. Sousa, G. Coppola, A. M. Falcao, A. Joao Rodrigues, D. H. Geschwind, N. Sousa, M. Correia-Neves, and J. A. Palha. 2009. Kinetic profile of the transcriptome changes induced in the choroid plexus by peripheral inflammation. *J Cereb Blood Flow Metab* 29:921-932.
421. Banks, W. A. and S. M. Robinson. 2010. Minimal penetration of lipopolysaccharide across the murine blood-brain barrier. *Brain, Behavior, and Immunity* 24:102-109.
422. Varma, T. K., C. Y. Lin, T. E. Toliver-Kinsky, and E. R. Sherwood. 2002. Endotoxin-Induced Gamma Interferon Production: Contributing Cell Types and Key Regulatory Factors. *Clinical and Diagnostic Laboratory Immunology* 9:530-543.
423. Wang, J., I. L. Campbell, and H. Zhang. 2008. Systemic interferon- α regulates interferon-stimulated genes in the central nervous system. *Mol Psychiatry* 13:293-301.

424. Wang, J. and I. L. Campbell. 2005. Innate STAT1-dependent genomic response of neurons to the antiviral cytokine alpha interferon. *Journal of Virology* 79:8295-8302.
425. Wang, X., X. Li, D. B. Schmidt, J. J. Foley, F. C. Barone, R. S. Ames, and H. M. Sarau. 2000. Identification and molecular characterization of rat CXCR3: receptor expression and interferon-inducible protein-10 binding are increased in focal stroke. *Molecular pharmacology* 57:1190-1198.
426. Kolb, S. A., B. Sporer, F. Lahrtz, U. Koedel, H. W. Pfister, and A. Fontana. 1999. Identification of a T cell chemotactic factor in the cerebrospinal fluid of HIV-1-infected individuals as interferon- γ inducible protein 10. *Journal of Neuroimmunology* 93:172-181.
427. Farber, J. M. 1997. Mig and IP-10: CXC chemokines that target lymphocytes. *Journal of leukocyte biology* 61:246-257.
428. Reyes, T. M., J. R. Walker, C. DeCino, J. B. Hogenesch, and P. E. Sawchenko. 2003. Categorically distinct acute stressors elicit dissimilar transcriptional profiles in the paraventricular nucleus of the hypothalamus. *The Journal of Neuroscience* 23:5607-5616.
429. Foster, S. L., D. C. Hargreaves, and R. Medzhitov. 2007. Gene-specific control of inflammation by TLR-induced chromatin modifications. *Nature* 447:972-978.
430. Rayhane, N. m., C. Fitting, and J. M. Cavaillon. 1999. Dissociation of IFN- γ from IL-12 and IL-18 production during endotoxin tolerance. *Journal of Endotoxin Research* 5:319-324.
431. Akira, S. and K. Takeda. 2004. Toll-like receptor signalling. *Nat Rev Immunol* 4:499-511.
432. Chen, R., H. Zhou, J. Beltran, L. Malellari, and S. L. Chang. 2005. Differential expression of cytokines in the brain and serum during endotoxin tolerance. *Journal of Neuroimmunology* 163:53-72.
433. Faggioni, R., G. Fantuzzi, P. Villa, W. Buurman, L. J. van Tits, and P. Ghezzi. 1995. Independent down-regulation of central and peripheral tumor necrosis factor production as a result of lipopolysaccharide tolerance in mice. *Infection and Immunity* 63:1473-1477.
434. Liew, F. Y., D. Xu, E. K. Brint, and L. A. O'Neill. 2005. Negative regulation of toll-like receptor-mediated immune responses. *Nature Reviews Immunology* 5:446-458.
435. Fong, Y., K. J. Tracey, L. L. Moldawer, D. G. Hesse, K. B. Manogue, J. S. Kenney, A. T. Lee, G. C. Kuo, A. C. Allison, and S. F. Lowry. 1989. Antibodies to cachectin/tumor necrosis factor reduce interleukin 1 beta and interleukin 6 appearance during lethal bacteremia. *The Journal of Experimental Medicine* 170:1627-1633.
436. Terrando, N., C. Monaco, D. Ma, B. M. J. Foxwell, M. Feldmann, and M. Maze. 2010. Tumor necrosis factor- α triggers a cytokine cascade yielding

postoperative cognitive decline. *Proceedings of the National Academy of Sciences* 107:20518-20522.

437. Allantaz-Frager, F., F. Turrel-Davin, F. Venet, C. Monnin, A. I. Saint Jean, V. Barbalat, E. Cerrato, A. Pachot, A. Lepape, and G. Monneret. 2013. Identification of Biomarkers of Response to IFN γ during Endotoxin Tolerance: Application to Septic Shock. *PLoS one* 8:e68218.
438. Field, R., S. Champion, C. Warren, C. Murray, and C. Cunningham. 2010. Systemic challenge with the TLR3 agonist poly I: C induces amplified IFN α/β and IL-1 β responses in the diseased brain and exacerbates chronic neurodegeneration. *Brain, Behavior, and Immunity* 24:996-1007.
439. Sakaguchi, S., H. Negishi, M. Asagiri, C. Nakajima, T. Mizutani, A. Takaoka, K. Honda, and T. Taniguchi. 2003. Essential role of IRF-3 in lipopolysaccharide-induced interferon- β gene expression and endotoxin shock. *Biochemical and Biophysical Research Communications* 306:860-866.
440. Yamamoto, M., S. Sato, H. Hemmi, K. Hoshino, T. Kaisho, H. Sanjo, O. Takeuchi, M. Sugiyama, M. Okabe, K. Takeda, and S. Akira. 2003. Role of Adaptor TRIF in the MyD88-Independent Toll-Like Receptor Signaling Pathway. *Science* 301:640-643.
441. Qin, S., J. B. Rottman, P. Myers, N. Kassam, M. Weinblatt, M. Loetscher, A. E. Koch, B. Moser, and C. R. Mackay. 1998. The chemokine receptors CXCR3 and CCR5 mark subsets of T cells associated with certain inflammatory reactions. *J Clin Invest* 101:746-754.
442. Pajek, Daniela, McKimmie, Clive S., Haxton, Ben, Johnston, Nicholas, Fooks, Anthony R., and Graham, Gerard J. Defining the chemokine basis for leukocyte recruitment during viral encephalitis. *Journal of Virology* . 2014.

Ref Type: In Press

443. Roy, M., J. F. Richard, A. Dumas, and L. Vallieres. 2012. CXCL1 can be regulated by IL-6 and promotes granulocyte adhesion to brain capillaries during bacterial toxin exposure and encephalomyelitis. *Journal of Neuroinflammation* 9:18.
444. Rubio, N. and F. Sanz-Rodriguez. 2007. Induction of the CXCL1 (KC) chemokine in mouse astrocytes by infection with the murine encephalomyelitis virus of Theiler. *Virology* 358:98-108.
445. Pineau, I., L. Sun, D. Bastien, and S. Lacroix. 2010. Astrocytes initiate inflammation in the injured mouse spinal cord by promoting the entry of neutrophils and inflammatory monocytes in an IL-1 receptor/MyD88-dependent fashion. *Brain, Behavior, and Immunity* 24:540-553.
446. Omari, K. M., G. John, R. Lango, and C. S. Raine. 2006. Role for CXCR2 and CXCL1 on glia in multiple sclerosis. *Glia* 53:24-31.
447. Shaftel, S. S., T. J. Carlson, J. A. Olschowka, S. Kyrkanides, S. B. Matousek, and M. K. O'Banion. 2007. Chronic interleukin-1 β expression in

- mouse brain leads to leukocyte infiltration and neutrophil-independent blood-brain barrier permeability without overt neurodegeneration. *The Journal of Neuroscience* 27:9301-9309.
448. Shi, C., T. Jia, S. Mendez-Ferrer, T. Hohl, N. Serbina, L. Lipuma, I. Leiner, M. Li, P. Frenette, and E. Pamer. 2011. Bone Marrow Mesenchymal Stem and Progenitor Cells Induce Monocyte Emigration in Response to Circulating Toll-like Receptor Ligands. *Immunity* 34:590-601.
 449. Larangeira, A. P., A. R. Silva, R. N. Gomes, C. Penido, M. G. M. O. Henriques, H. C. Castro-Faria-Neto, and P. T. Bozza. 2001. Mechanisms of allergen-and LPS-induced bone marrow eosinophil mobilization and eosinophil accumulation into the pleural cavity: a role for CD11b/CD18 complex. *Inflammation Research* 50:309-316.
 450. Sato, Y., S. F. van Eeden, D. English, and J. C. Hogg. 1998. Bacteremic pneumococcal pneumonia: Bone marrow release and pulmonary sequestration of neutrophils. *Critical care medicine* 26:501-509.
 451. Quesenberry, P., J. Halperin, M. Ryan, and F. J. Stohlman. 1975. Tolerance to the granulocyte-releasing and colony-stimulating factor elevating effects of endotoxin. *Blood* 45:789-800.
 452. Trifilo, M. J., C. C. Bergmann, W. A. Kuziel, and T. E. Lane. 2003. CC chemokine ligand 3 (CCL3) regulates CD8⁺-T-cell effector function and migration following viral infection. *Journal of Virology* 77:4004-4014.
 453. Inngjerdingen, M., B. Damaj, and A. A. Maghazachi. 2001. Expression and regulation of chemokine receptors in human natural killer cells. *Blood* 97:367-375.
 454. Lee, Y. K., D. H. Kwak, K. W. Oh, S. Y. Nam, B. J. Lee, Y. W. Yun, Y. B. Kim, S. B. Han, and J. T. Hong. 2009. CCR5 deficiency induces astrocyte activation, A β deposit and impaired memory function. *Neurobiology of Learning and Memory* 92:356-363.
 455. Musante, V., F. Longordo, E. Neri, M. Pedrazzi, F. Kalfas, P. Severi, M. Raiteri, and A. Pittaluga. 2008. RANTES Modulates the Release of Glutamate in Human Neocortex. *The Journal of Neuroscience* 28:12231-12240.
 456. Sui, Y., L. Stehno-Bittel, S. Li, R. Loganathan, N. K. Dhillon, D. Pinson, A. Nath, D. Kolson, O. Narayan, and S. Buch. 2006. CXCL10-induced cell death in neurons: role of calcium dysregulation. *European Journal of Neuroscience* 23:957-964.
 457. van Weering, H. R. J., H. W. G. M. Boddeke, J. Vinet, N. Brouwer, A. H. de Haas, N. van Rooijen, A. R. Thomsen, and K. P. H. Biber. 2011. CXCL10/CXCR3 signaling in glia cells differentially affects NMDA-induced cell death in CA and DG neurons of the mouse hippocampus. *Hippocampus* 21:220-232.
 458. Foster, R., A. Kandaneeratchi, C. Beasley, B. Williams, N. Khan, M. K. Fagerhol, and I. P. Overall. 2006. Calprotectin in microglia from frontal

cortex is up-regulated in schizophrenia: evidence for an inflammatory process? *European Journal of Neuroscience* 24:3561-3566.

459. Aktas, O., B. Kieseier, and H. P. Hartung. 2010. Neuroprotection, regeneration and immunomodulation: broadening the therapeutic repertoire in multiple sclerosis. *Trends in Neurosciences* 33:140-152.
460. Dogan, R. N., A. Elhofy, and W. J. Karpus. 2008. Production of CCL2 by central nervous system cells regulates development of murine experimental autoimmune encephalomyelitis through the recruitment of TNF-and iNOS-expressing macrophages and myeloid dendritic cells. *The Journal of Immunology* 180:7376-7384.
461. Hamann, I., F. Zipp, and C. Infante-Duarte. 2008. Therapeutic targeting of chemokine signaling in Multiple Sclerosis. *Journal of the neurological sciences* 274:31-38.
462. Mellergård, J., M. Edström, M. Vrethem, J. Ernerudh, and C. Dahle. 2010. Natalizumab treatment in multiple sclerosis: marked decline of chemokines and cytokines in cerebrospinal fluid. *Multiple Sclerosis* 16:208-217.
463. Baugh, L. R., A. A. Hill, E. L. Brown, and C. P. Hunter. 2001. Quantitative analysis of mRNA amplification by in vitro transcription. *Nucleic Acids Research* 29:e29.
464. Wang, J. and A. J. Dunn. 1999. The role of interleukin-6 in the activation of the hypothalamo-pituitary-adrenocortical axis and brain indoleamines by endotoxin and interleukin-1 β . *Brain Research* 815:337-348.
465. Földes, A., Z. Némethy, O. Szalay, and K. J. Kovács. 2000. Anaphylactoid reactions activate hypothalamo-pituitary-adrenocortical axis: comparison with endotoxic reactions. *Brain Research Bulletin* 52:573-579.
466. Uribe, R. M., S. Lee, and C. Rivier. 1999. Endotoxin Stimulates Nitric Oxide Production in the Paraventricular Nucleus of the Hypothalamus through Nitric Oxide Synthase I: Correlation with Hypothalamic-Pituitary-Adrenal Axis Activation. *Endocrinology* 140:5971-5981.
467. Lestage, J., D. Verrier, K. Palin, and R. Dantzer. 2002. The enzyme indoleamine 2,3-dioxygenase is induced in the mouse brain in response to peripheral administration of lipopolysaccharide and superantigen. *Brain, Behavior, and Immunity* 16:596-601.
468. Youn, H. S., J. Y. Lee, K. A. Fitzgerald, H. A. Young, S. Akira, and D. H. Hwang. 2005. Specific inhibition of MyD88-independent signaling pathways of TLR3 and TLR4 by resveratrol: molecular targets are TBK1 and RIP1 in TRIF complex. *The Journal of Immunology* 175:3339-3346.
469. Piao, W., C. Song, H. Chen, M. A. Quevedo Diaz, L. M. Wahl, K. A. Fitzgerald, L. Li, and A. E. Medvedev. 2009. Endotoxin tolerance dysregulates MyD88- and Toll/IL-1R domain-containing adapter inducing IFN- β -dependent pathways and increases expression of negative regulators of TLR signaling. *Journal of leukocyte biology* 86:863-875.

470. Schellenberg, A., R. Buist, M. Del Bigio, H. Toft-Hansen, R. Khorooshi, T. Owens, and J. Peeling. 2012. Blood-brain barrier disruption in CCL2 transgenic mice during pertussis toxin-induced brain inflammation. *Fluids and Barriers of the CNS* 9:10.
471. Kraus, M. R., A. Schäfer, H. Faller, H. Csef, and M. Scheurlen. 2003. Psychiatric symptoms in patients with chronic hepatitis C receiving interferon alfa-2b therapy. *J Clin Psychiatry* 64:708-714.
472. Kraus, M. R., A. Schäfer, K. Schöttker, C. Keicher, B. Weissbrich, I. Hofbauer, and M. Scheurlen. 2008. Therapy of interferon-induced depression in chronic hepatitis C with citalopram: a randomised, double-blind, placebo-controlled study. *Gut* 57:531-536.
473. Neilley, L. K., D. S. Goodin, D. E. Goodkin, and S. L. Hauser. 1996. Side effect profile of interferon beta-1b in MS: Results of an open label trial. *Neurology* 46:552-553.
474. Hua, L. L. and S. C. Lee. 2000. Distinct patterns of stimulus-inducible chemokine mRNA accumulation in human fetal astrocytes and microglia. *Glia* 30:74-81.
475. Farber, J. M. 1993. HuMig: A New Human Member of the Chemokine Family of Cytokines. *Biochemical and Biophysical Research Communications* 192:223-230.
476. Kaplan, G., A. D. Luster, G. Hancock, and Z. A. Cohn. 1987. The expression of a gamma interferon-induced protein (IP-10) in delayed immune responses in human skin. *The Journal of Experimental Medicine* 166:1098-1108.
477. Vanguri, P. and J. M. Farber. 1994. IFN and virus-inducible expression of an immediate early gene, *crg-2/IP-10*, and a delayed gene, *I-A alpha* in astrocytes and microglia. *The Journal of Immunology* 152:1411-1418.
478. Antonelli, A., S. M. Ferrari, P. Fallahi, E. Ghiri, C. Crescioli, P. Romagnani, P. Vitti, M. Serio, and E. Ferrannini. 2010. Interferon-alpha, -beta and -gamma induce CXCL9 and CXCL10 secretion by human thyrocytes: Modulation by peroxisome proliferator-activated receptor-gamma agonists. *Cytokine* 50:260-267.
479. Génin, P., M. Algarté, P. Roof, R. Lin, and J. Hiscott. 2000. Regulation of RANTES Chemokine Gene Expression Requires Cooperativity Between NF- κ B and IFN-Regulatory Factor Transcription Factors. *The Journal of Immunology* 164:5352-5361.
480. Lin, R., C. Heylbroeck, P. Genin, P. M. Pitha, and J. Hiscott. 1999. Essential role of interferon regulatory factor 3 in direct activation of RANTES chemokine transcription. *Molecular and Cellular Biology* 19:959-966.
481. Andersen, J., S. VanScoy, T. F. Cheng, D. Gomez, and N. C. Reich. 2008. IRF-3-dependent and augmented target genes during viral infection. *Genes and immunity* 9:168-175.

482. Burke, S. J., D. Lu, T. E. Sparer, T. Masi, M. R. Goff, M. D. Karlstad, and J. J. Collier. 2014. NF- κ B and STAT1 control CXCL1 and CXCL2 gene transcription. *American Journal of Physiology-Endocrinology and Metabolism* 306:E131-E149.
483. Xu, J., M. D. Zhu, X. Zhang, H. Tian, J. H. Zhang, X. B. Wu, and Y. J. Gao. 2014. NF κ B-mediated CXCL1 production in spinal cord astrocytes contributes to the maintenance of bone cancer pain in mice. *Journal of Neuroinflammation* 11:38.
484. Skelly, D. T., E. Hennesy, M. A. Dansereau, and C. Cunningham. 2013. A Systematic Analysis of the Peripheral and CNS Effects of Systemic LPS, IL-1 β , TNF- α and IL-6 Challenges in C57BL/6 Mice. *PloS one* 8:e69123.
485. Segel, G. B., M. W. Halterman, and M. A. Lichtman. 2011. The paradox of the neutrophil's role in tissue injury. *Journal of leukocyte biology* 89:359-372.
486. Üllen, A., E. Singewald, V. Konya, G. Fauler, H. Reicher, C. Nussold, A. Hammer, D. Kratky, A. Heinemann, P. Holzer, E. Malle, and W. Sattler. 2013. Myeloperoxidase-Derived Oxidants Induce Blood-Brain Barrier Dysfunction *In Vitro* and *In Vivo*. *PloS one* 8:e64034.
487. Parker, L. C., E. C. Jones, L. R. Prince, S. K. Dower, M. K. B. Whyte, and I. Sabroe. 2005. Endotoxin tolerance induces selective alterations in neutrophil function. *Journal of leukocyte biology* 78:1301-1305.
488. Carpentier, P. A., D. S. Duncan, and S. D. Miller. 2008. Glial toll-like receptor signaling in central nervous system infection and autoimmunity. *Brain, Behavior, and Immunity* 22:140-147.
489. Lalvani, A., R. Brookes, S. Hambleton, W. J. Britton, A. V. S. Hill, and A. J. McMichael. 1997. Rapid Effector Function in CD8⁺ Memory T Cells. *The Journal of Experimental Medicine* 186:859-865.
490. Young, K. G., S. MacLean, R. Dudani, L. Krishnan, and S. Sad. 2011. CD8⁺ T Cells Primed in the Periphery Provide Time-Bound Immune-Surveillance to the Central Nervous System. *The Journal of Immunology* 187:1192-1200.
491. Kwok, L. Y., H. Miletic, S. Lütjen, S. Soltek, M. Deckert, and D. Schlüter. 2002. Protective Immunosurveillance of the Central Nervous System by Listeria-Specific CD4 and CD8 T Cells in Systemic Listeriosis in the Absence of Intracerebral Listeria. *The Journal of Immunology* 169:2010-2019.
492. Drevets, D. A., M. J. Dillon, J. S. Schawang, N. van Rooijen, J. Ehrchen, C. Sunderkötter, and P. J. M. Leenen. 2004. The Ly-6Chigh Monocyte Subpopulation Transports Listeria monocytogenes into the Brain during Systemic Infection of Mice. *The Journal of Immunology* 172:4418-4424.
493. Howe, C. L., R. G. LaFrance-Corey, R. S. Sundsbak, and S. J. LaFrance. 2012. Inflammatory monocytes damage the hippocampus during acute picornavirus infection of the brain. *J Neuroinflammation* 9:50.

494. Djukic, M., A. Mildner, H. Schmidt, D. Czesnik, W. Brück, J. Priller, R. Nau, and M. Prinz. 2006. Circulating monocytes engraft in the brain, differentiate into microglia and contribute to the pathology following meningitis in mice. *Brain* 129:2394-2403.
495. Simard, A. R., D. Soulet, G. Gowing, J. P. Julien, and S. Rivest. 2006. Bone Marrow-Derived Microglia Play a Critical Role in Restricting Senile Plaque Formation in Alzheimer's Disease. *Neuron* 49:489-502.
496. Naert, G. and S. Rivest. 2012. Hematopoietic CC-chemokine receptor 2 (CCR2) competent cells are protective for the cognitive impairments and amyloid pathology in a transgenic mouse model of Alzheimer's disease. *Molecular Medicine* 18:297.
497. Puma, C., M. Danik, R. Quirion, F. Ramon, and S. Williams. 2001. The chemokine interleukin-8 acutely reduces Ca²⁺ currents in identified cholinergic septal neurons expressing CXCR1 and CXCR2 receptor mRNAs. *Journal of Neurochemistry* 78:960-971.
498. Giovannelli, A., C. Limatola, D. Ragozzino, A. M. Mileo, A. Ruggieri, M. T. Ciotti, D. Mercanti, A. Santoni, and F. Eusebi. 1998. CXC chemokines interleukin-8 (IL-8) and growth-related gene product α (GRO α) modulate Purkinje neuron activity in mouse cerebellum. *Journal of Neuroimmunology* 92:122-132.
499. Gillard, S. E., M. Lu, R. M. Mastracci, and R. J. Miller. 2002. Expression of functional chemokine receptors by rat cerebellar neurons. *Journal of Neuroimmunology* 124:16-28.
500. Oh, S. B., T. Endoh, A. A. Simen, D. Ren, and R. J. Miller. 2002. Regulation of calcium currents by chemokines and their receptors. *Journal of Neuroimmunology* 123:66-75.
501. Boutet, A., H. Salim, P. Leclerc, and M. Tardieu. 2001. Cellular expression of functional chemokine receptor CCR5 and CXCR4 in human embryonic neurons. *Neuroscience Letters* 311:105-108.
502. Meucci, O., A. Fatatis, A. A. Simen, T. J. Bushell, P. W. Gray, and R. J. Miller. 1998. Chemokines regulate hippocampal neuronal signaling and gp120 neurotoxicity. *Proceedings of the National Academy of Sciences* 95:14500-14505.
503. Rostene, W., P. Kitabgi, and S. M. Parsadaniantz. 2007. Chemokines: a new class of neuromodulator? *Nat Rev Neurosci* 8:895-903.
504. Di Prisco, S., M. Summa, V. Chellakudam, P. I. A. Rossi, and A. Pittaluga. 2012. RANTES-mediated control of excitatory amino acid release in mouse spinal cord. *Journal of Neurochemistry* 121:428-437.
505. Limatola, C., M. T. Ciotti, D. Mercanti, A. Santoni, and F. Eusebi. 2002. Signaling pathways activated by chemokine receptor CXCR2 and AMPA-type glutamate receptors and involvement in granule cells survival. *Journal of Neuroimmunology* 123:9-17.

506. Nelson, T. E. and D. L. Gruol. 2004. The chemokine CXCL10 modulates excitatory activity and intracellular calcium signaling in cultured hippocampal neurons. *Journal of Neuroimmunology* 156:74-87.
507. Vlkolinský, R., G. R. Siggins, I. L. Campbell, and T. Krucker. 2004. Acute exposure to CXC chemokine ligand 10, but not its chronic astroglial production, alters synaptic plasticity in mouse hippocampal slices. *Journal of Neuroimmunology* 150:37-47.
508. Limatola, C., M. T. Ciotti, D. Mercanti, F. Vacca, D. Ragozzino, A. Giovannelli, A. Santoni, F. Eusebi, and R. Miledi. 2000. The chemokine growth-related gene product β protects rat cerebellar granule cells from apoptotic cell death through α -amino-3-hydroxy-5-methyl-4-isoxazolepropionate receptors. *Proceedings of the National Academy of Sciences* 97:6197-6201.
509. Tripathy, D., L. Thirumangalakudi, and P. Grammas. 2010. RANTES upregulation in the Alzheimer's disease brain: A possible neuroprotective role. *Neurobiol Aging* 31:8-16.
510. Zhang, F., S. Y. Yao, W. O. Whetsell, and S. Sriram. 2013. Astroglipathy and oligodendroglipathy are early events in CNS demyelination. *Glia* 61:1261-1273.
511. Felts, P. A., A. M. Woolston, H. B. Fernando, S. Asquith, N. A. Gregson, O. J. Mizzi, and K. J. Smith. 2005. Inflammation and primary demyelination induced by the intraspinal injection of lipopolysaccharide. *Brain* 128:1649-1666.
512. Hosking, M. P., E. Tirotta, R. M. Ransohoff, and T. E. Lane. 2010. CXCR2 signaling protects oligodendrocytes and restricts demyelination in a mouse model of viral-induced demyelination. *PloS one* 5:e11340.
513. Gamo, K., S. Kiryu-Seo, H. Konishi, S. Aoki, K. Matsushima, K. Wada, and H. Kiyama. 2008. G-protein-coupled receptor screen reveals a role for chemokine receptor CCR5 in suppressing microglial neurotoxicity. *The Journal of Neuroscience* 28:11980-11988.
514. Luo, Y., M. A. Berman, Q. Zhai, F. R. Fischer, S. R. Abromson-Leeman, Y. Zhang, W. A. Kuziel, C. Gerard, and M. E. Dorf. 2002. RANTES stimulates inflammatory cascades and receptor modulation in murine astrocytes. *Glia* 39:19-30.
515. Luo, Y., F. R. Fischer, W. W. Hancock, and M. E. Dorf. 2000. Macrophage Inflammatory Protein-2 and KC Induce Chemokine Production by Mouse Astrocytes. *The Journal of Immunology* 165:4015-4023.
516. Kalkonde, Y. V., R. Shelton, M. Villarreal, J. Sigala, P. K. Mishra, S. S. Ahuja, E. Barea-Rodriguez, P. Moretti, and S. K. Ahuja. 2011. The CC chemokine receptor 5 regulates olfactory and social recognition in mice. *Neuroscience* 197:153-161.
517. Nomura, F., S. Akashi, Y. Sakao, S. Sato, T. Kawai, M. Matsumoto, K. Nakanishi, M. Kimoto, K. Miyake, K. Takeda, and S. Akira. 2000. Cutting

Edge: Endotoxin Tolerance in Mouse Peritoneal Macrophages Correlates with Down-Regulation of Surface Toll-Like Receptor 4 Expression. *The Journal of Immunology* 164:3476-3479.

518. Hayley, S., J. Scharf, and H. Anisman. 2013. Central administration of murine interferon- α induces depressive-like behavioral, brain cytokine and neurochemical alterations in mice: A mini-review and original experiments. *Brain, Behavior, and Immunity* 31:115-127.